THE EFFECT OF RECOMBINANT HUMAN PARATHYROID HORMONE AND RECOMBINANT HUMAN GROWTH HORMONE ON BONE CELL VIABILITY

ANTIOPI VOULTSIADOU

A Thesis submitted for the degree of Doctor of Philosophy

The University of Edinburgh

May 2009

Thesis Abstract

Parathyroid hormone (PTH) and growth hormone (GH) are known to decline with ageing and have been associated with the process of apoptosis in the osteoblast and osteocyte cell populations. The presence of viable osteocytes in bone is an important parameter in maintaining bone quality while osteocyte death by apoptosis during ageing has been associated with loss of bone strength. PTH (1-34) administration as part of hormone replacement therapy (HRT) has been shown to exert positive effects via the stimulation of bone formation and improved bone microarchitecture, mainly through the inhibition of osteoblast and osteocyte apoptosis. GH on the other hand has been shown to exert positive effects on bone formation, but due to financial cost not many clinical trials have been performed. However *in vivo* studies have demonstrated the positive effects of GH on osteoblasts and osteocytes with a direct or indirect manner, possibly through the stimulation of growth factors and mainly IGF-I. Although their potential use as anabolic treatments has long been recognised and their effects on osteoblasts and osteocytes have been studied for many years, their effects on the maintenance of the osteocytic population *in vivo* are less clear. Work in this thesis has investigated whether recombinant human parathyroid hormone (rhPTH) and recombinant human growth hormone (rhGH) can inhibit osteocyte apoptosis, either due to ageing or damage as well as the potential of these hormones to trigger specific gene response on the osteoblast in the ageing rat skeleton.

An *in vitro* study in this thesis has indicated the protective effects of rhPTH and rhGH in osteocyte cultures following physical injury *in vitro*. These data have provided evidence for the first time of effects of these hormones in the repair of cell membranes following disruption. In this study, physical membrane disruption to MLO-Y4 cells *in vitro* was taken to represent physical injury-which is one aspect of microdamage to osteocytes in bone. These findings may provide a new understanding of how osteocytes sense and respond to injury and the potential of therapeutical compounds to maintain osteocyte viability in disease and old age.

rhPTH and rhGH treatment was shown to reduced osteocyte apoptosis in aged female rat bone, while improved trabecular architecture was observed in response to rhPTH treatment but not to rhGH. These data point to the potential of these hormones to be used as anabolic treatments. However the molecular mechanisms by which rhPTH and rhGH maintain the osteocytic population and lead to bone formation are not well understood.

The effects of mechanical loading on the maintenance of the osteocytic population were investigated in human cancellous bone explants *ex vivo* in the presence or absence of rhPTH. Osteocyte viability was increased and a significant reduction in osteocyte apoptosis was observed compared to unloading conditions after 7 days in culture. Furthermore alkaline phosphatase a marker of an osteogenic repsonse was increased by mechanical stimulation in the presence or absence of rhPTH compared to unloading conditions, indicating a stimulatory effect on osteoblasts. Moreover SOST gene expression was decreased in the presence or absence of mechanical stimulation following administration of rhPTH. These data pointed to important anabolic effects induced by mechanical stimulation in the presence or absence of rhPTH.

Finally a laser microdisection study using the tibias of old female rats presented in this thesis provides the basis for future studies aimed to identify specific osteoblastic genes regulated by rhPTH and rhGH at different anatomical sites of bone. Such data would provide the necessary information to elucidate the molecular mechanisms that regulate rhPTH and rhGH and their effects on bone.

In this study identification of the anti-apoptotic and protective effects of rhPTH and rhGH on osteocytes *in vivo*, *in vitro* and *ex vivo* highlighted important information on their bioactivity *in vivo*. Moreover an attempt to elucidate the molecular mechanisms behind rhPTH and rhGH effects on osteoblasts *in vivo* has been presented and provides the basis for future studies that may prove useful in identifying specific drug targets for the treatment of pathological bone.

Declaration

I hereby declare that this thesis has been composed by myself and is the result of my own work. I was assisted by Novartis Pharmaceuticals (Basel, Switzerland) by microarray and bioinformatics analysis, as clearly indicated throughout the text of the thesis. This work has neither been submitted for any other degree.

Antiopi Voultsiadou
May 2009

Acknowledgements

I would like to thank my PhD supervisors; Dr. Brendon Noble and Dr. Val Mann for their guidance and support that helped me complete my PhD studies.

I am particularly grateful to Dr Brendon Noble not only for his support and effective guidance but also for his constructive and creative criticism throughout my PhD studies. I am very grateful to Dr Val Mann for her encouragement and support. Her guidance and valuable advice have enlightened me when this thesis seemed endless. I would also like to thank all the people working in MTEC who have all made my time more enjoyable during my studies and have supported me to finish this PhD.

A special acknowledgement goes to my family for their patience, support; optimism and loving care that helped me complete my PhD. Special thanks go to my friends Yolanta and Christina who both helped me continuously and supported me throughout my PhD studies. It has been great to share the ups and downs with them for all these years. Finally I would like to thank Prof. Hamish Simpson, Dr. Carolyn Greig, Phil, Duncan, Jordi, Aimee, Natassa, Sally-Anne and Kostas for their support and for always being there to help me through hard times and make me smile.

I am also grateful to Dr. Juerg Gasser (Novartis Pharmaceuticals, Basel, Switzerland) for microarray and bioinformatics analysis as well as useful comments and support.

To my dear parents Petros and Anastasia,
and my siblings Eva, Thomai and Thomas

Contents

CHAPTER 5: Differential Gene Expression Between Osteoblastic Populations at Different Anatomical Sites: Use of Laser Capture Microscopy and Microarray.

Figure Index

Table Index

Abbreviations

ALP	alkaline phosphatase
ANOVA	analysis of variance
ASBMR	american society of bone and mineral research
ATP	adenine triphosphate
BMD	bone mineral density
BMPs	bone morhogenetic proteins
BMSC	bone marrow stromal cells
BMUs	basic multicellular units
bp	base pairs
BA	bone area
BS	bone surface
BV	bone volume
B.Pm	bone perimeter
cDNA	complementary DNA
CAD	caspase-activated Dnase
C-	carbon
^{o}C	degrees celcius
Ca^{+2}	calcium ion
Caspases	cysteine aspartate proteases
CAT	catalase
Cbfa1	core-binding factor a -1
CFU	colony forming unit
CFU-GM	colony forming unit of the granulocyte-macrophage series
cm	centimeter
CO_2	carbon dioxide
Cx	connexin
2D	2-dimensional
3D	3-dimensional
DAPI	4', 6-Diamidino-2-phenylindole

dATP	2'-deoxy-adenosine 5'-triphosphate
dCTP	2'-deoxy-cytidine 5'-triphosphate
DEPC	diethylpyrocarbonate
DERKO	double estrogen receptor knock out
DFF45	DNA fragmentation factor 45
dGTP	2'-deoxy-guanosine 5'-triphosphate
DHEA	dehydroepiandrosterone
DIG	digoxigenin
dLS	double labelled surface
DMEM	Dulbecco's Modified Eagle's Medium
DMSO	dimethyl sulfoxide
DNA	deoxyribonucleic acid
DNase I	deoxyribonuclease I
dNTP	deoxynucleoside triphosphate
dUTP	2'-deoxy-uracil 5'-triphosphate
E_1	estrone
E_2	17β-estradiol (estrogen)
E_3	estriol
EBPs	estrogen binding proteins
ecNOs	endothelial cell nitric oxide synthase
EDTA	ethylenediaminetetraactic acid
EGF	endothelial growth factor
EGFR	epidermal growth factor receptor
ER	estrogen receptor
EREs	estrogen response elements
ERK	extracellular signal regulated kinase
αERKO	estrogen receptor alpha knock out
βERKO	estrogen receptor beta knock out
ERα	estrogen receptor alpha
ERβ	estrogen receptor beta
FasL	Fas ligand

FBS	fetal bovine serum
FGF	fibroblast growth factor
FITC	fluorescein isothiocyanate
GH	growth hormone
GHR	growth hormone receptor
GHRH	growth hormone-releasing hormone
GHBP	growth hormone binding protein
GLAST	glutamate and aspartate transporter
GNRH	gonadotrophin-releasing hormone
L-Glu	L-glutamine
GnRH	gonadotrophin-releasing hormone analogs
GPx	glutathione peroxidase
GR	glucocorticoid receptor
GRP30	G-protein coupled receptor 30
GSH	Glutathione
H-	hydrogen atom
H^+	hydrogen proton
HBSS	Hank's balanced salt solution
H_2DCF-DA	2',7'-dichlorodihydrofluorescein-diacetate
H_2O	water
H_2O_2	hydrogen peroxide
HeLa cells	Henrietta Lacks cells
HRT	hormone replacement therapy
Hz	Hertz
ICAD	inhibitor of caspase activated deoxyribonuclease
IFN-γ	interferon-gamma
IGF	insulin-like growth factor
IGF-1R	IGF-1 receptor
Ihh	indian hedgehog
IL-1	interleukin-1
IL-8	interleukin-8

Ir.L.t	interlabel time
Ir.L.Th	interlabel thickness
i. S	intersection surface
kg	kilogram
KO	knock out
L	litre
LCMM	laser capture microdissection microscopy
LCM	laser microdissection
LCS	light chain shifting
LDH	lactate dehydrogenase
LDL	low density lipoproteins
LRP5	low density lipoprotein receptor-related protein 5
M	molar
MAPK	mitogen-activated protein kinase
MAR	mineral apposition rate
MCSF	macrophage colony stimulating factor 1
MEK1/2	MAPK/ERK kinase
MEM	minimum essential medium Eagle
α-MEM	α-modified minimum essential medium
mg	milligram
Mg	magnesium
ml	millilitre
mm	millimetre
mmol	millimole
mM	millimolar
mRNA	messenger ribonucleic acid
MSC	mesenchymal stem cells
MS	mineralising surface
NAD	α-nicotinamide adenine dinucleotide
NADPH	nicotinamide adenine dinucleotide phosphate hydrogen
NBT	nitroblue tetrazolium

NCS	newborn calf serum
ng	nanogram
nm	nanometer
NO	nitric oxide
NT	nick translation
O-	oxygen atom
$O_2^{\cdot-}$	superoxide
OF45	osteoblast/osteocyte factor 45
-OH	hydroxyl group
$OH^{\cdot}$	hydroxyl radical
OCN	osteocalcin
OPG	osteoprotegerin
OPN	osteopontin
OVX	ovariectomy
OSF	osteoblast-specific factor
Osx	osterix
PCR	polymerase chain reaction
P/S	penicillin/streptomycin
PARP	poly(ADP-ribose) polymerase
PBS	phosphate-buffered saline
PDGF	platelet-derived growth factor
PGE_2	prostaglandin E_2
PHEX	Phosphate-regulating gene with homology to endopeptidases on the X chromosome
PI	propidium iodide
PI3-Kinase	phosphoinositol 3-kinase
PTH	parathyroid hormone
PTHrP	parathyroid hormone-related protein
PTH1R	parathyroid hormone receptor 1
PTH2R	parathyroid hormone receptor 2
PTH3R	parathyroid hormone receptor 3

RANK	receptor for activation of nuclear factor kB
RANKL	receptor activator of NF-kB ligand
rhGH	recombinant human growth hormone
rhPTH	recombinant human parathyroid hormone
RNA	ribonucleic acid
ROI	region of interest
RO_2	peroxyl radical
ROS	reactive oxygen species
RT	room temperature
RT-PCR	reverse transcription polymerase chain reaction
S.E.	standard error of the mean
SERMs	selective estrogen receptor modulators
sLS	single labelled surface
SOD	superoxide dismutase
SOST	sclerostin gene
SS	somatostatin
Tb. N	trabecular number
TV	tissue volume
TA	total tissue area
TS	tissue surface
Tb.Th	trabecular thickness
Tb. Sp	trabecular separation
Tb. N	trabecular number
TESPA	3-aminopropylnethoxy-silane
TGF-a	transforming growth factor-alpha
TGF-β	transforming growth factor-beta
TNF	tumor necrosis factor
TNF-a	tumor necrosis factor-alpha
TRAP	tartrate resistant acid phosphatase
VDR	vitamin D receptor
VEH	vehicle

μM	micromolar

CHAPTER 1

Introduction: Bone and Parathyroid and Growth Hormones

Introduction

1.1 Bone as an organ

Bone is a rigid form of connective tissue that, together with cartilage, makes up the skeletal system. It serves three main functions; it supports locomotion as a site of muscle attachment; it protects vital organs, such as the brain and bone marrow; and it functions as a metabolic tissue, acting as a reserve of calcium and phosphate ions that participate in serum homeostasis (Baron, 1996, Felsenfeld et al., 1999).

Bone is a dynamic tissue that has the ability to adapt to its architecture through continuous cycles of modelling and remodelling in order to adapt to structural and mechanical requirements (Wolf 1982, Turner 1992, Parfitt 1994).

The cells involved in the processes of bone modeling and remodeling are under a coordinated control in order to attain a balance between bone formation and resorption. This consists of systemic hormones such as parathyroid hormone (PTH), 1,25dihydroxyvitamin D3 and calcitonin, growth hormone (GH) and steroid hormones as well as growth factors such as transforming growth factor-β (TGF-β), fibroblast growth factor (FGF's), platelet-derived growth factor (PDGF) and insulin growth factor (IGF). These hormones and growth factors mainly stimulate and regulate bone formation while cytokines such as members of the interleukin family and tumour necrosis factor (TNF) act to stimulate osteoclastic bone resorption (Rodan 1992, Hill P. A., 1998, Sommerfeldt and Rubin, 2001).

Imbalances in these fine tuned interactions may lead to abnormal turnover cycles, characterized by insufficient formation of bone resorbing or bone forming cells, increased resorptive or forming activity or abnormal formation of mineral crystals leading to diseases such as osteoporosis, Paget's disease, osteolytic and osteoscelrotic bone diseases (Rodan and Martin 2000, Compston JE, 2007).

1.2 Bone organisation

Bone consists of hydroxyapatite crystals, collagenous proteins which make up approximately 85-90% of the total protein in bone(collagen type I) and the remaining 10-15%f the bone total protein is composed of non-collagenous proteins, either serum derived or exogenous proteins which bind to hydroxyapatite due to their acidic nature (Baron 1996). Macroscopically, bones can be divided into flat bones, such as bones of the skull and scapula, long bones such as the tibia and femur and irregular bones such as vertebrae, maxillae and cranial bones.

Long bones (Figure 1.1) consist of cortical and trabecular bone (Baron 1996) that contribute to its function as the load-bearing parts of the skeleton. Cortical bone is a dense structure forming the outer shell of the long bones and enclosing the medullary cavity. Cortical bone consists of osteons oriented in the direction of maximal stress; each osteon is composed of a blood vessel enclosed in a Harvesian canal, which is surrounded by concentric lamellae of collagen fibres and interstitial bone (areas of cortical bone surrounded by cement lines that do not contain an osteon). The outer surface of the cortical bone is called the periosteum and the inner the endosteum (Eihorn 1996).

Trabecular or cancellous bone is a porous network found in the vertebrae and the metaphyses of long bones. It has a spongy appearance and is composed of a network of rod and plate-like elements that make the overall organ lighter and allowing space for marrow; trabecular plates are oriented in such a way to resist mechanical load (Weiner 1999, Sikavitsas et al., 2001) Trabecular bone accounts for about 20% of total bone mass the remaining 80% is cortical bone, but for about 61% of the bone surface area. The main role of trabecular bone is to absorb more energy imparted during mechanical load; due to its structure it is capable of tolerating deformation and distributing mechanical loads from the articular cartilage to the cortical shaft, to avoid structural damage (Keaveny and Yeh, 2002).

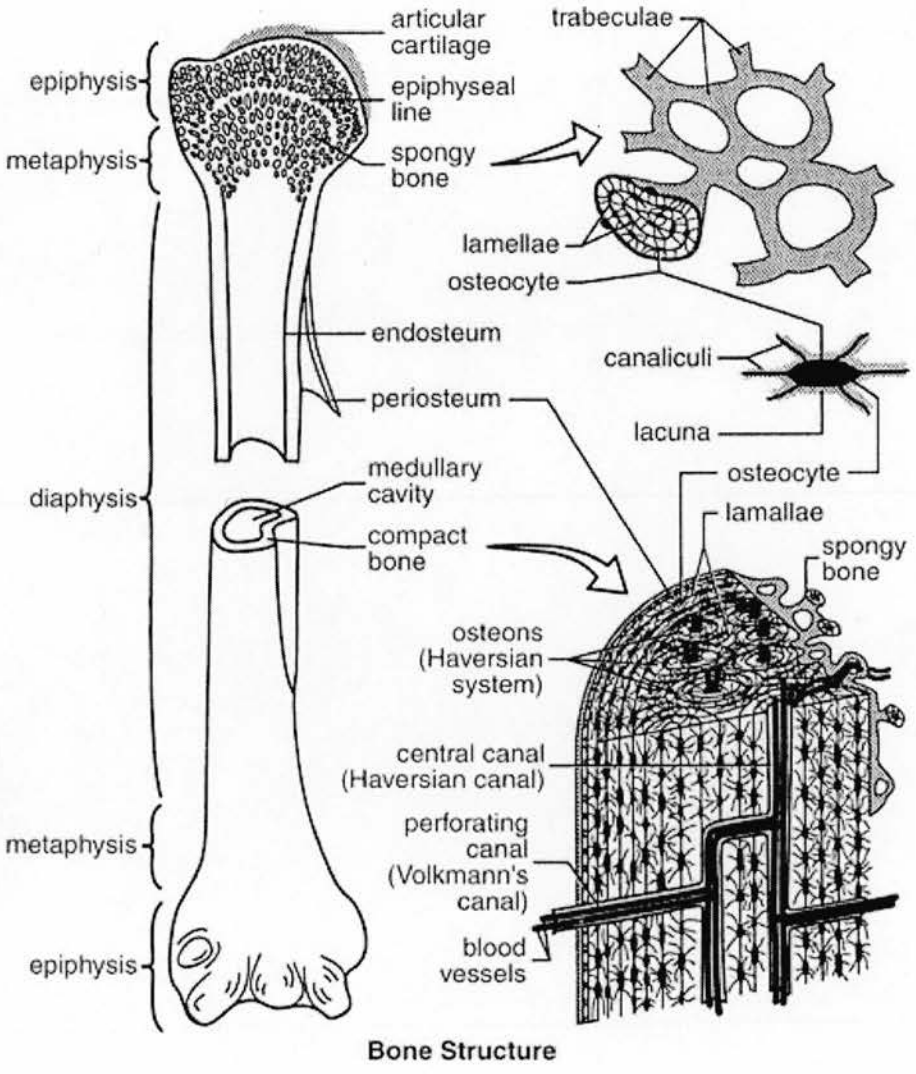

Figure 1.1 Schematic diagram of a long bone. Either end of a long bone consists of the epiphysis, characterised by internal trabecular structure, while the central region known as the diaphysis consists mainly of cortical bone. Diaphysis and epiphyses are separated by the metaphysis which includes both trabecular and cortical bone and is found below a zone of cartilage in which bone growth takes place known as the growth plate. (Taken from http://media.wiley.com/Lux/84/21784.nfg001.jpg)

1.3 Modeling

During growth, skeletal architecture is established and controlled by the process of bone modeling. Modeling can be split into 1. the intramembranous ossification, responsible for the formation of flat bones and the thickening of long bones and 2. the endochondral ossification that forms the long bones. During intramembranous ossification, mesenchymal cells differentiate into preosteoblasts and osteoblasts that synthesize woven bone. Woven bone is characterized by irregular calcification and arrangement of collagen fibres and high osteocyte cell density, which is replaced by lamellar bone over time (Turner 1992, Weiner and Wagner 1998, Sikavitsas 2001).

During the process of endochondral ossification mesenchymal stem cells differentiate into prechondroblasts and chondroblasts that form a cartilaginous matrix and then differentiate into chondrocytes that will eventually form the growth plate and engender longitudinal growth (Parfitt 1976, Carter et al 1996). As chondroblasts continue to proliferate, chondrocytes move away from the proliferative zone and become hypertrophic. They then initiate the mineralization process of the cartilaginous matrix and eventually undergoe apoptosis. This process is controlled by a number of factors such as parathyroid hormone-related protein (PTHrP), Indian hedgehog (Ihh), and bone morphogenetic proteins (BMPs) (Strewler 2001). Osteoclasts then come into action to resorb the calcified matrix, while osteoblasts use the matrix as a template to form the woven bone (Boyde 1980, Parfitt 1994, Weiner and Wagner 1998, Baron 1996).

1.4 Bone remodeling

Bone remodeling otherwise known as bone turnover is a complex process occurring on trabecular and cortical bone surfaces. During this process old or damaged bone is replaced by new (Mundy 1995). Remodeling is essential for bones to adapt to mechanical strains, repair microdamage and maintain mineral homeostasis; about 2-10% of the whole adult skeleton is constantly undergoing remodeling (Parfitt 1994, Burr et al. 1985, Eriksen et al. 2007).

In endochondral and trabecular bone remodeling the source of osteoblasts and osteoclasts is the stromal and haematopoietic precursors in the bone marrow, respectively. In periosteal remodelling osteoblasts are derived from the periosteal mesenchymal cells and the osteoclasts from the peripheral blood haematopoietic precursors (Rodan 1992, Prockop 1997, Teitelbaum 2000).

Bone turnover occurs in basic multicellular units (BMUs) (Frost, 1969) and involves a sequence of events, that include formation and activation of osteoclasts that carry out bone resorption; osteoblasts replace the resorbed bone by secreting osteoid that over time becomes calcified returning that site to a quiescent state. The average length required to complete the remodeling cycle is about 5 months (Recker et al., 1988) but it differs in cortical and trabecular bone with the trabecular one being lengthier (Figure 1.2). The osteoblasts will either line the surface of new bone to either undergo apoptosis or to differentiate into osteocytes and become embedded into the bone matrix.

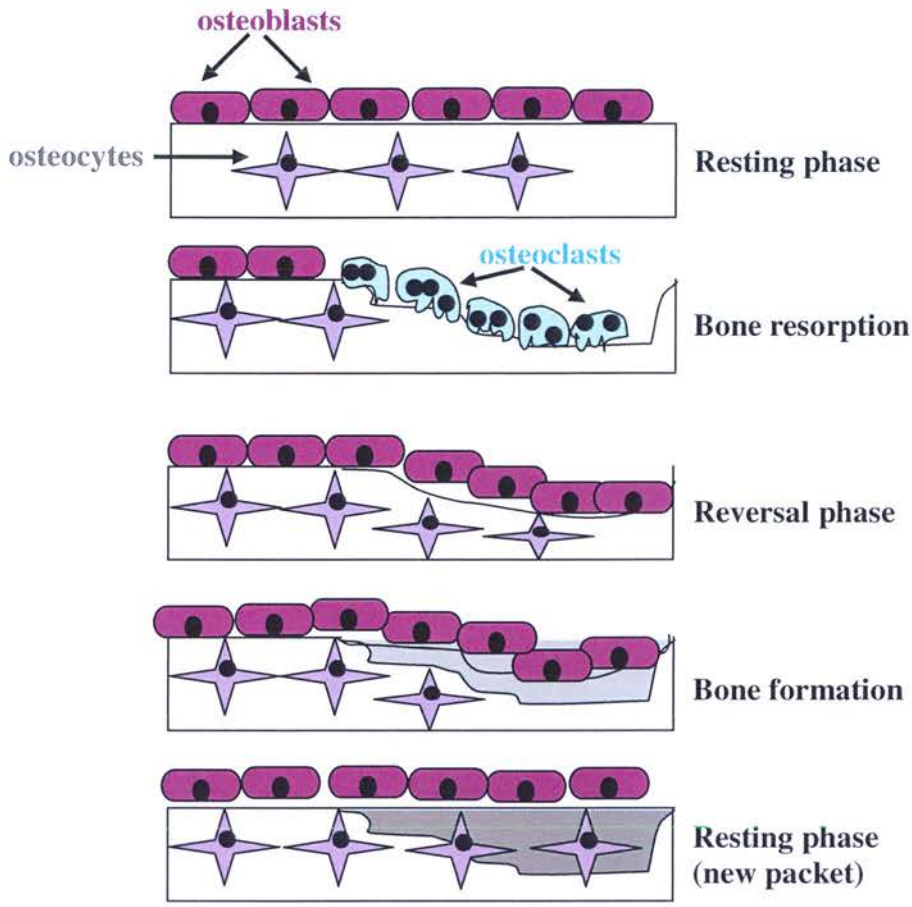

Figure 1.2 Remodeling Process. The remodeling process involves two distinct stages: bone resorption (breakdown) and bone formation. When calcium is needed in the body; osteoclasts attach to the bone and break it down to release calcium. The osteoblasts then move in to the cavities that the osteoclasts left and release collagen and proteins in these cavities and stimulate bone mineralization. Some of these osteoblasts will remain as part of the matrix and become embedded into the bone to form osteocytes

1.5 Bone cells

Osteoblasts, osteoclasts, bone lining cells and osteocytes are the four cell types found in bone. Osteoblasts, osteoclasts and bone lining cells are mainly located at the endosteal bone surface, whereas osteocytes are found embedded within the mineralized bone matrix. Osteoclasts are the bone resorbing cells whereas osteoblasts are the bone forming cells. Osteocytes and bone lining cells are defined by their location but new research suggests that they may have a role in the balance of bone metabolism.

1.5.1 Osteoblasts

The osteoblasts are fully differentiated mononuclear bone forming cells derived from mesenchymal stem cells (MSC). These cells arise from the mesenchyme during development and give rise to a number of different progenitors in the bone marrow stroma (Prockop 1997). These stem cells will form single colonies known as colony forming units (CFU's), heterogeneous in size, morphology and differentiation potential. The CFU's are under the control of different hormones, growth factors and cytokines, as well as transcription factors that guide CFU's to become osteoblasts, adipoblasts, chondroblasts, myoblasts or fibroblasts (Ducy et al., 2000).

Osteoblasts are characterized by a round nucleus and a cuboidal shape with prominent Golgi complexes and a well-developed endoplasmic reticulum (Puzas 1996). They are also characterized by cytoplasmic processes extending into the osteoid, with which they communicate with the osteocytes in their canaliculi and gap junctions to communicate with other osteoblasts (Baron 1996). Their main action is to secrete type I collagen and non-collagenous proteins of the bone matrix, and regulate the mineralization process, although the exact mechanism is unknown. The production of collagen is an early event, taking place after the proliferation of osteoblast precursors, followed by the expression of alkaline phosphatase (ALP) and reaches maximal levels before mineralization (Yoon et al., 1987). ALP is an enzyme needed for the mineralization of bone matrix however ALP is not exclusively expressed in bone and is also found in a wide variety of tissues such as the liver, spleen, intestine kidney and placenta. In bone ALP is considered as a marker of osteoblasts at late differentiation stage. During matrix mineralization, a number of genes

such as osteopontin and osteoclacin are activated and the produced non-collagenous proteins are deposited in the matrix. In addition to those proteins proteoglycans and glycoproteins are synthesized and secreted, some of these proteins produced by the osteoblasts leak into the blood circulation, and different immunoassays are available to quantitate the bone formation rate e.g by the measurement of alkaline phosphatase isoenzymes in plasma.

The control of differentiation into an osteogenic lineage is controlled by osteoblast-specific factors (OSFs). OSF2 or Cbfa1 (recently renamed Runx2) is a member of the runt homology domain transcription factor family, which was first identified based on its ability to regulate osteocalcin (OCN); and has been found to be essential as a transcriptional activator of osteoblast differentiation (Ducy et al., 2000). The importance of Runx2 was demonstrated by gene targeting experiments in which Runx-2 deficient mice developed a cartilaginous skeleton without any osteoblasts with subsequent death of the animals due to respiratory distress (Komori et al., 1997, Otto et al. 1997). It is the earliest known marker of osteoblast differentiation and can be stimulated by multiple signal transduction pathways such as the mitogen-activated protein kinase (MAPK) pathway, which in turn is stimulated by a number of signals including those initiated by osteogenic growth factors like bone morphogenetic proteins (BMPs), mechanical loading and hormones such as parathyroid hormone (PTH) (Franceschi and Xiao 2003). Nakashima et al. (2002) have identified a novel transcription factor, called osterix (Osx) that also regulates osteoblast differentiation and bone formation. Osx appears to act downstream of Runx2. It was shown in the same study that there is no bone formation in Osx null mice, suggesting that it is essential for osteoblast differentiation. Moreover it was shown by Celil et al. (2005) that during osteogenic lineage progression, in addition to BMP-2/Smad pathway, insulin-like growth factor I (IGF-I) and MAPK signaling may be mediated by Osx.

Osteoblasts and adipocytes are able to transdifferentiate, demonstrating the plasticity of the progenitors (Park et al., 1999). Surprisingly, the inhibition of gap junctions converts the osteoblasts into cells with an adipocyte phenotype (Schiller et al. 2001) showing the

importance of cellular communication during osteognesis. These findings are suggestive of a bipotential adipocyte-osteoblast precursor cell, and the balance between bone formation and bone marrow adipogenesis may provide the solution towards a therapeutic target to prevent or treat conditions with inadequate bone formation and excessive adipogenesis.

The osteoprogenitors go through three stages that can be divided as 1. proliferation, 2. extracellular matrix production and 3. mineralization; towards fully differentiated osteoblasts. During these stages a number a complex markers such as collagen type I, ALP and non-collagenous proteins are expressed. The diversity of this process suggests that not all osteoblasts are the same; and they may develop via different regulatory mechanisms and they may be functionally and even molecularly different from each other. These differences may explain the different trabecular architecture seen at different skeletal sites.

1.5.2 Osteoclasts

Osteoclasts are the bone resorbing, multinucleated cells containing an average of 4-20 nuclei. However the number of nuclei per osteoclast is extremely variable, with an average number 1-6 nuclei in rodents, but more in others species such as cats or humans with about 7-26 nuclei (Vaananen et al., 2008). In addition, in some pathological situations like Paget's disease, each osteoclast can contain more than 100 nuclei(Boissy et al., 2002). They are located on the calcified bone surface, usually at the endosteal site and they act to resorb the mineral and organic phases in bone or calcified cartilage. Osteoclasts are characterized by abundant Golgi complexes, numerous mitochondria and lysosomal vesicle trafficking (Vaananen et al., 2008).

Osteoclasts arise from haematopoietic stem cells within the bone marrow, following the monocyte-macrophage lineage. Osteoclast differentiation is regulated by a number of cytokines and growth factors such as osteoprotegerin (OPG), receptor activator of nuclear factor kappa B ligand (RANKL) and receptor activator of nuclear factor kappa B (RANK). Following proliferation mononuclear precursors close to the bone surface are

fused into multinucleated osteoclasts; the mechanisms of fusion and determination of resorption site are still unknown (Vaananen et al., 2000).

The resorption cycle can be divided into 5 phases that include 1. osteoclast attachment, 2. osteoclast polarization, 3. formation of the sealing zone, 4. resorption and 5. cell detachment and death (Vaananen et al. 2000). Once the osteoclast is attached for resorption it undergoes polarization changes. In the resorbing osteoclast a ruffled border is formed, and this area becomes the bone resorbing site that is sealed off from the surroundings by a sealing zone. The ruffled border area is then acidified by the fusion of intracellular vesicles and by the V-type ATPase proton pump, ensuring rapid dissolution of minerals, by migration of the osteoclast along the site destined to be removed, as migration tracks have been observed in vitro and in vivo (Palokangas et al. 1997). After the osteoclast has resorbed bone and transported the degraded matrix products into the extracellular space, it will possibly undergoe apoptosis by the same molecular pathways as other cell types (Xing and Boyce 2005).

1.5.3 Bone lining cells

The bone lining cells as their name implies are located on the bone surface. These are non terminally differentiated cells that have been reported to revert to an active osteoblast phenotype e.g following PTH treatment (Gasser, 1998). The surface of the bone which, is not undergoing remodeling, is covered by a 1-2 μm thick layer of unmineralized collagen matrix and a layer of flat elongated cells. These cells other than being called bone lining cells are known by a number of other names such as 'inactive osteoblasts' and 'surface osteocytes', suggesting that they are descendents of osteoblasts (Parfitt 1994). There is very little known of their origin, proliferation, differentiation and function, and they only contain a few organelles, including endoplasmic reticulum, free ribosomes and mitochondria (Miller et al. 1980). It has been demonstrated that bone lining cells are in contact with osteocyte dendrites and that this system regulates ionic flow between bone and plasma (Rubinacci et al. 1998).

1.5.4 Osteocytes

Osteocytes (Figure 1.3) are the most abundant cells in bone with approximately ten times more osteocytes than osteoblasts in adult human bone (Parfitt 1977). Osteocytes are terminally differentiated osteoblasts that have become embedded within the mineralized bone matrix (Aarden et al. 1994, Noble BS 2008).

It has been suggested that about 10-20% of osteoblasts will differentiate into osteocytes (Aubin et al. 1996); however the signals regulating this process are not fully understood. The evidence for the osteoblast-osteocyte differentiation comes from ultrastuctural studies, reporting how some osteoblasts are buried inside the matrix (Palumbo et al. 1990). Osteocyte communication within the osteocyte syncytium and other cells on the bone surface is via dendritic processes that radiate in all directions and pass through the canaliculi in bone (Palumbo et al. 1990, Aarden et al. 1994).

Osteocyte location and the lack of antibodies directed against specific osteocyte markers, makes it hard to study their characteristics, and there is limited number of studies to date describing as such. Avian postmitotic osteocytic-like cells (Van der Plaas et al. 1994) have been isolated and purified using the mAb OB7.3 antibody (Nijweide and Mulder 1986, 1992) that is thought to be specific for the chicken Phosphate-regulating gene with homology to endopeptidases on X chromosome (PHEX) endoprotease (Westbroek et al. 2002) likely to be forming part of the osteocyte factor 45/ matrix extracellular phosphoglycoprotein (OF45/MEPE) signaling pathway (MacDougall et al. 2001, Gowen et al. 2003). Studies have localized the OF45 mRNA on mature osteoblasts and osteocytes in the skeleton of rats and mice (Petersen et al. 2000, Igarashi et al. 2002) suggesting that OF45 might be involved in the mineralization process and the differentiation of osteoblasts to osteocytes. Other molecules involved in this process would be matrix metalloproteinases (MMPs), dentin matrix protein-1 (DMP-1), Klotho gene, TGFb inducible early gene-1 (TIEG), lysophosphatidic acid (LPA) and E11 which is a possible marker of the osteocytic phenotype and it has been proposed to regulate formation and maintenance of the osteocytic as well as the osteoblastic cellular processes (Wetterwald et al. 1996, Schulze et al. 1999, Hadjiargyrou et al. 2001, Noble BS. 2008).

The MLO-Y4 osteocyte-like cell line (Figure 1.4) has been extensively used and lots of information regarding osteocytic characteristics comes from data based on its use. The osteocalcin promoter was used to target simian virus (SV) 40 large T-antigen oncogene into the osteocytes of transgenic mice (Kato et al. 1997). These cells are characterized by long dendritic processes, high osteoclacin secretion, osteopontin and connexin 43 expression, low collagen type I, low alkaline phosphatase expression (Kato et al. 1997) and E11 expression (Bonewald, 2007). Other cell lines include the MLO-D1, -D6, -A5 and –C2 osteocyte like cells proposed to represent various stages of the differentiation form osteoblasts to osteocytes (Kato et al. 2001), but are not yet well characterized.

A number of functions have been proposed for osteocytes, including their role in the mineralization process (Ikeda et al. 1996) and bone resorption known as osteocytic osteolysis, as demonstrated by the lacunae size in diseases and collagenase production (Shimizu et al. 1990, Fuller and Chambers 1995,) although this function remains controversial (Boyde 1980, Marotti et al. 1990, Van der Plaas et al. 1994). Other studies have demonstrated an inhibitory signal from osteocytes to neighboring osteoblasts that negatively regulates bone formation (Marotti et al. 1996). It was only recently that a number of studies (van Bezooijen et al. 2004; 2005, Poole et al. 2005) identified this signal to be the protein sclerostin, which belongs to the DAN family of glycoproteins, the product of the SOST gene responsible for sclerosteosis, a rare skeletal dysplasia characterized by progressive bone thickening and sclerosis of the skeleton (Brunkow et al. 2001, Gardner et al., 2005). Sclerosteosis is due to loss of function mutations of the SOST gene, which encodes for the protein sclerostin that is produced by mature osteocytes and inhibits bone formation (van Bezooijen et al. 2004). It is hypothesized that in patients with sclerosteosis and sclerostin deficiency, the bone phenotype is probably due to increased bone formation that is not associated with increased bone resorption, leading to a positive bone balance and increased bone mass (van Bezooijen et al., 2005). Although investigations in this field are still ongoing it was initially thought that sclerostin functions as a BMP antagonist, but it is now known that it antagonizes canonical Wnt signaling by binding to Wnt co-receptors, low density lipoprotein receptor

related protein (Lrp) 5 and 6 (Li et al. 2005). Thus high bone mass observed in sclerosteosis and Van Buchem disease may result from increased Wnt signaling due to the absence of insensitivity to sclerostin (Sutherland et al. 2004, ten Dijke et al. 2008).

In contrast to this theory, other studies, following examination of the lacunar occupancy at different stages of remodeling, revealed that forming as well as resorbing osteons contained higher osteocyte density and lacunar occupancy, when compared to quiescent osteons (Power et al. 2002). Furthermore evidence has been presented to show that the controlled death of osteocytes via means of apoptosis may be providing the signals that direct turnover, since apoptotic osteocytes have been observed in close association with resorbing areas (Noble et al. 1997, Verborgt et al. 2000, Kogianni et al. 2008) and most importantly prior to initiation of bone resorption (Noble et al. 2003). However, in order for the osteocytes to respond to this signal they should be able to sense such a requirement.

It has been speculated that osteocytes due to their location within the bone matrix as well as the communicating network they form, may be the mechanosensors (Lanyon 1993, Klein Nulend et al. 1995, Zhang et al. 1997, Noble et al. 2003) and communicate a metabolic signal to the bone effector cells (Duncan and Turner 1995, Lean et al. 1996, Aarden et al. 1996, Klein Nulend et al. 1995, Yellowley et al. 2000).

Several hormones known to regulate the bone turnover process have also been shown to affect osteocyte survival and function, following binding to their receptors located on the osteocytes, or via indirect routes. Osteocytes have been shown to undergoe apoptosis in response to glucocorticoids both in vivo (Weinstein et al. 1998) and in vitro (Kogianni et al. 2004); respond to PTHrP and PTH binding (Rao et al. 1983, Fermor et al. 1995), which were shown to alter cx43 expression and induce osteocyte apoptosis possibly regulating osteocyte communication and survival (Divieti et al. 2001). Osteocytes have also been demonstrated to respond to intermittent PTH administration by downregulating expression of sclerostin, which is hypothesized to maintain bone lining cells in a

quiescent state on the bone surface, therefore allowing lining cells to return to an active bone forming state (Keller et al. 2005, Poole et al. 2005, Leupin et al., 2007).

1.6 Mechanical loading and bone

Mechanical loading of bone causes the deformation of bone matrix generates strain and intraosseous fluid flow occurs through the interconnected pore space in the bone. Bone fluid flow leads to a strain generated streaming potential, which is hypothesized to initiate the mechanotransduction pathway (Hong et al, 2007). Frost in 1988 introduced the term mechanostat, which describes the ability of bone to adapt its structure to suit its function. This process requires bone cells to detect mechanical signals and change bone architecture accordingly. Bone continuously adjusts to strains by changing its shape, mass or microarchitecure. For example, reduction in mechanical strain due to disuse like in cases of prolonged bed-rest, space flight or reduced physical activity in old age results in increased bone resorption and bone loss (Inman et al. 1999, Bonewald and Johnson 2008), whereas under physiological strains, at a frequency of about 2 Hz, which corresponds to the stride frequency observed during natural locomotion (Mosley and Lanyon, 1998) bone mass is maintained.

Mechanical loading is known to control both modeling and remodeling processes, having an important role in bone structure and shape during growth and its maintenance in adult life (Rubin 1984, Rubin and Lanyon 1987, Carter 1996, Mosley et al. 1997), however the mechanism is not completely understood.

Evidence has suggested that bone has an ability to repair accumulated microdamage due to everyday use (Parfitt 2001) via sensing changes in the distribution of strain within the bone microenvironment and targeting bone for removal by osteoclasts (Burr and Martin 1993, Parfitt 2002). A number of studies support the same idea, since it was demonstrated that microdamage induced by loading on canine (Burr and Martin 1993) or rat bone (Verborgt et al. 2000, Noble et al. 2003) was targeted for removal by osteoclastic cells more frequently than would have been expected by chance alone (Burr et al. 1985, Mori and Burr 1993, Burr and Martin 1993, Parfitt et al. 2001) followed by increased

remodeling activity. The mechanism directing those activities is still unknown, but it is hypothesized to be mediated by the osteocyte (Kakizaki et al. 1971, Kenzora et al. 1978, Kamijou 1994, Mori et al. 1997, Marrotti et al. 1998, Hazenberg et al., 2007, Bonewald and Johnson 2008).

Bone is lost in the absence of loading and maintained or increased in the presence of loading. The bone cells with potential to sense mechanical strains and translate them into biochemical signals include bone lining cells, osteoblasts and osteocytes, however due to their distribution thourghout bone, osteocytes are thought to be one if not the major cell type to sense mechanical strains (Bonewald and Johnson, 2008). It has been recently shown that targeted deletion of osteocytes results in bone loss and bone does not respond to unloading (Bonewald and Johnson, 2008).

But the question is how osteocytes sense mechanical loading, for this reason a number of models, such as substrate tension and bending, fluid shear and a combination of these have been developed in an effort to answer this question. There is some controversy regarding the type of *in vitro* experimental model that would better mimic the *in vivo* environment of loading. The fluid flow that occurs in bone during *in vivo* situations is another factor that needs to be considered, since it serves a number of functions such as nutrient transfer as well as creating fluid shear stress forces on the cell membrane and cell processes. Current theory has it, that cells are more responsive to fluid shear than to mechanical strain (Turner et al. 1994, Tan SD et al., 2008). To address these questions an *ex-vivo* bioreactor system (Zetos^{TM}) has been developed to study the effects of mechanical loading on bone explants, which is the subject of chapter 4 and will be discussed in detail there.

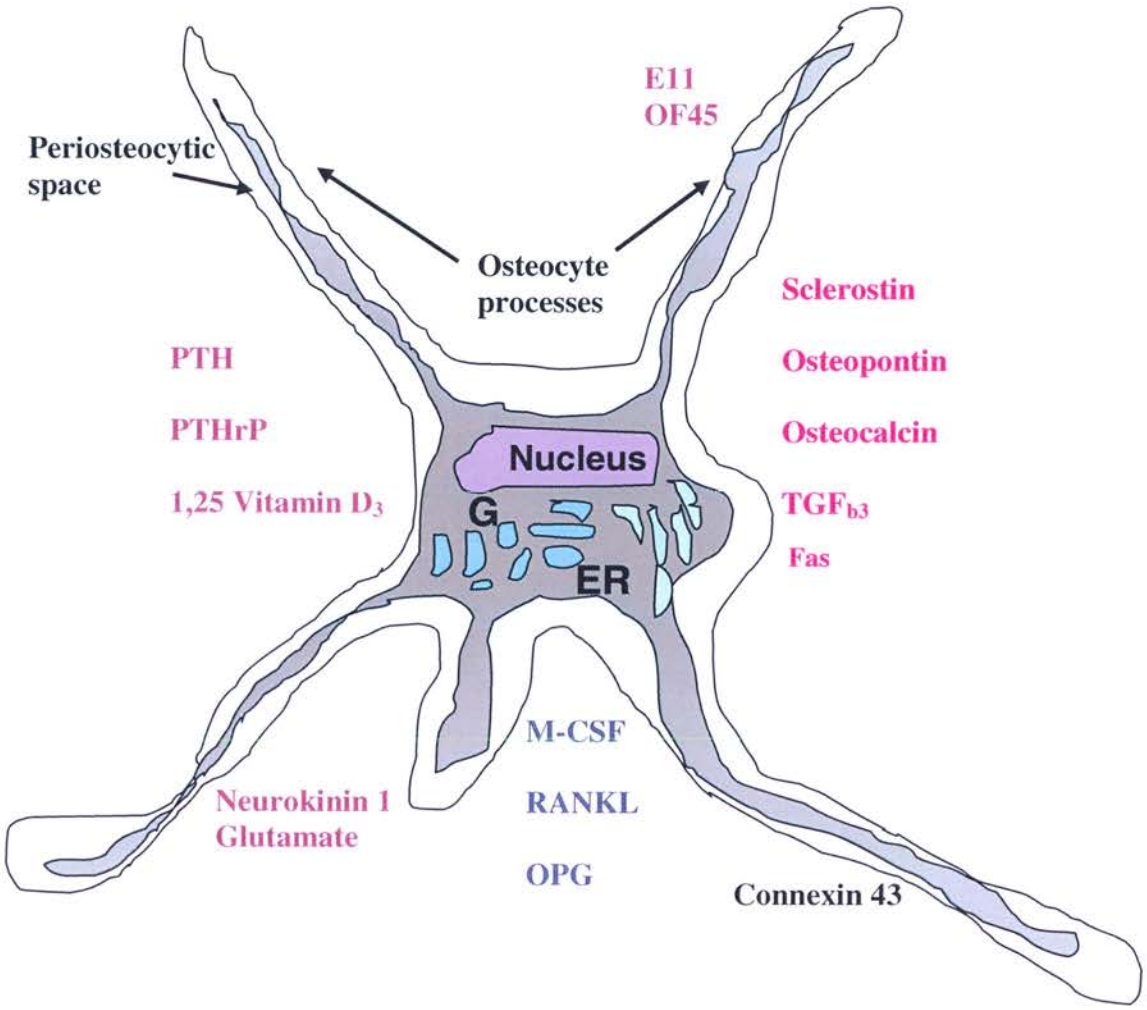

Figure 1.3 The osteocyte. The osteocyte contains a large Gogli apparatus (G), an endoplasmic reticulum (ER) and a basal nucleus. The osteocytes expresses molecules involved in the targeting of bone formation and resorption and are under the influence of hormones, neuronal factors and mechanical stimuli.

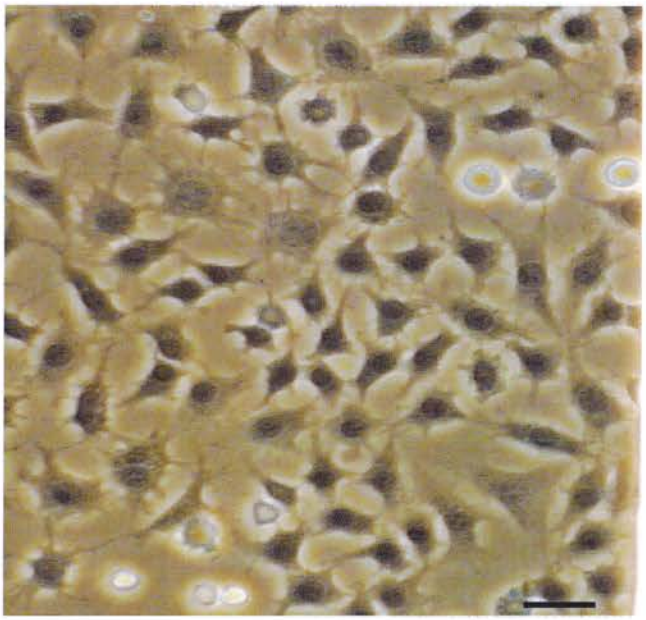

Figure 1.4 MLO-Y4 osteocytes in culture. Representative image of MLO-Y4 osteocyte-like cell line isolated and characterized by Kato et al., 1997, demonstrating large cytoplasmic extensions which enable contact between neighbor osteocytes. Image was taken using phase contrast light microscopy. Bar represents10 μm.

1.7 Ageing and microdamage

Osteocyte death has long been associated with ageing (Frost 1960). Certain situations such as osteoarthritis (Wong et al. 1987) and hip fracture (Dunstan et al. 1990, Dunstan et al. 1993) have also demonstrated a decrease in osteocyte viability. The general view is that osteocytes can live for decades (Knothe Tate et al. 2004), but it has been demonstrated that 40% of osteocytes in ear ossicles which do not receive any mechanical stimulation during fetal development are dead within the second year of life (Marotti et al. 1998), emphasizing the importance of mechanical loading in osteocyte survival. It was later confirmed that osteocyte density indeed declines with age and that the age of bone, rather than the age of an individual, would be more important in determining the fate of osteocytes (Qiu et al. 2002).

The age related loss of osteocytes has been associated with impaired bone remodeling, during the removal of microdamage (Compston 2007). Microdamage is a phenomenon that occurs in bone as a result of repetitive events of cycling loading; accumulation of small cracks in the mineralized matrix leads to reduced strength of bones, but bone is capable of removing the damage by targeted remodeling (Mori and Burr 1993). It has been suggested that about 10-20% of remodelling in the adult human bone is targeted while the rest is non-targeted remodelling (Parfitt, 2002). An increase in remodelling has been reported after the generation of microdamage (Mori and Burr 1993), suggesting that targeted remodelling involves the active removal of damaged matrix by osteoclasts. The signals that activate the osteoclastic bone resorption at the damage site are unknown but it is hypothesized that they originate from the apoptotic death of the osteocytes (Verborgt et al. 2000, Noble et al. 2003, Kogianni et al. 2008). Osteocyte death was observed to precede osteoclast invasion in the damaged regions (Noble et al. 2003) and increased osteocyte apoptosis was associated with the up regulation of the proapoptotic Bax protein (Verborgt et al. 2002). The question that still remains to be answered is the nature of this signal.

1.8 Cell death

Cell death is a phenomenon conserved throughout evolution and can be classified as either 1. necrotic death that refers to the morphology seen when cells or tissues die from severe injury, chemical, physical or toxic. This phenomenon is accompanied by inflammation and changes in tissue architecture and 2. apoptotic cell death, which is the programmed cell death, as a result of the induction of an internal suicide program.

Apoptosis is initiated by a variety of stimuli including lack of extracellular survival factors, administration of steroid hormones, viral infections, oxidative stress, ionising radiation and DNA damage (Kobayashi et al, 2008). The process of apoptosis is regulated by the function of several proteins such as the bcl-2 proteins, death receptors, the p53 protein and the caspases (Dragovich et al. 1998). Caspases (Cysteine ASpartate ProteASES), are cysteine proteases that cleave their target molecules at very specific sites, following aspartate residues (asp-x). (Allen, et al. 1998, Thornberry et al. 1998). Caspases play a central role in the apoptotic maschinery as they mediate the apoptotic process in cells from the initial stages (initiator caspases) to their package in apoptotic bodies for elimination by phagocytosis (effector caspases). Apoptosis is an essential homeostatic mechanism for the healthy development and maintenance of tissues e.g finger formation during fetal development or skin regeneration following sunburn (Cotman and Anderson 1995); via regulation of the size and function of organs through the removal of harmful, excess or damaged cells (Hall et al. 1994, Pradhan et al. 1997). Apoptotic cells are characterized by membrane blebbing, chromatin condensation, disappearance of the nucleolus, alterations of the cell surface, DNA cleavage and fragmentation of the cell into apoptotic bodies.

The apoptotic bodies, containing ribosomes, morphologically intact mitochondria, and cleaved nuclear DNA, are cleared by phagocytosis in order to avoid the generation of an inflammatory response within the body (Kerr et al.1972, Savill et al. 1997). Apoptosis involves an initiating phase, decision, execution and clearing phase (Guchelaar et al. 1997) although the exact sequence of events is not well defined and is thought to involve

some complex interactions (decision events) between the cells destined to apoptose and nearby phagocytes (Reddien et al. 2007).

1.9 Apoptosis and bone

In bone tissue there is evidence of both necrotic and apoptotic cell death. Necrosis has been demonstrated in response to exposure to radiation (Sugimoto et al. 1993), steroid use (Watanabe et al. 1989), ischemia (Rosingh and James 1968) and leads to the formation of dead bone separated from healthy bone (Wong et al. 1987). There is also evidence indicating that bone cells such as osteoclasts, osteoblasts and osteocytes as well as chondrocytes undergoe apoptosis during development, bone remodelling as well as in disease indicating that apoptotic cell death is essential for skeletal development and maintenance throughout life. During endochondral ossification and fracture healing, when cartilaginous tissue is replaced by woven bone, hypertrophic chondrocytes undergoe apoptosis (Lee et al. 1998). The mechanism of such actions is unknown but it is hypothesized to act as a signal to osteoclasts for their removal (Bronckers et al. 2000). Osteoclasts have been shown to undergoe apoptosis following completion of bone resorption (Hughes and Boyce 1997, Xing and Boyce 2005) as well as in response to anti-resorptive agents such as estrogen and bisphosphonates (Kameda et al. 1997, Hughes et al. 1996, 1995; Papapoulos et al. 1997, Rodan 1998, Rogers et al. 1999). Osteoblasts on the other hand have also been suggested to undergo apoptosis at the end of the bone formation cycle in order to regulate the number of osteoblasts present during bone remodelling (Jilka et al. 1998, Landry et al. 1997) or in response to glucocorticoids in mouse (Weinstein et al., 1998, Plotkin et al., 1999) and human (Weinstein et al. 1998), but not in rat (Silvestrini 2000) and to various cytokines in vitro such as TNF-a, IL-1, IFN-γ (Ozeki et al. 2002) and FasL (Kawakami et al. 1997, Jilka et al. 1998).

1.10 Osteocyte apoptosis

Frost was the first to describe the death of osteocytes *in vivo* when he observed an increasing incidence of empty lacunae with increasing age (Frost 1960). The mechanisms by which osteocytes die was initially thought to be due to necrosis, but recent studies have provided insight into the apoptotic osteocyte cell morphology, demonstrating DNA fragmentation, chromatin condensation and cell shrinkage in both pathological and healthy bones (Noble et al. 1997).

Several studies have reported an association between osteocyte apoptosis and the regulation of bone turnover in growing bone (Noble et al. 1997). The viability of osteocytes is affected by the presence or absence of hormones, which influence the maintenance of bone homeostasis such as glucocorticoids (Weinstein et al. 1998, Mazzioti et al., 2007) or estrogen (Tomkinson et al. 1997, 1998, Huber et al., 2007). Intermittent administration of PTH has also been suggested to reduce osteocyte apoptosis in the mouse vertebra *in vivo* as well as in MLO-Y4 osteocytes *in vitro* (Jilka et al. 1999).

During orthodontic tooth movement (Hamaya et al. 2000) or in surrounding areas induced by fatigue microdamage (Verborgt et al. 2000, Waldorff et al., 2007) large numbers of apoptotic osteocytes have been observed. Furthermore unloading has been linked to an increase in osteocyte apoptosis in murine (Aguirre et al. 2006) and rat bone (Basso et al. 2006) *in vivo* and *in vitro* (Bakker et al. 2004), shown in rat bone to be reversed upon reloading (Basso et al. 2006). Moreover Mann et al. (2006) using an *ex vivo* bioreactor system showed that loading reduces osteocyte apoptosis in human trabecular bone explants. In addition Noble et al (1997) have shown that there is a U-shape relationship between osteocyte survival and the strains they experience, with normal physiological strains reducing apoptosis, whereas damagingly high levels of loading induced apoptosis. In the latter case, the transient increase in the proportion of apoptotic osteocytes in response to high levels of mechanical loading was immediately followed by subsequent intracortical remodelling providing the first evidence that the presence of apoptotic osteocytes within bone might regulate specific site-directed remodelling (Noble et al. 2003). These findings indicate that osteocyte apoptosis is a

process observed both in normal and pathological bone conditions and it might be essential in influencing the remodelling process towards specific sites.

1.11 Parathyroid Hormone: background

Parathyroid hormone (PTH) is an 84 amino acid polypeptide secreted by the parathyroid glands. PTH is essential for the maintenance of calcium homeostasis via direct actions on its main target organs, bone and kidney, and by indirect actions on the gastrointestinal tract (Sanders and Harvey, 2008). PTH acts to increase the concentration of calcium in blood in three ways. It enhances the release of calcium from the bones; it enhances reabsorption of calcium from renal tubules; and it enhances the absorption of calcium from the intestine by increasing the production of vitamin D (Vanhouten et al., 2004) The principal form of biologically active PTH is its intact molecule 1-84 which is the key endocrine regulator of calcium homeostasis (Poole, 2005) but the Kupffer cells in the liver cleave it into the 1-34 form and smaller C- terminal fragments.

In the kidney PTH has three major biological functions essential for the regulation of mineral ion homeostasis: enhancement of active reabsorption of calcium from distal tubules and the thick ascending limb, inhibition of phosphate reabsorption and enhancement of calcium absorption in the intestine by increasing the production of vitamin D (Al-Badr and Martin, 2008). Vitamin D activation occurs in the kidney, where PTH up regulates the activity of the renal 1-α-hydroxylase, thereby enhancing the synthesis of vitamin D which in turn increases the intestinal absorption of calcium and phosphate (Leder et al., 2005). As a result of these PTH actions blood calcium concentration rises and blood phosphate concentration declines with the concentration of extracellular calcium being the most important physiological regulator of the minute-to-minute secretion of PTH. In figure 1.5 the main actions of PTH are outlined.

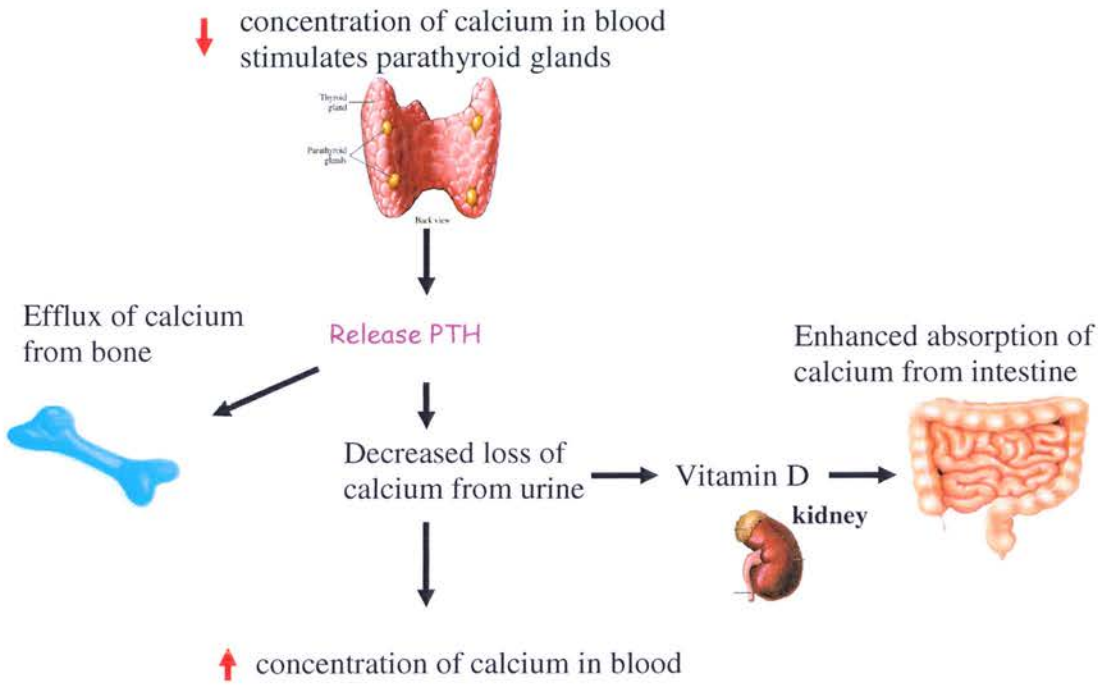

Figure 1.5 Calcium homeostasis and PTH actions In response to low calcium concentrations in the blood, parathyroid glands secrete PTH. PTH in turn stimulates release of calcium from bone, stimulating bone resorption, decreases urinary loss of calcium and indirectly stimulated calcium absorption in the small intestine via stimulation of vitamin D in the kidney.

1.12 Parathyroid hormone Receptors and Bone

There are two known parathyroid hormone receptors termed PTH1R and PTH2R. These receptors are members of the 7 transmembrane G protein coupled family (Jüppner, 1994). PTH1R is the classical PTH receptor and is expressed in high levels in the target tissues; bone and kidney, and regulates calcium ion homeostasis through activation of adenylate cyclase and phospholipase C (Offermanns et al. , 1996 and Mannstadt et al., 1999, Pioszak and Xu, 2008). This receptor is also found in a large variety of other fetal and adult tissues and at high concentrations in growth plate chondrocytes. This makes it very important in cartilage and bone development, because it mediates the parathyroid receptor protein (PTHrP) dependent regulation of chondrocyte proliferation and differentiation (Kroneberg, 2003). PTH2R is primarily expressed in the central nervous system, pancreas, testis and placenta (Usdin et al., 2002). However most biological functions mediated through this receptor remain to be determined, it is hypothesized that it may have a role in the regulation of renal blood flow, as the TIP peptide from brain has been shown to dilate the renal vessels in a PTH1R indepent manner as well as being expressed in the intrarenal arterial tree (Usdin et al., 1995, Eichinger et al, 2002).

Recently, three receptors for PTH have been isolated from zebrafish, two of these receptors are homologues to PTH1R and PTH2R while the third one (PTH3R) appears to be novel and has not been identified in mammalian cells to date (Juppner, 1999, Gensure et al., 2004).

The PTH1R seems to be the most important receptor mediating the actions of PTH (Murray et al., 2005). PTH- dependent regulation of mineral homeostasis is mainly mediated through the PTH1R receptor (Merendino et al., 1986, Potts and Gardella, 2007). Most of the PTH1R receptor dependent actions involve activation of adenylyl cyclase while some actions seem to require phospholipase C-mediated events. PTH receptors on osteocytes and osteoblasts have been demonstrated in situ by Fermor and Skerry (1995) and on isolated cells (van der Plas et al., 1994).

A number of studies have reported that there are no obvious PTH receptors on osteoclasts and as such the effects of PTH are indirect (Rouleau et al., 1988).On the other hand there are reports suggesting that there may in fact be PTH receptors on mature osteoclasts (Teti et al., 1991, Agarwala and Gay, 1999, Murray et al., 2005). Although it has not yet been resolved whether PTH has direct effects on the osteoclast, it is true that it does have indirect effects (Ono et al., 2007). The significance of the PTH1R in bone tissue has been described via the use of knock out (KO) animal models. Ablation of the PTH1R gene in mice results in neonatal lethality and severe defects in endochondral bone formation that is characterized by impaired proliferation and accelerated chondrocyte maturation and mineralization (Lanske et al., 1996). Some of these mice survive via chodrocyte specific expression of constitutively active PTH1Rs, but display abnormalities in tooth development and bone while it has not yet been possible to study the mineral ion homeostasis (Schipani et al., 1997).

The primary role of PTH *per se* and of PTH1R in maintaining the ion homeostasis has been confirmed via the ablation of the PTH gene (Miao et al., 2001, 2002), that lead to hypocalcaemia and hyperphosphatemia, whereas activating mutations in the PTH1R cause hypercalcemia and hypophosphatemia (Schipani et al., 1996 and Parfitt et al. 1996) Mice lacking the PTH gene show abnormalities in mineralization and formation of primary spongiosa of long bones, which are not observed in PTHrP- null mice and it is hypothesized to reflect loss of PTH specific actions in bone (Miao et al., 2001).

1.13 Parathyroid hormone and osteocytes

PTH receptors on osteocytes have been demonstrated in situ by Fermor and Skerry in 1995 and on isolated osteocytes in culture by van der Plas et al. in 1994. A number of reports (van der Plas et al., 1994, Liang et al., 1999) demonstrate the expression of early response genes such as increase of cAMP, of c-fos, c-jun and IL-6 in response to short term treatment with PTH in osteocytes. In another study c-fos could only be detected in osteocytes subjected to mechanical stimulation and PTH treatment, indicating that PTH supports the mechanical responsiveness of osteocytes (Chow et al., 1998b).PTH has been

reported to induce connexin 43 (Cx43) gene expression and gap junctional communication in osteoblasts (Schiller et al., 1992) and there is some evidence that the same in terms of Cx43 reorganization is induced by PTH in osteocytic cells (Divieti et al., 2001). The activation of PTH receptors in osteocytes has been reported to potentiate calcium influx via stretched activated channels (Miyauchi et al., 2000) suggesting another mechanism for PTH action. PTH receptors are considered very important in mediating the effects of mechanical loading and the anti-apoptotic effects of PTH in osteocytes (Bringhurst, 2002).

Interestingly recent reports have indicated that PTH suppresses SOST gene expression *in vivo* and *in vitro*, and that sclerostin may be the direct target for PTH action, which can partially explain the anabolic actions of PTH in bone (Bellido et al., 2005, Bellido, 2006, Keller and Kneissel, 2005)

1.14 Parathyroid hormone and bone cells

Clinical trials in the 1970's and 1980's suggested that PTH could restore bone in osteoporotic patients (Dempster et al., 1993). Such observations were the start point of intense research in the past decade on the actions of PTH on bone. Direct PTH administration to osteoblasts *in vitro* has led to high levels of cellular gap junction complexes formed by the cells as well as changes in cell shape. These results emphasize the importance of the quick response of the cells to PTH which may also explain the process of the osteoblastic cells as they function in situ. (Massas, Benayahu, 1998). Further research has indicated that the osteoblast and its progenitors are the primary *in vivo* targets for PTH action (Dempster et al., 1993, Ogita et al., 2008), where stimulation of bone formation occurs primarily in endocortical surfaces (Oxlund et al., 1993). *In vitro* studies have shown that PTH promotes the commitment of osteoblast precursors (Ishizuya et al., 1997, Ogita et al., 2008) and inhibits osteoblast apoptosis (Jilka et al., 1999). *In vivo,* PTH induces a transient increase in osteoblast apoptosis (Stanislaus et al., 2000). The controversy between *in vitro* and *in vivo* studies may be explained by the study of Chen et al. (2002) who demonstrated that PTH has anti-apoptotic effects on undifferentiated mesenchymal stem cells (MSCs) but is pro-apoptotic to more mature cells. PTH has also been shown to have an indirect effect on osteoclast activation with a

follow up calcium release by enhanced bone resorption (Murrils et al., 1990). This action was later confirmed and explained via the stimulation of the osteoblastic RANKL expression (Yasuda et al., 1998b) and MCSF synthesis (Suda et al., 1999). With complicated actions partially understood on both osteoblasts and osteoclasts the net effect of PTH on the skeleton can either be anabolic or catabolic, depending on the dose of PTH, the mode of administration, the animal species and the specific skeletal site (Compston, 2007). Moreover a number of clinical trials demonstrated the efficacy of rhPTH (1-34) otherwise known as teriparatide as a bone anabolic agent (McLung, 2004).

1.15 Effects of parathyroid hormone on bone tissue

The actions of PTH on bone are complex and only partially understood. For the PTH actions on bone the presence of several different cells types, including the osteoblasts, bone marrow stromal cells, hematopoietic precursors of osteoclasts and mature osteoclasts (Ling et al., 2004, Poole and reeve, 2005) are necessary. PTH administration leads to the release of calcium near the surface of bone. Continuous administration of PTH (or increased PTH secretion as seen in primary hyperparathyroidism) leads to an increased number and activity of osteoclasts, while intermittent administration paradoxically leads to increased amounts of trabecular bone (Suzuki et al., 2008). The primary PTH responsive cells in bone are the osteoblasts and its precursors. Tam et al. (1982) were the first to identify the differential effects of continuous and intermittent administration of PTH on net bone apposition rate.

To date, it has been proposed that intermittent PTH administration exerts its anabolic effects in three steps, 1. stimulation of preosteoblast proliferation; 2. promotion of differentiation of preosteoblasts and osteoblasts; and 3. via the inhibition of osteoblast apoptosis (Bijlezikian JP., 2008). It is still unclear whether the proliferation of preosteoblasts is increased, but *in vivo* experiments in rats' receiving intermittent PTH showed an increase in the number of osteoprogenitors indicating that PTH stimulates the proliferation of osteoblasts (Nishida et al., 1994, Kostenuik et al., 1999).

Studies in rats and humans, in which histomorphometric and bone formation markers were evaluated, have shown an increase in bone forming surfaces and markers, following intermittent PTH administration providing evidence that an increase in differentiation of osteoblasts is occurring in preference to proliferation (Meng et al., 1996, Dobnig and Turner, 1997) . Also recent microarray data from osteoblastic cell lines is supportive of the hypothesis that PTH exerts its anabolic actions via an increase in osteoblast differentiation (Qin et al., 2003, Li et al., 2007).

The other mechanism with which PTH induces an anabolic response in bone is by inhibition of osteoblast apoptosis. Daily injections with PTH in adult mice with either normal bone mass or osteopenia, increased bone formation by preventing apoptosis of mature osteoblasts (Jilka et al., 1999). Using a rat model it was shown that intermittent administration of PTH could both induce an initial transient increase in apoptosis and inhibit the activities of a group of caspases extracted from entire distal metaphyses (Stanislaus et al, 2000). These studies highlight the importance of this mechanism in growing and developing animals, but further research is required to elucidate the relationship of PTH and osteoblast apoptosis.

PTH affects bone resorption via indirect actions through the osteoblast. Osteoclast recruitment, differentiation and activation occur via direct interaction between RANKL on the osteoblast and its receptor RANK on the pre-osteoclast. This interaction can be inhibited by the decoy receptor OPG and thus, the RANKL: OPG ratio will determine the degree of osteoclast differentiation and activation (Yasuda et al., 1998). Recent studies demonstrated that the various modes of PTH administration regulate the RANKL: OPG ratio differently, resulting in different effects on bone resorption. Continuous PTH infusion in rats, sustained a decrease in mRNA for OPG and a prolonged increase in mRNA for RANKL (Ma et al., 2001) that was observed over twenty four hours, showing that continuous administration favors continued differentiation, recruitment and activation of osteoclasts. Further evidence is provided from studies with cultured marrow cells; continuous PTH administration produced increased numbers of osteoclasts and caused a 25-fold increase in the RANKL: OPG ratio. On the other hand when PTH was

administered intermittently increased osteoblast differentiation markers were demonstrated, with little effect on the RANKL: OPG ratio (Locklin et al., 2003). PTH can exert either anabolic or catabolic effects on bone and for these reasons it has become an intense area of research with the scope of elucidating the mechanism that underlie those actions and lead to the design of new pharmaceutical compounds.

1.16 Parathyroid hormone related protein

Parathyroid hormone related protein (PTHrP) is a family of proteins produced by most tissues in the body. A segment of PTHrP is closely related to PTH but its peptides have a broader spectrum of effects. PTH and some of the PTHrP peptides bind to the same receptor, but PTHrP peptides also bind to several other receptors (Strewler, 2000). PTHrP is widely expressed in a number of fetal tissues and has a number of functions such as in the control of endochondral bone formation, the development of the mammary epithelium and the eruption of teeth (Kronenberg HM, 2003, Wysolmerski et al., 1998 and Philbrick et al., 1998)

In cartilage and bone development most of the information in the role of PTHrP comes from the use of knockout mice. In cartilage the first such experiment was reported in 1994, in which the PTHrP null mouse was a neonatal lethal (Karaplis et al., 1994). The formation of the cartilaginous growth plate is an essential step for normal linear growth. The critical control point in this process is the chondrocyte differentiation, to become terminally differentiated chondrocytes. PTHrP normally regulates the rate of this program and its deletion results in a rapid progression of this program with the classic chondrodysplasia phenotype that is lethal at birth (Harrington et al., 2007)

The abnormalities observed in the endochondral skeleton are a consequence of the absence of PTHrP regulation of chondrocyte development (Karaplis et al., 1994, Kronenberg, 2003). It was later reported that heterozygous PTHrP-null mice are normal at birth but acquire trabecular osteopenia in their long bones from the age of three months (Amizuka et al., 1996), with subsequent reduced bone formation and mineral apposition, as well as formation and survival of osteoblasts. PTHrP is also expressed in the

periosteum and in the insertion sites of tendons and ligaments into cortical bone, the function of PTHrP at those sites is unknown but it is hypothesized that PTHrP may be induced at those sites by mechanical forces, and serve to regulate localized bone formation and/or bone formation (Chen et al., 2006).

1.17 Growth Hormone: background

Growth hormone (GH) stimulates growth and cell reproduction in humans and other animals. It is a 191 amino acids single chain polypeptide hormone and it's a major participant in growth and metabolism (Figure 1.6). It is synthesized, stored and secreted by the somatotroph cells of the anterior pituitary gland (Zofkova, 2003). It has a variety of functions in the body, with the most important being the postnatal longitudinal bone growth and the increase of height throughout childhood. There are a number of diseases, such as growth hormone deficiency in children and adults that can be treated through the therapeutic use of rhGH. Acromegalies due to excess secretion of GH show an increase in bone remodelling as measured by biochemical parameters of osteoblastic activity such as alklaline phosphatase (ALP) and osteocalsin production (Ohlsson et al., 1998). The levels of GH secretion decline with age, by approximately 14% per decade from young adult life, and the changes in body composition associated with ageing such as reduction in bone mass are similar to those adults with GH deficiency (Shalet et al., 1998, Velduis and Bowers, 2003).

GH affects several tissues including the liver, muscle, kidney and bone and its effects are generally anabolic. GH directly stimulates division and multiplication of chondrocytes as well as stimulating production of insulin-like growth factor 1 (IGF-1), via its actions on the liver which is the GH's main target organ and the principal site of IGF-1 production (Giustina et al., 2008). IGF-1 has growth stimulating effects on a number of target tissues, making it both an endocrine and autocrine/paracrine hormone, it also exerts its effects on osteoblasts and chondrocytes which will be discussed later to promote bone growth (Zofkova 2003).

In addition to bone growth, GH has other effects on the body; these would include, increase in calcium retention, increased muscle mass (Corpas et al. 1993) promotion of lypolysis (Davidson 1987), reduction of glucose uptake by the liver as well as promotion of gluconeogenesis in the liver and it contributes to the maintenance and function of pancreatic islets and stimulates the immune system (Chen et al. 1998). Recent studies have shown that through direct actions on the brain, GH may modulate emotion, stress response, and behavior (Yoshizato et al. 1998, Abizaid et al., 2008).

The production of GH is modulated by stress, exercise, nutrition, sleep and GH itself (Barb et al., 2008). However the primary controllers are two hypothalamic hormones and a hormone from the stomach. The first hormone is the growth hormone-releasing hormone (GHRH) which is a hypothalamic peptide that stimulates both the synthesis and secretion of growth hormone. The second one is somatostatin (SS) which is a peptide produced by several tissues in the body, including the hypothalamus, the main function of somatostatin is to inhibit growth hormone release in response to GHRH and to other stimulatory factors such as low blood glucose concentration. Lastly ghrelin is a peptide hormone secreted from the stomach, ghrelin binds to receptors on somatotrophs and potently stimulates secretion of growth hormone (Bouillon 1991, Slootweg 1993, Kojima et al., 1999, Barb et al., 2008).

The mechanism of GH action on bone is not yet clear and there are two hypotheses of two possible mechanisms of action: the *somatomedin hypothesis* which states that GH stimulates production of IGF-I, which in turn stimulates longitudinal bone growth (Salmon and Daughaday 1957), and the *dual effector theory*, which states that GH acts on progenitor cells and IGF-I stimulates subsequent clonal expansion (Green et al. 1993).

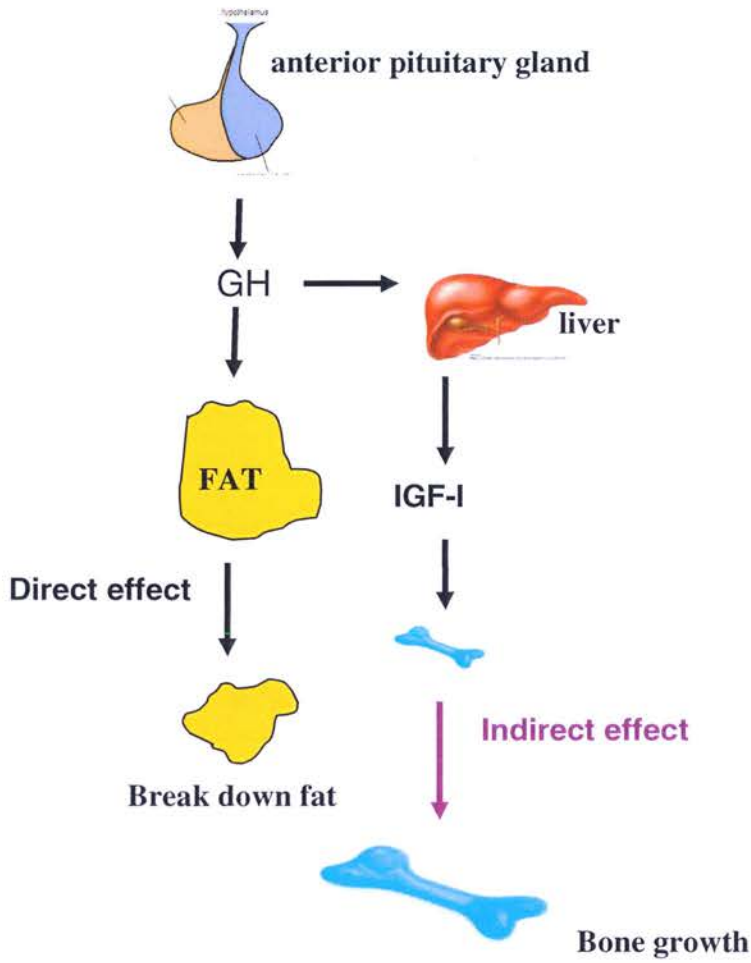

Figure 1.6 Diagram of Growth Hormone Actions. Physiological stimuli such as changes in energy levels and decreased fatty acid concentrations increase GH secretion from the somatotroph cells within the lateral wings of the anterior pituitary gland. The major role of growth hormone in growth is to stimulate the liver to secrete IGF-I, which in turn stimulates proliferation of chondrocytes, resulting in bone growth.

1.18 GH/IFG-I axis and bone

Growth hormone is probably the most important regulator of IGF-I production (Niu and Rosen 2005) and the GH/IGF-I axis is the main regulator for growth. There are other growth systems but appear to play minor role compared to the GH/IGF-I system since it has been documented that only about 17% of the total body size of an adult mouse can be attained without the precipitation of GH and IGF-I (Lupu et al. 2001).

The major target of GH is hepatic insulin growth factor I (IGF-I), the endocrine actions of IGF-I include its role in stimulating chondrocyte proliferation at the growth plate, glucose homeostasis in muscle and fat as well as skeletal and muscle maintenance (Lupu et al. 2001). IGF-I also stimulates tubular reabsorption of phosphate and can directly regulate vitamin D activity in the kidney, with subsequent increase in calcium absorption and transport of phosphate a necessary component of skeletal mineralization (Caverzasio et al. 1990, Lanfranco et al., 2003, Giordano et al., 2008).

Mohan et al. (2003) demonstrated the contribution of the GH/IGF-I axis to the development of peak BMD. The skeletal changes in IGF-I knockout (KO), IGF-II KO, and GH-deficient mice were measured at three different developmental changes; the prepubertal, pubertal and postpubertal in the femur by dual x-ray absorpiometry. They demonstrated skeletal growth failure in different degrees in the absence of growth factors. In summary it was suggested that mice deficient in IGF-I show a greater impairment in bone accretion than IGF-II or GH deficient mice; and the GH/IGF-I axis but not the IGF-II, is critical for puberty induced bone growth.

1.19 Growth hormone Receptors and Bone

The first tissue in which GH binding sites were identified was the liver mainly due to the abundance of receptors located there, however later more tissues that possess growth hormone receptors (GHRs) were identified including the muscle, adipose, mammary gland, bone, kidney, embryonic stem cells and immune tissues (Kelly et al. 1991, Ohlsson et al. 1993, Giustina et al., 2008) and more recently the brain (Yoshizato et al. 1998).

The GHR is a member of the cytokine/hemopoietic growth factor receptor family (Kelly et al. 1993).GH signaling via its receptor has been shown to be mediated through cascades of protein phosphorylation resulting in activation of nuclear proteins and transcription factors. The GHR itself is not a tyrosine kinase, but after binding of GH to its receptor an association with a protein JAK2 occurs, JAK2 is then phosphorylated and in turn it phosphorylates the GHR (Kopchick and Andry 2000).

Barnard et al. (1991) were the first to show specific high-affinity GHRs on the osteoblast – like cells UMR 106.06. The presence of these receptors was later confirmed in primary human and mouse osteoblasts (Nilsson et al. 1995, Slootweg et al. 1996). Lobie and colleagues (1992) demonstrated GHRs on rat chondrocytes, osteoblasts and osteoclasts while osteocytes were generally found to be immunonegative, while Abu et al. (1997) reported GHR expression on few osteocytes at remodelling sites. Only recently GHRs were identified in the frontal bone osteocytes at the onset of the flatfish metamorphosis (Hildahl et al. 2008).

Evidence as to the function of the GHR in growth development came from the generation of mice containing a disrupted GHR/GHBP (growth hormone binding protein) gene through homologous recombination (Zhou et al. 1997). Homozygous mice showed postnatal growth retardation, dwarfism, and did not display GHRs or GHBPs, these mice grew to half the size of their non-transgenic littermates, showed lowered IGF-I levels and increased GH concentrations. Heterozygous mice were slightly smaller compared to non-transgenic mice and had reduced levels of GHR, GHBP and IGF-I circulation. Female GHR knockout mice are fertile and they experience delayed puberty, but when IGF-I replacement therapy is administered it results in advancement of puberty back to normal levels, highlighting the importance of GH dependent IGF-I production (Danilovich et al. 1999).

1.20 Growth hormone and bone cells

In bone tissue, growth hormone receptors are active on osteoblast and osteoclasts but not on mature osteocytes (Lobie et al. 1992). GH stimulates osteoblasts and osteoclasts directly or indirectly via IGF-I. The effects of GH on the osteoblasts have been studied in a number of osteoblastic cell lines and primary isolated osteoblasts from various sources, such as human, chicken, rat and mouse as well as the SaOS-2 human and UMR 106.01 rat osteocarcoma cell line. GH has been demonstrated to induce proliferation of primary isolated rat, mouse, chicken, human and rat osteosarcoma cells as well as mesenchymal precursor cells (Ernst and Froesch 1988, Slootweg et al. 1988, Scheven et al. 1991, Nilsson et al. 1995, Kang et al., 2007).

GH has been demonstrated to act directly on the osteoblast *in vitro*, while its actions are partly mediated by IGF-I *in vivo*. This was demonstrated in calvarial osteoblasts where the IGF-I receptor was disrupted *in vitro* and *in vivo*. GH stimulated IGF-I production and inhibited osteoblast apoptosis in osteoblasts lacking the IGF-I receptor *in vitro*. *In vivo* wild type mice for the IGF-I receptor treated with GH showed doubling of osteoblast numbers, while they remained the same in mice lacking the IGF-I receptor. These results indicate that although direct IGF- 1R-independent actions of GH on osteoblast apoptosis can be demonstrated *in vitro*, IGF-1R is required for anabolic effects of GH in osteoblasts *in vivo* (DiGirolamo et al., 2007). This was also demonstrated via stimulation of phenotypic functions of osteoblasts such as alkaline phosphatase, osteocalcin, and type I collagen (Morel et al. 1993, Chenu et al. 1990).

IGF-I is thought to play a role for the GH actions on the osteoblasts. Stimulation of osteoblastic IGF-I production by GH has been demonstrated by some studies (Morel et al. 1993, Chenu et al. 1990) but not by others (Kanzaki et al. 1995). To identify the importance of IGF-I in mediating the actions of GH, endogenous IGF-I was sequestered by an antiserum to IGF in osteoblast-like cells; as a result the proliferative action of GH was abolished (Ernst and Froesch 1988) demonstrating that local IGF-I is important for GH induced cell proliferation.

GH has been shown to increase the number of osteoclasts in the metaphysis if the proximal tibia of hypophysectomized rats (Lewinson et al. 1993), but the mechanism of this action is unclear. GHRs have been identified in in mouse marrow cultures (Ranjo et al. 1996) and in mouse hemopoietic blast cells (Nishiyama et al. 1996). In the study by Nishiyama et al. (1996) it was found that GH stimulates osteoclastic bone resorption through both direct and indirect actions on osteoclast differentiation and indirect activation of mature osteoclasts.

Factors that may mediate the indirect GH-regulated osteoclast formation include IGF-I and IL-6, both of which are involved in osteoclast formation and have been shown to be regulated by GH (Nishiyama et al. 1996, Slootweg et al. 1992, Saggese et al. 1995, Swolin et al. 1996, Mochizuki et al. 1992, Giustina et al., 2008).

It has been shown that IGF-I stimulates activation and formation in cultures of mouse bone cells (Mochizuki et al. 1992) and that the osteoblasts mediate IGF-I stimulated formation of osteoclasts in mouse marrow cultures as well as activation of rat osteoclasts (Hill et al. 1995). The physiology of GH-induced effects on osteoclast is still unclear and further studies are necessary to try and elucidate the exact mechanisms of GH actions on the osteoclast.

1.21 Growth hormone and osteocytes

GH receptors have been identified in osteoblasts and osteoclasts but not on mature osteocytes (Lobie et al., 1992). Only recently GHRs were reported in the frontal bone osteocytes at the onset of the flatfish metamorphosis (Hildahl et al. 2008). To date the effects of GH *in vitro* have been studied in bone tissue cultures which offer the advantage of preserved intercellular interactions. Stracke et al. (1984) reported that GH increased ALP activity in the culture medium from embryonal rat tibias in tissue culture. Similar observations were later confirmed by Maor et al. (1999). Rat cartilage pieces were cultured on top of collagen sponges in the absence or presence of GH. Three day incubation with GH caused an increase in DNA synthesis and size of the specimen. The effect of GH was more pronounced after six days in culture, at which time a network of

trabeculae was noted throughout the extracellular matrix. The trabeculae contained osteocyte-like cells and positive staining for osteocalcin and osteopontin provided further support that the newly formed trabeculae was comprised on bone matrix components. Utretated cultures lacked bone-like strucures, demonstating that GH directly induced bone formation *in vitro*.

Similarly in vivo GH treatment influences bone mass, bone metabolism and mechanical strength of bones. When GH was administered in hypophysectomized (HX) rats an increase in bone formation was observed. Furthermore in bone from HX rats a decrease in mRNA levels of IGF-I was found, and the levels were restored after GH replacement (Bikle et al. 1995). This observation strongly suggests that GH has a direct effect on bone cells. In normal rats GH administration has been found to increase cortical bone (Andreassen et al. 1995). Corresponding to the increased bone mass there is also an increase in mechanical strength of the whole bone. Due to the absence of evidence supporting the presence of GHRs in mammalian osteocytes it can only be speculated that GH exerts indirect effects on them. Future studies are necessary to improve our understanding of the physiology of GH-induced effect on osteocytes.

1.22 Effects of growth hormone on bone tissue

Postnatal longitudinal bone growth results by the direct effect of GH on bone tissue, as a result of cell proliferation of chondrocytes in the epiphyseal growth plate. This was demonstrated after the rate of proliferation decreased following hypophysectomy with subsequent narrowing of the growth plate. When GH was administered the rate of cell proliferation and the width of growth plate were restored (Isakson et al. 1985, Nilsson et al., 2005).

The effect of GH directly on cartilage *in vivo* was tested by injecting GH locally into the epiphyseal growth plate of the proximal tibia in hypophysectomized rats. Stimulation of longitudinal bone growth was demonstrated as well as an increase in the width of the cartilage in the growth plate suggestive of stimulation of chondrogenesis (Isakosn et al.

1992). In another study in rats injection of GH locally at the growth plate stimulated longitudinal bone growth (Isakson et al. 1985).

GH has also been reported to influence bone metabolism by modulating PTH secretion and its circadian levels (Lancer et al., 1976, Giustina et al., 2008). This effect is partially mediated by changes in serum phosphate levels (Ahmad et al., 2003). Serum PTH peaks at around 17.00 hours coinciding with the serum phosphate peak (Estepa et al., 1999), GH favors phosphate retention via an increase in the renal threshold for phosphate. In addition both GH and IGF-I activate the renal 1α-hydroxylase and inhibit 24-hydroxylase, with an increase in the production of active 1, 25 dihydroxyvitamin D3 (Wei et al., 1997). These mechanisms may contribute to bone mineralization.

Another factor suggested to mediate the effects of GH on longitudinal bone growth is IGF-I, mainly in its regulation of bone remodeling. IGF-I is hypothesized to have a mitogenic predisposition on osteoblasts and have been suspected to have potential as a formation-stimulating drug. In a clinical study it was shown that IGF-I increases biochemical markers for both bone formation and bone resorption (Johansson et al. 1992). In another study of men with idiopathic osteoporosis, GH and IGF-I were administered and their effects on bone metabolism were compared after 7 days; it was shown that IGF-I increased biochemical markers for bone formation but not bone resorption while GH increased markers for both bone formation and resorption, indicating different mechanisms of actions at the cellular level of the two peptides (Johansson et a. 1996).

In rats IGF-I treatment results in periosteal bone formation and both increased and decreased bone formation has been reported in the cancellous bone (Bagi et al. 1994, Ibbotson et al. 1992). On the other hand in primates GH but not IGF-I has been shown to increase bone formation (Sass et al. 1997), while in growth hormone deficiency (GHD) patients GH treatment increases bone mass but is not clear whether IGF-I has the same capacity (Ohlsson et al. 1998, Baroncelli et al., 2003).

1.23 Current Osteoporosis Treatments

HRT is prescribed after menopause to help with the unwanted symptoms of hot flushes; night sweats; irregular heart beat; mood swings and chronic diseases such as osteoporosis and to maintain the quality of life of an individual.

A number of treatments are currently available for osteoporosis, which are mainly focused in preventing bone resorption (Allen et al., 2004). Examples of antiresorptive medications include estrogens and Selective Estrogen Receptor Modulators (SERMS) e.g. raloxifene that suppress bone remodelling thus maintaining the function of osteoblasts and osteocytes; the bisphosphonates, which inhibit osteoclast activity by inducing osteoclast apoptosis; and finally calcitonin that inhibits osteoclast activity without affecting the osteoblast collagen production (Stepan et al., 2003). All the above treatments have been found to reduce fracture risk mainly through their effects on the osteoclasts (the bone resorbing cells). On the other hand anabolic treatments which have started receiving a lot of interest recently affect the osteoblasts (the bone forming cells). Anabolic agents include rhPTH 1-34, rhGH, strontium and statins that directly stimulate bone formation.

rhPTH (1-34) is the only anabolic agent approved for use for the treatment of osteoporosis, produced by Lilly referred to as teriparatide. PTH treatment increases bone turnover, stimulating the osteoblasts to a greater extent than osteoclasts (McCloung et al. 2005). The formation of new bone with PTH improves bone microarchitecture, including improved trabecular connectivity and enhanced cortical thickness (Misof et al. 2003). It has also been shown to possibly affect bone size and geometry, with beneficial effects on bone strength (Parfitt 2002, Burr, 2005). For individuals with severe osteoporosis PTH might produce more benefits to help in reducing their high risk of fracture, but there is still no data to support this concept.

GH is another anabolic agent that when administered in postmenopausal osteoporotic women and men with idiopathic osteoporosis it was shown to increase the markers for bone resorption and formation within the first week of administration (Andreassen and Oxlund 2000). Because of the financial cost for GH treatment there have not been performed many clinical trials, so it has been suggested that GH-releasing factors may be used for the stimulation of the GH/IGF-I axis. Compared to PTH which is an injectable treatment the advantage of GH-releasing factors is that they can be administered orally (Ohlsson et al. 1998).

Moreover in rat studies receiving GH on withdrawal the labeling persists six weeks later indicating that new bone is preserved upon cessation of treatment contrary to PTH treatment where bone is quickly resorbed after withdrawal from treatment, and treatment with antiresorptives should follow to maintain the new bone formed (Ejersted et al. 1998).

1.24 Summary

High osteocyte density has been associated with regions characterised by resorption and formation activity (Power et al. 2002) while absence of osteocytes is associated with low occurrence or absence of remodelling surfaces (Marotti et al. 1998) and accumulation of microdamage in conditions such as ageing (Mori et al. 1997) and osteonecrosis (Kenzora et al. 1978). In addition, high incidence of osteocyte apoptosis has been associated with a range of conditions including glucocorticoid treatment (Gu et al. 2005), estrogen withdrawal (Tomkinson et al. 1997, Weinstein et al. 2000) elevated PTH (Bringhurst 2000), androgen action (Wiren et al. 2006) and both underloaded and overloaded bone (Noble et al. 2003). My key hypothesis is that rhPTH and rhGH are essential growth factors in 1) promoting osteocytic cell population survival in ageing and in response to mechanical stimulation and 2) directing osteoblast bone forming activity in helping to build new bone. To test these hypotheses I:

1. Examined the ability of rhPTH and rhGH to promote cell survival of MLO-Y4 osteocyte like cells *in vitro* to a wound injury model.
2. Examined the ability of rhPTH and rhGH to promote osteocyte survival in skeletally mature female rats *in vivo*.
3. Examined the ability of rhPTH in the presence of absence of mechanical stimulation to promote osteocyte survival in human bone explants as it has been previously shown that these two parameters can have a synergistic effect on osteocyte viability and bone formation. And
4. Examined the ability of rhPTH and rhGH in directing the bone forming activity of osteoblast cells using LCM and gene microarray at different anatomical sites of bone (periosteal vs. endosteal) in skeletally mature female rats *in vivo*.

CHAPTER 2

The Protective Effects of Recombinant Human Parathyroid and Recombinant Human Growth Hormones on Osteocyte Plasma Membrane Repair *in vitro*

Abstract

Microdamage in bone contributes to fractures and is hypothesized to act as a stimulus for bone remodeling. Through their apoptotic death, osteocytes are thought to provide signals that activate osteoclastic bone resorption at the damage site. The cause of osteocyte death near the microdamage site is unknown but it may be related to either mechanically sensitive signaling pathways, direct physical damage of the osteocyte itself or the canalicular system that supplies necessary nutrients and oxygen. In light of a number of studies suggesting that the rapid repair of plasma membrane disruption is possible and essential to cell survival in other cell types, here the ability of osteocytes to survive damage was tested. The rapidity of the repair was estimated using propidium iodide (PI) and sytox green staining. Also the relationship of osteocyte membrane repair with rhPTH and rhGH, known to be de-regulated with ageing was investigated.

A cell-wounding model using the osteocyte-like cell line MLO-Y4 was developed. PI uptake was used to estimate cell wounding and repair over time. For follow-up experiments PI and Sytox green staining were used to estimate the repair of individual cells injured over time. MLO-Y4s were incubated in the presence or absence of either rhPTH or rhGH for one hour after which time they where injured using a sharp blade. As the repair process is know to be calcium dependent in other cell types, the requirement for calcium in MLO-Y4 cells in this process in the presence or absence of rhPTH and rhGH was also investigated.

It was found that large numbers of osteocytes were capable of re-sealing their plasma membrane within the first minute following mechanical injury in the presence or absence of rhPTH and rhGH. Interestingly the repair process was accelerated following incubation with either rhPTH or rhGH, in the presence or absence of calcium in the growth media, but the mechanisms of this process are unknown. These findings may provide a new understanding of how osteocytes sense and respond to injury and the potential of therapeutic compounds to maintain osteocyte viability in disease and old age.

2.1 Introduction

In the skeleton the number of viable osteocytes decreases with age (Frost 1960, Dunstan et al. 1993), and it is likely that this age-related decrease is occurring in the proportion of bone that is not being actively remodeled (Chan and Duque 2002). In the elderly there is more damage accumulating and less healthy bone with the sites of lower osteocyte lacuna density containing more damage (Noble 2003). Microdamage occurs in bone as a result of normal functional and repetitive loading due to every day use with subsequent accumulation of small cracks in the bone matrix (Reilly and Currey, 2000, Qui et al. 2005, Nagaraja et al. 2007) that is increased during strenuous exercise (Brukner 1966). Osteocytes are extremely sensitive to alterations in the local physical environment (Skerry et al., 1989) and are thought to be involved in microdamage detection and remodeling (Parfitt 1993, Bentolila et al. 1998).

Bone is capable of removing the accumulating microdamage through the actions of the osteoclasts and the osteoblasts, during bone remodeling (Burr and Martin, 1993; Mori and Burr, 1993; Parfitt, 2001), which is impaired in the ageing skeleton for reasons that still remain unknown (Compston 2007). Osteocytes are vital in bone remodeling and produce signal molecules to regulate this process. Mechanotransduction is the process by which cells in a living tissue – such as osteocytes –perceive physical stimuli and respond with biochemical signals (Dodd et al., 1999). Osteocytes respond to altered load through changes in gene and protein expression (Dodd et al., 1999). Mechanical stimuli within the physiological range maintain osteocyte viability (Noble et al. 1997, Plotkin et al., 2005).

On the other hand, excessive strains result in microdamage and osteocyte apoptosis (Verborgt et al., 2000, Noble et al., 2000, 2003). The mechanism by which microdamage induces cell death is debated. Previously studies have suggested that apoptosis may occur as a result of direct physical damage to the cell membrane (Colopy et al. 2004, O'Brien et al. 2005), activation of mechanically sensitive signaling pathways or damage to the light chain shifting (LCS) and disruption of nutrient and oxygen provision (Frost 1960, Knothe-Tate 1998, Dodd 1999). However these factors cannot be considered in isolation. It is hypothesized that osteocyte death is associated with the production of signals

involved in the activation of the remodeling process. However, controversy arises over whether signaling molecules are generated following osteocyte apoptosis. It has recently been demonstrated that induction of bone damage is associated with an increase in osteocyte death by apoptosis. This was demonstrated by Noble and colleagues (1997, 2003) using the rat model of fatigue fracture, where osteocyte apoptosis was associated with cortical bone resorption induced by mechanical loading, pointing to the hypothesis that osteocytes provide signals that activate osteoclastic bone resorption at the damage site through their apoptotic death (Noble et al., 2000). Ruptured osteocyte processes may also secrete compounds, which diffuse throughout the matrix and stimulate osteoclasts (Hazenberg 2007). In support of this theory Kurata and colleagues (2006) demonstrated the release of molecules such as RANKL, which induces osteoclastogenesis following osteocyte damage.

As mentioned earlier it has been suggested that apoptosis may occur as a result of direct physical damage to the cell membrane (Colopy et al. 2004, O'Brien et al. 2005). However recent reports demonstrated the ability of cells to repair membrane disruptions following physical injury within seconds (McNeil and Steinhardt 1997, McNeil and Terasaki 2001) due to the inherent 'self-sealing' capacity of biological membranes (McNeil 2002). Such a response is vital for cell survival, and has been found to be calcium dependent. The 'Patch Hypothesis'- first proposed by Terasaki and colleagues (1997) describes de-novo barrier formation and membrane fusion, triggered by the entrance of extracellular calcium following cell injury. A number of vesicles accumulate and fuse with one another to form a patch vesicle which fuses with the phospholipid bilayer, providing a reparative protein barrier (McNeil and Steinhardt, 2003). In bone rapid resealing of membrane disruptions would be vital in maintaining osteocyte viability and bone quality as well as removal of damage and remodeling.

In light of studies suggesting that the rapid repair of plasma membrane disruption is possible and essential to cell survival in other cell types (McNeil and Kirchhausen 2005), the ability of MLO-Y4 osteocyte-like cells to survive physical damage was tested and the rapidity of the repair estimated for the first time in osteocytes. The ability of rhPTH and

rhGH to influence the repair process of the damaged cell membrane was also tested. Both PTH and GH affect bone growth and maintenance either directly or indirectly. PTH has been shown to increase bone mass by adding bone on both endosteal and periosteal envelopes as well as affecting the bone remodeling process, similarly GH influences bone growth and skeletal maintenance either directly or indirectly via stimulation of IGF-I production (Reijnders et al. 2007, Sundeep et al. 2008).

Loss of osteocytes in bone is associated with an impairment of the damage repair system, with older people having more damage. PTH and GH decline with ageing thus possibly influencing the repair system. Moreover they have been found to modify calcium channels; PTH has been demonstrated to activate the calcium channels in rat and chicken osteocytes (Miyauchi et al. 2000, Selim et al. 2005). GH on the other hand has been shown to increase intracellular calcium concentrations about twofold within two minutes of addition in adipocyte cultures (Shikha et al., 1998). Taking into account that in other cells types such as skin cells and the sea urchin, the repair process has been shown to be calcium dependent (McNeil and Kirchhausen 2005), a possibility that these hormones may be able to influence the repair process in a calcium dependent manner arises.

In this study membrane-disruption to MLO-Y4s *in vitro* was taken to represent direct physical injury to osteocytes *in vivo*. The purpose of this study was to investigate the hypothesis that direct physical damage to osteocytes causes' cell death (Colopy 2004, O'Brien 2005) and the effect of rhPTH and rhGH with the process of cell membrane resealing following physical injury. Staining techniques were used to demonstrate the ability of MLO-Y4 cells to survive and rapidly repair following physical membrane disruption. These findings provide us with an insight of how osteocytes respond to injury as well as the potential of therapeutic compounds to maintain osteocyte viability in disease and old age.

2.2 Materials and methods

All chemicals were purchased from Sigma, UK, unless otherwise stated. All tissue culture reagents were purchased form Invitrogen, UK and all tissue culture plastics from Corning, UK. All tissue culture procedures were performed in a laminar flow hood (class 2) receiving HEPA-filtered air, using sterile equipment.

2.2.1 Cell culture and maintenance

The murine long-bone derived osteocyte-like MLO-Y4 cell line was cultured in Modified Eagles Medium Alpha (α-MEM) supplemented with 5% foetal bovine serum (FBS), 5% newborn calf serum (NCS), 1% penicillin/streptomycin (P/S) and 1% L-glutamine (Kato et al., 1997). Cells were grown in continuous monolayer culture in sterile 75 cm^2 tissue culture flasks. Flasks were coated with 0.1M collagen type I from rat tail prior to use. Growth media were stored at 4°C and warmed to 37 °C prior to use. Cells were maintained in an incubator at 37 °C in a 95% humidified atmosphere of O2:CO2 in the ratio of 95%:5%. Subculturing was performed twice weekly upon reaching 90% confluency. The cell monolayer was detached with addition of 1ml of trypsin solution at 2.5mg/l for 5 minutes, followed by addition of 10ml of growth medium. 1ml of the cell suspension was added to anew flask containing 9mls of fresh growth medium and placed in the incubator.

2.2.2 Cell treatment

The MLO-Y4 osteocytes were plated at a density of 3.5 x 104 cells per ml in 24 well plates, 24 hours prior to experimentation. Following appropriate treatment cells were returned to the incubator at 37°C for the appropriate time following individual treatment. Experiments were carried out a minimum of three times, and each treatment was represented by 4 wells in each experiment. Cells were observed in 6 fields per well resulting in 24 fields per treatment group using a x20 magnification lens for all estimates allowing similar numbers of cells to be counted per field in all experiments using an inverted microscope fitted with DXM 1200 camera (Nikon UK Limited). All compounds used for cell treatments were diluted in complete α-MEM media.

2.2.3 Hormone treatments

The MLO-Y4 cells were pre-treated for one hour with rhPTH and rhGH (both provided by NOVARTIS) diluted in α– MEM medium supplemented with 5% FBS, 5% NCS, 1% P/S and 1% L-glutamine at the concentrations of 50nM/ml and 100ng/ml respectively followed by cell injury. Cells were also pre-treated for one hour prior to injury with TGF-b3 at concentrations of 1ng/ml, 10ng/ml and 50ng/ml and Vitamin C at concentrations of 1μM/ml, 50μM/ml and 100μM/ml for one hour prior to injury.

2.2.4 Serum deprivation

The MLO-Y4 cells were grown to confluency in complete α– MEM media prior to incubation for 16 hours in low serum α– MEM media, which contained 0.1% FBS, 1% P/S and 1% L-glutamine. Experiments were then performed according to individual experimental protocols.

2.2.5 Calcium deprivation

Hanks balanced salt solution

Inorganic balanced salt solutions in tissue culture have long been used and their functions can be divided into four principal ones: 1. serve as irrigating, transporting and diluting fluids while maintaining intra- and extracellular osmotic balance, 2. provide cells with water and certain bulk inorganic ions, 3. provide principal source of energy combined with a carbohydrate for cell metabolism and 4. provide a buffering system to maintain the medium within the physiologic pH range (Hanks, 1976). For the purposes of the experiments presented here Hanks solution which contains all necessary salts except calcium chloride was used to deprive cells of extracellular calcium. Hanks salt solution was supplemented with 5% FBS, 5% NCS, 1% P/S and 1% L-glutamine.

The MLO-Y4 cells were incubated in Hanks media for half an hour prior to initiation of cell treatments with rhPTH and rhGH. Following experimental treatments cell injury was induced and cell repair over time was estimated.

For follow up experiments calcium chloride diluted in Hanks at a final concentration of 1.6mM (which is the final concentration of calcium chloride in α– MEM media was sterile filtered and added in cultures pre-treated with Hanks pre- and post- injury.

2.2.6 Cell injury

A cell-wounding model was developed for the injury of the MLO-Y4 osteocytes. Cells were injured using a sterile sharp blade and a cut was induced in the middle of the well to disrupt plasma cell membrane of cells below the blade (figure 2.1) in order to follow up repair over time at different time points from 0 seconds - 15seconds (T(0)), 5minutes, 30 minutes and 24 hours. Following those time points, repair was also followed up at shorter time points from 0 seconds – 16 seconds (T (0)), to 1 minute, 2 minutes, 3 minutes, 4 minutes and 5minutes.Cells at a distance of 0.2mm either side of the cut were counted for the analysis.

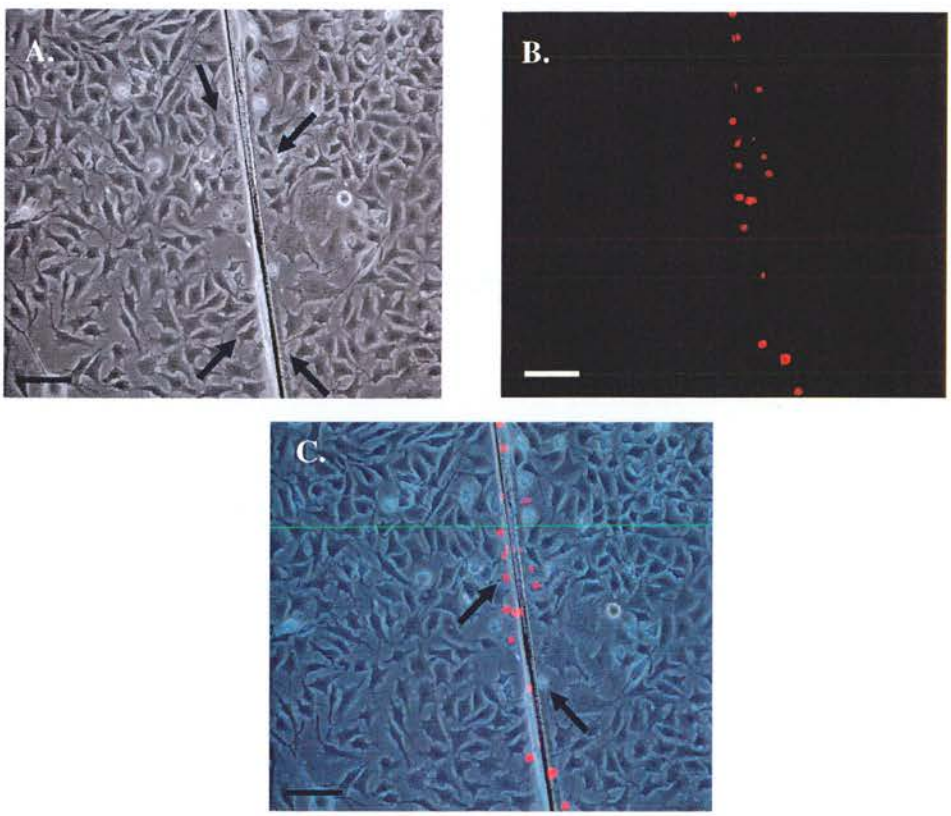

Figure 2.1 Induction of injury in MLO-Y4 cells in culture. Representative image of injured MLO-Y4 cells in culture (A, B). Cells were injured by cutting through the middle of the well using a sharp blade. Cells were stained with PI to identify those with a compromised plasma membrane (B). Cut was found to induce cell injury (C).Arrows indicate injured cells on the cut. Bar represents100 μm.

2.2.7 Determination of Cell repair over time

2.2.7.1 Propidium Iodide stain

For the identification of cells with a compromised cell membrane i.e. cells that have not repaired over time following the experimental procedure propidium iodide (PI) stain was used. PI is a compound that stains nuclear DNA, giving a red fluorescent image when subjected to UV light illumination at 535nm. PI is most often used to differentiate between necrotic and apoptotic cells while being excluded from healthy cells, with an intact cell membrane (Lecoeur 2002). PI is rapidly taken up by cells and binds to DNA by intercalating between the bases with little or no sequence preference and with a stoichiometry of one dye per 4-5 base pairs of DNA (Moore et al. 1998). Once the dye is bound to nucleic acid, its fluorescence is enhanced 20- to 30- fold fluoresces as bright red. For the T (0) 100 µl of PI were added in the culture media prior to injury at a final concentration of 2.5ng/ml diluted in α– MEM media. In separate wells for the follow up time points PI was added after injury was induced, to identify cells with a compromised cell membrane over time (figure 2.2). Following experimental treatments, cells were fixed in 4% paraformaldehyde for 10 minutes, washed three times in PBS and air-dried. Cells were then stained with DAPI for total cell counts as described below and examined using fluorescent microscopy.

2.2.7.2 DAPI stain

For total cell number counts on the cut 4',6- Diamino-2- phenylindole (DAPI) compound that stains nuclear DNA, and fluoresces as bright blue when subjected to UV light illumination at 358nm was used. DAPI is a stain that is rapidly taken up by cells and forms enhanced fluorescent complexes with double-stranded DNA due to either forming a highly energetic interaction or stable hydrogen bonds with the minor groove of the double helix (Cowden et al., 1981). Following experimental treatments, and staining with PI as described above cells were incubated with DAPI at a concentration of 2.5ng/ml for 5-10 minutes, washed in PBS and examined by fluorescence microscopy and digital image capture. Four wells represented each time-point in each 24-well plate and eight fields per well were taken, which resulted in 192 fields counted per plate. Each experiment was repeated at least three times.

Percentage of non-repaired cells (%) =

$$\frac{\text{Number of PI positive cells}}{\text{Number of DAPI stained cells}} \times 100$$

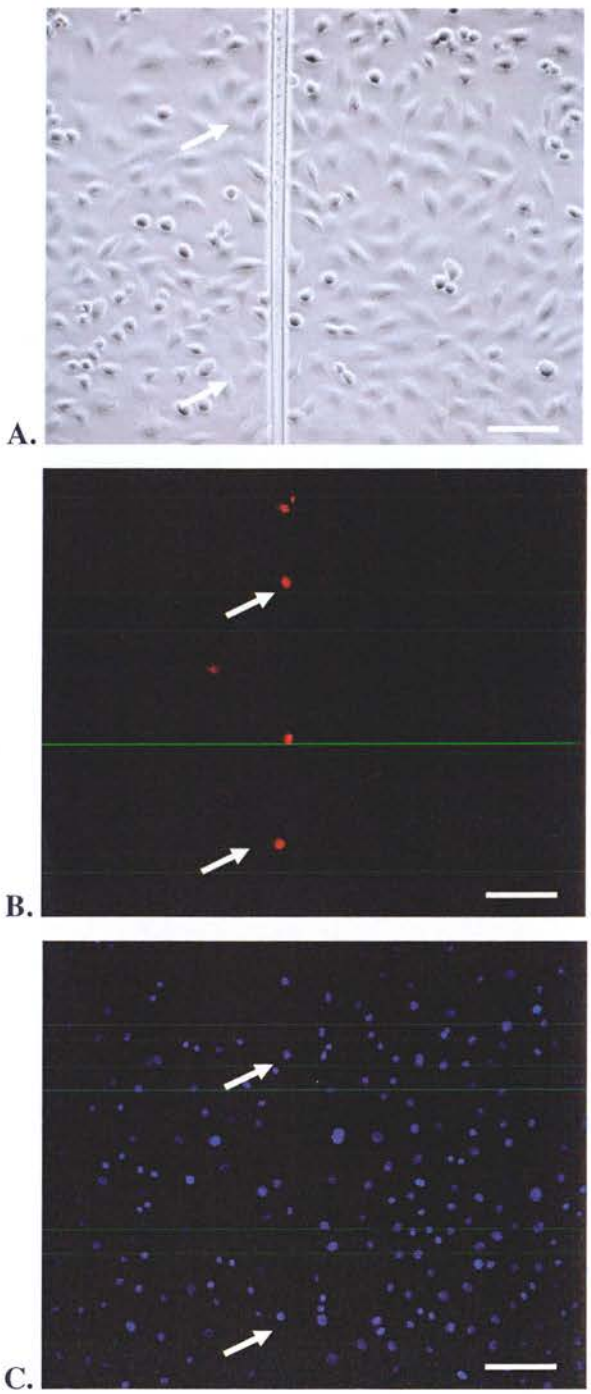

Figure 2.2 MLO-Y4 cells in culture post injury. PI was added in media following injury in MLO-Y4 cells in culture (**A**) to identify the cells with a compromised plasma membrane (**B**). Cells were then fixed and DAPI stained (**C**) for total cell counts on the cut. Arrows indicate cells injured on the cut. Bar represents100 μm.

2.2.7.3 SYTOX green stain

To follow the course of repair of individual cells, two membrane permeant dyes were used, one to identify the cells damaged at start (PI) and a second one to determine whether repair of the cells damaged at start occurred (Sytox green) (Figure 2.3). Sytox green is a nucleic acid stain that rapidly penetrates cells with compromised plasma membranes while being excluded from live cells. It stains nuclear DNA and fluoresces as bright green when subjected to UV light illumination at 490nm. Sytox green is most often used in dead-live assays to identify necrotic cells (Roth et al. 1997). Following experimental treatments 100µl of PI was added to the bathing media prior to injury for each of the different time points to identify the number of cells injured at the start. Following incubation with PI for 15 seconds cells were washed with a – MEM media to remove excess PI. For the T (0) time point cells upon removal of PI were immediately stained for 10 seconds with 100µl Sytox green at a final concentration of 1µM/ml diluted in α-MEM media and then fixed in 4% paraformaldehyde . For the later time points cells were washed and then placed back in the incubator in a- MEM media. At the end of each experimental time point media were removed and cells were incubated for 10 seconds in Sytox green prior to being fixed in 4% paraformaldehyde and were then examined using fluorescence microscopy. Cells that were PI positive and Sytox negative were cells that were injured and then repaired their membrane thus excluding Sytox green stain. PI negative and Sytox green positive were considered as uninjured cells that later became permeant to the dye, possibly undergoing unrelated death into the dish.

$$\textbf{Percentage repaired cells } (\%) = \left(\frac{\text{PI + Sytox –ve}}{\text{(PI +ve) + (PI +ve / Sytox +ve)}} \right) \text{x } 100$$

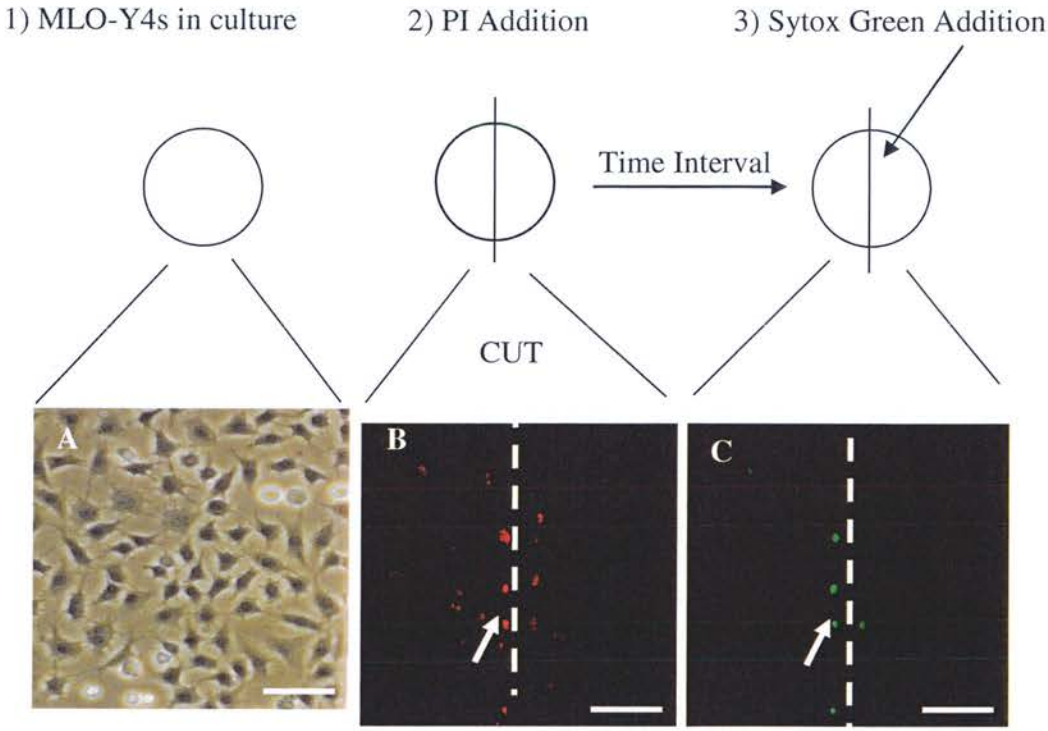

Figure 2.3 Double staining experiments. A. MLO-Y4s in culture. **B.** Addition of PI prior to induction of injury, followed by removal of the media and cells were washed, and fresh media replaced for the set time intervals prior to staining with Sytox green **C.** Addition of Sytox green and incubation for about 10 seconds prior to removal and fixing with PFA. Arrows indicate cells injured on the cut and did not repair. Bar represents100 μm.

2.2.7.4 In situ analysis of osteocyte DNA fragmentation using Nick Translation technique

To identify cells undergoing apoptosis a DNA nick translation technique, (Noble et al. 1995; 1997) was used. Only the larger number of single DNA breaks, associated with apoptosis rather than necrosis, were detected. The technique allows the identification of early DNA breaks prior to loss of the DNA content and prior to plasma membrane permeabilisation (Petit et al., 1995).The cells were fixed in 4% paraformaldehyde (Sigma, UK) for 10 minutes and then washed in phosphate buffer saline (PBS) (Oxoid, UK) for 5 minutes three times. For the positive control a well was treated with deoxyribonuclease I (DNase) at a concentration of 0.2 mg/ml in PBS (Sigma, UK) for 30 minutes to induce DNA breaks (figure 2.4). All wells apart from the negative control (figure 2.5) that was treated with the following reaction mixture in the absence of DNA polymerase I, were treated with a reaction mixture that consisted of 3 mmol/L digoxigenin (DIG)-labelled dUTP (DIG-11-dUTP); 3 mmol/L each of dGTP, dATP, and dCTP; 50 mmol/L Tris HCl, pH 7.5; 5 mmol/L $MgCl_2$, 0.1 mmol/L dithiothreitol, 0.5 mL/100 ml DNA polymerase I for 45 minutes at 37 ^{0}C in a humified chamber. At the end of the incubation period all wells were washed in PBS and incubated with fluorescein isothiocyanate (FITC)-labelled anti-DIG antibody (all reagents obtained from Roche Diagnostics Corporation, UK) and 5% normal sheep serum (Sigma) in PBS, for 1 hour in a humidified chamber at room temperature (RT). After washing in PBS all wells were stained for nuclear DNA with DAPI (Sigma, UK) at 2mg/ml for 10 minutes, washed thoroughly in PBS and mounted with fluorescent mounting medium (DAKO, UK). Wells were visualized by fluorescent microscopy using a DXM1200 camera mounted on Eclipse E800 microscope (Nikon) using 20X/0.50 □/0.17WD2.1 magnification lens (x20). Osteocytes stained positive for both the FITC label and DAPI were considered as osteocytes containing fragmented DNA.

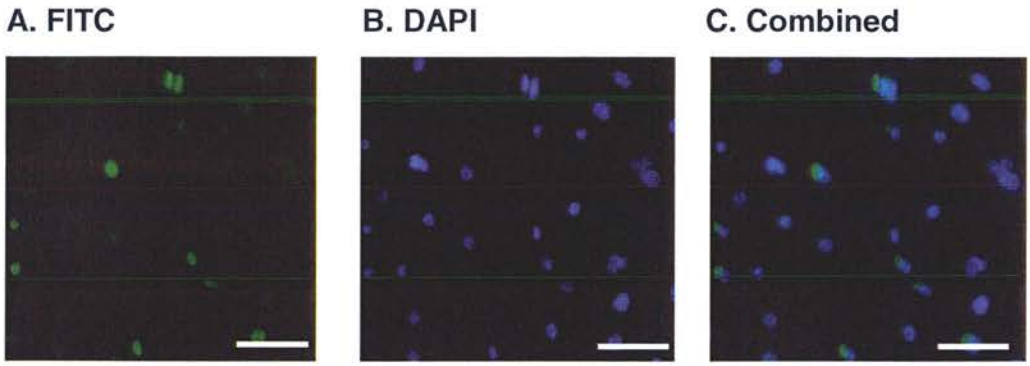

Figure 2.4 In situ demonstration of a positive control for the nick translation method. MLOY-4 cells in tissue culture wells were treated with the nick translation mixture. All nuclei stained green for the FITC signal **(A, C)** since the cells were incubated with deoxyribonuclease I (DNase) in order to produce DNA breaks prior to reaction with the nick translation mixture (x 20). Nuclei were stained blue with DAPI **(B)**. Bar represents 10 μm.

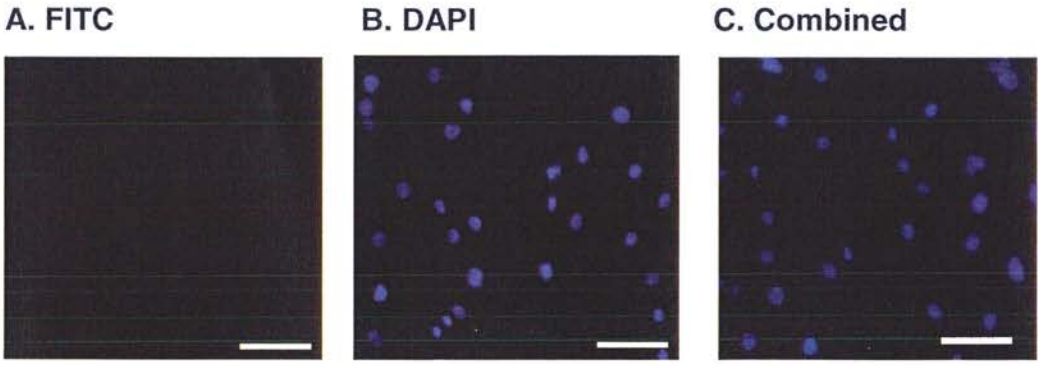

Figure 2.5 In situ demonstration of a negative control for the nick translation method. MLOY-4 cells were treated with the nick translation mixture in the absence of polymerase I. Nuclei were stained blue with DAPI **(B).** No FITC signal was observed indicating the inability of oligonucleotides to be incorporated into the DNA breaks in the absence of DNA polymerase I and be recognized by the anti-DIG-FITC labelled antibody **(A, C)** (x 20). Bar represents 10μm.

2.2.8 Statistical Analysis

For all data analyses the statistical software package SPSS 14.1 for Windows was used. All data was checked for normal distribution by applying the Kolmogorov-Smirnov test. In cases where the randomly selected sample data were shown to have a normal (Gaussian) distribution (95% of data would fall within plus or minus 1.96 standard deviations from the mean value) parametric statistical tests such as one-way Analysis of Variance (ANOVA) and the post-hoc Tukey-Kramer and Bonferroni test were performed to determine statistical significance between the treatment groups. The Tukey-Kramer post hoc test was employed in all statistical analyses to determine significance between the treatment groups as it allows for comparison of more than two means without introducing the type I error associated with multiple t-tests (Zar 1984, Fielding and Gilbert 2000). Results are expressed as means ± SEM. $p<0.05$ was considered to be statistically significant, representative of n=3 experiments.

2.3 Results

2.3.1. MLO-Y4 cells repair their cell plasma membrane in a time dependent-manner.

MLO-Y4 osteocytes were injured using a sharp blade as described in the methods section §2.2.6 and PI was added prior to injury for the 0 seconds - 30 seconds time point and then in other culture wells post injury at 5 minutes, 30 minutes and 24 hours. It was found that large numbers of osteocytes were capable of re-sealing their plasma membrane following injury in a time dependent-manner (figure 2.4). The number of cells counted per field was at the range of 25-35 cells. Between 0 seconds – 30 seconds 19 % ± 1.79 of the cells had been damaged as demonstrated by PI uptake; however repair was increased over time so that only 11 % ± 0.93 ($p<0.05$) were damaged at 5 minutes, 6 % ± 0.35 ($p<0.001$) at 30 minutes and only 3% ± 0.32 cells still damaged after 24 hours. Whereas the pre-cut control cultures were found to be at 2 % ± 0.18, indicating that the damage was caused due to physical injury.

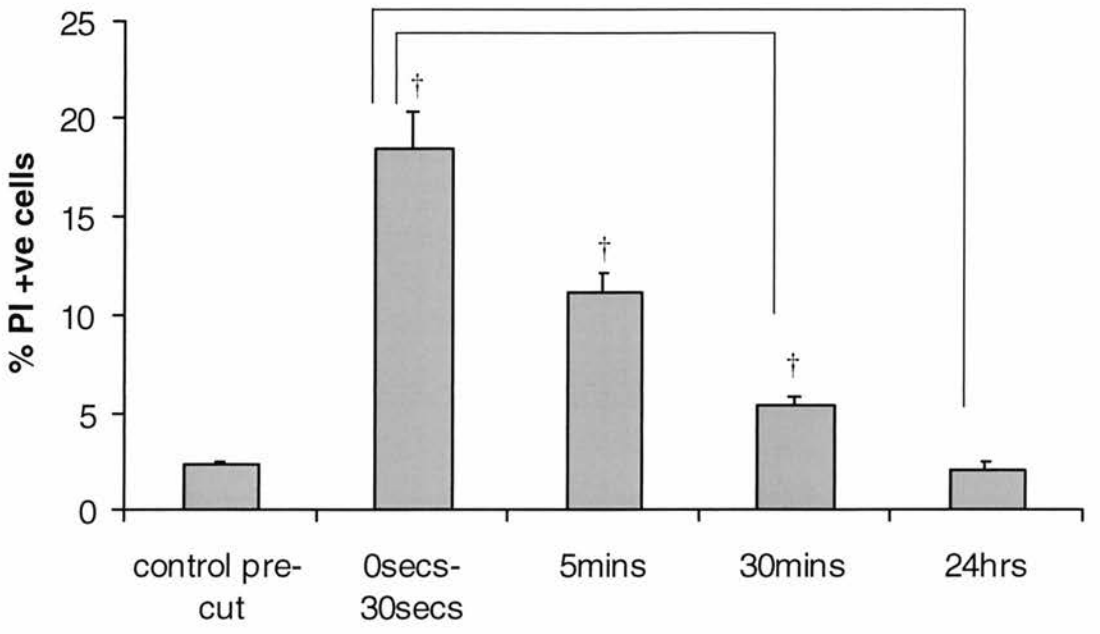

Figure 2.4 MLO-Y4 osteocyte like cells repair their plasma cell membrane in a time dependent manner. Osteocytes were plated and allowed to set overnight prior induction of injury in control media. Cell injury was induced at time 0 and PI was added for the 0-30 seconds' time point prior to induction of injury and then at the time points of 5minutes, 30 minutes and 24 hours, to identify cells that remained leaky to PI (cells that did not repair over time). By 24 hours the PI positive cells reach similar levels as that of the pre-cut cultures. Graphs represent mean percentages of PI positive cells ± SEM † represents $p<0.05$ compared the previous time point.

2.3.2. Incubation of MLO-Y4 cells prior to injury with rhPTH or rhGH enhances the repair process.

Following the observations that MLO-Y4 cells repair their cell membrane over time, the prospect of rhGH and rhPTH influencing the cell repair process was examined. MLO-Y4 osteocytes were pre-treated for an hour with the known anti-apoptotic doses of 50nM/ml rhPTH or 100ng/ml rhGH. Following incubation with these hormones, physical injury was induced and PI was added at 0seconds-30seconds time point and then post injury at 5 minutes, 30 minutes and 24 hours. At the end of each experimental time point cells were fixed and stained with DAPI for total cell counts on the cut (Figure 2.5). It was found that rhPTH significantly increased the cell repair at the earliest time point compared to control cultures (10% ±0.15 vs. 19% ± 0.17 respectively, $p<0.05$) with the repair increasing over time so that at 5 minutes (6% ± 0.26 vs. 7 % ± 0.28, $p>0.05$) cells were still damaged in the rhPTH-treated cultures compared to the control cultures. Both the control and rhPTH-treated cultures reached similar levels of repair by 24 hours (1% ±0.11 vs. 3 % ±0.11) respectively (figure 2A). Similarly rhGH significantly increased the cell repair process over time compared to the control (12% ± 0.17 vs. 19% ± 0.17, $p<0.05$) at 0seconds-30seconds, and (6 % ± 0.14 vs. 7 % ± 0.28, $p>0.05$) still damaged at 5 minutes in the rhGH treated cultures compared to the control. By 24 hours both rhGH and control cultures reached similar levels of repair (2% ± 0.08 vs. 1% ±0.11, $p>0.05$) respecyively still being damaged (Figure 2B).

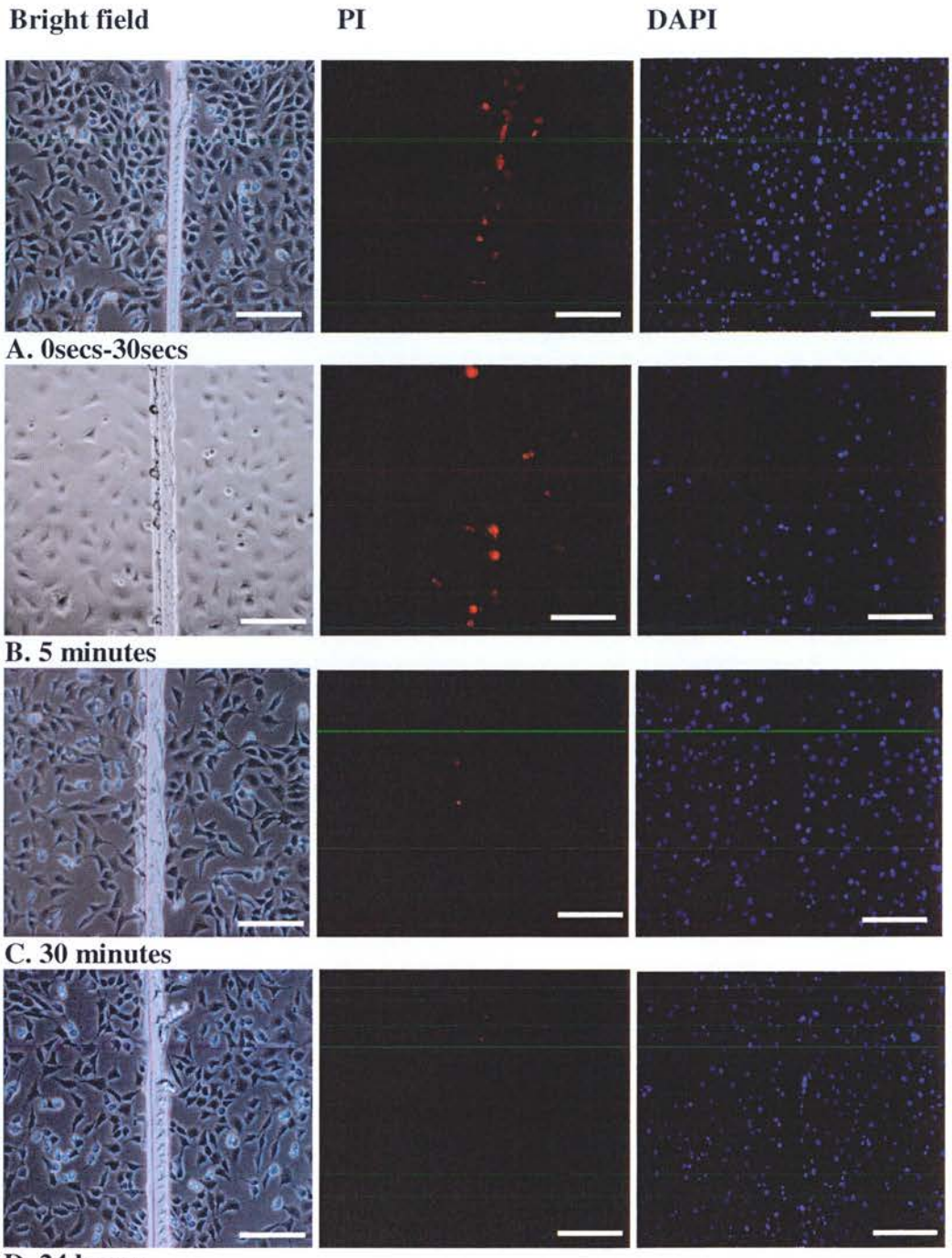

Figure 2.6 Representatives of Bright field, PI and DAPI staining experiments from 0secs – 30 secs to 24 hours. Cells were stained with PI post induction of injury to identify cells with a compromised plasma membrane and with DAPI following fixation of cells for total cell counts on the cut, in different cultures for each time point. **A.** 0 secs-30 secs time point, **B.** 5 minutes time point, **C.** 30 minutes time point and **D.** 24 hours time point. Bar represents 100 μm.

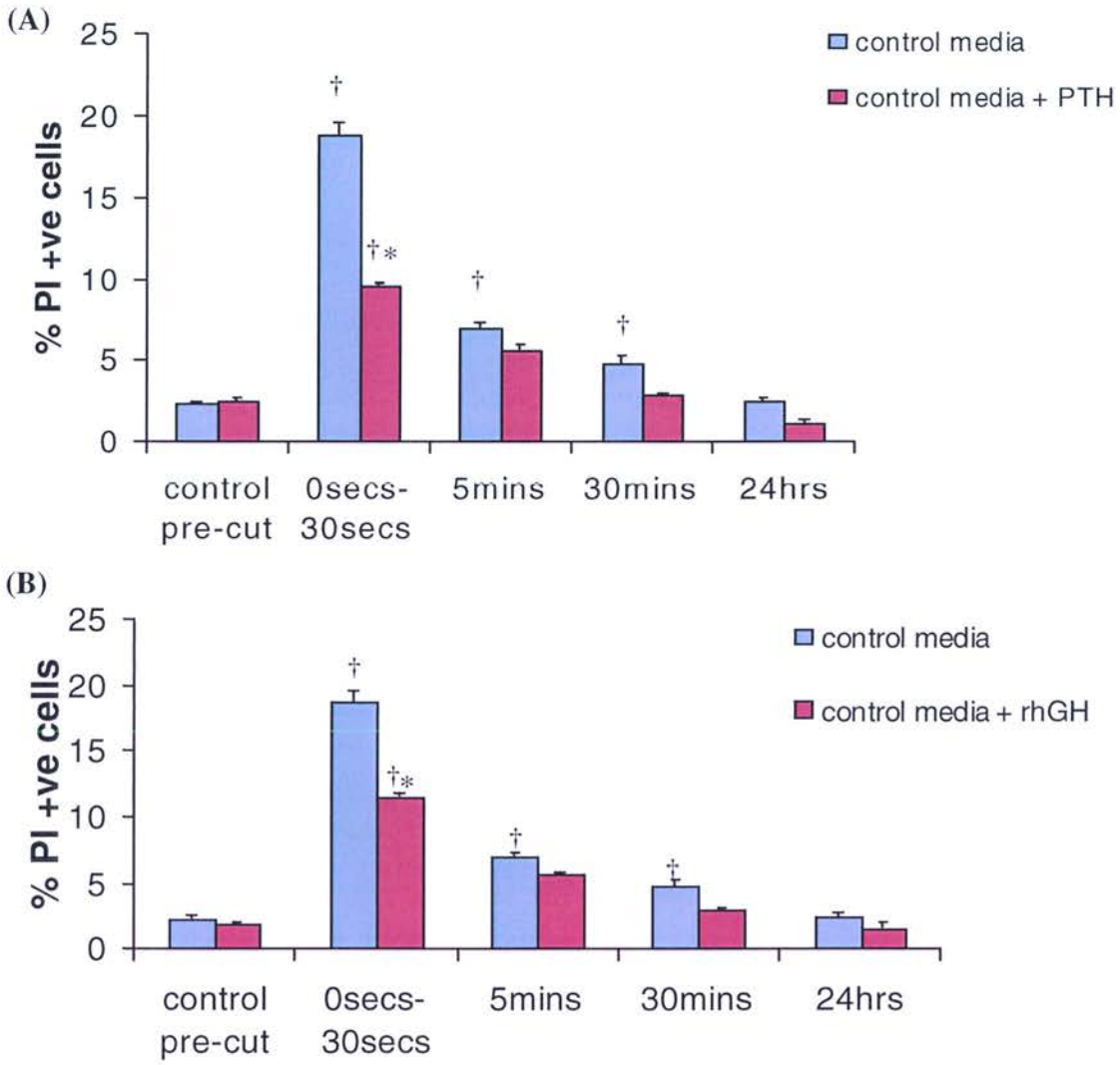

Figure 2.6 MLO-Y4 osteocytes like cells repair their plasma cell membrane faster in the presence of rhPTH or rhGH. Cells were pre-incubated for 1 hour with either 50nM rhPTH or 100ng/ml rhGH followed by cell injury. Cells repaired their cell membrane faster in the presence of rhPTH (**A**) or rhGH (**B**). Graphs represent mean percentages of PI positive cells ± S.E, * = $p<0.05$ denote significant differences of control cultures compared to rhPTH or rhGH treated cultures at the same time point. † represents $p<0.05$ compared to the same treatment at the previous time point.

2.3.3. Pre-incubation of MLO-Y4 cells with TGF- β3 and Vitamin C do not induce the same response as that of rhPTH and rhGH.

MLO-Y4 cells were pre-incubated with TGF- β3 (Figure 2.7A) in a range of doses (1, 10 and 50ng/ml) and with L-ascorbic acid (vitamin C) (10, 50 and 100 μM) (Figure 2.7B). Repair of cells over time was similar at all time points in both treated and untreated cultures, except the 5 minutes time point for the 100 μM of vitamin C compared to control at that time point (12% vs. 20%, $p<0.05$). No significant differences were found between the pre-treated cultures with TGF- β3 and vitamin C in terms of cell repair over time when compared to the control cultures.

2.3.4. Cell membrane repair upon induction of mechanical injury in the presence or absence of rhPTH and rhGH occurs within the first minute.

The resealing of cell membranes has been reported to occur within a few seconds (McNeil et al. 2005). From the data presented in this study it was observed that the repair was taking place within the first 5 minutes with significant differences noted at the T(0) in pre-treated cultures with rhPTH and rhGH compared to the control (figure 2.8 A, B). To define more specifically the time period at which repair occurred PI was added every minute over a 5 minute time period, followed by fixation of cells and DAPI staining for total cell counts. Repair was significantly accelerated at 0secs-30secs in the cultures pre-treated with rhGH and rhPTH compared to the control cultures (14% ± 0.86, 12% ± 0.69 vs. 23% ± 2.01, $p<0.05$, respectively). At 1 minute cell plasma membrane was significantly accelerated in the presence of rhGH and rhPTH compared to control cultures (9% ± 0.26, 8% ± 0.28 vs. 15% ± 1.00, $p<0.05$, $p<0.001$, respectively). Similarly at 2 minutes repair was also accelerated in the presence of rhGH and rhPTH compared to control cultures (7% ± 0.57, 6% ± 0.28 vs. 12% ± 1.13, $p<0.05$, respectively). At 3 minutes statistically significant differences were noted between the rhPTH tretated cultures and the control cultures (5% ± 0.30 vs. 8% ± 1.14, $p<0.05$). For subsequent time-points no statistically significant differences were noted between rhPTH and rhGH treated to control cultures.

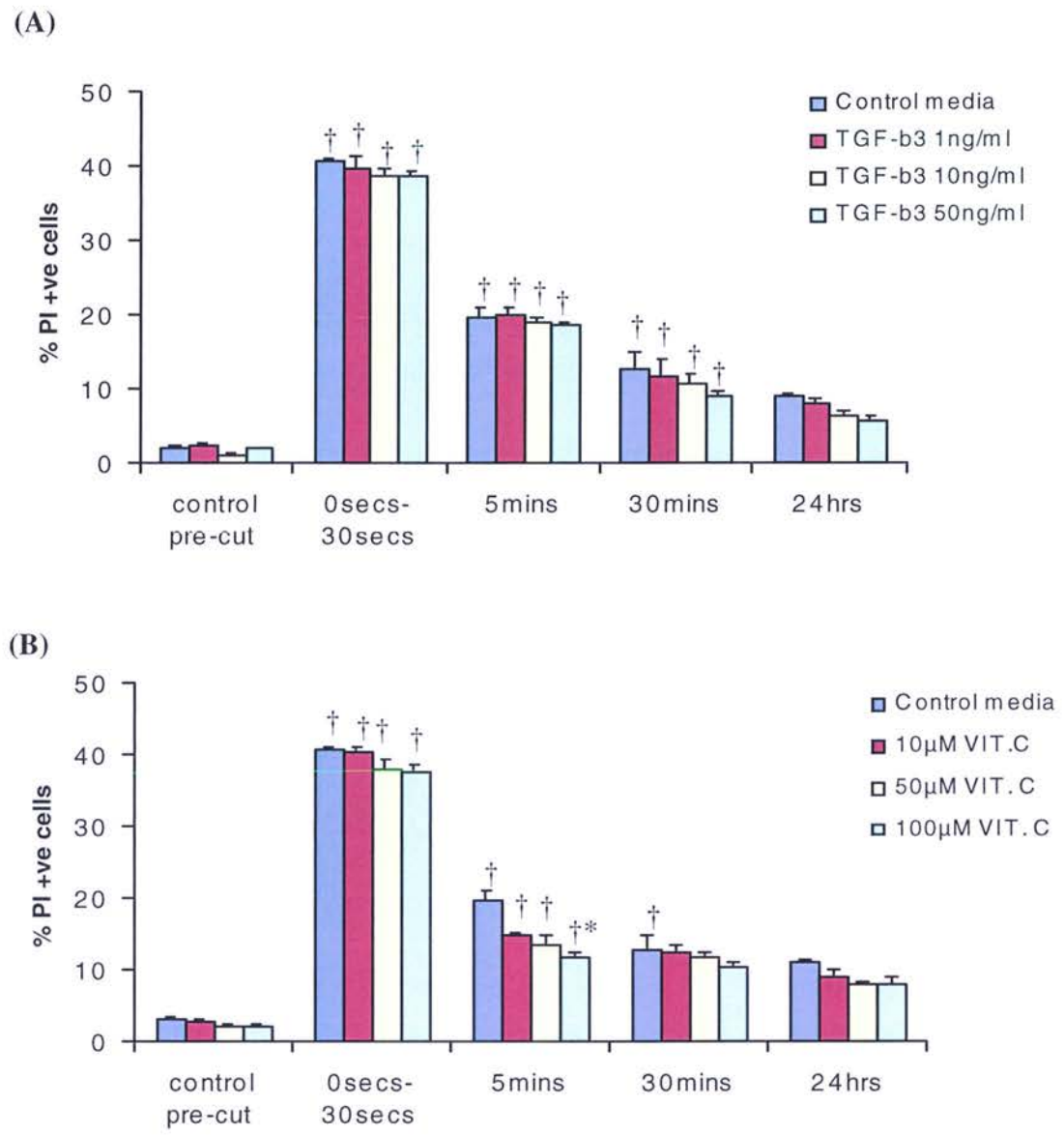

Figure 2.7 TGF-b3 and Vitamin C do not induce the same response as that of rhPTH and rhGH in cell repair. Osteocytes were incubated in the presence of TGF-b3 (**A**) and Vitamin C (**B**) for 1 hour prior to induction of injury. Cell injury was induced as described in methods. Graphs represent mean percentages of PI positive cells ± SEM, * = $p<0.05$ denote significant differences for the 100µM of Vit. C compared to control at the same time point. † represents $p<0.05$ compared to the same treatment at the previous time point. No significant differences were found between treatments and control cultures.

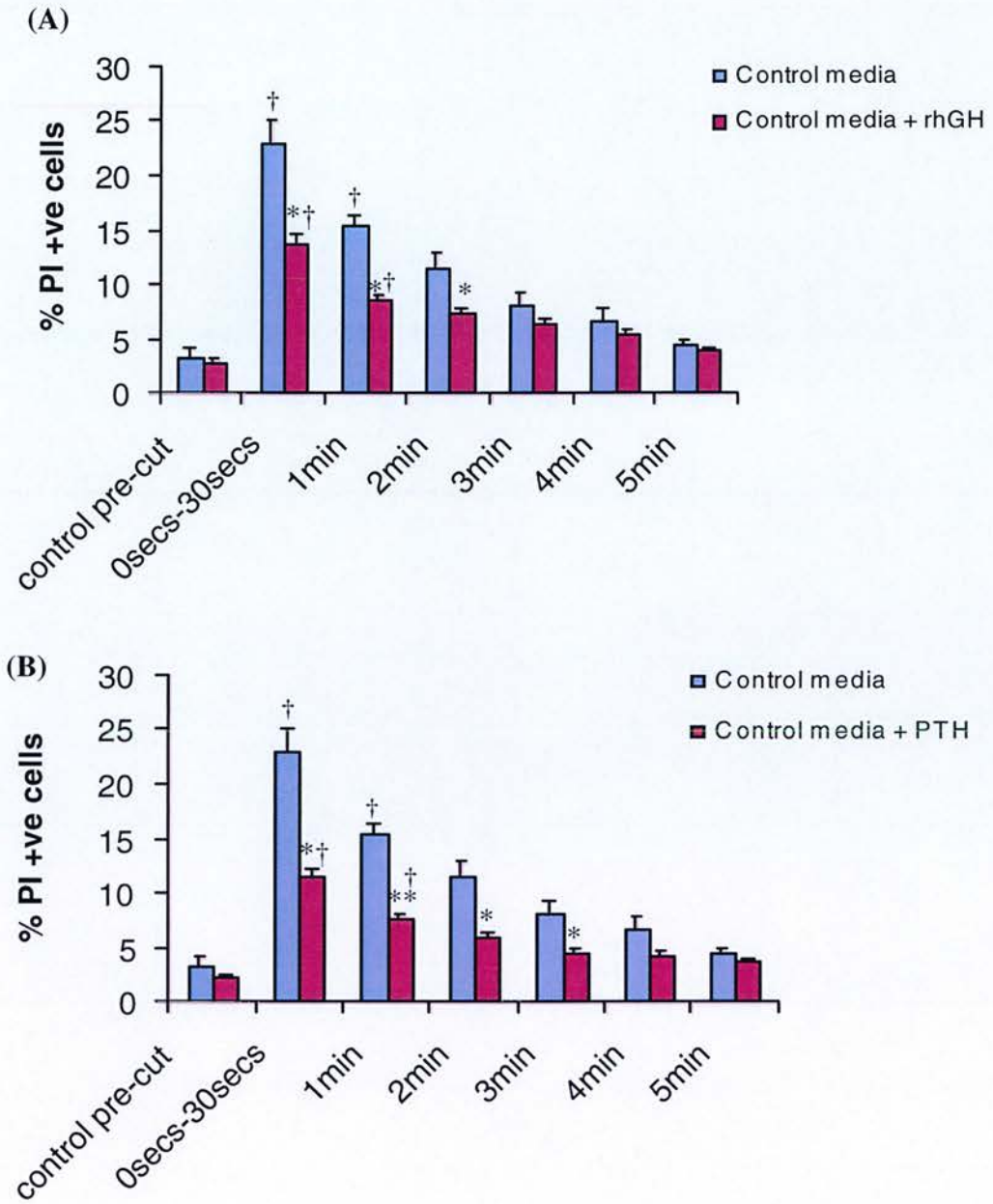

Figure 2.8 MLO-Y4 cells plasma membrane repair occurs within the first five minutes. MLO-Y4 cells were incubated for 1 hour in the presence of rhPTH and rhGH prior to induction of injury. The majority of cells repair their plasma membrane within the first minute of induction of injury with a significant effect of rhGH (**A**) and rhPTH (**B**) compared to control cultures ($p< 0.05$). Graphs represent mean percentages of PI positive cells ± SEM, * = $p<0.05$ and ** = $p< 0.001$ denote significant differences when hormonal treatments compared to control cultures. † represents $p<0.05$ compared to the same treatment at the previous time point.

2.3.5 Cell repair is enhanced in the presence of rhPTH or rhGH as shown by double staining with PI and Sytox green.

In order to identify cells injured at the start of the time course and subsequent repair of these cells, double staining experiments using PI and Sytox green were carried out. PI was added in the bathing media prior to induction of injury to identify cells damaged at start. Cells were stained with Sytox green at the end of each time point to identify cells that did nor repair over time (Figure 2.9) from 0secs – 30 secs up to 24 hours (figure 2.10D) and 0 secs – 30 secs to 5 minutes (figure 2.11D) time periods. These experiments provided evidence of a constant cell number injured at each time point in the presence or absence of rhPTH or rhGH (figure 2.10A-C, figure 2.11A-C), with no significant differences noted between the numbers of cells injured initially at each time point. Similarly to previous experiments at 0secs-30secs cell membrane repair was statistically significant enhanced in the presence of rhGH or rhPTH compared to control cultures (31% ± 1.71, 34% ± 0.86 vs. 24 % ± 1.69, $p<0.05$, respectively). At 5 minutes in the presence of rhGH or rhPTH cell repair was statistically enhanced compared to control cultures (70% ± 0.52, 68% ± 0.59 vs. 58% ± 0.74, $p<0.05$, respectively). For the time points at 30 minutes and 24 hours no statistically significant changes were noted between control and treated cultures. Most of the cell membrane repair was noted to occur within the first minute post injury and pre-incubation with either rhPTH or rhGH significantly accelerated the repair process compared to control cultures as shown in figure 2.11D. At the 0secs-30secs time point post injury statistically significant differences were noted between the cultures pre-treated with rhGH or rhPTH to control cultures (29% ± 1.71, 32% ± 0.86 vs. 16% ± 1.69, $p<0.05$, respectively). At 1 minute statistically significant differences were noted between the rhGH or rhPTH treated to control cultures (52% ± 0.26, 51% ± 0.27 vs. 30% ± 1.15, $p<0.05$, respectively). Repair of cell membrane repair continued to occur for up to 3minutes however no statistically significant differences were noted between treated and control cultures.

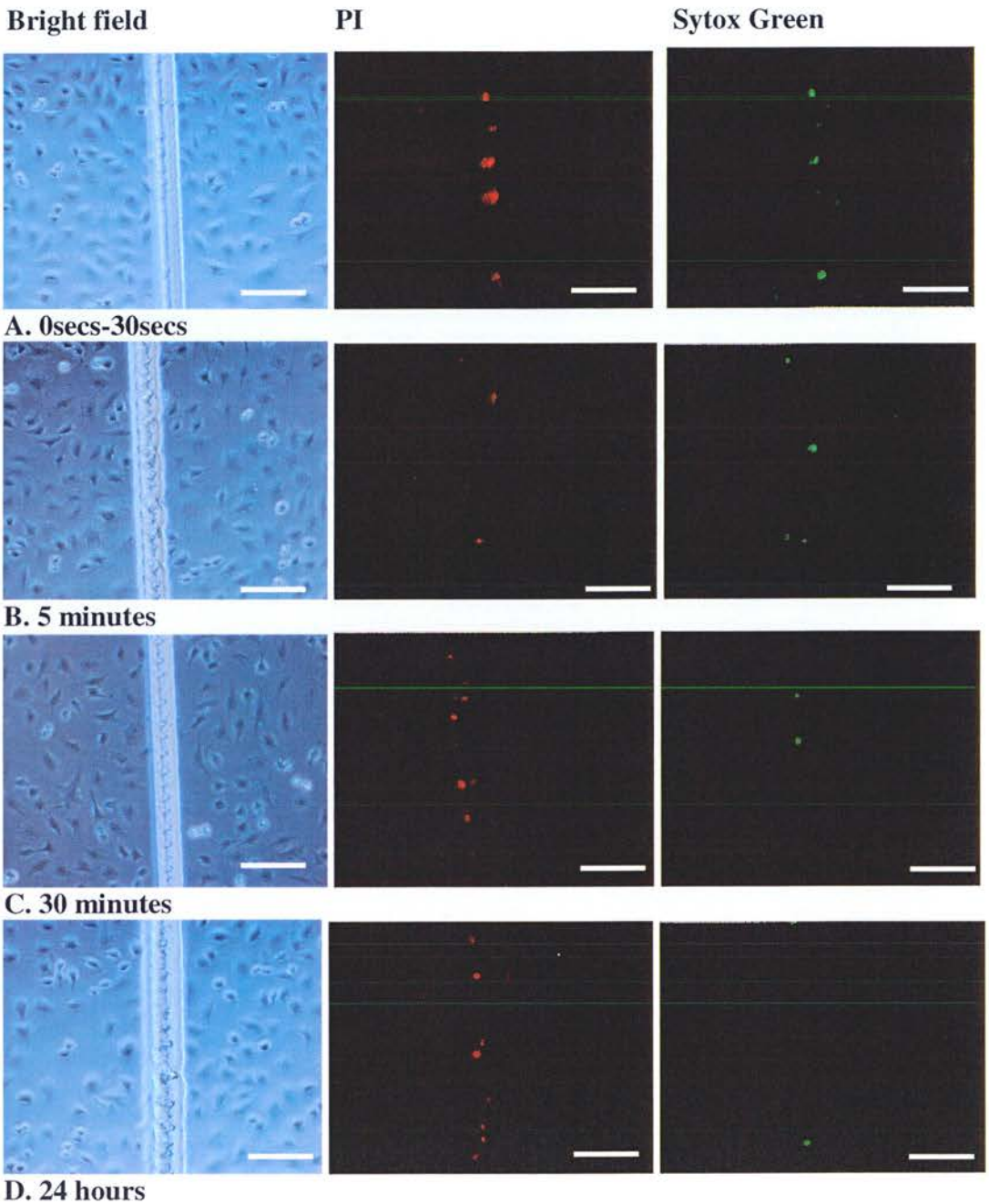

Figure 2.9 Representatives of the double staining experiments with PI and Sytox green from 0secs – 30 secs to 24 hours. Cells were stained with PI prior to induction of injury and at follow up time points with Sytox green prior to fixation. **A.** 0 secs- 30 secs time point, **B.** 5 minutes time point, **C.** 30 minutes time point and **D.** 24 hours time point. Bar represents100 μm.

(A) Control media

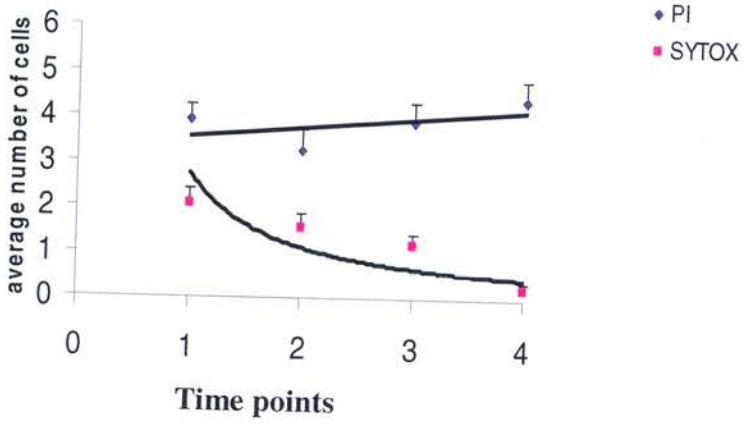

(B) rhGH

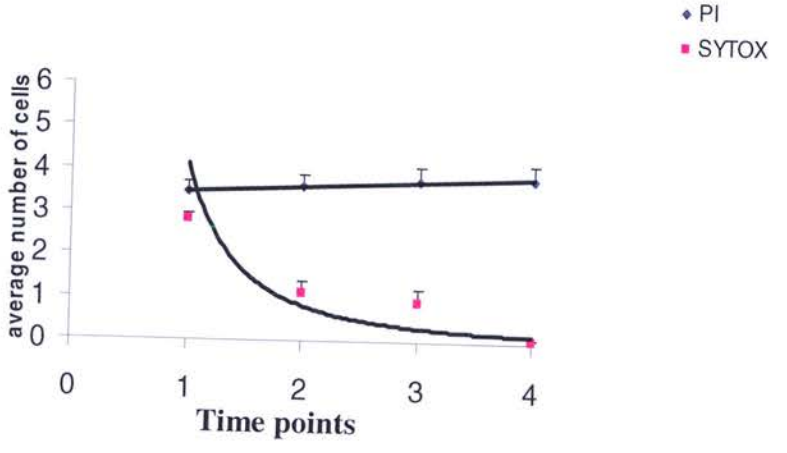

(C) rhPTH

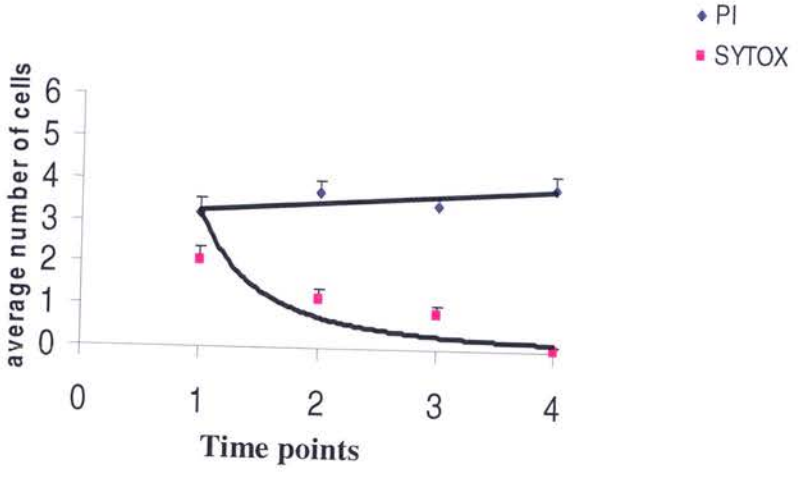

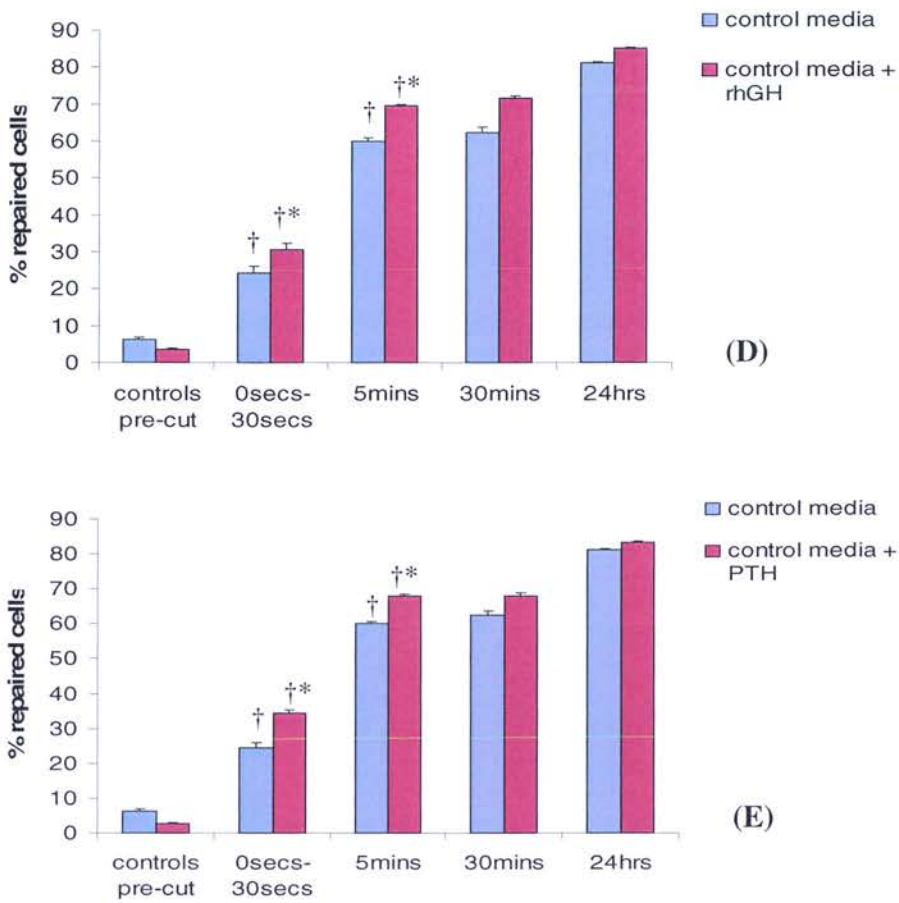

Figure 2.10 Double staining of MLO-Y4 cells in response to rhPTH and rhGH treatment from 0 secs- 30secs to 24 hours. Cells were stained with PI prior to injury to identify the cells injured at each time point. For each time point media was removed and cells stained with Sytox green prior to fixation to identify cells that did not repair their plasma membrane over time. Graphs **A**, **B** and **C** show the average number of cells positively stained with PI and Sytox green in the absence of rhPTH or rhGH (**A**), in the presence of rhGH (**B**) and in the presence of rhPTH (**C**) for PI and Sytox green, these graphs demonstrate a constant number of cells injured at each different time point (PI linear relationship) and a decrease in the number of damaged cells (Sytox positive) over time. Repair is accelerated at earlier time points in the presence of rhGH (**D**) and rhPTH (**E**). Graphs represent mean percentages of repaired cells ± SEM, * = $p<0.05$ denotes significant differences when treatments compared to control cultures at the same time point. † represents $p<0.05$ compared to the same treatment at the previous time point.

(A) Control Media

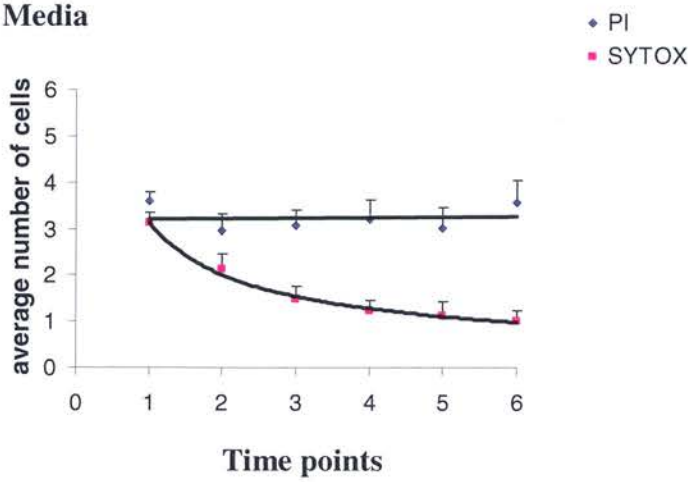

(B) rhGH

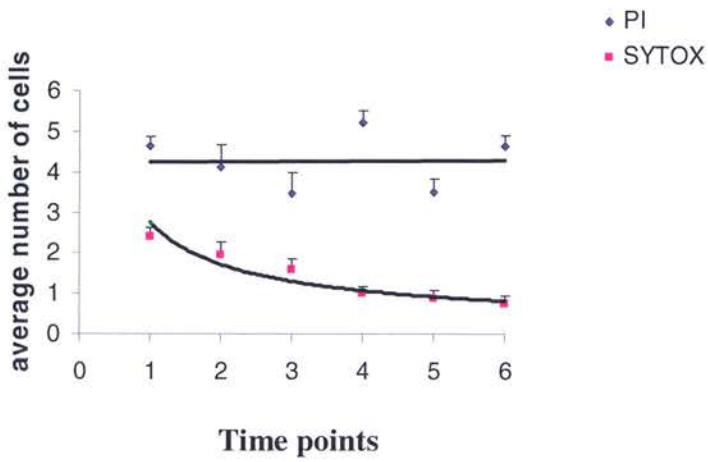

(C) rhPTH

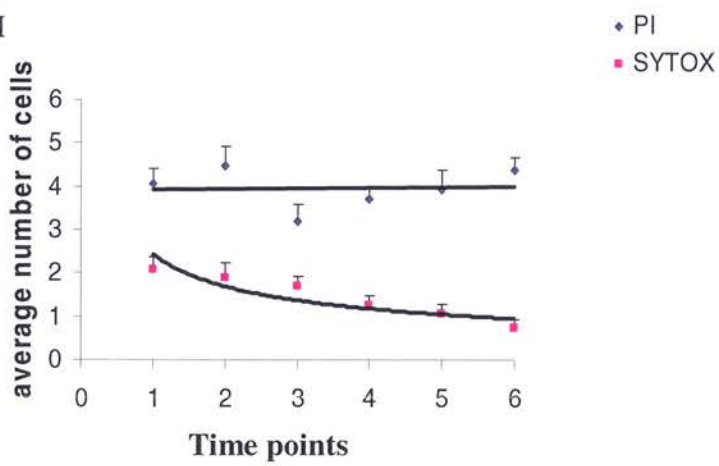

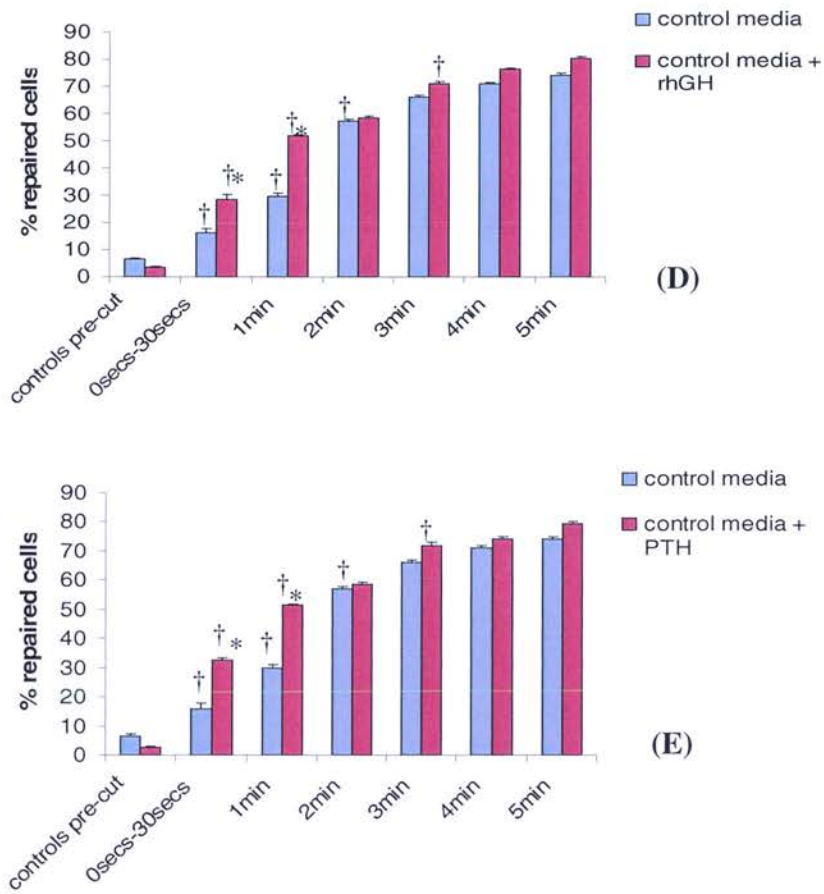

Figure 2.11 Double staining with PI and Sytox green in response to rhPTH and rhGH treatment from 0 secs - 30secs to 5 minutes. Repair of cells following physical injury from 0secs.-30secs to 5 minutes. Most of the repair occurs within the first minute post injury and pre-incubation with rhGH (**D**) or rhPTH (**E**) accelerates the process. Graphs **A**, **B** and **C** show the average number of cells positively stained in the absence (**A**) of rhPTH or rhGH, in the presence of rhGH (**B**) and in the presence of rhPTH (**C**) for PI and Sytox green, these graphs demonstrate a constant number of cells injured at each different time point (PI linear relationship) and a decrease in the number of damaged cells (Sytox positive) over time. Graphs represent mean percentages of non-repaired cells ± SEM, * = $p<0.05$ denote significant differences when hormonal treatments compared to control cultures at the same time point. † represents $p<0.05$ compared to the same treatment at the previous time point.

2.3.6 rhPTH and rhGH exert protective effects upon induction of injury in serum-deprived osteocytes.

MLO-Y4 osteocytes were incubated in 0.1% FBS for 16 hours, in order to deprive cells in culture from growth factors, after which time they were incubated for an hour with rhGH (figure 2.12A) or rhPTH (figure 2.12B). Injury was then induced followed by PI and DAPI staining. In more detail at 0secs-30secs cells in the 0.1% FBS cultures did not repair following injury when compared to control, 0.1% FBS+rhGH and control+rhGH cultures (27% ± 0.59 vs. 19% ± 0.71, 16% ± 0.74, 12% ± 0.17, respectively, $p<0.001$). Similarly at 5 minutes cells in 0.1% FBS cultures did not repair following injury when compared to control, 0.1% FBS+rhGH and control+rhGH cultures(24% ± 0.45 vs. 10% ± 0.31, 10% ± 1.07, 6% ± 0.14, respectively, $p<0.001$). At 30 minutes cells in 0.1% FBS cultures did not repair following injury when compared to control, 0.1% FBS+rhGH and control+rhGH cultures(21% ± 0.39 vs. 8% ± 0.24, 3% ± 0.15, 3% ± 0.011, respectively, p0.05). At 24 hours cells the same as in previous time points was observed with the cells in 0.1% FBS cultures not repairing following injury when compared to control, 0.1% FBS+rhGH and control+rhGH cultures (24% ± 0.23 vs. 4% ± 0.37, 3% ± 0.45, 3% ± 0.14, respectively, $p<0.001$). Similarly to rhGH in the presence of rhPTH at 0secs-30secs cells in the 0.1% FBS cultures did not repair following injury when compared to control, 0.1% FBS+rhPTH and control+rhPTH cultures (27% ± 0.17 vs. 18% ± 0.47, 11% ± 0.47, 10% ± 0.15, respectively, $p<0.001$). At 5 minutes cells in 0.1% FBS cultures did not repair following injury when compared to control, 0.1% FBS+rhPTH and control+rhPTH cultures (24% ± 0.43 vs. 11% ± 0.26, 7% ± 0.18, 6% ± 0.30, respectively, $p<0.05$). At 30 minutes as before cells in 0.1% FBS cultures did not repair following injury when compared to control, 0.1% FBS+rhPTH and control+rhPTH cultures (21% ± 0.68 vs. 9 % ± 0.11, 3.2% ± 0.13, 3% ± 0.27, respectively, $p<0.05$). Similarly at 24 hours cells in 0.1% FBS cultures did not repair their plasma membrane when compared to control, 0.1% FBS+rhPTH and control+rhPTH cultures (24% ± 0.23 vs. 8% ± 0.37, 3% ± 0.23, 2% ± 0.13, respectively, $p <0.001$). Pre-incubation of low serum cultures with rhPTH or rhGH significantly enhanced the repair process of cells, indicative of protective effects of these compounds.

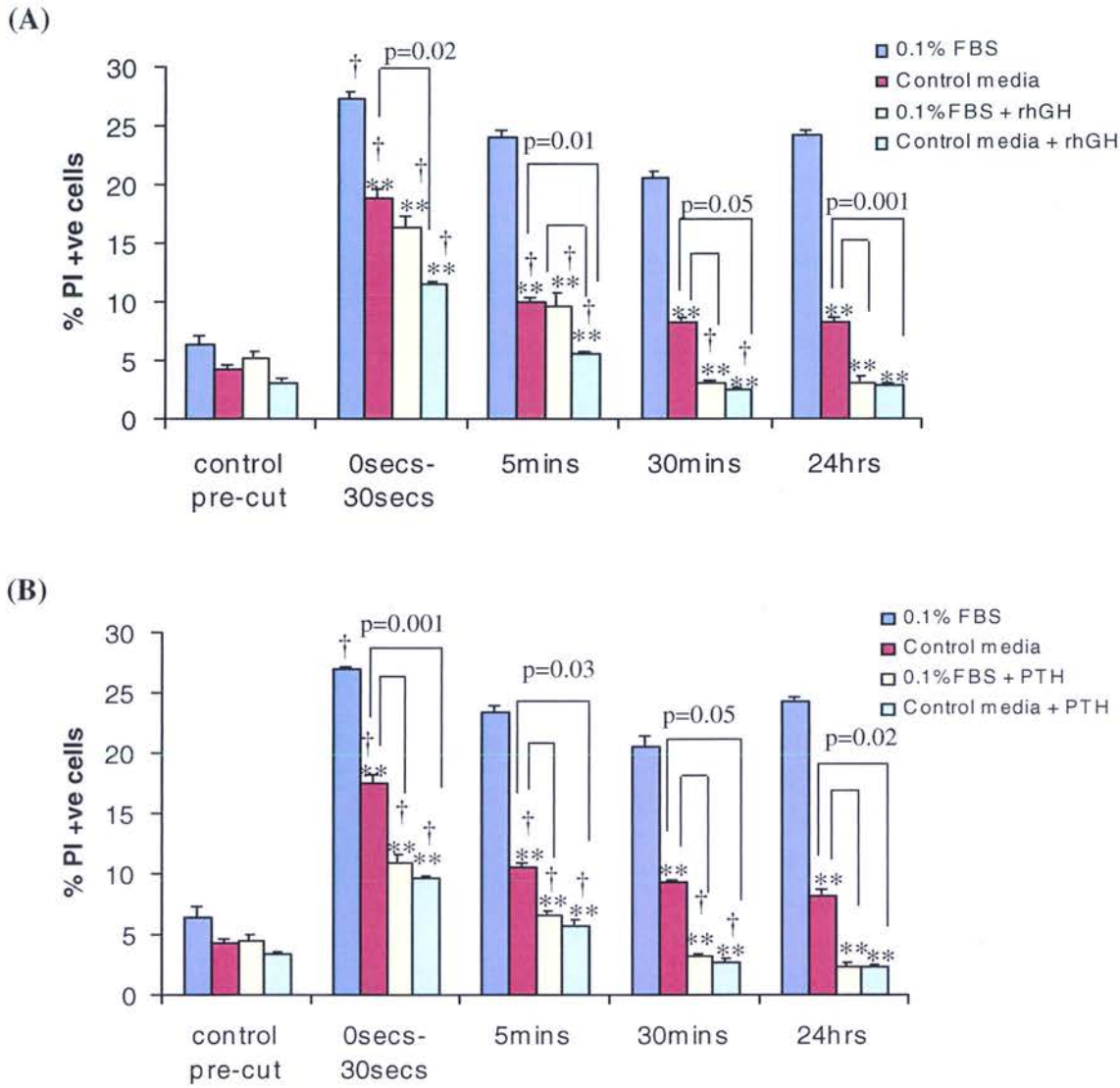

Figure 2.12 Pre-incubation with rhPTH and rhGH following overnight incubation of MLO-Y4 osteocytes in low serum enhances cell membrane repair. Osteocytes were incubated overnight in 0.1% FBS followed by pre-incubation of an hour with either rhPTH or rhGH. Following injury cells in low serum controls did not repair as cells in control media (a-MEM) or those pre-incubated with rhGH (**A**) or rhPTH (**B**) in control or 0.1% FBS media. Graphs represent mean percentages of PI positive cells ± SEM, * = $p<0.05$ and ** = $p< 0.001$ denote significant differences of treatments and control cultures compared to 0.1% FBS cultures at the same time point. † represents $p<0.05$ compared to the same treatment at the previous time point.

2.3.7 Effects of extracellular calcium removal in cell membrane repair on cultures of MLO-Y4 osteocytes.

The repair process is calcium dependent in other cell types (Terasaki et al., 1997); the same hypothesis was tested in osteocyte cells in culture. Cells were incubated in HANKS solution (which is an inorganic balanced salt solution, containing all necessary salts except calcium chloride) for half an hour prior to induction of injury followed by PI and DAPI staining. It has been previously reported that the removal of extracellular calcium causes dissociation of cell-cell contacts and changes in cell shape, such as retraction and rounding (Xin et al., 2005). Such changes didn't appear to occur in the cultures examined in these experiments following light microscopy observation. Extracellular calcium deprivation was found to significantly affect the repair process at all time points, when compared to controls (Figure 2.13). At 0secs. – 30 seconds the percentages of injured cells in the calcium deprived cultures were significantly higher compared to the control (51% ± 0.47 vs. 19 ± 0.71, respectively, $p<0.001$). At 5 minutes there was a significant decrease in the controls compared to calcium deprived cultures (10% ± 0.31 vs. 41% ± 1.23, respectively, $p<0.001$) with the same observation at 30 minutes (4% ± 0.64 vs. 38% ± 1.45, respectively, $p<0.001$). To test these findings calcium chloride at a final concentration of 1.6mM was added in the HANKS calcium deprived cultures pre- and post- injury (Figure 2.14), to test if the cell repair can reach similar levels as that of the controls. These findings showed no significant differences between addition of calcium chloride prior or post injury, however there were significant difference noted between the calcium deprived (HANKS) and the calcium deprived with addition of calcium chloride cultures. There were also significant differences noted between the HANKS treated cultures with addition of calcium chloride compared to the control media cultures for the early time points. In table 2.1 the mean percentages ± SEM of damaged cells are presented for each time point and individual treatments.

Table 2.1	HANKS	HANKS+ CaCl PI	HANKS+ CaCl AI	Control media	Significance HANKS to other treatments
0-30secs	51%±0.47	33%±1.28	32% ±0.33	27% ±0.96	p<0.001
5 mins	36% ±3.46	18% ±0.54	16% ±0.23	13% ±0.61	p<0.001
30 mins	31% ±3.79	15 % ±0.19	14% ±0.30	9% ±0.06	p<0.001

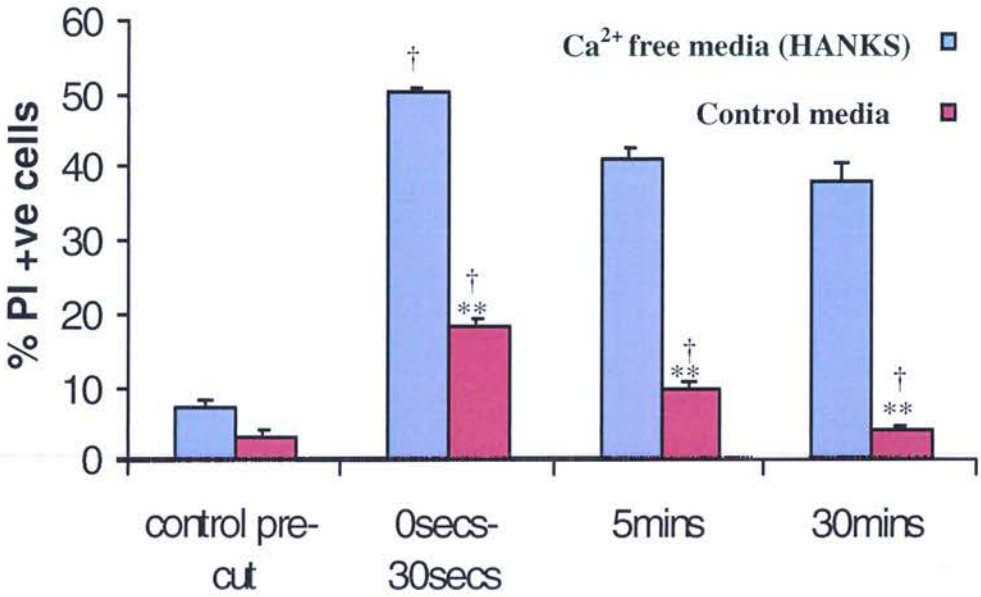

Figure 2.13 Extracellular calcium is important for cell membrane repair following injury. Cells were incubated for 30 minutes with HANKS media to deprive them from extracellular calcium. Cell repair in the calcium deprived cell cultures was compromised and no significant differences were noted between the time points. Cells in control media repaired their cell membrane following injury in a time dependent manner and significant differences in cell repair were noted between the time points. Graphs represent mean percentages of PI positive cells ± SEM, ** = $p< 0.001$ denote significant differences of control media cultures compared to HANKS calcium deprived cultures at the same time point. † represents $p<0.05$ compared to the same treatment at the previous time point.

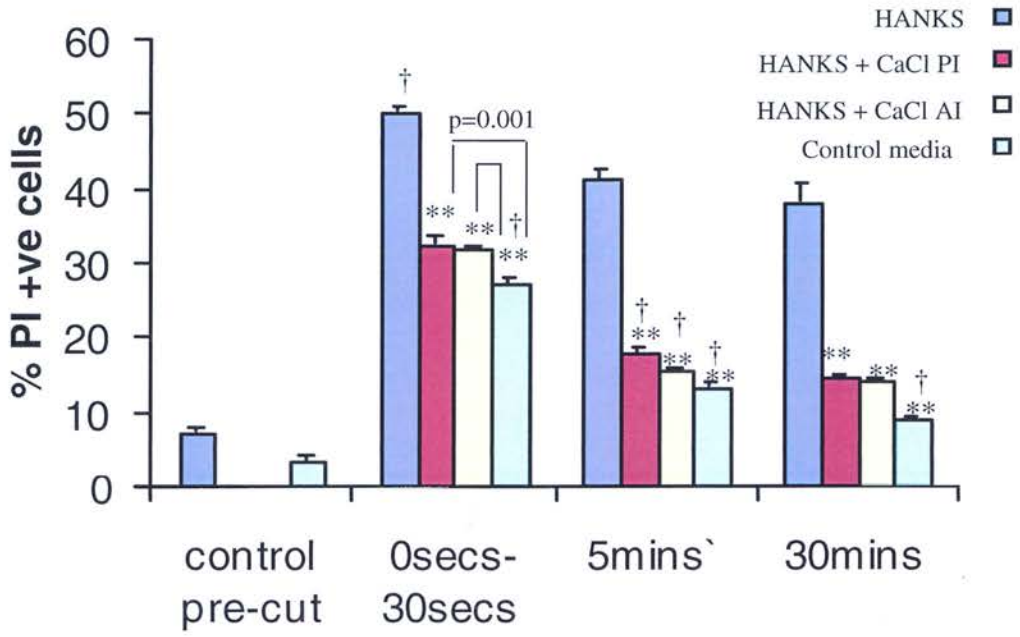

Figure 2.14 Addition of calcium chloride in HANKS calcium deprived cultures accelerates the repair process. Cells were incubated for 30 minutes with HANKS media to deprive them from extracellular calcium. Calcium chloride at a final concentration of 1.6mM was added in the HANKS cultures prior (PI) and post injury (AI) and repair was documented. There were no significant differences noted between addition of calcium chloride prior or post injury, however there were significant difference noted between the calcium deprived (HANKS) and the calcium deprived with addition of calcium chloride cultures. Also there were significant differences found between the HANKS treated cultures with addition of calcium chloride compared to the control media cultures for the early time points. Graphs represent mean percentages of PI positive cells ± SEM, ** = $p< 0.001$ denote significant differences of all treatment cultures compared to HANKS calcium deprived cultures at the same time point. † represents $p<0.05$ compared to the same treatment at the previous time point.

2.3.8. Effects of rhPTH and rhGH on cell membrane repair in the absence of extracellular calcium.

Following deprivation of extracellular calcium in HANKS media cells were pre-treated with rhPTH or rhGH, at the end of the incubation injury was induced. The calcium deprived cultures treated with rhGH (Figure 2.15A) and those treated with rhPTH (Figure 2.15B) showed significant differences compared to the HANKS cultures. However the repair process of these cultures could not reach same levels of repair as that of control or control in the presence of rhPTH or rhGH. In more detail at 0secs-30secs statistically significant differences in cell membrane repair were noted between the HANKS cultures compared to the HANKS+rhGH, control and control+rhGH cultures (50% ± 0.47 vs. 24% ± 1.17, 19% ± 0.71, 13% ± 0.17, respectively, p=0.001). Similarly at 5 minutes statistically significant differences were noted between the HANKS cultures compared to the HANKS+rhGH, control and control+rhGH cultures (37% ± 2.16 vs. 18% ± 0.61, 7.% ± 0.31, 6% ± 0.14, respectively, p=0.05). At 30 minutes statistically significant differences were noted between the HANKS cultures compared to the HANKS+rhGH, control and control+rhGH cultures (33% ± 1.79 vs. 16% ± 0.55, 6% ± 0.24, 3% ± 0.11, respsectively, $p<0.05$). Similarly to rhGH treatment, rhPTH treatment resulted in statistically significant differences at 0secs-30secs between the HANKS cultures compared to the HANKS+rhPTH, control and control+rhPTH cultures (50% ± 0.47 vs. 26% ± 0.58, 19% ± 0.71, 10% ± 0.15, respectively, p=0.001). At 5 minutes statistically significant differences were noted between the HANKS cultures compared to the HANKS+rhPTH, control and control+rhPTH cultures (37% ± 2.16 vs. 18% ± 0.28, 7% ± 0.31, 5% ± 0.30, respectively, p=0.01). Similarly at 30 minutes differences were noted between the HANKS cultures compared to the HANKS+rhPTH, control and control+rhPTH cultures (33% ± 1.79 vs. 15 % ± 0.62, 6% ± 0.24, 2% ± 0.27, respectively, $p<0.05$).

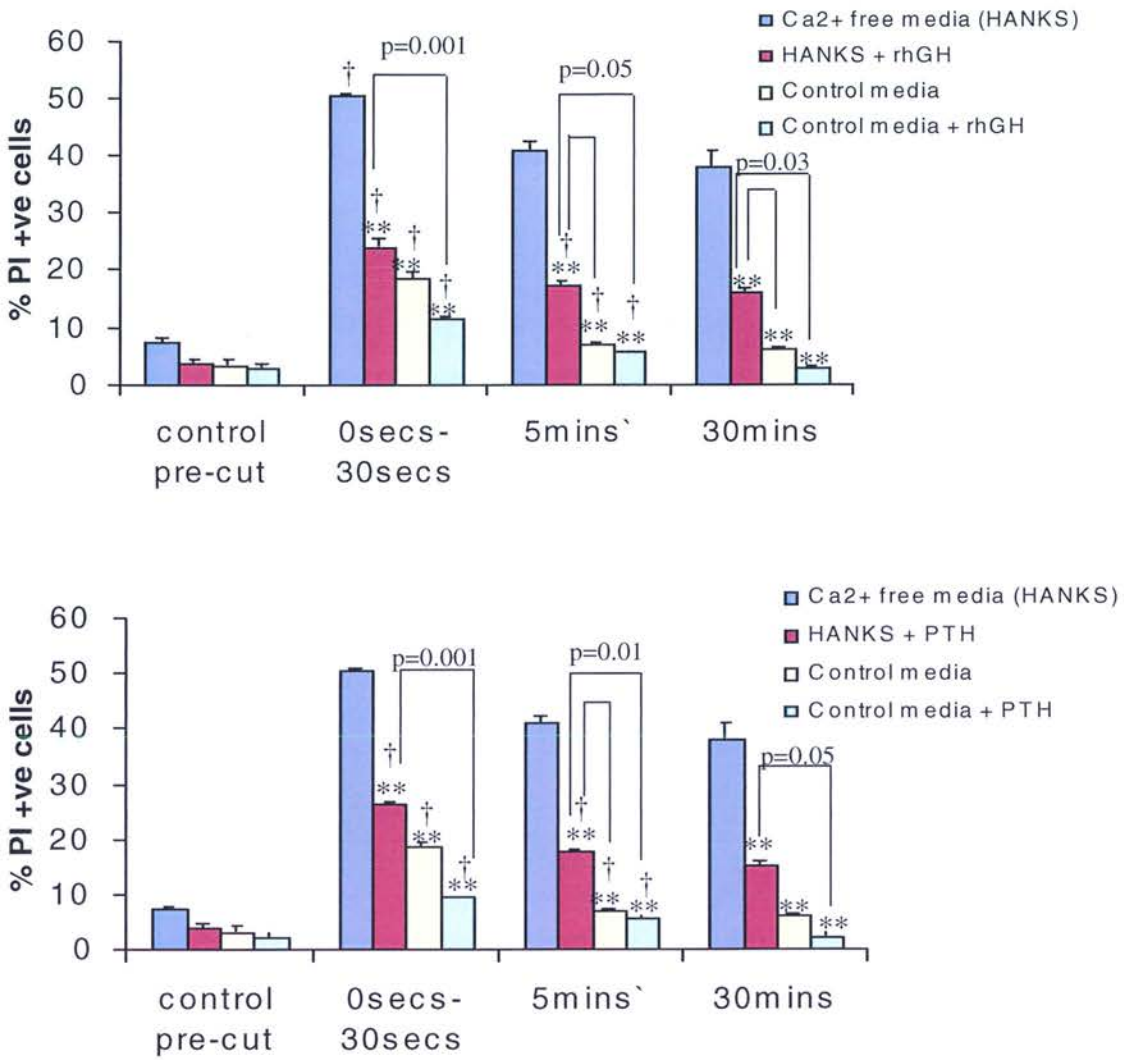

Figure 2.15 Pre-incubation of calcium deprived cultures with rhPTH or rhGH affects the repair process. Cells were calcium deprived in HANKS media followed by pre-incubation with rhPTH or rhGH for an hour. Following addition of rhGH (**A**) or rhPTH (**B**) in calcium deprived cultures the repair process was significantly accelerated as cells repair in a time dependent manner when compared to calcium deprived cultures. However the repair process of these cultures could not reach same levels of repair as that of control or control in the presence of rhPTH or rhGH. Graphs represent mean percentages of PI positive cells ± SEM, ** = $p< 0.001$ denote significant differences of all treatment cultures compared to HANKS calcium deprived cultures at the same time point. † represents $p<0.05$ compared to the same treatment at the previous time point.

2.3.9. Osteocyte apoptosis using in situ nick translation technique.

Following observations that osteocytes were not dying immediately following injury, due to necrosis, in situ nick translation technique was used to define whether they were undergoing apoptosis at later time points. But due to the model used to induce cell injury it was not clear which cells were undergoing apoptosis since all visible cells on the cut were stained positive for all time points examined (figure 2.16).

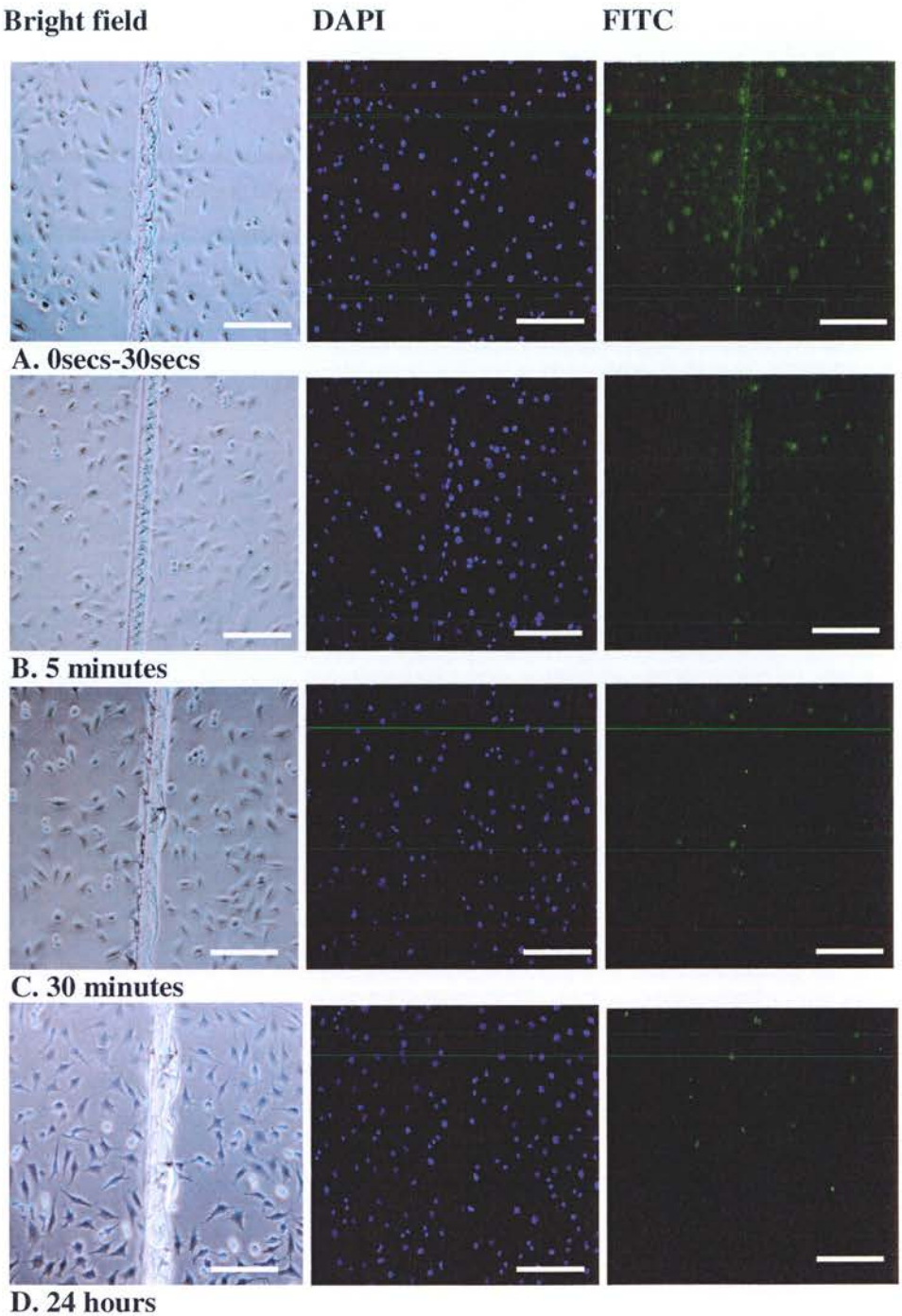

Figure 2.16 Nick translation representatives for all three treatment groups. Representative images of MLO-Y4 -osteocyte like cells following injury *in vitro* at different time points. Following fixation cells were reacted with the nick translation mixture in order to identify apoptotic osteocytes (FITC-green). Red arrows identify apoptotic osteocytes. Bar = 100 μm.

2.4 Discussion

It is widely accepted (McNeil, 1997, 2001, 2002) that cell membranes are 'self-sealing' in a number of different cell types, in support of this concept, experimental conditions using laser wounding, electroporation or needle scratch have been developed that allow cell membrane disruprions to reseal in the laboratory, (McNeil and Kirchhausen, 2005). The biological question of interest presented in this chapter, however, is whether MLO-Y4 cells have the capacity to reseal and survive cell membrane disruptions *in vitro* and whether this process is affected by the presence of rhPTH and rhGH.

Before this work, observations *in vivo* supported the hypothesis that direct cell injury causes osteocyte apoptosis (Colopy et al. 2004, O'Brien et al. 2005). These studies reported death of osteocytes due to disruptions near microcracks, however they did not apply techniques to study osteocyte apoptosis and base all conclusions to light microscopy and as such no secure conclusions can be made to link microdamage to cell death. Alternative interpretations of these results are of course possible, because the perturbations inflicted might have introduced unintended effects. Here it is shown that MLO-Y4 cells are able to survive and repair following physical membrane disruption.

A simple *in vitro* model for injuring cells in culture was developed. Briefly cells were injured using a sharp blade *in vitro* in 24-well plates by making a light scratch over the cell surface.The MLO-Y4 osteocyte like cell line was used, due to the difficulties of obtaining large numbers of primary osteocytes. Cell repair was followed at different time points and it was found that whilst scalpel damage induced significant injury, osteocyte repair was rapid, the majority occurring within the first few minutes following damage. Such rapid repair is confirmed by previous studies (McNeil 1997, 2001, 2002), which describe a resealing response, occurring within seconds following cell injury to prevent loss of cytoplasmic contents, calcium influx and subsequent cell death (McNeil 2000).

Although repair occurred in the absence of these hormones, following incubation for an hour with rhPTH or rhGH was shown to have a beneficial effect, reducing the number of

injured cells dramatically within the first five minutes. The choice of concentrations for both compounds was based on what has been published before in the literature regarding the known anti-apoptotic effective concentrations of these hormones *in vitro* (Kassem et al. 1993, Jilka et al. 1999). In order to determine whether the effect of rhPTH and rhGH in accelerating the repair process was specific to those two compounds, TGF-β3, a growth factor regulating a broad range of biological processes as well as wound healing (Janssens et al. 2005) and Vitamin C- a potent antioxidant (Padayatty et al., 2003) were also used over the time period of 24 hours in the same experimental context as that of rhGH and rhPTH. Antioxidant compounds such as vitamin C, vitamin E and estrogen protect osteocytes from apoptosis induced from oxidant attack (Mann et al., 2005). These compounds did not induce the same response as rhPTH or rhGH, indicative of the protective effects these hormones have on osteocytes in culture. However there was a significant difference observed at the highest concentration of vitamin C when compared to the control cultures at the 5 minute time point, which is suggestive of the possibility that longer incubation periods or higher concentrations of antioxidant compounds may be able to elicit protective effects to osteocytes.

To estimate cell wounding and repair over time three different tracking dyes were used. In initial experiments cell wounding and repair was estimated using PI staining, which stained cells with a compromised cell membrane at different time points and DAPI stain was used to estimate the total cell numbers for 0.2mm of either site of the cut. For follow up experiments due to the inability to determine initial percentages of damaged cells, questions arose over the nature of the beneficial effect seen in the presence of rhPTH and rhGH. For instance, whether rhPTH and rhGH allowed cells to heal more quickly, or increased resistance of cells to scalpel damage. Double staining experiments using PI and Sytox green helped to clarify this point. It was found that the initial number of damaged (PI positive) cells was similar in the presence and absence of rhPTH and rhGH. Therefore it could be concluded that rhPTH and rhGH were most likely increasing the overall rate of repair following damage.

Pre-incubation for an hour with rhPTH and rhGH had a significant effect on the rapidity of the cell membrane repair when compared to control cultures. Cell repair was followed at a number of different time-points, from 30 seconds to 24 hours at initial experiments. The majority of cells repaired within the first five minutes. Following this observation shorter experiments from 30 seconds to 5 minutes were carried out. In these experiments rhPTH and rhGH had a similar effect in accelerating the repair process when compared to the control cultures. To my knowledge there is no such report of similar effects in the literature, thus more studies are needed to investigate these findings. However there are a number of studies in the literature reporting the repair process of cell membrane *in vitro* in different tissues such as endothelium, skeletal, cardiac muscle and skin (McNeil 1993, 1997, 2001, 2002). At the cell level, most of the studies of membrane repair have been performed in sea urchin fibroblasts (McNeil and Terasaki 2001, McNeil 2000) and the repair process was reported to occur within the first 5 seconds of induction of injury to these cells. Nevertheless in neurons it has been reported that repair can take as long as 90 minutes. In this study the repair was increased over time with 18.5% of the cells that had been damaged as demonstrated by PI uptake at 0 seconds – 30 seconds increasing over time with only 3% of cells still damaged after 24 hours.

The mechanism of this rapid membrane resealing has been shown to be calcium dependent (McNeil et al. 2003). According to the patch hypothesis influx of calcium into the cytosol through the membrane disruption elevates cytosolic calcium locally. The cytoskeleton then breaks down and although the precise repair mechanism is still unknown, current reports propose that resealing is directly mediated by the delivery of intracellular membrane to the cells surface (Idone et al., 2008). According to these models the vesicles fuse with one another, forming a larger patch vesicle that fill up the disrupted site (McNeil et al. 2000) or decrease plasma membrane tension to elicit an exocytotic addition of vesicles to the plasma membrane (Togo et al. 2000). The force required to allow a decrease in membrane tension comes from the adherence of a phospholipid bilayer to the underlying cytoskeleton, thus disruption elicited exocytosis is proposed to promote lipid flow and hence resealing (Miyake and McNeil 2003).

In the present study the involvement of extracellular calcium in the resealing process in the absence or presence of rhPTH or rhGH was tested. Preliminary data is suggestive of calcium being involved in the resealing process of MLO-Y4 cells. When injury was induced in HANKS (calcium chloride absent) cultures the cells where unable to repair the membrane disruption when compared to the control cultures, but interestingly upon addition of calcium chloride in these cultures the repair process was restored close to control levels. It has been reported in other studies that resealing of small disruptions such as those induced by electroporation do not require extracellular calcium and have been reported as spontaneous sealing of the membrane without the participation of internal membranes (Fein and Terasaki, 2005). However in the study presented here the disruptions were of a higher magnitude than those of electroporation induced disruptions. Another possibility that would explain these findings is that the membrane added during wound sealing adds enough calcium permeability to change the membrane potential. On the other hand if we suppose that calcium is not involved in the resealing process the possibility that the permeability is present in the plasma membrane before injury but is inactivated and the injury does not produce a large enough signal to activate permeability can provide an alternative explanation to these findings. While calcium was not directly linked to the response to rhPTH and rhGH in this study, both of these hormones have been reported to affect calcium trafficking. Studies of calcium trafficking in the presence of PTH and GH have demonstrated an effect by those hormones. Nanomolar concentrations of PTH and GH have been shown to increase calcium in target cells within a couple of minutes (Gesek and Friedman 1992, Samra et al. 1992, Gaur et al. 1998). Such observations may explain the effect of rhPTH and rhGH in calcium deprived cultures and the rapidity of disruption repair. The calcium content has not been quantified in this study and such an investigation would be useful in providing more in depth information regarding the involvement of calcium in cell repair in MLO-Y4 cells. These findings highlight the importance of physiological levels of extracellular calcium for the repair of cell membrane disruptions.

Both PTH and GH have been reported to have anti-apoptotic effects and stimulate growth factor production, including IGF-I (Herndon et al. 1995, Eriksen et al. 1996, Aarts et al.

2001, Compston 2007). PTH has been reported to enhance the survival of serum deprived chondrocytes and save them from apoptosis (Aarts et al. 2001), GH on the other hand has been reported to stimulate IGF-I production and affect wound healing and tissue repair, however, the mechanism by which it improves wound healing remains in question (Herndon et al. 1995). Cells deprived of growth factors undergoe cell death and apoptosis (Goyeneche et al. 2006). The effect of growth factor deprivation in cell membrane repair, via means of serum starvation of cells overnight was investigated. Serum deprived cultures showed a slower repair over time compared to control cultures. When cells were pre-treated with rhPTH and rhGH the repair process was significantly improved compared to serum deprived cultures in the absence of rhPTH or rhGH and similar to control cultures pre-treated with rhPTH and rhGH. These data suggest that rhPTH and rhGH can enhance the repair process even in serum starved cells after a short incubation period. This response may be related to the stimulation of cells to produce growth factors either within their cytosol or in the extracellular fluids. Upon disruption they stimulate potential signals to enter into the wounded cell; and possibly expression of other genes that either facilitate cell survival against the disruption injury or promote tissue recovery or protect the tissue from mechanical stresses. Support for this hypothesis comes from studies of basic fibroblast growth factors (bFGF and aFGF) (McNeil and Steinhardt 1997). When these polypeptides are found in the extracellular environment they are potent growth factors and when they are localized in cytosolic and nuclear compartments of cells, they have been shown to be released into extracellular medium upon disruption of membranes which are survived by the cell, possibly due to the release of these factors.

Evidence has been presented to suggest that when mechanical forces are experimentally imposed upon osteocyte-like cells wounding of the plasma cell membrane occurs, which is survived by the cell. Staining with PI and Sytox green has identified wounding and repair of cells over time. Both rhGH and rhPTH had a protective effect over osteocytes in culture and accelerated the repair process following injury. It can be concluded that about 80% of these cells survive injury and efficiently repair their cell plasma membrane, and are fully capable of both locomotion and proliferation as documented by our real-time 24 hour long time-lapse videos. However this is a preliminary study and a number of

limitations were identified in the design of the experiment. It is clear that the repair process is rapid and in order to accurately determine the time-frame, further work is required to characterize the initial time point. In the present study the initial time point was defined as the first 30 seconds but as reported in other studies (McNeil and Terasaki 2001, McNeil 2000) repair can occur within the first 5 seconds of induction of injury. This could involve time-lapse microscopy of individual cells damaged by laser, or experimentation with other dyes that would be taken up faster by the cells.

The present study was carried out using an MLO-Y4 osteocyte-like cell line which does not represent primary osteocytes as such it is important that future work is undertaken on well characterized primary cells, obtained from sequential digestion, to confirm the observations made here. Moreover these cells do not express calcium channels in their resting phase but they do upon hormone stimulation (Gu et al., 2001), thus further studies would be useful to identify the exact mechanism of cell repair and calcium trafficking in MLO-Y4 cells. These experiments show that rhPTH and rhGH increase the rate of repair following damage, but do not address the final outcome, in terms of whether cells are actually saved through this acceleration of healing and as such we can only speculate as to the benefit of accelerated repair *in vivo.* Though it is clear that the cells are not dying immediately (by necrosis), we cannot rule out the possibility of apoptosis. However as documented in 24 hour time-lapse movies of wounded cells, these cells are able to heal their cell membrane and survive injury. In this study an attempt to study the fate of all cells wounded was made using the in situ nick translation techinque , however due to the scalplel damage caused to the plastic of the well it was hard to identify the cells on the cut following in situ nick translation staining. Thus an improved injury model would be necessary to study the fate of these cells following injury.

Plasma membrane disruption is a frequent and physiological event, and rapid resealing is therefore a fundamental biological adaptation (McNeil, 2005). The present work establishes the hypothesis that MLO-Y4 cells are able to repair following injury and the rate of the repair process is accelerated in the presence of rhPTH and rhGH, by mechanisms that are still unknown. It is hypothesized that osteocyte death related to

microdamage may not be due to the physical damage of the osteocyte itself, but it may be related to either mechanically sensitive signaling pathways, direct physical damage of the canalicular system that supplies necessary nutrients and oxygen. *In vivo* the osteocyte network is vital for the detection of microdamage and activation of the remodeling process for its removal (Burr and Martin 1993, Mori and Burr 1993, Dodd et al. 1999, Parfitt 2001) therefore accelerated repair via the use of therapeutical compounds may be beneficial in maintaining the structural integrity of bone.

CHAPTER 3

Recombinant Human Parathyroid and Recombinant Human Growth Hormone Inhibit Osteocyte Apoptosis In Aged Female Rats. Implications for Bone Quality Maintenance in the Ageing Female Rat Skeleton

Abstract

Parathyroid and growth hormone has been previously shown to exert positive effects on bone, including the maintenance of osteocytes, via inhibition of their apoptotic cell death. This study has investigated the effects of these hormones on osteocyte viability and apoptosis. Their effect on bone architectural changes as well as sclerostin expression by osteocytes in aged female rats was also tested.

Eighteen, virgin female Sprague-Dawley rats aged 15 months were divided into three treatment groups. The control group received vehicle by gavage (n=6), the second group received rhPTH (1-34) at a dose of 50 μg/kg (n=6) once daily, and the third group received rhGH once daily at a dose of 2.5 mg/kg (n=6), by subcutaneous injection. Tibias and femurs were removed; snap frozen and examined histologically at 14 days following the start of treatment. For all three groups in the region of secondary spongiosa osteocytes were examined for viability using the lactate dehydrogenase enzyme activity assay (LDH assay), for apoptosis using an in situ nick-translation (NT) technique and for sclerostin expression using immunostaining. There was a trend towards a decrease in osteocyte apoptosis in response to rhPTH and rhGH treatments but the difference was not statistically significant. Moreover a trend towards a decrease in osteocytes expressing sclerostin was observed, with no statistical significance noted. Architectural changes in the trabecular bone were also documented using the femurs of the same animals by means of three-dimensional micro-computed tomography. Significant changes compared to the control group in trabecular architecture were observed in the rhPTH treated group but not in the rhGH group.

These observations demonstrate that these hormones can exert inhibitory effects upon osteocyte apoptosis and rhPTH can improve the trabecular architecture in aged animals, pointing to their potential to be used as anabolic treatments.

3.1 Introduction

In the previous chapter evidence has been presented regarding the effects of rhPTH and rhGH in MLO-Y4 osteocyte-like cells. Both compounds have been shown to exert a protective effect on osteocytes following physical injury *in vitro*, pointing to a potential use of these compounds to protect the osteocytic population in ageing and disease states. In the study presented here the effects of these hormones on osteocytes were examined *in vivo* in aged skeletally mature female rats.

Osteocyte loss via apoptosis or necrosis has long been associated with the ageing process (Dunstan et al. 1993, Frost 1960), and as a consequence their presence within bone has been associated with its ability to respond to mechanical stimuli (Lanyon et al. 1993), remodel efficiently and repair accumulated microdamage (Burr et al. 1985, Parfitt 2001, Noble et al. 2003). These findings indicate that bone quality is closely associated with the presence of osteocytes and the communicating network they form through their cytoplasmic processes within the bone matrix (Dunstan et al. 1993).

Osteocyte death by apoptosis has been associated with a range of conditions including glucocorticoid treatment (Gu et al. 2005), estrogen withdrawal (Tomkinson et al. 1997, Weinstein et al. 2000), elevated PTH (Bringhurst 2000), androgen action (Wiren et al. 2006) and both underloaded and overloaded bone (Noble et al. 2003).

Osteocytes possess receptors for a number of hormones including the receptors for PTH (Divieti, 2005). On the other hand GH receptors have only been shown on osteoblasts and osteoclasts but not on mature rat osteocytes (Lobie et al. 1992), leading to the assumption that it affects them indirectly, possibly via stimulation of growth factors, mainly being IGF-I. Moreover GH levels decline by approximately 14% per decade from young adult life, and the associated reduction in bone mass similar to that seen in adults with growth hormone deficiency is indicative of influencing the skeleton (Shalet et al., 1998).

In animal studies an increase in bone mass in both ovariectomized and normal rats following administration of GH and PTH has been documented (Andreassen, H. Oxlund,

2001, Alexander et al. 2001). Combined treatment with PTH and GH has been shown to stimulate enhanced bone formation mainly at the endocortical surface, which was found to be greater than that induced by PTH administration alone, whereas GH treatment has been shown not to influence the endocortical surface (Adreassen and Oxlund, 2000). In studies of post menopausal women administration of GH and intermittent PTH have shown an increase in bone turnover as well as a reversal of bone loss induced by estrogen deficiency in the case of PTH (Saaf et al., 1999, Alexander et al. 2001).

Anabolic treatments have become the focus of intense research lately due to their potential to stimulate bone formation. The only anabolic agent currently approved for the treatment of osteoporosis, is teriparatide; the human PTH analog 1-34. Its use has been associated with an increase in bone density and bone turnover (Girotra et al., 2006). The mechanisms underlying the anabolic effects of PTH are not well understood but depending on the mode of administration it exerts either anabolic (intermittent administration) or catabolic (continuous administration) effects. When intermittently administered, PTH appears to increase bone mass by stimulating the osteoblasts at all levels of their life cycle including recruitment, proliferation, differentiation and apoptosis (Wang et al., 2006). Intermittent administration of PTH in accelerated senescence resistant mouse strain (SAMR 1) mice has also been shown to decrease apoptosis in osteocytes (Jilka et al., 2002). Similar anti-apoptotic effects were observed in MLO-Y4 osteocyte-like cells (Bringhurst, 2002). These findings indicate that PTH exerts complex actions in bone and a net positive or negative outcome dependant on the kinetics of PTH exposure. Further identification of novel genes involved and studies of their molecular mechanisms of action are required to elucidate PTH effects on bone.

Recently, the SOST gene and its protein product, sclerostin, have been identified as potent negative regulators of bone formation (Keller and Kneissel, 2004). SOST is expressed by mature osteocytes and its protein product sclerostin has been proposed to act as a signal directed to osteoblasts or to lining cells; following completion of mineralization in the matrix surrounding the osteocyte in order to limit further osteoblast activity (Poole et al. 2005) and/or to indirectly activate osteoclast resorption. In the

present study sclerostin expression via means of immunostaining in the osteocytes was investigated in the three treatment groups analyzed, as it has been reported to be involved in the PTH anabolic response (Li et al. 2005, Poole et al. 2005, van Bezooijen et al. 2005).

In contrast to the effects exerted by PTH, the anabolic effects of GH are not direct to the osteocytes, since the GH receptor is found only on the surface of osteoblasts and osteoclasts but not on the mature osteocytes (Andreassen, H. Oxlund, 2001). GH is the most important regulator of IGF-I production (Niu and Rosen, 2005), which is known to stimulate chondrocyte proliferation at the growth plate as well as skeletal and muscle maintenance (Lupu et al., 2001). IGF-I not only exerts proliferative effects on tissues but also anti-apoptotic effects, as has been demonstrated in cell cultures of some tumors (Granerus et al. 2001). IGF-I production may provide some insight as to the mechanism of GH effects on osteocytes. IGF-I receptors have been shown on osteocytes which may explain the indirect anti-apoptotic effect of GH via IGF-I production (Okazaki et al. 2003). GH administration has been shown to increase bone formation and resorption and to enhance cortical bone mass and mechanical strength, these effects are thought to be mediated by the GH-IGF-I axis (Adreassen and Oxlund, 2001).

In this study the use of rhPTH and rhGH on the maintenance of osteocyte viability and prevention of the increase in the proportion of osteocytes undergoing apoptosis in aged intact female rats, was investigated. Finally the architectural changes in the trabecular bone following short term hormonal treatment were examined.

In order to detect changes in osteocyte viability methods to detect both osteocyte apoptosis and viability were employed. Apoptotic osteocytes were identified by the use of the Nick Translation (NT) technique (Noble et al. 1997), while viable osteocytes at the time of sampling were determined by using the Lactate Dehydrogenase Assay (LDH) (Noble et al. 2003). Architectural changes in the trabecular bone were analysed by means of three-dimensional micro-computed tomography (μCT).

3.2 Materials and Methods

3.2.1 Animals

Eighteen, female Sprague-Dawley rats were purchased (Harlan UK Ltd., Shaws Farm, Blackthorn, Bicester, Oxon, UK) at the age of three months and allowed to age until the age of 18 months. A standard rodent diet (RM1; Special Diet Services Ltd, UK) and tap water were available *ad libitum*, with twelve hours light (6:00 a.m. to 6:00 p.m.) and twelve hours darkness. Animal experimentation was conducted in compliance with national ethical guidelines.

The animals were grouped into three treatment groups, so that each group contained 6 animals. Group 1, the control group, which received vehicle (1% Carboxy-methylcellulose) by gavage using a stomach tube. Group 2 received rhPTH fragment 1-34 (provided by NOVARTIS, Basel, Switzerland) once daily at a dose of 50 μg/kg body weight via subcutaneous injection, dissolved in 0.15M saline.Group 3 received rhGH (provided by NOVARTIS) once daily at a dose of 2.5 mg/kg body weight via subcutaneous injection, dissolved in distilled water. The animals were weighed every day prior to treatment and the dose of the compounds was adjusted in accordance with the actual body weight. The duration of the experiment was fourteen days.

At the end of the experimental period all animals were killed by exsanguination the tibias were harvested and dissected free of muscle, immersed in 5% polyvinyl alcohol (Sigma, UK) and frozen to –70°C in super cooled hexane (BDH, UK), prior to storage and analysis. Transverse cryostat sections of 7μm thickness were cut onto ultra pure tape for sections (Taab Laboratories, UK) from the left tibia from the control, the rhPTH and the rhGH groups and were then transferred to Super frost slides(Western Laboratory Services, UK) for further analysis. Three sections of each sample were used in order to determine each of the measurement criteria. These sections were spaced at least three sections apart to avoid sampling the same osteocyte nucleus twice.

3.2.2 Cell viability assessment in situ

Viable osteocytes at the time of sampling were identified in cryostat sections by means of their lactate dehydrogenase (LDH) activity.Lactate dehydrogenase is a cytoplasmic enzyme that catalyzes the oxidation of L-lactate to pyruvate via the reduction of nicotinamide adenine dinucleotide (NAD^+) to NADH (Stryer L. 1995).

$$\text{L-lactate} + NAD^+ \xrightleftharpoons{\text{LDH}} \text{Pyruvate} + NADH + H^+$$

The metabolic activity of the cells was assessed by their capacity to convert NBT to a coloured product since the colour is the outcome of metabolic activity (Widholm, 1972). The proton atom (H^+) released during the reduction of NAD^+ to NADH reduces NBT to give a dark blue coloured product only in the metabolically active cells with intact cell membranes. Histochemical staining was undertaken using the method of Noble and Stevens (Noble and Stevens 2003). 7μm unfixed tissue sections were incubated in 1.75 mg/ml disodium salt (a-nicotinamide adenine dinucleotide, NAD) (Roche Diagnostics Corporation, UK), 60 mmol/L lactic acid, 3 mg/ml nitroblue tetrazolium (NBT) (Sigma, UK) and 40% Polypep (Sigma, UK), pH 8.0, for 3h at 37°C in a humidified chamber. Finally, sections were rinsed in warm water to remove the reaction mixture, fixed in 4% paraformaldehyde for 10 minutes, washed in PBS and then mounted in DAKO mounting medium (Fisher Scientific Ltd, UK). Sections were examined under transmitted light and the number of dark blue stained LDH positive osteocytes (figure 3.1), considered to be viable per bone area (mm^2), and was quantified using the BIOQUANT OSTEO software. Images were captured with a DXM1200 camera mounted on Eclipse E800 microscope (Nikon) using 20X/0.50 / 0.17WD2.1 magnification lens.

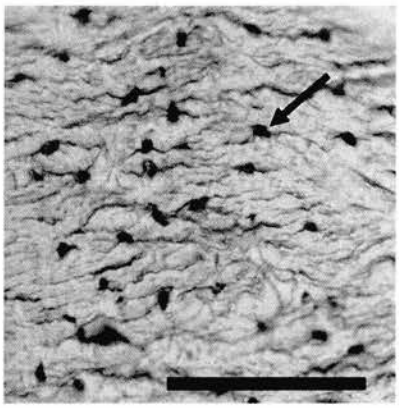

Figure 3.1 Histochemical reaction of LDH enzyme in rat sections in situ. Representative image of a section obtained from a control animal and stained for LDH activity. Viable osteocytes were distinguished by the presence of LDH activity in cells. Blue arrow identifies a viable LDH-positive osteocyte. Bar represents 100μm.

3.2.3 In situ analysis of osteocyte DNA fragmentation using Nick Translation technique

The percentage of osteocytes demonstrating significant levels of DNA fragmentation was determined using a DNA nick translation technique, (Noble et al. 1995; 1997). Only the larger number of single DNA breaks, associated with apoptosis rather than necrosis, were detected. The technique allows the identification of early DNA breaks prior to loss of the DNA content and prior to plasma membrane permeabilisation (Petit et al., 1995).The 7 μm thick cryostat sections were fixed in 4% paraformaldehyde (Sigma, UK) for 10 minutes and then washed in phosphate buffer saline (PBS) (Oxoid, UK) for 5 minutes three times, prior to demineralisation in 0.25 mol/L ethylenediamine tetra-acetate (EDTA) (Sigma, UK) in 50 mmol/L Tris HCL, pH 7.4, for 10 minutes. The sections were then washed in PBS. For the positive control a section was treated with deoxyribonuclease I (DNase) at a concentration of 0.2 mg/ml in PBS (Sigma, UK) for 30 minutes to induce DNA breaks (figure 3.2). All sections apart from the negative control (figure 3.3) that was treated with the following reaction mixture in the absence of DNA polymerase I, were treated with a reaction mixture that consisted of 3 mmol/L digoxigenin (DIG)-labelled dUTP (DIG-11-dUTP); 3 mmol/L each of dGTP, dATP, and dCTP; 50 mmol/L Tris HCl, pH 7.5; 5 mmol/L $MgCl_2$, 0.1 mmol/L dithiothreitol, 0.5 mL/100 ml DNA polymerase I for 45 minutes at 37 ^{0}C in a humified chamber. At the end of the incubation period all sections were washed in PBS and incubated with fluorescein isothiocyanate (FITC)-labelled anti-DIG antibody (all reagents obtained from Roche Diagnostics Corporation, UK) and 5% normal sheep serum (Sigma) in PBS, for 1 hour in a humidified chamber at room temperature (RT). After washing in PBS all sections were stained for nuclear DNA with DAPI (Sigma, UK) at 2mg/ml for 10 minutes, washed thoroughly in PBS and mounted with fluorescent mounting medium (DAKO, UK). Sections were visualized by fluorescent microscopy using a DXM1200 camera mounted on Eclipse E800 microscope (Nikon) using 20X/0.50 / 0.17WD2.1 magnification lens (x20). Osteocytes stained positive for both the FITC label and DAPI were considered as osteocytes containing fragmented DNA.

A. FITC B. DAPI C. Combined

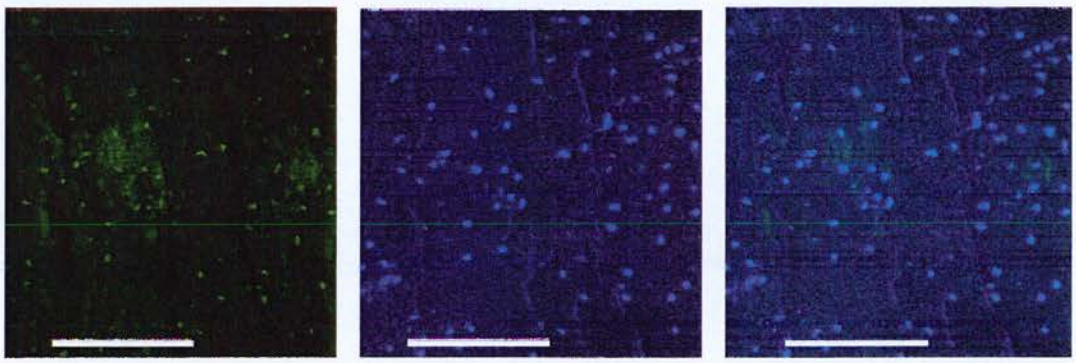

Figure 3.2 In situ demonstration of a positive control for the nick translation method. A section of cortical bone was taken from the tibia of a control animal. All nuclei stained green for the FITC signal **(A, C)** since the section was incubated with deoxyribonuclease I (DNase) in order to produce DNA breaks prior to reaction with the nick translation mixture (x 20). Nuclei were stained blue with DAPI **(B)**. Bar represents 100 μm.

A. FITC B. DAPI C. Combined

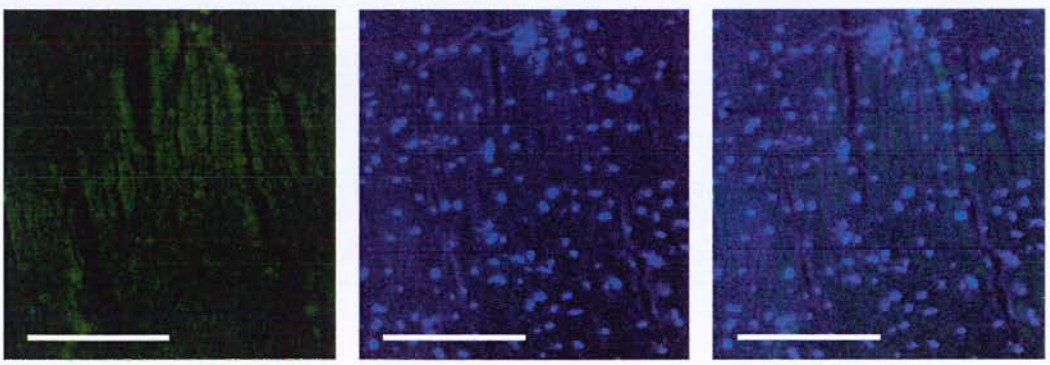

Figure 3.3 In situ demonstration of a negative control for the nick translation method. Sections were treated with the nick translation mixture without the presence of DNA polymerase I. Nuclei were stained blue with DAPI **(B).** No FITC signal was observed indicating the inability of oligonucleotides to be incorporated into the DNA breaks in the absence of DNA polymerase I and be recognized by the anti-DIG-FITC labelled antibody **(A, C)** (x 20). Bar represents 100 μm.

3.2.4 Quantification of osteocyte viability and apoptotic criteria

Transverse cryostat sections 7 μm thick were obtained from the secondary spongiosa region moving towards the diaphysis for 2.5 mm. To calculate the percentage of apoptotic osteocytes three non-consecutive sections from each biopsy were used. Using the nick translation technique the number of apoptotic osteocytes relative to the total number of cells that stained positive for DAPI was calculated to give the percentage of apoptotic osteocytes. Adjacent sections from the same area were used to determine the density of viable osteocytes (the number of LDH positive osteocytes per mm^2) using the *in situ* LDH viability assay. A minimum of eight non-overlapping fields of view were randomly selected from each of the sections so that more of 70% of the total bone area was analyzed.

The following criteria were used to calculate the percentage of apoptotic osteocytes and the percentage of viable osteocytes following the treatments described above.

Percentage of apoptotic osteocytes (%) =

$$\frac{\text{Average number of FITC positive osteocytes}}{\text{Average number of PI stained osteocytes}} \times 100$$

Density of viable osteocytes (mm^2) =

$$\frac{\text{The number of LDH positive osteocytes}}{\text{The area of bone in the field of measurement per } mm^2}$$

3.2.5 Sclerostin staining

For the identification of sclerostin-positive osteocytes in the rat tibia 7 μm thick cryostat sections were fixed in 4% paraformaldehyde (Sigma, UK) for 10 minutes and then washed in phosphate buffer saline (PBS) (Oxoid, UK) three times for 5 minutes, prior to demineralisation in 0.25 mol/L ethylenediamine tetra-acetate (EDTA) (Sigma, UK) in 50 mmol/L Tris HCL, pH 7.4, for 10 minutes. The sections were then washed in PBS and incubated in 0.3% H_2O_2 (Sigma, UK) in methanol for 15 minutes at room temperature. Sections were then washed in PBS three times for 5minutes prior to incubation for 1 hour in 10% normal rabbit serum in PBS. The sections were then incubated with 1:100 diluted goat polyclonal anti-mouse sclerostin antibody in PBS (R&D Systems) at 4°C overnight in a humidified chamber. For the negative control (Figure 3.4) sections were incubated in goat serum diluted at 1:100 in 2% normal rabbit serum. At the end of the incubation period sections were washed three times for 5 minutes in PBS and incubated for 1 hour at room temperature with 1:200 diluted rabbit-anti goat-HRP (Autogen Bioclear). Sections were then washed with PBS and immunodetection was performed using DAB chromogen for 20 seconds. After washing in PBS all sections were stained for nuclear DNA with DAPI (Sigma, UK) at 2mg/ml for 10 minutes, washed thoroughly in PBS and mounted with fluorescent mounting medium (DAKO, UK). Sections were visualized by light and fluorescent microscopy using a DXM1200 camera mounted on Eclipse E800 microscope (Nikon) using 20X/0.50 / 0.17WD2.1 magnification lens (x20). Osteocytes stained positive for sclerostin were considered as osteocytes expressing sclerostin (Figure 3.5).The following criteria were used to calculate the percentage of sclerostin positive osteocytes:

Density of sclerostin positive osteocytes (mm^2) =

$$\frac{\text{The number of sclerostin positive osteocytes}}{\text{The area of bone in the field of measurement per } mm^2}$$

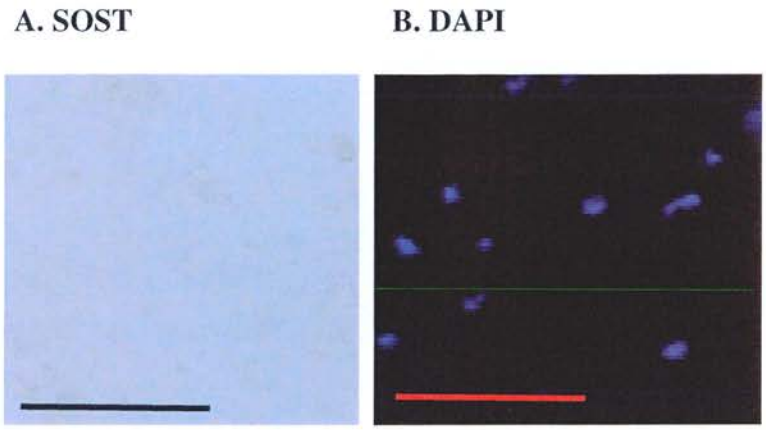

Figure 3.4 Immunohistochemical demonstration of a negative control for sclerostin staining. Sections were treated with the goat serum diluted at 1:100 in 2% normal rabbit serum mixture without the presence of sclerostin antibody. Nuclei were stained blue with DAPI **(B).** No sclerostin signal was observed **(A)**. Bar represents 100 μm.

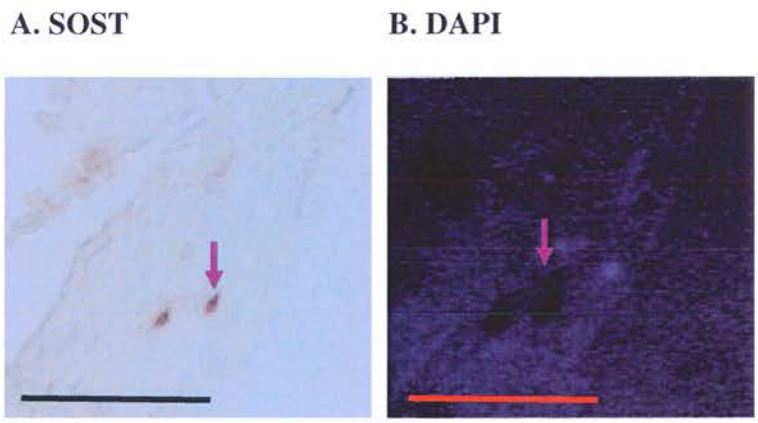

Figure 3.5 Immunohistochemical reaction of sclerostin expression in rat section. A section of trabecular bone was taken from a control animal. Osteocytes stained positive for sclerostin are brown as indicated by the arrow **(A)** Nuclei stained positive for DAPI **(B)**. Bar represents 100μm.

3.2.6 Micro-computed Tomography (micro-CT)

The rat femurs and not the tibias, (due to the fact that the tibias were all embedded in PVA and could not fit into the scanner), were removed from -80°C storage and placed in a plastic tube mounted vertically in the Skyscan 1172 for micro-CT imaging. The system is composed of a sealed microfocus X-ray tube and a CCD camera. Images were obtained at 60V and 167μA. Specimens were studied packed with dry ice to remain frozen during scan, since it could take from 10 up to 20 minutes for a scan to complete as time passes. The pixel size used was 10μm with a rotation of 360° .The area of interest scanned was for 2mm towards the diaphysis with reference to the growth plate as the starting point. Reconstruction was carried out using the Skyscan Nrecon software. Trabeculae were selected with reference to the growth plate. A cross sectional slice was selected as growth plate reference slice, by moving slice by slice from the end of the growth plate through to the metaphysis and selecting the cross sectional level at which the primary spongiosa is obvious. Such a reference slice can be identified in all the scans. The regions of interest were selected with reference to the growth plate reference slice. Within the trabecular region separation from the cortical bone was performed using a free hand drawing tool for separating the regions of interest. The trabecular region commenced about 0.215- 1.74 mm from the growth plate in the direction of the metaphysis. After defining the region of interest (ROI) 2D and 3D histomorphometric parameters were obtained.

Microstructural measurements were obtained using a processing algorithm to produce binary images separating the trabecular and intertrabecular regions(marrow space). For 2D analysis, the total tissue area (TA: mm^2), bone perimeter (B.Pm: mm) and bone area (BA: mm^2) are determined directly from the ROI, while the trabecular number (Tb.N: /mm) was calculated as a derived parameter using Parfitt's definitions (1987), according to the parallel plate model, following the equation: **Tb.N 5 (BV/TV)/Tb.Th**

Tissue volume (TV: mm3), bone volume (BV: mm^3), bone surface (BS: mm^2), and the Tb.N (/mm) were directly measured. The fractional bone volume was obtained by BV/TV

(%).Trabecular thickness (Tb.Th) was then obtained following the equation of the parallel plate model: **Tb.Th 5 2/ (BS/BV)**

Trabecular separation (Tb. Sp) was also obtained by the parallel plate model following the equation: **Tb.Sp 5 (1/Tb.N) 2 Tb.Th**

3.2.8 Histomorphometry

Bone histomorphometry provides information regarding bone structure and remodeling process in a location within bone biopsies (Chavassieux and Delmas 2006). Histomorphometric indices are divided into primary such as measurements of bone surface (BS), volume (BV) (Parfitt 1987) and the derived measurements some of which would include mineralizing surface (MS) or bone formation rate (BFR/BS).

Using light microscopy, the bone surfaces were traced on sections from the samples maintained in the Zetos^{TM} system and analysis of bone surface (BS) was carried out using the bone histomorphometry software BIOQUANT OSTEO (Bioquant Image Analysis Corporation, USA). The sections used were collected from the 2.5mm distance and were stained for alkaline phosphatase activity as described earlier and measurement of bone surfaces was performed using the formula:

BS (mm) = Total Bone Surface - Artificial edges

3.2.9 Statistical Analysis

For all data analyses the statistical software package SPSS 14.1 for Windows was used. All data was checked for normal distribution by applying the Kolmogorov-Smirnov test. In cases where the randomly selected sample data were shown to have a normal (Gaussian) distribution parametric statistical tests such as one-way Analysis of Variance (ANOVA) and the post-hoc Tukey-Kramer and Bonferroni test were performed to determine statistical significance between the treatment groups. For comparison between percentages of osteocyte apoptosis used in this study, the square root of each percentage was transformed into its arcsine, which enabled the distribution of the data to be nearly normal allowing therefore the use of parametric tests. Tukey-Kramer post hoc test was also employed in all statistical analyses to determine significance between the treatment groups as it allows for comparison of more than two means without introducing the type I error associated with multiple t-tests (Zar 1984, Fielding and Gilbert 2000). Results are expressed as means ± SEM $p<0.05$ was considered to be statistically significant.

3.3 Results

3.3.1 Recombinant human parathyroid hormone (rhPTH) and recombinant human growth hormone (rhGH) treatment increases osteocyte viability in the rat tibia.

Following fourteen days of treatment with rhPTH at 50 μg/kg/day and rhGH at 2.5 mg/kg/day (Figure 3.6) was associated with significant increases in the number of viable osteocytes in both treatment groups. rhPTH treatment increased osteocyte viability to 506 ± 3.2 compared to 345 ± 5.4 in the control ($p= 0.001$). Similar effects to rhPTH treatment were observed with rhGH treatment which also increased osteocyte viability to 460 ± 9.1 compared to 345 ± 5.4 in the control ($p<0.05$) (figure 3.7).

3.3.2 Recombinant human parathyroid hormone (rhPTH) and recombinant human growth hormone (rhGH) treatment reduces osteocyte apoptosis in the rat tibia.

Treatment with rhPTH (50 μg/kg/day) and rhGH (2.5 mg/kg/day) resulted in a small decrease in the percentage of osteocytes undergoing apoptosis in the tibia (figure 3.8); however no statistically significant differences were observed. The proportion of osteocytes undergoing apoptosis was decreased to 0.52% ± 0.05 in the rhPTH treatment group and 0.56% ± 0.06 in the rhGH treatment compared to 0.59% ± 0.02 in the control group ($p>0.05$) (figure 3.9).

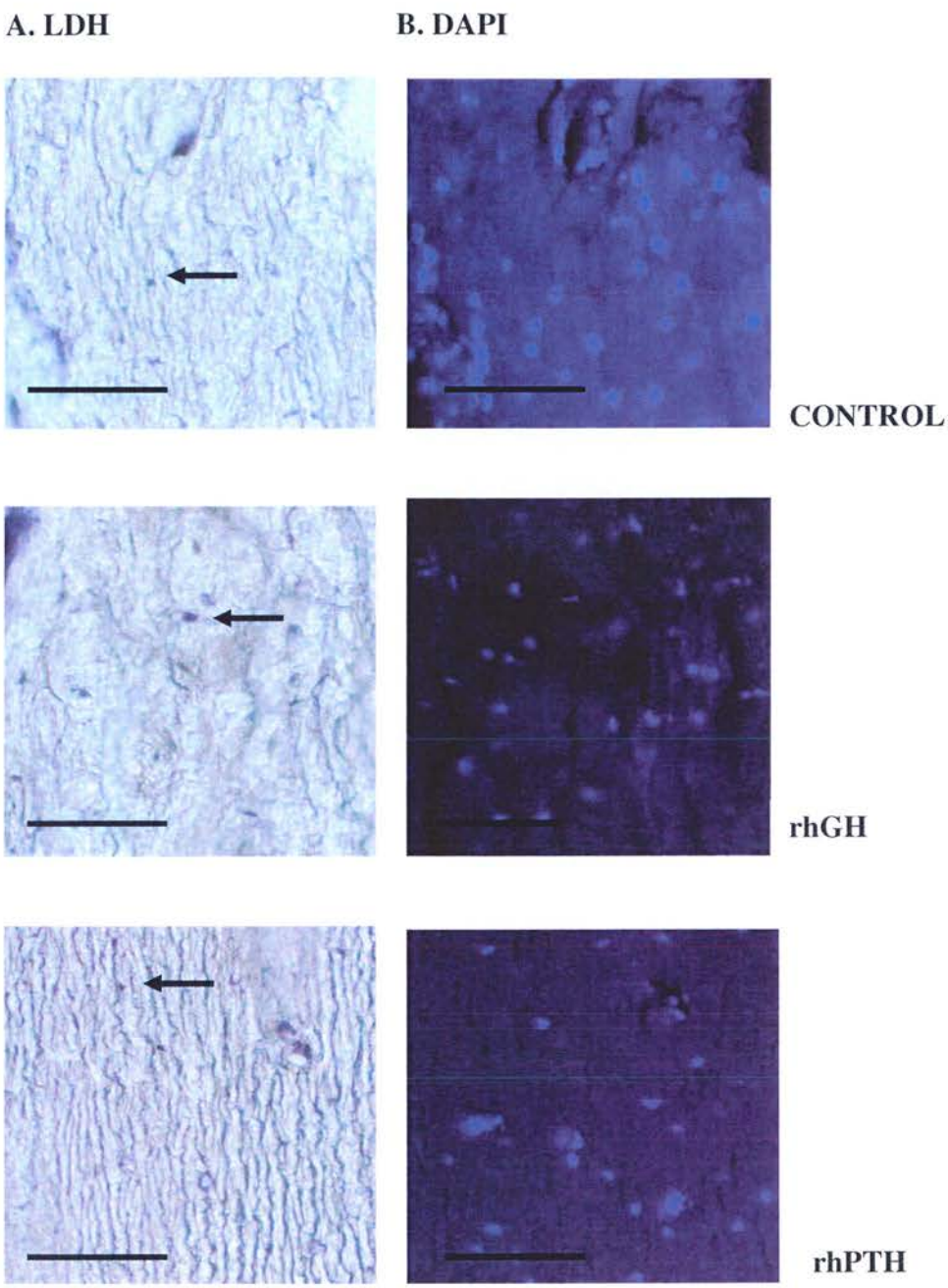

Figure 3.6 LDH representatives for all three treatment groups. Representative images of sections obtained from the secondary spongiosa of a control animal, an rhGH treated animal and an rhPTH treated animal, and stained for LDH activity. Viable osteocytes were distinguished by the presence of LDH activity in cells. Black arrows identify viable LDH-positive osteocytes. Bar represents 100μm.

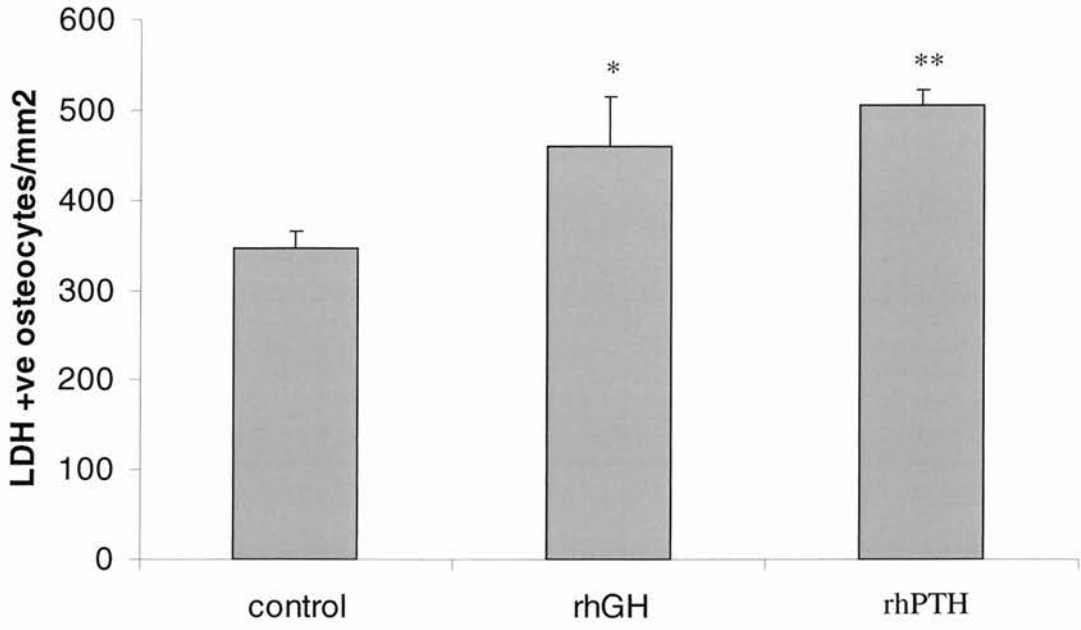

Figure 3.7 The number of LDH positive osteocytes per bone area following 14 days of treatment with rhPTH and rhGH. The number of viable osteocytes (LDH positive cells) per bone area (mm^2) 14 days post-hormone treatment. Hormone treatment increased the numbers of viable osteocytes. Sections were studied for the presence of cellular LDH activity. Results are expressed as the number of total osteocytes displaying positive staining for LDH ± SEM * = $p<0.05$ and ** = $p<0.001$ denote significant differences when compared to control.

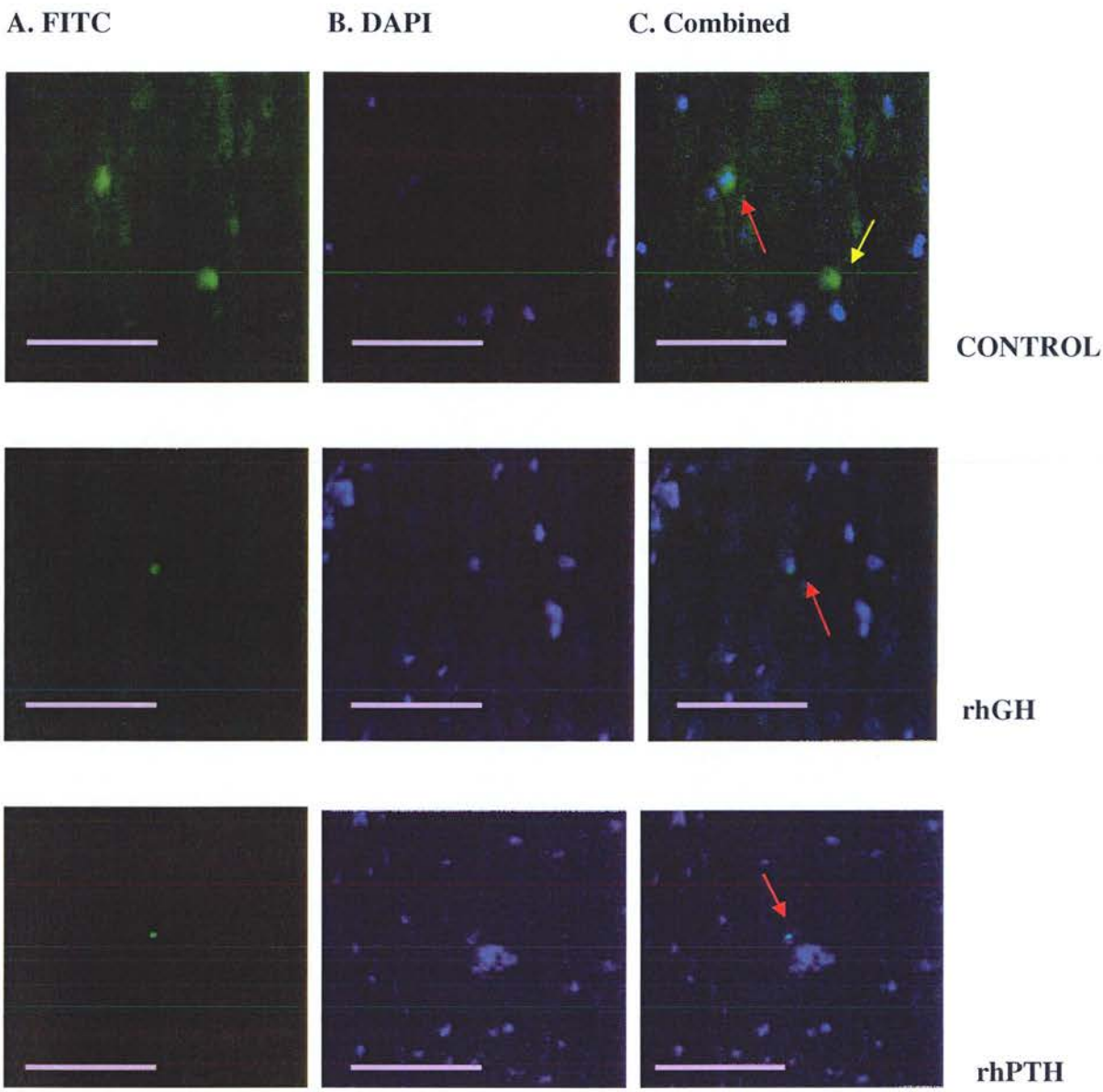

Figure 3.8 Nick translation representatives for all three treatment groups. Representative images from the secondary spongiosa of rat sections treated with rhGH and rhPTH in vivo for 14 days and reacted with the nick translation mixture in order to identify apoptotic osteocytes (FITC-green). Red arrows identify apoptotic osteocytes. Bar represents 100 μm.

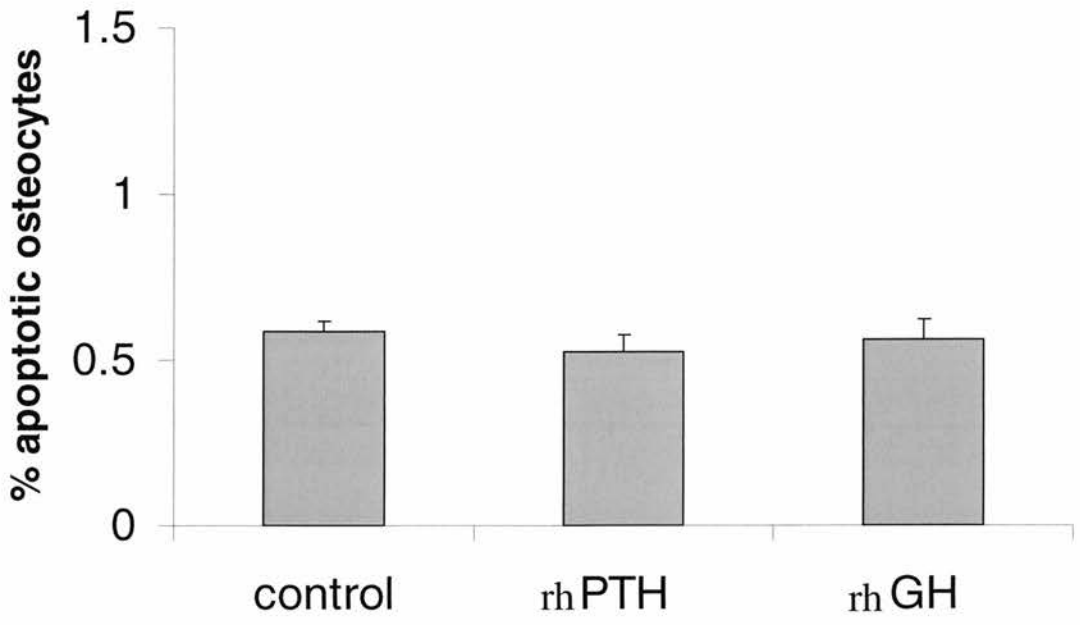

Figure 3.9 The percentage of osteocytes displaying evidence of DNA fragmentation in situ after 14 days of rhPTH and rhGH hormonal treatment. rhPTH and rhGH treatment resulted in a trend towards a decrease in the percentage of osteocyte undergoing apoptosis in situ after 14 days of treatment. Sections were obtained from the secondary spongiosa of the tibia and studied for the presence of fragmented DNA material using an in situ nick translation technique. Results are expressed as the mean percentage of total osteocytes displaying positive staining for fragmented DNA ± SEM.

3.3.3 Trabecular structure parameters measured using micro-computed tomography (μCT).

Trabecular structure parameters were measured using μCT as described in §3.2.6. Trabecular bone volume (BV/TV) and trabecular thickness (Tb.Th) were greater in the rhPTH and rhGH treatment groups compared to the control group (figure 3.10). Trabecular separation (Tb.Sp) was lower in the rhPTH and rhGH compared to the control. Analysis by means of μCT revealed that BV/TV was significantly greater in the rhPTH group compared to the control group (46% ± 7.41 vs. 20% ± 5.81 respectively, $p<0.05$). In contrast no significant difference was found in the BV/TV measurement between the rhGH treatment group and the control group (31% ± 3.17 vs. 20% ± 5.81, respectively, $p>0.05$). Trabecular thickness (Tb.Th.) was significantly greater in the rhPTH treatment group compared to the control (122μm ± 10.38 vs. 81μm ± 12.1 respectively, $p<0.05$), whereas no difference was observed between the rhGH group treatment and the control group (95μm ± 0.61 vs. 81μm ± 18.1 respectively). Trabecular separation (Tb.Sp.) was significantly lower in the rhPTH treatment group compared to the control (168μm ± 2.9 vs. 251 μm ± 1.71 respectively, $p<0.05$), whereas no significant difference was found between the rhGH treatment group and the control group (195μm ± 3.9 vs. 251μm ± 1.71) respectively (figure 3.11).

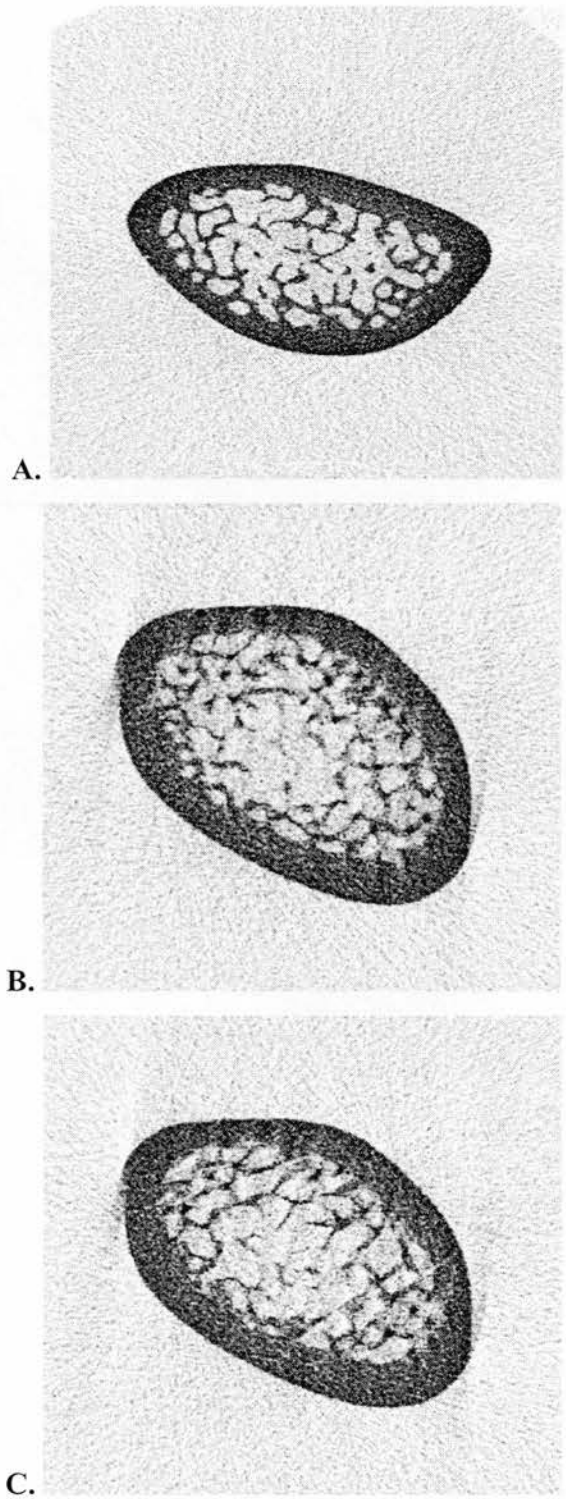

Figure 3.10 Two-dimensional images of the femoral metaphysis using micro-computed tomography. Representative 2D images derived from the μCT analysis for (A) Control, (B) rhPTH and (C) rhGH.

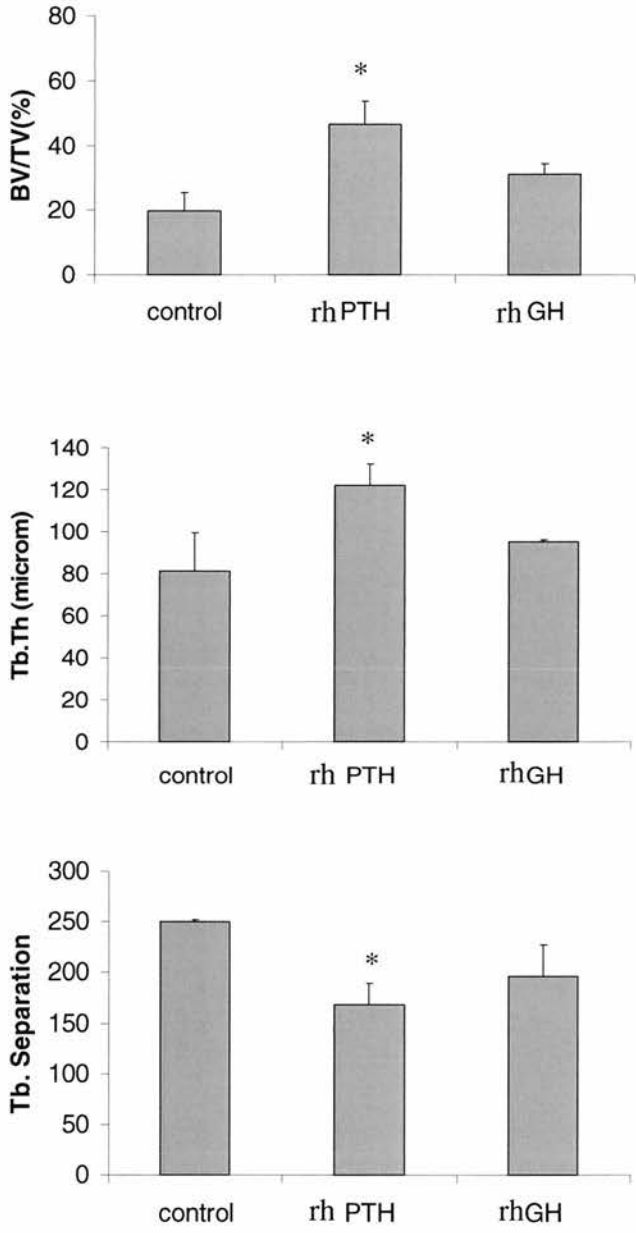

Figure 3.11 Effects of rhPTH and rhGH treatment on the three-dimensional structure in trabecular bone of the distal femur. rhPTH treatment significantly increased BV/TV and Tb.Th and decreased Tb.Sp compared to the control. No significant differences were found between the rhGH treatment and the control. Results are expressed as mean percentages of individual indices ± SEM * = $p<0.05$ denote significant differences when compared to control.

3.3.4 The effect of rhPTH and rhGH on osteocyte sclerostin expression.

Sclerostin was located in osteocytes, whereas lining cells and osteoblasts were negative. The immunostained osteocytes were mainly located in the inner bones areas, while a few positive osteocytes were visible near the endosteal surfaces. Treatment with rhPTH (50μg/kg/day) and rhGH (2.5mg/kg/day) resulted in non significant differences in the numbers of osteocytes expressing sclerostin, when compared to control (53 ± 1.16, 64 ± 7.17 vs. 63 ± 4.1, respectively, $p>0.05$) (figure 3.12). Figure 3.13 shows representative images of sclerostin staining for the three treatment groups.

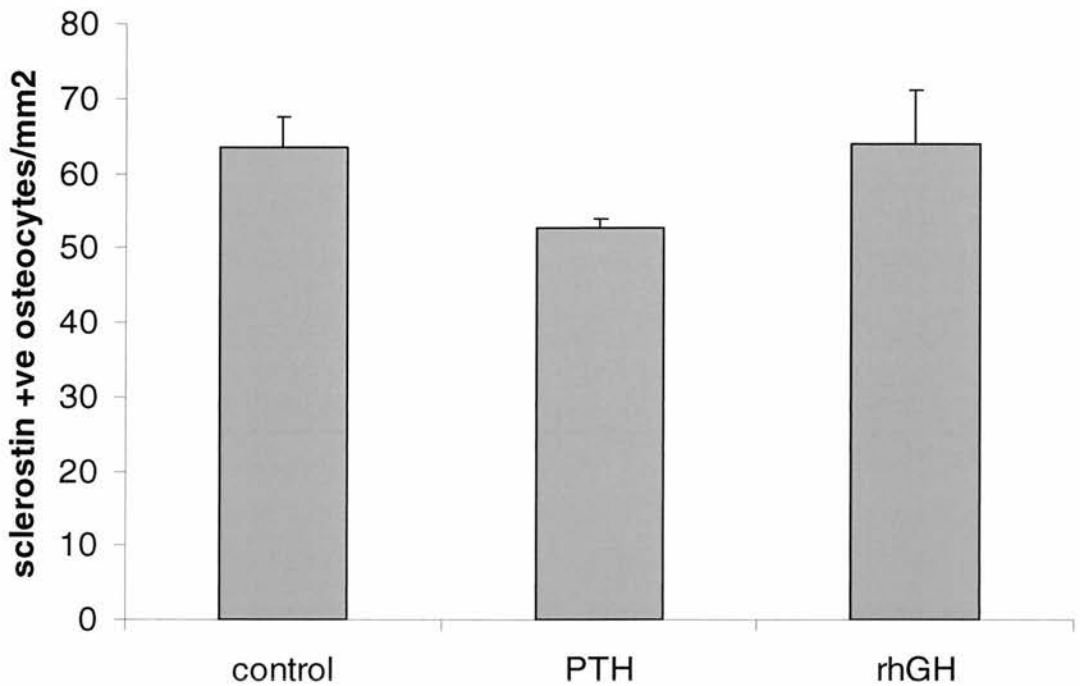

Figure 3.12 The number of sclerostin positive osteocytes per bone area in the rat tibial metaphysis. The number of sclerostin positive osteocytes was not significantly altered between treatment groups. Sections were studied for the presence of sclerostin expression, via means of immunostaining. Results are presented as numbers of sclerostin positive osteocytes ± SEM.

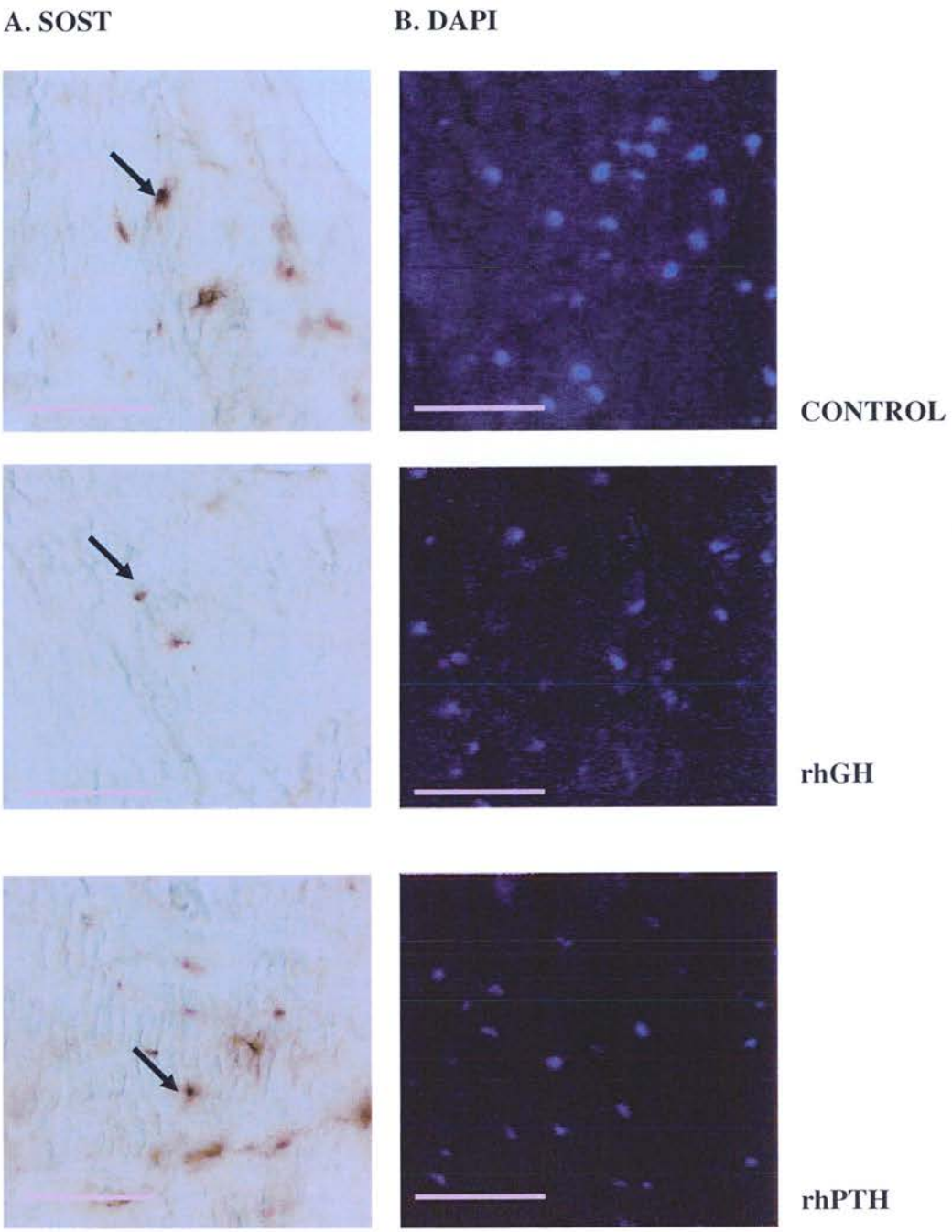

Figure 3.13 Representative images for sclerostin staining for the three treatment groups. Representative sections of trabecular rat bone stained for sclerostin expression in rat osteocytes. Arrow identifies sclerostin positive osteocytes. Bar represents 100μm.

3.4 Discussion

In the previous chapter evidence has been presented to demonstrate the protective effects of rhPTH and rhGH in osteocyte-like cells *in vitro*. In the study presented here the effects of these compounds were tested *in vivo*. Evidence has been presented to show that short term hormone treatment can promote osteocyte viability as well as improving bone architecture, in the aged female rat.

The decline of osteocyte numbers has been related with ageing and disease states such as osteoporosis, with the number of viable osteocytes in the human femur declining from 90% in the first decade to 20% in the 9th decade (Dunstan et al. 1993), resulting in skeletal fragility and increased fracture incidence. Anabolic treatments such as PTH and GH hold much promise in restoring bone mass and architecture. To test this hypothesis in the present study rhPTH and rhGH were administered in aged female rats.

In this study a decrease in osteocyte apoptosis from age-related apoptosis in the tibia of female rats following rhPTH treatment was observed; but the differences were not statistically significant. A possible explanation for this finding lies on the short duration of the experiment or the advanced age of the animals. It seems possible that the gain in bone volume as noted by the micro-CT analysis was primarily due to an increase in trabecular thickness, possibly due to an increase in osteoblast number and to a lesser degree in osteoblast activity, as it was previously shown in older animals, where PTH treatment rapidly activated bone lining cells to express the osteoblast phenotype (Dobnig and Turner, 1995). Several other studies in adult and aged rats have shown that the increase in bone mass induced by PTH is predominantly due to trabecular thickening (Turner et al. 1998, Wronski et al.1999, Kneissel et al. 2001) and not due to the suppression of osteoblast and osteocyte apoptosis. These data suggests that the process of ageing and the increase in quiescent bone surfaces covered with bone lining cells forms the basis for the anabolic effects of PTH on bone. Support for this hypothesis comes from reports where the PTH-induced bone gain appears to result from direct activation of bone lining cells on cancellous and cortical surfaces (Gasser 2003).

At present the molecular mechanisms of PTH anabolic actions are not fully understood. However the recently identified gene SOST and its protein product sclerostin have been recognized as potent negative regulators of bone formation (van Bezooijen RL. 2007, Bellido et al. 2005, Keller and Kneissel 2005, Li et al. 2005, Boyden et al. 2002, Brunkow et al. 2001). In the present study sclerostin expression in the secondary metaphyseal trabeculae of the rat tibia was investigated. rhPTH treatment resulted in a decrease in the number of sclerostin positive osteocytes with no statistically significant differences noted. Sclerostin positive osteocytes where located in the inner zone of bone, which is in agreement with previous studies (van Besooijen et al. 2006, Poole et al. 2005, Silvestrini et al. 2007), supporting the finding that it is only expressed by mature osteocytes. This finding is suggestive of the possibility that sclerostin down regulation may not have an important role in mediating the anabolic effects of rhPTH in skeletally mature animals. On the other hand bone architectural changes occurred in the rhPTH treated group, as shown by the bone formation indices via means of micro-CT. Although no fluorescent markers of bone formation had been administered and no secure assessment of the degree of bone formation could be formulated, an enhancement in bone architecture in rhPTH treated rats was shown by a significant rise in trabecular thickness together with a tendency towards a rise in BV/TV and towards a fall in trabecular separation. It is possible to hypothesize that PTH-mediated sclerostin reduction could be critical in regulating bone remodeling. However no secure conclusions can be drawn regarding the role of sclerostin from the data presented in this study since sclerostin is a delayed secreted product of osteocytes (Poole et al. 2005) and possibly SOST gene expression and protein quantification may provide more information regarding its effect *in vivo*. Along the same line rhGH treatment did not change the number of sclerostin positive osteocytes compared to the other treatment groups, there is no other report in the literature regarding rhGH and sclerostin expression and further studies are necessary to confirm these findings.

On the other hand rhGH treatment has been reported to increase the markers for bone resorption and formation within the first week of administration in postmenopausal osteoporotic women and men with idiopathic osteoporosis (Andreassen and Oxlund

2000, Andreassen et al. 1996). Fluorochrome labeling has shown that GH induces periosteal bone deposition at the diaphysial bone surfaces of long bones without influencing the endocortical surfaces of these bones (Andreassen et al, 2000). On withdrawal from GH the labeling persists six weeks later indicating that new bone is preserved upon cessation of treatment contrary to PTH treatment where bone is quickly resorbed after withdrawal from treatment (Ejersted et al. 1998). In line with these findings, in this study improvements in bone volume, trabecular separation and thickness where observed as indicated by micro-CT analysis of the femurs, compared to control, following rhGH treatment; however these differences where found not to be statistically significant. This may be explained by the fact that in old rats no linear growth occurs and as such treatment with rhGH does not influence bone volume or trabecular thickness.

However rhGH administration in this study had a significant effect on osteocyte viability, with a non statistically significant effect on apoptosis. This finding as for rhPTH treatment could be due to the duration of the experiment or the age of the animals. In addition as mentioned earlier mature osteocytes do not possess GH receptors and as such rhGH administration is unlikely to stimulate osteocytes directly. However *in vitro* and *in vivo* studies have revealed that GH can stimulate bone turnover either directly and/or indirectly through local IGF production, since it increases osteoblast number and activity (Neuberg et al. 1997, Wong et al. 2000, Ueland 2004, Niu and Rosen 2005). In bone, no reports exist so far to report any anti-apoptotic effects of IGFs on osteocytes; however the targeted overexpression of IGF-I in osteoblasts has been shown to increase the osteocyte lacunae occupancy without changing the osteoblast number, suggesting that IGF-I plays an autocrine role in osteocyte generation and life spun (Zhao et al. 2000).

In conclusion, treatment with rhPTH and rhGH increased osteocyte viability and resulted in a decrease in osteocyte apoptosis associated with ageing, with no statistical significance; and an improvement of trabecular architecture. The rhPTH effect was more marked than that of rhGH in terms of osteocyte viability and decrease in apoptosis as well as in micro-CT indices measured. These differences may be partially explained by the fact that osteocytes possess receptors for PTH but not for GH, thus GH treatment

exerts indirect effects to the osteocytes possibly through the GH/IGF-I axis, *in vivo*. Evidence to a GH protective effect *in vitro* via a potential stimulation of growth factors has also been presented in chapter 2, where osteocyte-like cells in low serum effectively repaired their plasma membrane and survived injury following treatment with rhGH. Although the exact signaling pathways of the effects of these hormones on bone were not investigated in this study, the current hypothesis that osteocytes are important in maintaining bone quality and affecting bone formation, possibly through the secretion of sclerostin (Keller and Kneissel 2005, Bellido et al. 2005) and resorption (Noble et al. 2003), receives lots of interest. However in this study no conclusions can be drawn regarding the effect of sclerostin in the skeletally mature rat; further studies are needed to determine whether changes in the osteocyte-derived sclerostin are involved in the control of bone formation by other hormones, locally produced growth factors, or mechanical stimuli as discussed in chapter 4; and whether regulation of other osteocyte products by PTH or GH are involved in the effects of these hormones in bone. Finally it should be noted that the original study design for this *in vivo* study was not intended for the analysis presented in this chapter but for the microarray study discussed in chapter 5. For this reason a number of experimental weaknesses can be identified. Firstly no fluorescent markers were administered so as to measure bone formation rate in the ageing rat skeleton following hormone treatment, to avoid disturbance of the cells of interest. Also the tibias were used for two different studies and as such only one tibia was available for analysis in each study, and because of the original study design the tibias were not processed differently for RNA and protein extractions which would be useful for further analysis.

CHAPTER 4

The Influence of Mechanical Stimulation and Recombinant Human Parathyroid Hormone on Osteocyte Apoptosis and Bone Viability in Human Trabecular Bone

Abstract

Data presented in the previous chapters have demonstrated the beneficial effects of rhPTH administration on the viability and apoptotic death of murine osteocytes *in vitro* and rat osteocytes *in vivo*. In this study the effect of an anabolic regime of rhPTH on the viability of osteocytes and osteoblast in human trabecular bone explants *ex vivo* in the presence and absence of mechanical stimulation using a 3D bioreactor system (Zetos^{TM}) was investigated.

Bone cores 10mm x 5mm in size prepared from human femoral head explants were incubated in the bioreactor for 7 days and subjected either to disuse conditions, physiological loading regime on a daily basis or rhPTH treatment every day as a 4 hours pulse in the presence or absence of mechanical loading. Following 7 days in culture; osteocyte viability as determined by LDH activity, apoptosis as determined by in situ nick translation technique, sclerostin and SOST gene expression and osteoblast alkaline phosphatase activity were measured.

Results suggested that application of mechanical loading at physiological levels improved osteocyte viability and significantly reduced osteocyte apoptosis compared to disuse conditions. Administration of rhPTH reduced osteocyte apoptosis in the presence and absence of mechanical stimulation. Furthermore application of mechanical stimulation did not change the numbers of osteocytes expressing sclerostin in the presence or absence of rhPTH compared to T (0) controls. Similar observations were made under unloading conditions in the presence or absence of rhPTH compared to T(0) controls. On the contrary the relative SOST gene expression (mRNA) decreased in the presence or absence of mechanical stimulation following administration of rhPTH.

These data have indicated that application of physiological loading in human bone using the bioreactor system inhibited osteocyte apoptosis and increased alkaline phosphatase activity. Furthermore, administration of rhPTH appeared to reduce apoptosis and improve viability of osteocytes.

4.1 Introduction

Wolff's law states that bone has the ability to adapt to its loading environment, (Wolf J., 1892); this is done through the remodeling process that is mediated by the bone cells-the osteoblasts, the osteocytes and the osteoclasts. Osteocytes have been shown to be able to sense the strains produced in their surrounding environment and produce or modify molecules such as nitric oxide (NO), prostaglandin (PGE_2) and collagen type I gene expression (Pitsillides et al. 1995, Ajubi et al. 1999). Production of these signals have a subsequent effect on the function of bone effector cells and regulation of the bone remodeling process in order to allow the skeleton to adapt efficiently to daily mechanical requirements (Burger et al. 1995, Lanyon 1993, Mullender and Huiskes 1997).

Studies have reported an age-related decline in osteocyte viability (Frost 1960, Dunstan et al. 1993, Qiu et al. 2005) which may result in reduced or impaired response in detection of mechanical strain and microdamage and lead to inappropriate bone remodelling, accumulation of microdamage in bone (Mori et al. 1997), loss of bone architecture and increased fracture risk (Burr et al. 1985, Parfitt 1993). The mechanism by which osteocytes may regulate the remodeling process is not fully understood. There are a number of reports in the literature which have provided evidence to suggest that the death of osteocytes through apoptosis might be providing the signals to regulate bone remodeling (Kaneko et al. 1997, Noble et al. 1997, Verborgt et al. 2000, Noble et al. 2003, Kogianni et al., 2004, Aguirre et al. 2006, Kogianni et al., 2008) since osteocyte apoptosis has been documented to be associated with increased resorptive activity in response to estrogen deficiency (Tomkinson et al. 1997, 1998) and exposure to glucocorticoids (Weinstein et al. 1998, Kogianni et al., 2004). Moreover it has been suggested that a U-shaped relationship exists between the survival of osteocytes and the loads produced in their environment in a way that low or excessive strains lead to osteocyte apoptosis following microdamage (Noble et al. 2003). This hypothesis might provide evidence for a possible causal mechanism by which signals derived from apoptotic osteocytes can regulate bone architecture (Noble et al. 2003).

For the growth, maintenance and repair of bone a number of non-mechanical agents such as PTH, which increases bone mass by adding bone on both endosteal and periosteal envelopes is necessary. However, hormone release appears to decline with age and that may be affecting the sensitivity of bone cells to mechanical loading (Jee and Tian, 2005). In this study the effect of rhPTH in the presence or absence of mechanical loading was tested. A line of evidence is available to show the effectiveness of combining PTH with mechanical loading. Gasser and colleagues (1998) reported that unloaded vertebral bodies in rats responded poorly to PTH administration, while Chow et al., (1998) found a synergistic effect of PTH and mechanical loading. Moreover it was found that trabecular bone density was higher in the regions of lumbar vertebrae under the highest compressive loading forces in women (Cann et al., 1997).

Mechanical loading improves bone mass and strength by stimulating the addition of new bone onto bone surfaces experiencing high strains, whereas sites experiencing small strains remain quiescent. At the cellular level the mechanisms involved in directing new bone formation to the high strain regions of a loaded bone are unclear (Robling et al. 2006). However significant progress has been made in understanding some of the basic mechanisms of mechanotransduction in bone. An important finding is the requirement for Wnt signaling through Lrp5 in mechanically induced bone formation, as mice with a loss of function mutation in Lrp5 were unable to respond anabolically to mechanical stimulation (Sawakami et al. 2006), suggestive of Wnt/Lrp5 signaling being an integral part of the mechanotransduction cascade in normal bone tissue.

Sclerostin, the protein product of SOST gene is a potent inhibitor of bone formation (Robling et al. 2008). Mutation in the SOST gene causes sclerosteosis and Van Buchem disease (Brunkow et al. 2001), patients with such mutations exhibit high bone mass. Sclerostin was originally characterized as a BMP antagonist but more recently it has been shown to bind to LRP5/6 (Li et al. 2005). Consequently, sclerostin raises the possibility for regulating mechanically induced signaling through the Lrp5 receptor; moreover sclerostin expression is specific to mature osteocytes (Poole et al. 2005, van Bezooijen et al. 2005) which are hypothesized to be the mechanosensor in bone, due to the population

density, distribution and extensive communication networks within bone (Cowin 2002). However there is little data to support this hypothesis (Cowin 2002) and as such the discovery of an osteocyte specific factor that has been shown to be mechanically regulated (Robling et al. 2008, 2006) and can reach the osteoblasts, with known effects on the Wnt/Lrp5 mechanotransduction signaling pathway , could be an alternative explanation for osteocytic mechanotransduction. In this study the regulation of SOST/sclerostin in the presence or absence of mechanical stimulation in a bioreactor following rhPTH administration was investigated in human osteocytes.

Studies have shown that the application of mechanical loading that produced strains within the physiological range appeared to preserve osteocyte viability compared to the unloaded conditions *in vivo* (Noble et al. 2003) and ex vivo (Lozupone et al. 1996) as well as to provide an osteogenic stimulus required by the bone tissue in order to maintain its structure and function (Frost 1988, Lanyon 1996, Robling 2000). When mechanical stress was applied on osteoblast-like cells, increased calcium content and ALP activity as well as DNA content was reported to be increased (Winter at al., 2002) showing that loading affects the osteoblast behavior as well.

Although there are a number of studies reporting the effectiveness of combining PTH with mechanical load in animals, such studies prove difficult to undertake in human bone due to inability to obtain human bone explants before and after exercise and maintaining viable cultures of bone explants *ex vivo* (Jones et al., 2003).

These difficulties can now be partially overcome by the use of the Zetos^{TM} culture system that allows the bone cells to interact with each other and the extracellular matrix; while the controlled application of mechanical loading or the administration of hormones and growth factors might enable the study of bone remodeling and growth factor or hormone interactions in normal and pathological bone in a controlled environment (Jones et al. 2003, Davies et al. 2006). The Zetos^{TM} culture system can provide a better understanding of skeletal physiology as the bone structure can be maintained in its 3D structure in near to physiological environment with a constant supply of nutrients and oxygen (Jones et al. 2003).

This study has investigated the effects of the controlled perfusion of rhPTH in an intermittent mode (anabolic action) in the presence or absence of mechanical loading; on the maintenance of the osteocytic population as well as SOST and sclerostin expression along with osteoblastic alkaline phosphatase activity in human bone after 7 days in culture in the Zetos ^{TM} bioreactor.

4.2 Materials and Methods

Unless indicated otherwise, all reagents were purchased from Sigma, UK. Preparation and culture of bone tissue was performed in a sterilised environment using sterile equipment.

4.2.1 Zetos^{TM} description

The Zetos^{TM} system consists of two parts; a set of diffusion chambers in which cancellous bone cores are maintained; which is connected to growth media supply via a peristaltic pump; and a computer-controlled loading device used to apply daily physiological mechanical stimulation to individual cores (Figure 4.1) (Davies et al. 2006). The system is designed to do three things: 1. apply all sorts of mechanical waveforms-frequencies and amplitudes to investigate mechanotransduction in bone and cartilage, 2. ensure the mechanical properties of the biological material and 3. maintain the material in as good a codition as possible. The bone cores are compressed axially by a piezoelectric actuator (PZA). Strain gauges on the PZA and a force sensor above it provide output signals of expansion and applied force, respectively. Force and specimen deformation are recorded and the bone stiffness determined (Jones et al. 2003).

Within the diffusion chambers individual bone cores are housed and supplemented with control media, and subjected to daily mechanical loading. Chambers contain a loading piston at the top plate which transmits the loading force to the bone core while the bottom plate is open in order to measure bone deformation at the bottom of the plate. The growth media is pumped continuously around the system by the use of a perfusion pump that can supply media to multiple chambers simultaneously. The loading device is controlled by a computer programme that can apply a defined load to the bone cores (Jones et al. 2003).

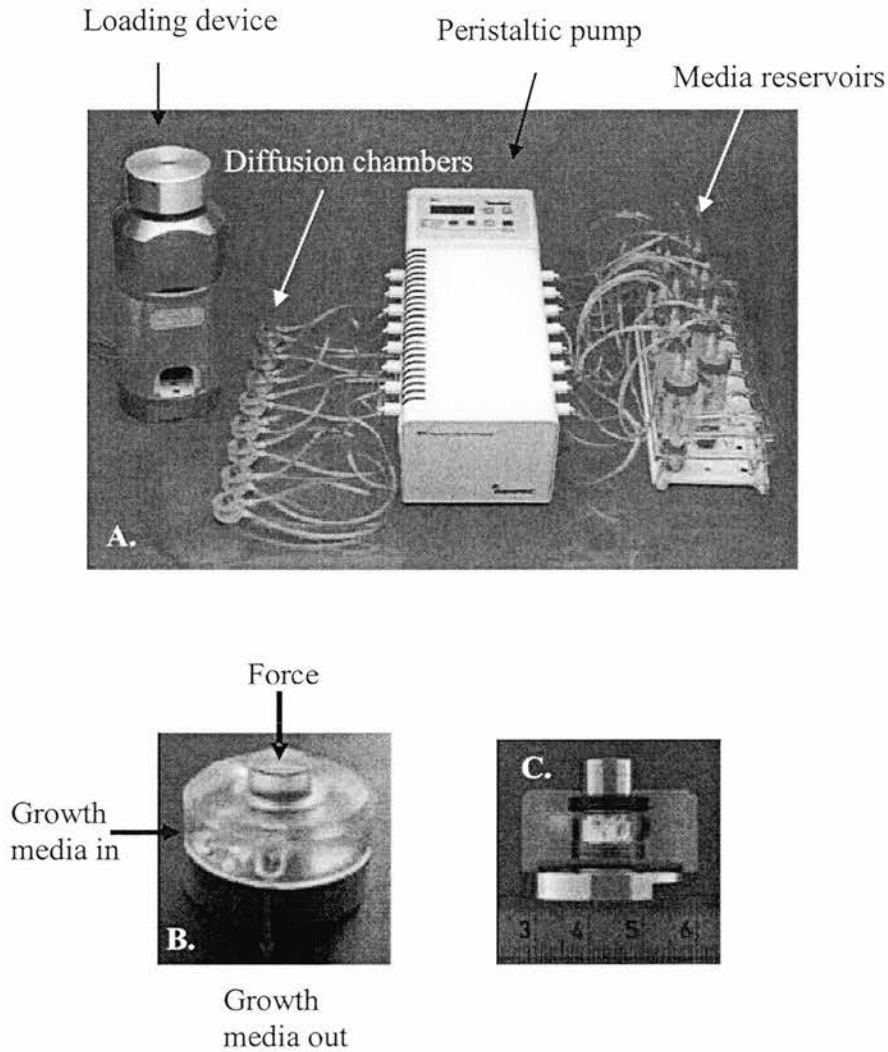

Figure 4.1 The Zetos™ system. The Zetos™ bioreactor consists of a loading device controlled by a computer and diffusion chambers perfused with media through individual reservoirs with the aid of a peristaltic pump (A). Zetos™ bone loading champer (B) and cross section of a bone specimen in a loading champer (C).

4.2.2 Preparation of human biopsies for culture

Excised femoral head tissue was obtained, with written consent and with the approval of the local ethical committee, from patients undergoing elective arthoplasty. A total of three patient samples were collected (Table 4.1).

The samples were collected in sterile PBS and transferred to the lab following surgery, with processing taking place within 2 hours. Femoral heads were first cut into 8mm slices in thickness using an Exackt 310 diamond-coated band saw (Figure 4.2). All preparation was performed under sterile conditions and during cutting and drilling the bone was irrigated with cold PBS in order to minimize heat-induced damage to the tissue and to prevent the bone from drying out (Davies et al. 2001). Cylindrical bone cores at 10mm in diameter were drilled from each of these 8 mm-thick slices (Figure 4.2) using a diamond-coated hollow drill (developed in house), while their height was adjusted to 5mm (± 2μm) with the Exackt 310 diamond coated band saw. The bone cores were then thoroughly washed three times for 10 min in Hank's Balanced Salt Solution (HBSS) at 37°C, and subsequently washed for 20 min in HBSS supplemented with the antibiotics Penicillin/Streptomycin (50IU/ml) (Invitrogen, UK), gentamycin (10mg/ml) and the antimycotic amphotericin B (4μg/ml). Cores from each individual patient were assigned into four groups (cores from each individual patient were used for one experiment); explants that were subjected daily to mechanical stimulation (n=3), explants that received daily rhPTH treatment and subjected to mechanical stimulation (n=3), explants that received daily rhPTH treatment in the absence of mechanical stimulation (n=3) and explants that did not receive neither rhPTH nor mechanical stimulation (n=3).

4.2.3 Controls of the study

As described in § 4.2.2, bone core samples that were left untreated were included in the Zetos ™ chambers in order to provide negative controls for mechanical stimulation or rhPTH treatment. Besides the untreated controls that were incubated in the Zetos™ bioreactor for 7 days, the study was provided with additional control samples that were not included in the Zetos™ chambers. Three bone cores from each patient T (0) were frozen immediately in cold hexane at the end of the harvesting procedure to provide an indication of the tissue state at the start of the experiments and to act as positive controls for cell viability assays.

Patient	1	2	3
Gender	Male	Female	Male
Age	46	57	60

Table 4.1. Patient samples

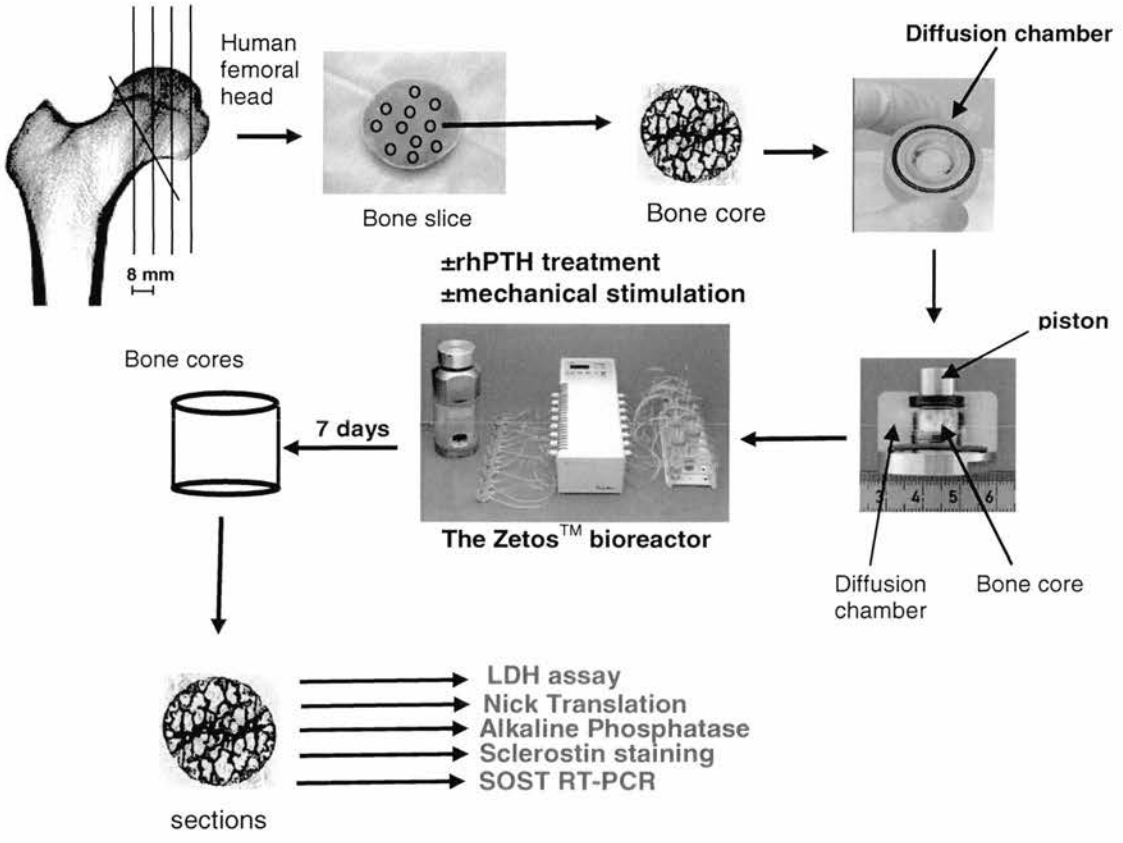

Figure 4.2. Schematic overview of the experimental setup using the 3D bioreactor system (Zetos™). Human trabecular bone cores were drilled from 8 mm-thick bone slices obtained from each individual human femoral head and housed within the diffusion chambers. Cores were assigned into four different treatment groups and maintained in the Zetos™ bioreactor for a period of 7 days. Following that period, cores were frozen and sections were collected from each core for subsequent analysis for osteocyte viability, apoptosis, alkaline phosphatase indices, sclerostin expression and SOST gene expression.

4.2.4 Maintenance of bone cores in the Zetos ^{TM} system

Individual cores were inserted in the diffusion chambers and were left overnight at 37 ^{0}C to settle prior to initiation of the experiment. Each diffusion chamber was connected to individual media reservoir via a peristaltic pump system allowing continual perfusion (7ml/hour) of the bone tissue with culture media. Individual bone cores were perfused with Dulbecco's Modified Eagle medium (DMEM) (Gibco, UK) containing 10% FCS, 10mM HEPES, 2mM L-glutamine (Gibco, UK), (10μg/ml) L-ascorbic acid-2-phosphate, 5mM β-glycerophosphate disodium hydrate, 0.14mM $NAHCO_3$ and Penicillin (50 IU/ml) Streptomycin (50μg/ml) (Gibco, UK). The bone cores were maintained in an environmental chamber set at 37°C for 7 days with media being replaced daily in order to provide adequate oxygen supply and clear out the cores receiving rhPTH treatment. Throughout the experimental period, the pH of the media in each diffusion chamber was closely monitored (~ pH 7.25) in order to ensure a physiological pH value during the maintenance of the cores in the Zetos^{TM} bioreactor.

4.2.5 Loading of the samples

A daily compressive mechanical loading of 5 minutes duration was applied to the bone cores on a daily basis; a 1 minute static load to ensure that the core is placed properly in the chamber followed by a 3 minute dynamic load. The applied forces resulted in strains of 3000 μstrain at a frequency of 1 Hz, in a waveform that corresponded to physiological jumping movement, based on preliminary studies in bovine bone (Figure 4.3), (Mann et al. 2004, 2006).

4.2.6 Treatment with rhPTH

rhPTH was prepared from an initial stock of 10mM and was further diluted to 7μM in normal medium. Samples then received treatment with rhPTH at 1μl/ml in normal medium to give a final concentration of 7nM. Treatment was administered at the beginning of the experiment (day 1) and was supplied as a 5 hour pulse every 24 hours for the 7 days of the experiment (figure 4.4).

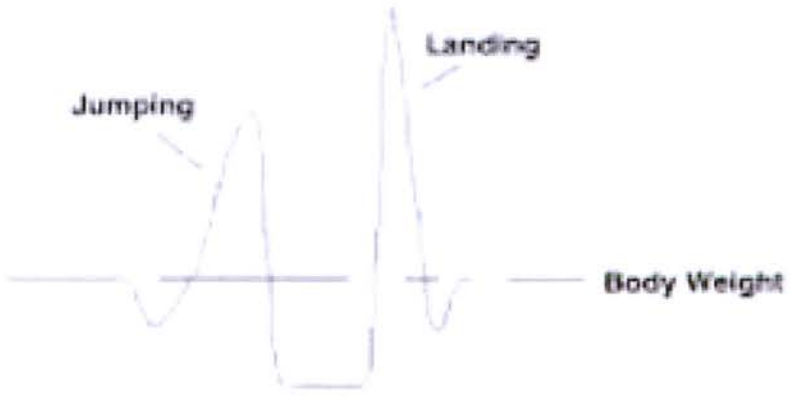

Figure 4.3. Waveform diagram for the jumping stimuli. The waveform shown above was used for a jumping signal that was used to provide the high impact stimulus used in this study.

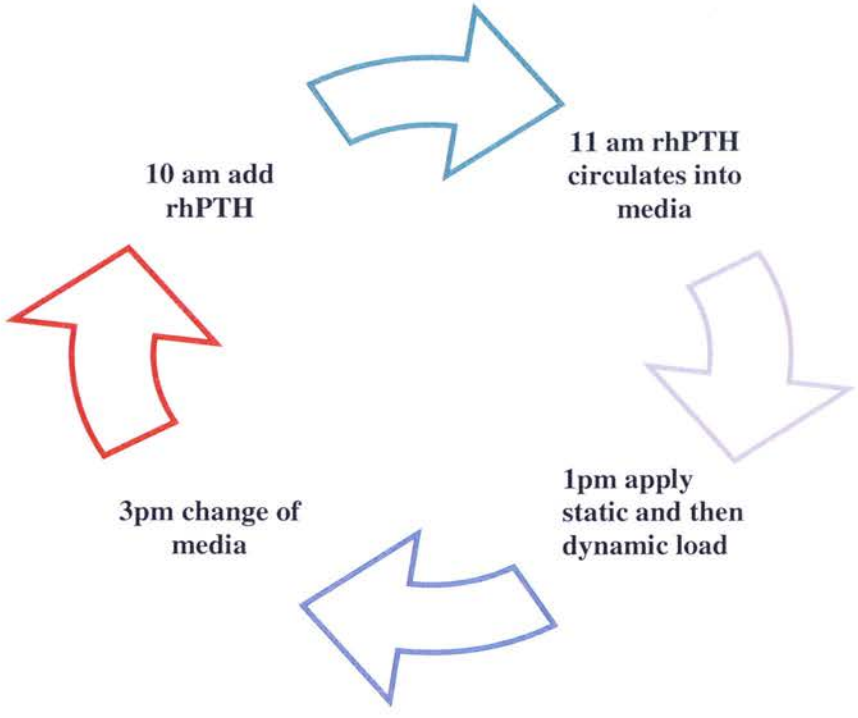

Figure 4.4 Schematic representation of the rhPTH treatment regime. rhPTH was administered as a 5 hour pulse in 24 hours.

4.2.7 Sample processing

After 7 days in the bioreactor, cores from each individual experiment were taken out of the champers and immersed in 5 % polyvinyl alcohol and snap frozen in hexane (BDH, UK) prior to storage at -70 ^{0}C. Transverse cryostat sections of 7μm in thickness were cut from the chilled material using an ultra pure tape for sections (Taab Laboratories, UK) and transferred to Superfrost slides (Western Laboratory Services, UK) for further analysis. The use of the ultra pure tape allowed better adhesion of the bone sections onto the slides. In order to broadly identify appropriate regions for subsequent analysis 6 sections were randomly collected from distances 0-0.5mm and 1-2.5mm from the upper surface of the bone cores as outlined in table 4.2 and figure 4.5.

4.2.8 Cell viability assessment in situ

Osteocytes that were viable at the time of sampling were identified in cryostat sections by means of their lactate dehydrogenase (LDH) activity as described in §3.2.2. The number of LDH positive osteocytes, representing the viable osteocytes, was expressed as a percentage of LDH positive osteocytes over the total number of cells. LDH staining was performed on four consecutive sections taken at 1 mm and 2.5 mm distances through each of the bone cores and six image fields were analyzed per section.

Percentage of viable osteocytes (%) =

$$\frac{\text{The number of LDH positive osteocytes}}{\text{The number of DAPI stained osteocytes}} \times 100$$

Treatments	No of cores /treatment /patient	No of sections /distance/ patient	Total no of sections/ distance/ treatment/ patient	No of fields/ Section/ patient	Total no of fields /distance /treatment/ patient
T0	3	4	12	6	72
Unloaded	3	4	12	6	72
Unloaded+rhPTH	3	4	12	6	72
Loaded	3	4	12	6	72
Loaded +rhPTH	3	4	12	6	72

Table 4.2. Outline of sections collected and fields analysed from each distance. Four sections were collected from each distance per core and six fields of view were analysed for each section, for each of the outcome measures.

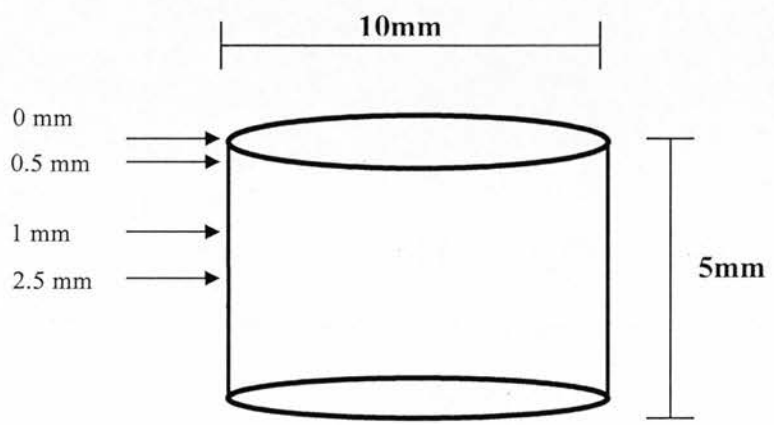

Figure 4.5. A schematic representation of the bone core. Bone cores are cylindrical in shape, 5 mm in height and 10 mm in diameter. (The arrows point to some of the distances away from the core surface at which cryostat sections were obtained in order to carry out the analysis).

4.2.9 In situ analysis of osteocyte DNA fragmentation using Nick Translation technique

The percentage of osteocytes demonstrating DNA breaks and therefore considered to be apoptotic was investigated using in situ DNA nick translation technique (Noble et al. 1997), as previously described in 3.2.3. Counterstaining was performed using DAPI, at 2.5ng/ml in order to enable identification of total osteocyte numbers in each section. Sections were then visualized by fluorescence microscopy in order to determine the ratio of the apoptotic osteocytes (FITC positive) over the total number of osteocytes (DAPI stained osteocytes). NT technique was employed on four consecutive sections per biopsy and a minimum of six fields of view were analyzed per section taken at 2.5mm distance through the bone cores covering in principle more than 70% of the total bone area at 20x magnification.

Percentage of apoptotic osteocytes (%) =

$$\frac{\text{Number of FITC positive osteocytes}}{\text{Number of DAPI stained osteocytes}} \times 100$$

4.2.10 Alkaline Phosphatase Staining

Alkaline phospatase (ALP) is a protein attached to the plasma membrane via a glycosyl-phosphatidinositol linkage (Noda, 1987) and catalyses the hydrolysis of phosphate monoesters.

$$R\text{-}O\text{-}PO3 + H2O \longrightarrow R\text{-}OH + HPO4\text{-}$$

ALP is a widely used marker of the osteoblast and has been suggested to participate in bone mineralization (Waymire et al., 1995). ALP positive bone surfaces were detected in 7μm cryosections taken at the 2.5 mm region of interest. ALP staining was performed on four consecutive sections taken at 2.5mm distance through each of the bone cores and six

image fields were analyzed per section. Sections were incubated at room temperature for 15 minutes in a solution of 1 mg/ml Fast Blue containing 40 µl (v/v) Naphthol-ASMX-mix, made in distilled water. The reaction was inhibited by washing the sections with PBS, followed by fixation in 4% paraformaldehyde for 10 minutes at room temperature. The percentage of ALP positive surface to total bone surface per field of view was measured using Bioquant Osteo Histomorphometry software (Bioquant Image Analysis Corporation, USA).

Percentage of alkaline phosphatase +ve area (%)
= (total bone area-alkaline phosphatase +ve area)*100

4.2.11 Sclerostin Staining

The percentage of osteocytes expressing sclerostin was investigated via means of immunostaining with a polyclonal anti-human sclerostin antibody (R&D Systems) as previously described in 3.2.5 (Figures 4.6, 4.7). Counterstaining was performed using DAPI, at 2.5ng/ml in order to enable identification of total osteocyte numbers in each section. Sections were then visualised by light and fluorescent microscopy in order to determine the ratio of the osteocytes expressing sclerostin over the total number of osteocytes (DAPI stained osteocytes). Sclerostin immunostaining was employed on four consecutive sections per biopsy and a minimum of six fields of view were analyzed per section taken at 2.5mm distance through the bone cores. The following criteria were used to calculate the percentage of sclerostin positive osteocytes:

Percentage of sclerostin positive osteocytes (%) =

$$\frac{\text{The number of sclerostin positive osteocytes}}{\text{The number of DAPI stained osteocytes}} \times 100$$

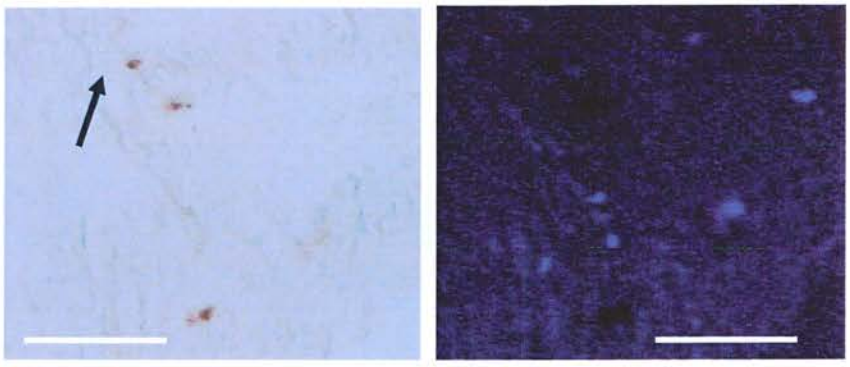

A. Sclerostin B. DAPI

Figure 4.6 Immunohistochemical reaction of sclerostin expression in sections of human bone explants. A section of trabecular bone was taken from a T (0) control sample. Osteocytes stained positive for sclerostin are brown as indicated by the arrow (A) Nuclei stained positive for DAPI (B). Bar represents 100μm.

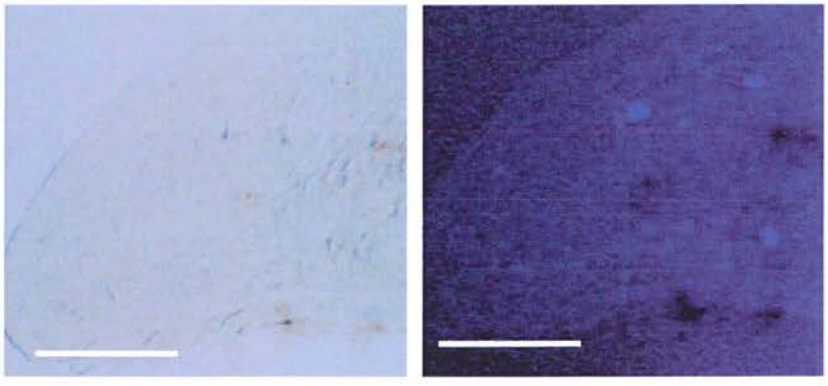

A. Sclerostin B. DAPI

Figure 4.7 Immunohistochemical demonstration of a negative control for sclerostin staining. Sections were treated with non-immune goat serum control diluted at 1:100 in 2% normal rabbit serum mixture in the absence of sclerostin antibody. Nuclei were stained blue with DAPI (B). No sclerostin signal was observed (A). Bar represents 100 μm.

4.2.12 RNA extraction from bone cores

For RNA extraction the bone cores were pulverized in liquid nitrogen using a mortar and pestle and the bone powder suspended in Trizol (Invitrogen).The homogenized sample was then incubated for 5 minutes at room temperature to allow the dissociation of nucleoproteins. The mix was then centrifuged (eppendorf centrifuge 5417R) to remove any debris and the supernatant was transferred to a new tube. 0.2 ml of chloroform were added and the samples vortexed for 15 seconds and incubated at room temperature for 2-3 minutes prior to centrifugation at 4°C for 15 minutes at 12,000 x g. The mixture then separates into a lower phenol-chloroform phase containing the DNA, an interphase that contains protein and a colorless upper aqueous phase containing the RNA. The upper aqueous phase was carefully aspirated into a new tube taking care to avoiding the interphase. An equal volume of isopropanol was added and the sample placed at -20 °C for a minimum of 20 minutes in order to precipitate the RNA. Following centrifugation at 12,000 x g for 10 minutes at 4°C the RNA was visible as a gel-like pellet at the bottom of the tube. The supernatant was then removed and the pellet was washed three times with 1ml of 75% ethanol at 7,500 x g for 5 minutes at 4°C. All leftover ethanol was removed after the final wash and the pellet was allowed to air-dry for approximately 10 minutes. The RNA pellet was then dissolved in 25 µl of RNAse free water. The RNA sample was then transferred on ice and stored immediately at -80°C.

4.2.13 Reverse Transcription Polymerase Chain Reaction (RT-PCR)

RNA samples were reverse transcribed to generate cDNA using the WT-Ovation™ RNA Amplification System (NuGEN) according to manufacturer's recommendations.

First Strand cDNA Synthesis Protocol

In a 2 µl of total RNA sample, 2µl of Strand Primer Mix (A1-2) reagent were added and the tube(s) was placed in a thermal cycler at:

65° C for 5 minutes

Cool to 4° C.

The tubes were then placed on ice and 6 µl of a master mix consisting of 5 µl First Strand Buffer Mix (A2-2) 0.5 µl of Nuclease Free Water (D1) and 0.5 µl of First Strand Enzyme Mix (A3).The tubes were then placed in a chilled thermal cycler at:

4 ° C 1 minute

25 ° C 10 minutes

42 ° C 10 minutes

70 ° C 15 minutes

4 ° C for ever

Following that the tubes were placed on ice to continue immediately with the second strand cDNA synthesis.

Second Strand cDNA Synthesis Protocol

A master mix combined of 9.75 µl of Second Strand Buffer Mix (B1-3) and 0.25 µl Second Strand Enzyme Mix (B2-2) was prepared and 10 µl were added to each of the First Strand Reaction tubes, mixed well by pippeting and placed in a thermal cycler for:

4 ° C 1 minute

25 ° C 10 minutes

50 ° C 30 minutes

70 ° C 5 minutes

4 ° C for ever

Samples were then placed on ice to continue immediately with Post Second Strand Enhancement Step.

Post Second Strand Enhancement Protocol

2 µl of the master mix combined of 1.9 µl Second Strand Buffer Mix (B1-3) and 0.1 µl of Reaction Enhancement Enzyme Mix (B3) were added to each of the Second Strand Reaction tubes, mixed by pippeting and placed on a chilled thermal cycler for:

4 ° C	1 minute
37 ° C	15 minutes
80 ° C	20 minutes
4 ° C	for ever

Samples were then placed on ice to continue with the SPIA Amplification.

SPIA Amplification Protocol

A master mix combined of 5 µl SPIA Buffer Mix (C2-4), 5 µl of SPIA Primer Mix and 10 µl SPIA Enzyme Mix was prepared and 20 µl were added to each of the Enhanced Second Strand reaction tubes, mixed and placed on a thermal cycler for:

4 ° C	1 minute
47 ° C	60 minutes
95 ° C	5 minutes

Samples were then placed on ice, prior to application of the Purification of Amplified cDNA Protocol.

Purification of Amplified cDNA Protocol

The Zymo Research DNA Clean and Concentrator -25 system was used for purification of the cDNA derived from the WT-Ovation™ RNA Amplification System.

320 µl of DNA Binding Buffer were added into the 40 µl of the amplified cDNA followed by vortexing. The mix was loaded onto the Zymo-Spin II Column and centrifuged at 10,000 x g for 10 seconds. The flow through was discarded and the sample was washed with 200 µl of 80% ethanol and then centrifuged at 10,000 x g for 10 seconds. The flow through was then discarded and another 200 µl of 80% ethanol were

added and the sample centrifuged at 10,000 x g for 30 seconds. The flow through was then discarded and the tip of the column was blotted onto filter paper to remove any residual wash buffer. The column was then placed in a clean 1.5 ml tube and 30 µl of nuclease free water were added and allowed to stand for 1 minute at room temperature prior to centrifuging at 10,000 x g for 30 seconds to elute the purified cDNA. The sample was then vortexed and placed at -20 °C until further use.

4.2.14 Quantitative Real-Time PCR Expression Analysis

Quantitative real-time PCR expression analysis was performed using an ABI Prism 7900 HT sequence detection system, TaqMan® Universal PCR Master mix, human 18 S rRNA pre-developed TaqMan® assay reagent for normalization and TaqMan® Assay-on-Demand™ products for human SOST (primers custom designed in house by Dr. Val Mann) were all purchaced from Applied Biosystems. All samples were run in triplicates. The TaqMan® Universal PCR Master mix was used for all the reaction components except primers, probe, and template. The final primer concentrations were 900 nM, and final probe concentrations were 50 nM. Cycling conditions were 50°C for 2 min, 95°C for 10 min, and 40 cycles of 95°C for 15 s and 60°C for 1 min. The data were collected and analyzed by the ABI Prism 7700 Sequence Detection System Software, version 2.1. The quantity (measured in copies/µl) was determined by the standard curve method, in which a standard curve generated by serial dilution (1×, 1:10, 1:100, 1:1,000, and 1:10,000) of a double-stranded fragment of known concentration was run with the unknown samples. No-template negative controls were constructed by substitution of nuclease-free water for cDNA. The quantity of each unknown was determined by plotting a standard curve (Threshold Cycle (C_T) vs. Starting Quantity) and calculating from the C_T of each sample the amount amplified. The normalized value was determined by multiplying the relative quantity of SOST for each sample by the relative quantity of 18S for that sample.

4.2.15 Histomorphometry

Bone histomorphometry was carried out as described in §3.2.8. Histomorphometric indices are divided into primary such as measurements of bone surface (BS), volume (BV) (Parfitt 1987) and the derived measurements some of which would include mineralizing surface (MS) or bone formation rate (BFR/BS).

Using light microscopy, the bone surfaces were traced on sections from the samples maintained in the Zetos^{TM} system and analysis of bone surface (BS) was carried out using the bone histomorphometry software BIOQUANT OSTEO (Bioquant Image Analysis Corporation, USA). The sections used were collected as described earlier and measurement of bone surfaces was performed using the formula:

BS (mm) = Total Bone Surface - Artificial edges

4.2.16 Statistical analysis

All data analyses were performed using the statistical software package SPSS for Windows 14.1. All data were checked for normality. In cases where the randomly selected sample data were shown to have a normal (Gaussian) distribution, the one-way Analysis of Variance (ANOVA) followed by the Tukey-Kramer and Bonferroni post hoc test were performed to determine statistical significance between treatment groups. For percentages or proportions that were not normally distributed the square root of each proportion was transformed into its arcsine which allowed the distribution of the data to be nearly normal enabling the use of parametric tests. Results were considered significant when $p<0.05$ denoted by * .The results are presented as means ± SEM.

4.3 Results

4.3.1. The effect of mechanical loading on osteocyte viability in the presence or absence of rhPTH at 1 and 2.5 mm distances.

In order to provide positive controls for the viability of osteocytes prior to the introduction of the cores to the Zetos^{TM} system, three samples were frozen immediately following the harvesting procedure, as described in methods, and were termed time zero (T0) controls. For each of the other treatment groups' three cores were introduced in the bioreactor and subjected to mechanical stimulation on a daily basis for 7 days. The treatment groups were divided in those that were maintained in the presence (termed as Load) (LD) or absence (termed as Unloaded) (UL) of mechanical stimulation and those maintained in the presence of mechanical stimulation and rhPTH alone treatment (termed as Loaded + PTH) (PTHLD) and those that received rhPTH treatment but no mechanical stimulation (termed as Unloaded + PTH) (PTH). After 7 days, all bone cores were removed from the bioreactor and were analyzed for cell viability using the LDH activity in order to determine any changes in the number of viable osteocytes following treatment as described above (Figure 4.9).

As shown in figure 4.8(A-C) at 1mm for patient 1 (P1) (Figure 4.8A) osteocyte viability in the unloaded sample was significantly lower to the T (0) control (30%± 2.63 vs. 87%± 11.1, p=0.016), while mechanical stimulation significantly increased osteocyte viability when compared to unloaded (53%± 4.09 vs. 30%± 2.63, p=0.018). rhPTH treatment significantly increased osteocyte viability in the absence or presence of mechanical stimulation when compared to unloaded (82%± 10.2 vs. 30%± 2.63 p=0.018, 58%± 4.44 vs. 30%± 2.63, p=0.033). For patient 2 (P2) (Figure 4.8B) the unloaded sample was significantly lower to the T (0) control (35%±3.18 vs. 74% ±5.60, $p<0.05$), while mechanical stimulation resulted in a trend towards an increase in osteocyte viability when compared to unloaded, with no statistically significant differences noted (52%±4.56 vs. 35%±3.18, $p>0.05$) Similarly rhPTH treatment showed a trend towards an increase in osteocyte viability in the absence or presence of mechanical stimulation when compared to unloaded, with no statistically significant differences noted (48 %±4.27, 52%±5.79 vs. 35%±3.18, respectively, $p>0.05$). In Patient 3 (P3) (Figure 4.8C), in the absence of

mechanical stimulation osteocyte viability was significantly decreased when compared to T(0) control (23%±4.23 vs. 77%±8.46, p=0.03) while in the presence of mechanical stimulation osteocyte viability was increased compared to unloaded (55%±12.8 vs. 23%±4.23, p=0.09). rhPTH treatment in the presence of mechanical stimulation significantly increased osteocyte viability compared to unloaded samples (60%±10.2 vs. 23%±4.23, p=0.012) while in the absence of mechanical stimulation no statistically significant differences were noted (35%±5.81vs. 23%±4.23, p>0.05) . Across all three patients the general trend observed at the distance of 1mm is that osteocyte viability is increased in the presence of mechanical stimulation whether rhPTH is present or not when compared to unloaded samples.

As shown in figure 4.8(D-F) at 2.5mm for P1 (Figure 4.8D) osteocyte viability in the unloaded sample was significantly lower to the T (0) control (27%± 2.62 vs. 70%± 7.73, p=0.001), while mechanical stimulation significantly increased osteocyte viability when compared to unloaded (52%± 7.01 vs. 27%± 2.62, p=0.001). rhPTH treatment significantly increased osteocyte viability in the absence of mechanical stimulation when compared to unloaded (77%± 10.7 vs. 27%± 2.62, p=0.001), while rhPTH in combination with mechanical stimulation increased osteocyte viability compared to unloaded however no statistically significant differences were noted (42%± 5.08 vs. 27%± 2.62, p>0.05).For P2 (Figure 4.8E) osteocyte viability was significantly higher in the T (0) control compared to unloaded (83.1% ±3.43 vs. 42.8%±5.04, p<0.001). Mechanical stimulation resulted in a trend towards an increase in osteocyte viability when compared to unloaded; with no statistically significant differences noted (54%±4.22 vs. 43%±5.04, p>0.05), however significant differences were observed in the presence of rhPTH treatment alone (36%±5.02 vs. 54%±4.22, p=0.027). rhPTH treatment in the presence of mechanical stimulation significantly increased osteocyte viability when compared to rhPTH treatment only (59%±4.7 vs. 36%±5.02, p=0.037). In P3 (Figure 4.8F), in the absence of mechanical stimulation osteocyte viability was significantly decreased compared to T (0) control (20%±3.6 vs. 83%±5.2, p=0.001) while in the presence of mechanical stimulation osteocyte viability was increased compared to unloaded (59%±6.2 vs. 20%±3.6, p=0.001). rhPTH treatment in the presence or absence of mechanical stimulation significantly increased osteocyte viability compared to unloaded

(37%±5.7 vs. 20%±3.6, p=0.006, 52%±4.47 vs. 20%±3.6, p=0.002, respectively). At the distance of 2.5 mm the trend observed across the three patients is that in that following rhPTH treatment in the presence or absence of mechanical stimulation osteocyte viability is increased compared to unloaded samples.

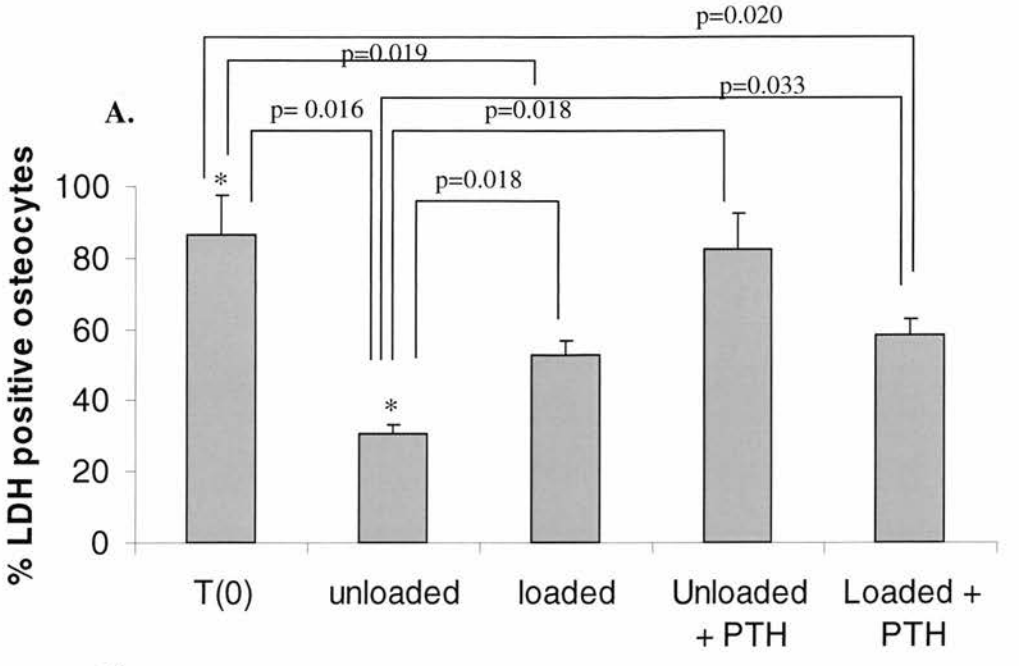
A.
p=0.020
p=0.019
p=0.033
p= 0.016
p=0.018
p=0.018
*
*
% LDH positive osteocytes
100
80
60
40
20
0
T(0)
unloaded
loaded
Unloaded + PTH
Loaded + PTH

P1

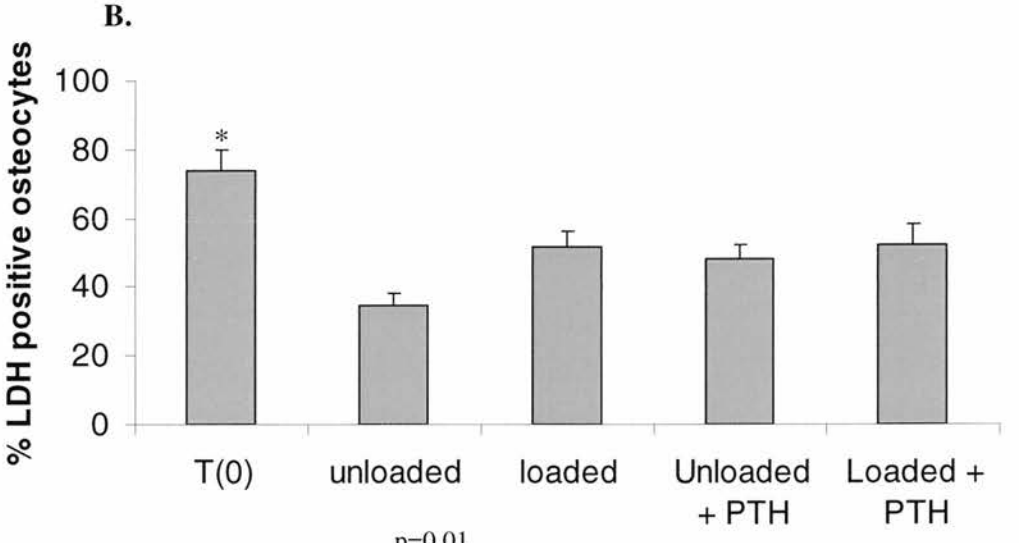
B.
*
% LDH positive osteocytes
100
80
60
40
20
0
T(0)
unloaded
loaded
Unloaded + PTH
Loaded + PTH

P2

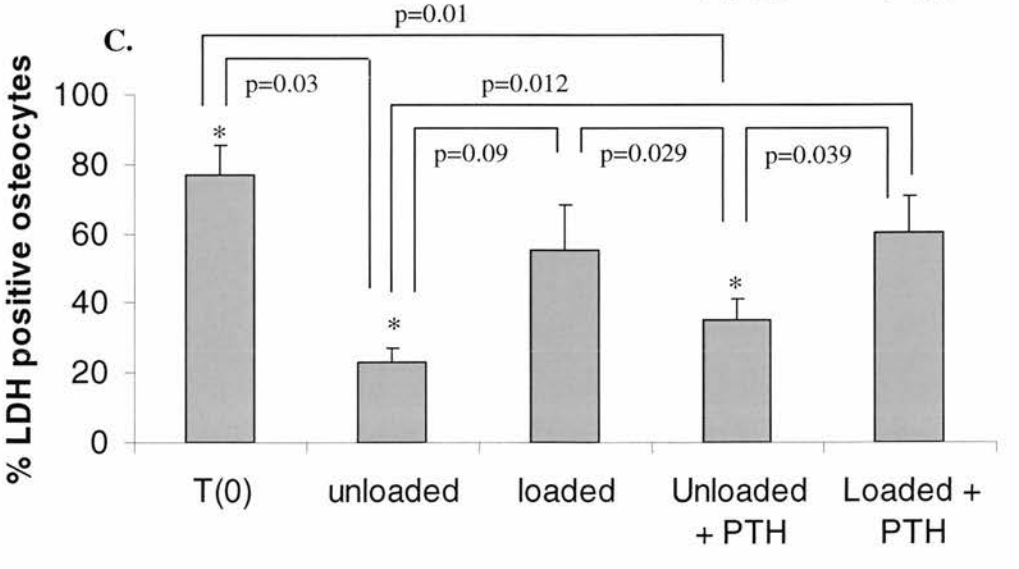
C.
p=0.01
p=0.03
p=0.012
p=0.09
p=0.029
p=0.039
*
*
*
% LDH positive osteocytes
100
80
60
40
20
0
T(0)
unloaded
loaded
Unloaded + PTH
Loaded + PTH

P3

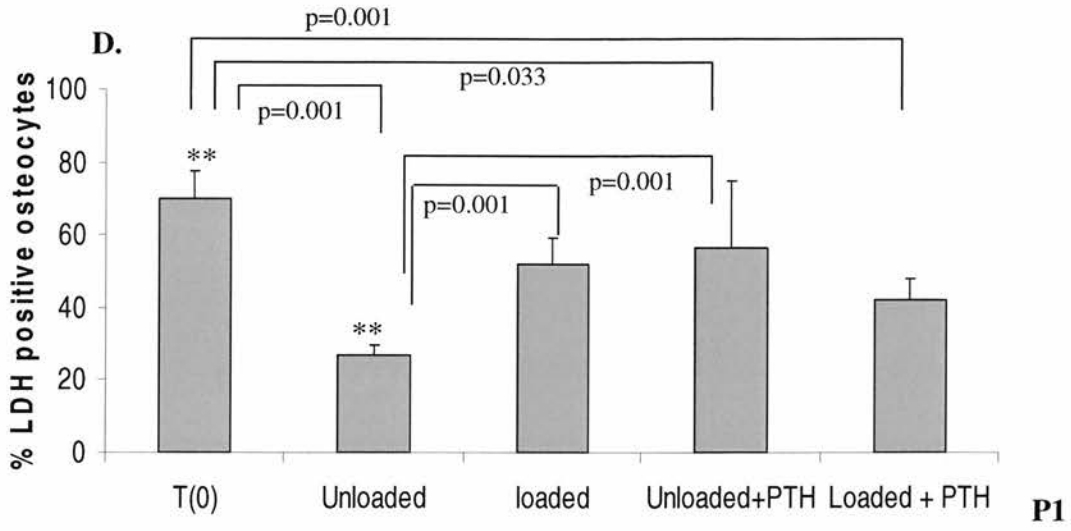
D.
p=0.001
p=0.033
p=0.001
p=0.001
p=0.001
% LDH positive osteocytes
100
80
60
40
20
0
**
**
T(0)
Unloaded
loaded
Unloaded+PTH
Loaded + PTH
P1

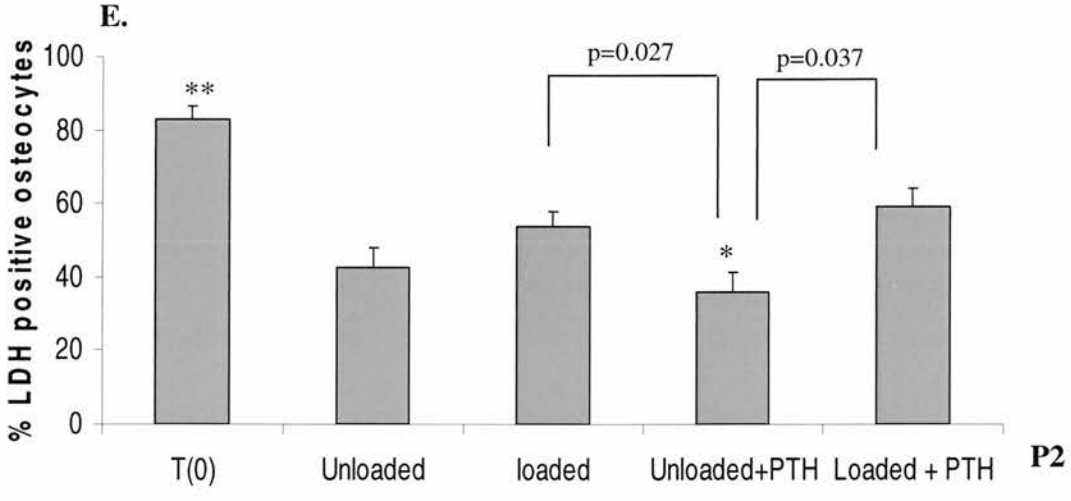
E.
p=0.027
p=0.037
% LDH positive osteocytes
100
80
60
40
20
0
**
*
T(0)
Unloaded
loaded
Unloaded+PTH
Loaded + PTH
P2

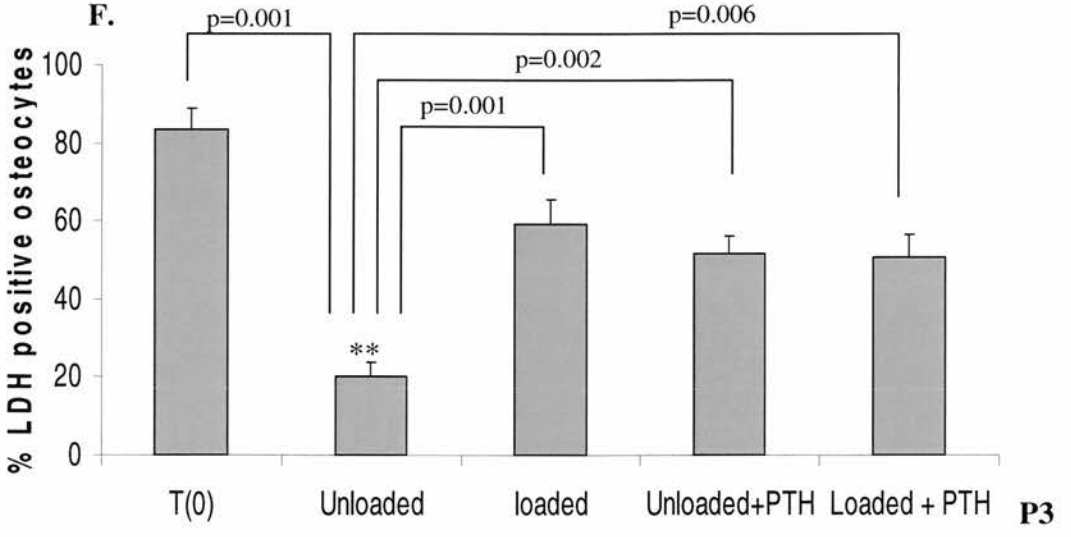
F.
p=0.001
p=0.006
p=0.002
p=0.001
% LDH positive osteocytes
100
80
60
40
20
0
**
T(0)
Unloaded
loaded
Unloaded+PTH
Loaded + PTH
P3

Figure 4.8 The percentage of LDH positive osteocytes in the presence or absence of mechanical stimulation and rhPTH. Bone cores from P1, P2 and P3 were maintained in the bioreactor for 7 days in the presence or absence of mechanical stimulation and the presence of rhPTH with mechanical or no mechanical stimulation. The T (0) controls were frozen as described above at the time of harvesting. Frozen sections collected at 1 (A-C) and 2.5 (D-F) mm and were examined for LDH activity in osteocytes (A-F).In the absence of mechanical stimulation for all patients osteocyte viability was significantly decreased compared to the T (0) controls, while mechanical stimulation increased osteocyte viability. rhPTH treatment increased osteocyte viability in while rhPTH in combination with mechanical stimulation had a more pronounced effect compared to rhPTH only. Results are expressed as the percentage of LDH positive osteocytes ± S.E.M * = $p<0.05$ and ** = $p<0.001$.

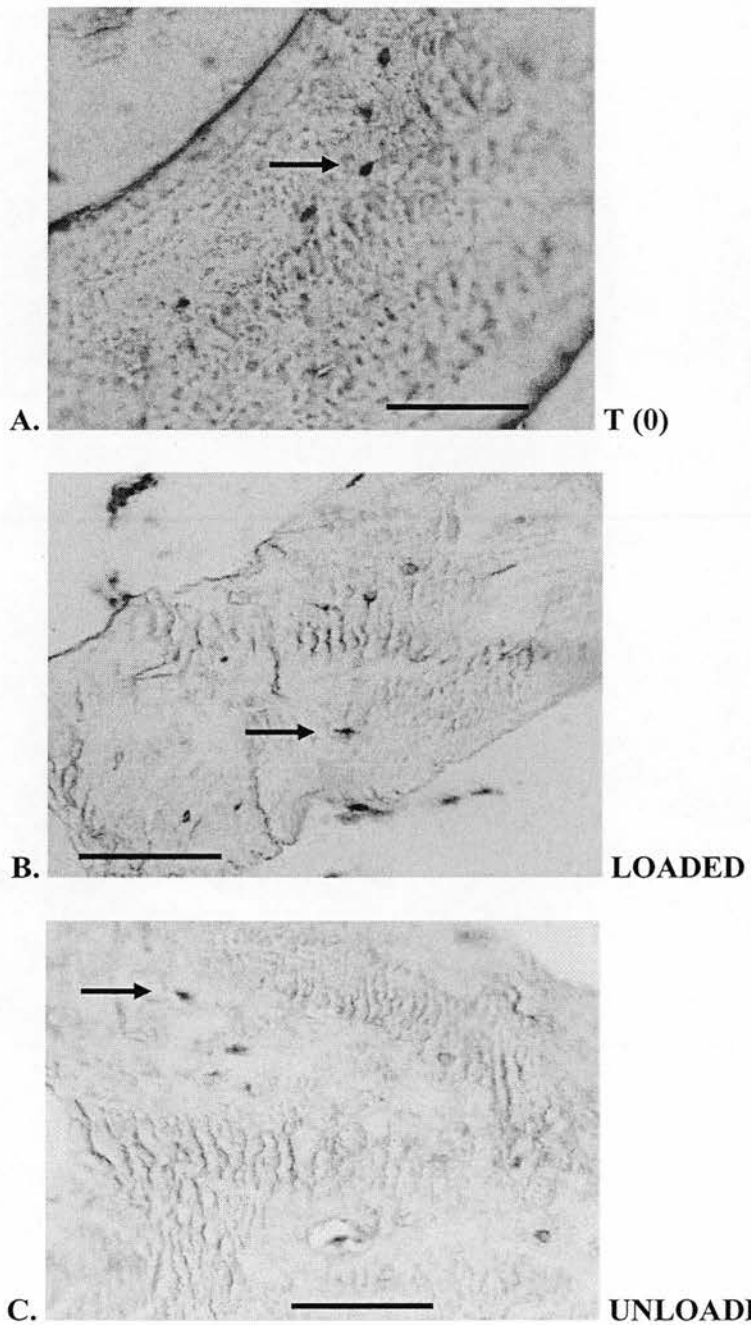

Figure 4.9 Histochemical reaction of LDH enzyme in sections of human bone explants cultured in the Zetos™ system for 7 days. Osteocyte lacunae showed either strong reaction with LDH indicating viable osteocytes or no reaction indicating empty lacunae or non viable osteocytes. Representative images from **A.** the T (0) control **B.** the mechanically stimulated sample **C.** the unloaded sample. Black arrow identifies a viable LDH-positive osteocyte. Bar represents 100μm.

4.3.2 The effect of mechanical loading on osteocyte apoptosis in the presence or absence of rhPTH.

Bone cores treated with rhPTH in the presence or absence of mechanical stimulation were also analyzed for osteocyte apoptosis at the distance of 2.5 mm (Figure 4.11). Application of mechanical loading reduced osteocyte apoptosis in all three patients compared to unloaded samples. More specifically in P1 (Figure 4.10A), osteocyte apoptosis in the unloaded sample was significantly increased compared to the T (0) control (0.94% ± 0.49 vs. 10% ± 1.89, p=0.005), while mechanical stimulation significantly decreased osteocyte apoptosis compared to the unloaded (2% ± 0.60 vs. 10% ± 1.89, p=0.011). rhPTH treatment decreased osteocyte apoptosis compared to unloaded, however no significant differences were noted (6% ± 1.21 vs. 10% ± 1.89). On the other hand rhPTH treatment in the presence of mechanical stimulation significantly decreased osteocyte apoptosis compared to unloaded (1 % ± 0.46vs. 10% ± 1.89, p=0.006) In P2 (Figure 4.10B), osteocyte apoptosis was significantly increased in the absence of mechanical stimulation compared to the T (0) control (10% ±1.39 vs.0.77% ± 0. 47, p=0.006). Mechanical stimulation significantly decreased osteocyte apoptosis compared to unloaded (2 % ± 0.49 vs. 10% ±1.39, p=0.025), while rhPTH treatment in the presence of mechanical stimulation significantly decreased osteocyte apoptosis compared to unloaded (1% ± 0.46 vs. 9 % ± 1.39, p=0.027). In P3 (Figure 4.10C) similar to P1 and P2, osteocyte apoptosis in the unloaded sample was significantly increased compared to the T (0) control (11% ± 1.89 vs. 0.75% ± 0.31, p=0.015), while mechanical stimulation significantly decreased osteocyte apoptosis compared to the unloaded (3% ± 0.75 vs. 11% ± 1.89, p=0.026). Similarly mechanical stimulation in combination with rhPTH treatment significantly decreased apoptosis compared to unloaded (2 % ± 0.54 vs. 11% ± 1.89, p=0.006). The general trend observed across all three patients is that mechanical stimulation significantly decreased osteocyte apoptosis compared to unloading conditions.

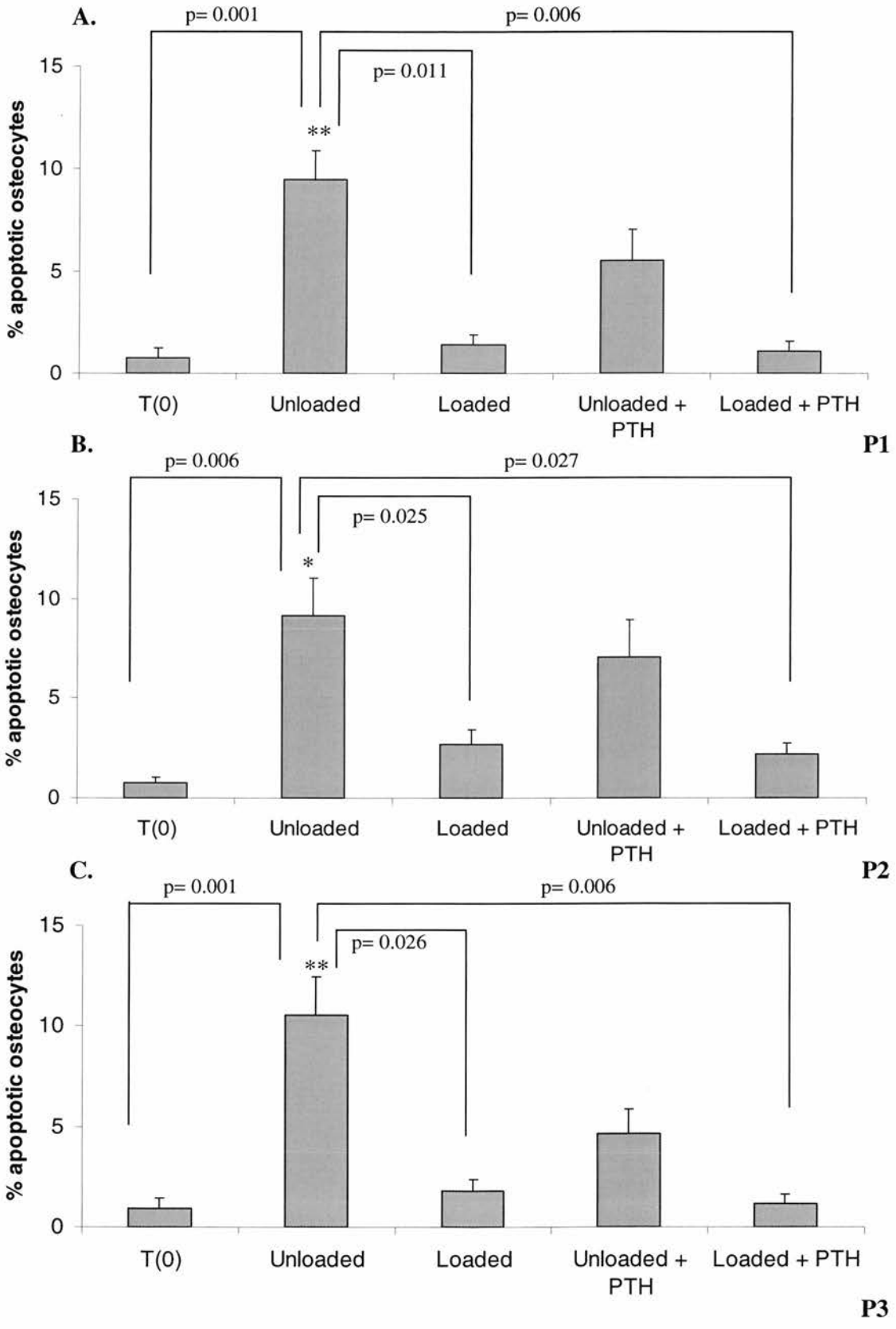
A.
p= 0.001
p= 0.006
p= 0.011
**
% apoptotic osteocytes
15
10
5
0
T(0)
Unloaded
Loaded
Unloaded + PTH
Loaded + PTH
P1
B.
p= 0.006
p= 0.027
p= 0.025
*
% apoptotic osteocytes
15
10
5
0
T(0)
Unloaded
Loaded
Unloaded + PTH
Loaded + PTH
P2
C.
p= 0.001
p= 0.006
p= 0.026
**
% apoptotic osteocytes
15
10
5
0
T(0)
Unloaded
Loaded
Unloaded + PTH
Loaded + PTH
P3

Figure 4.10 In situ evidence of DNA fragmentation in osteocytes subjected to mechanical stimulation in the presence or absence of rhPTH. Sections obtained from the 2.5mm distance were analyzed for osteocyte apoptosis using the in situ nick translation technique. (A-C). Treatment of cores under unloading conditions alone significantly increased the percentage of osteocyte apoptosis compared to the other treatments and the T (0) controls in P1 (A), P2 (B) and P3 (C). Combination treatment of rhPTH and mechanical stimulation in P1 (A), P2 (B) and P3 (C) significantly decreased osteocyte apoptosis compared to unloading conditions. Results are expressed as the percentage of osteocytes displaying positive staining for fragmented DNA over their total number ± S.E.M * = $p<0.05$ and ** = $p<0.001$ denote significant differences of T (0) to the other treatments.

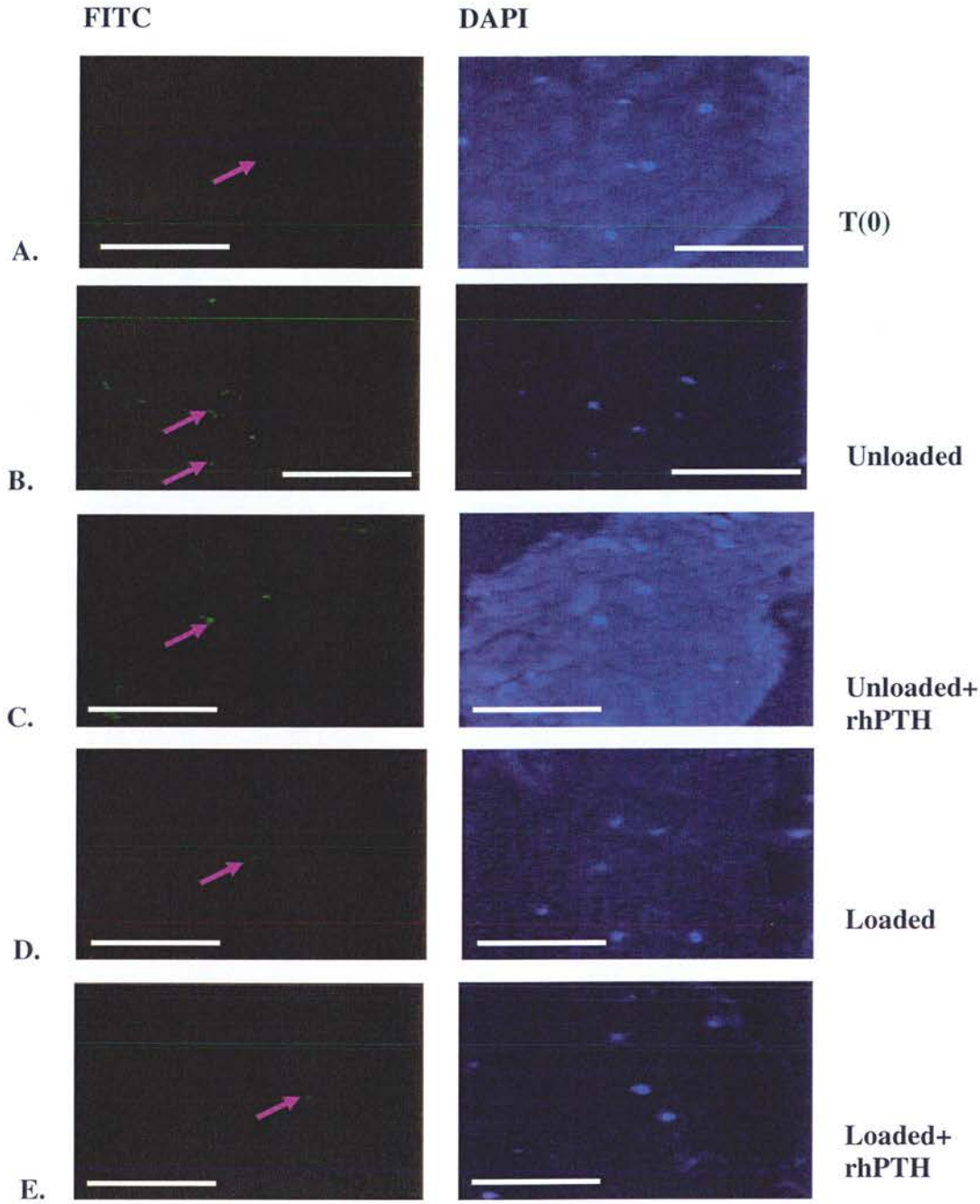

Figure 4.11 In situ evidence of DNA fragmentation in osteocytes subjected to mechanical stimulation in the presence or absence of rhPTH. The percentage of osteocyte apoptosis was quantified in sections at the distance of 2.5mm. Representative images of apoptotic osteocytes (FITC) and the corresponding total cell count (DAPI) in A. T (0) control, B. Unloaded samples, C. Unloaded samples in the presence of rhPTH, D. Loaded samples and E. Loaded samples in the presence of rhPTH. Arrow indicates apoptotic osteocytes. Bar represents 100μm.

4.3.3. The effect of mechanical loading on the percentage of alkaline phosphatase labeled bone surfaces in the presence or absence of rhPTH.

Bone cores treated with rhPTH in the presence or absence of mechanical loading were analyzed for indices of osteoblast activity at the distance of 2.5 mm. Cryostat sections were stained for alkaline phosphatase as described in the methods section (Figure 4.13). All three patients show a higher percentage of ALP positively labelled bone surface in the T (0) controls compared to both loaded and unloading conditions either presence or absence of rhPTH . As shown in figure 4.12(A-C) at 2.5mm for P1 (Figure 4.12A) T (0) control was statistically significant different to unloaded, loaded, and rhPTH treated samples in the absence or presence of mechanical stimulation (5%± 1.21 vs. 2%± 0.63, 2%± 0.43, 1 %± 0.39, 1.50%± 0.67, respectively, $p<0.05$), however no statistically significant differences were noted between other treatment groups. For P2 (Figure 4.12B) the percentage of positively labelled ALP bone surface was found to be significantly higher in the T (0) control compared to unloaded, loaded, and rhPTH treated samples in the absence or presence of mechanical stimulation (5%±0.92 vs. 0.92%±0.18, 0.59%±0.14, 1 %±0.43, 1%±0.37, respectively, $p<0.001$), while combination treatment of rhPTH and mechanical stimulation significantly increased ALP positively labelled surface compared to unloading conditions (1%±0.37 vs. 0.92%±0.18, $p=0.05$). In P3 (Figure 4.12C) the percentage of ALP labelled area was significantly higher in the T (0) control compared to unloaded (3%±0.61 vs. 2%±0.73 $p=0.026$). rhPTH treatment in the presence or absence of mechanical stimulation was also found significantly different to the T(0) control (2%±0.41, 2%±0.61 vs. 3 %±0.61, respectively, $p<0.05$).

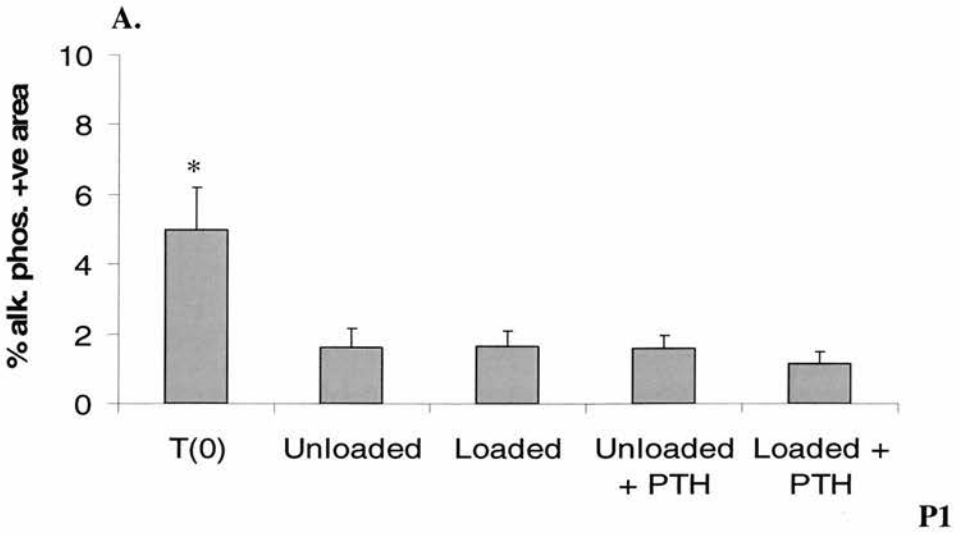
A.
% alk. phos. +ve area
10
8
6
4
2
0
*
T(0)
Unloaded
Loaded
Unloaded + PTH
Loaded + PTH

P1

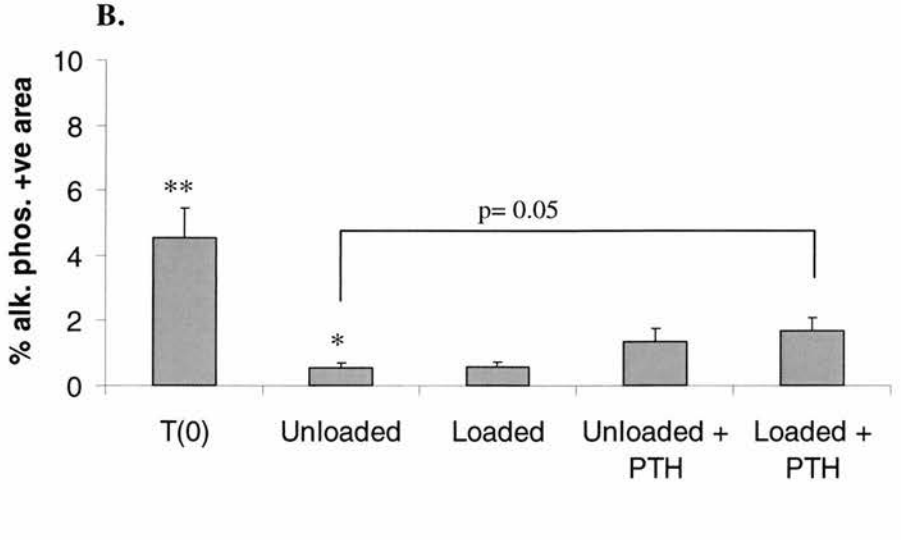
B.
% alk. phos. +ve area
10
8
6
4
2
0
**
*
p= 0.05
T(0)
Unloaded
Loaded
Unloaded + PTH
Loaded + PTH

P2

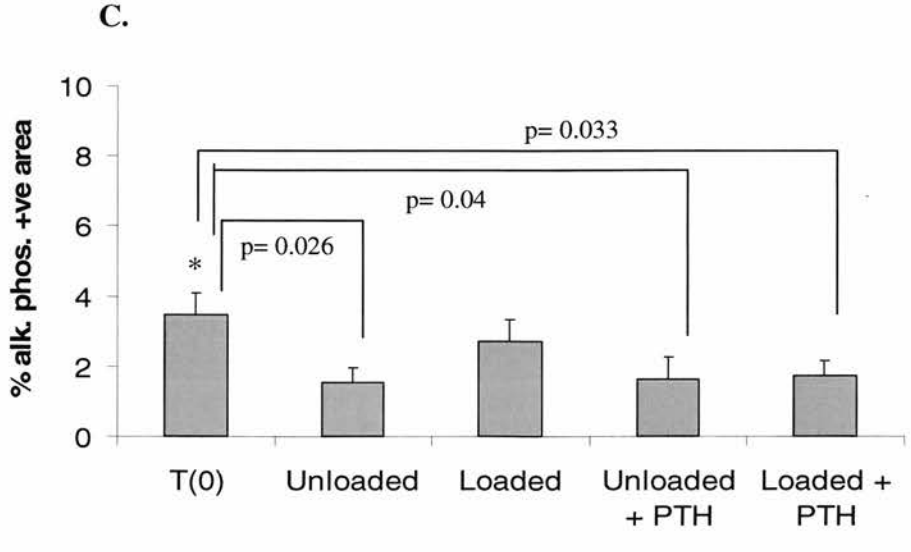
C.
% alk. phos. +ve area
10
8
6
4
2
0
*
p= 0.033
p= 0.04
p= 0.026
T(0)
Unloaded
Loaded
Unloaded + PTH
Loaded + PTH

P3

Figure 4.12 The percentage of alkaline phosphatase positive area in the presence or absence of mechanical stimulation and PTH. Frozen sections collected at the distance of 2.5mm obtained from bone cores from patients P1, P2 and P3 were examined for osteoblast activity indices in loading and unloading conditions in the presence or absence of rhPTH (**A-C**). In P1 (A) the percentage of positively labeled surface was found to be higher in the T (0) controls compared to the other treatment groups, while the presence of mechanical stimulation or rhPTH did not affect ALP expression. In P2 (B) the percentage of positively labeled bone surface was significantly higher in the T (0) control compared to the other treatment groups, while combination treatment of rhPTH and mechanical stimulation significantly increased ALP positively labeled surface compared to unloading conditions ($p=0.05$). In P3 (C) the percentage of positively labeled bone surface was higher in the T (0) control compared to unloading conditions in the presence or absence of rhPTH ($p<0.05$). Results are expressed as the percentage of ALP positively labelled area ± S.E.M * = $p<0.05$ and ** = $p<0.001$ denote significant differences of T (0) to the other treatments.

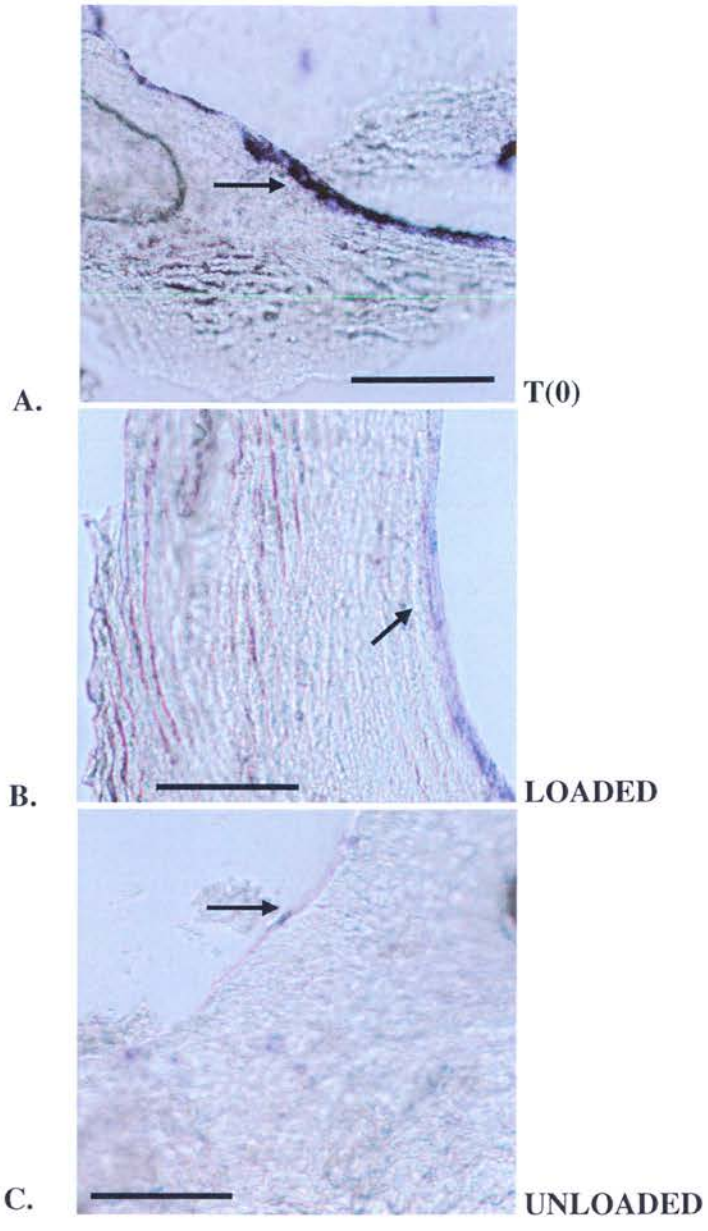

Figure 4.13 Histochemical reaction of alkaline phosphatase positive bone surfaces in sections of human bone explants cultured in the Zetos™ system for 7 days. ALP was stained using standard techniques, the ALP positive surfaces stain as purple. Representative images from **A**. the T (0) control. **B.** the mechanically stimulated sample **C.** the unloaded sample. Arrow indicates alkaline phosphatase positive stained surfaces. Bar represents 100μm.

4.3.4 The effect of rhPTH on osteocyte sclerostin expression in the presence or absence of mechanical stimulation.

Bone cores from the three patients treated with rhPTH in the presence or absence of mechanical stimulation were analyzed for sclerostin expression (Figure 4.14 A-C). For P1, P2 and P3 there were no significant differences noted between samples that where treated either in the presence or absence of mechanical stimulation as well as the presence or absence of rhPTH in the percentages of osteocytes expressing sclerostin. In more detail for P1 (A) in the absence of mechanical stimulation compared to the T (0) control (40% ± 1.20 vs. 43% ± 1.21, $p>0.05$) no difference was observed. Similarly in the presence of rhPTH in both loaded and unloaded conditions no reduction in the percentage of sclerostin positive osteocytes compared to the unloaded (39 % ± 0.57, 39 % ± 0.77 vs. 40 % ± 1.20, $p>0.05$) was observed. In P2 (B) similar observations to P1 were made with the presence of rhPTH in both loaded and unloaded conditions not affecting the percentage of sclerostin positive osteocytes (38% ± 0.30, 38%± 0.70 vs. 40 ± 0.52, $p>0.05$). Similarly loaded samples showed no difference in the percentage of sclerostin positive osteocytes when compared to samples in the presence of rhPTH in both unloaded and loaded conditions (40% ± 0.54 vs. 38% ± 0.30, 38% ± 0.70, $p>0.05$). Similar observations to P1 and P2 were made for P3 (C) with the presence of rhPTH in both loaded and unloaded samples showing no reduction in the percentage of sclerostin positive osteocytes compared to the unloaded (39%± 0.80, 39% ± 0.89 vs. 40% ± 0.60, $p>0.05$) and loaded samples (39% ± 0.80, 40% ± 0.89 vs. 40% ± 1.05, $p>0.05$).

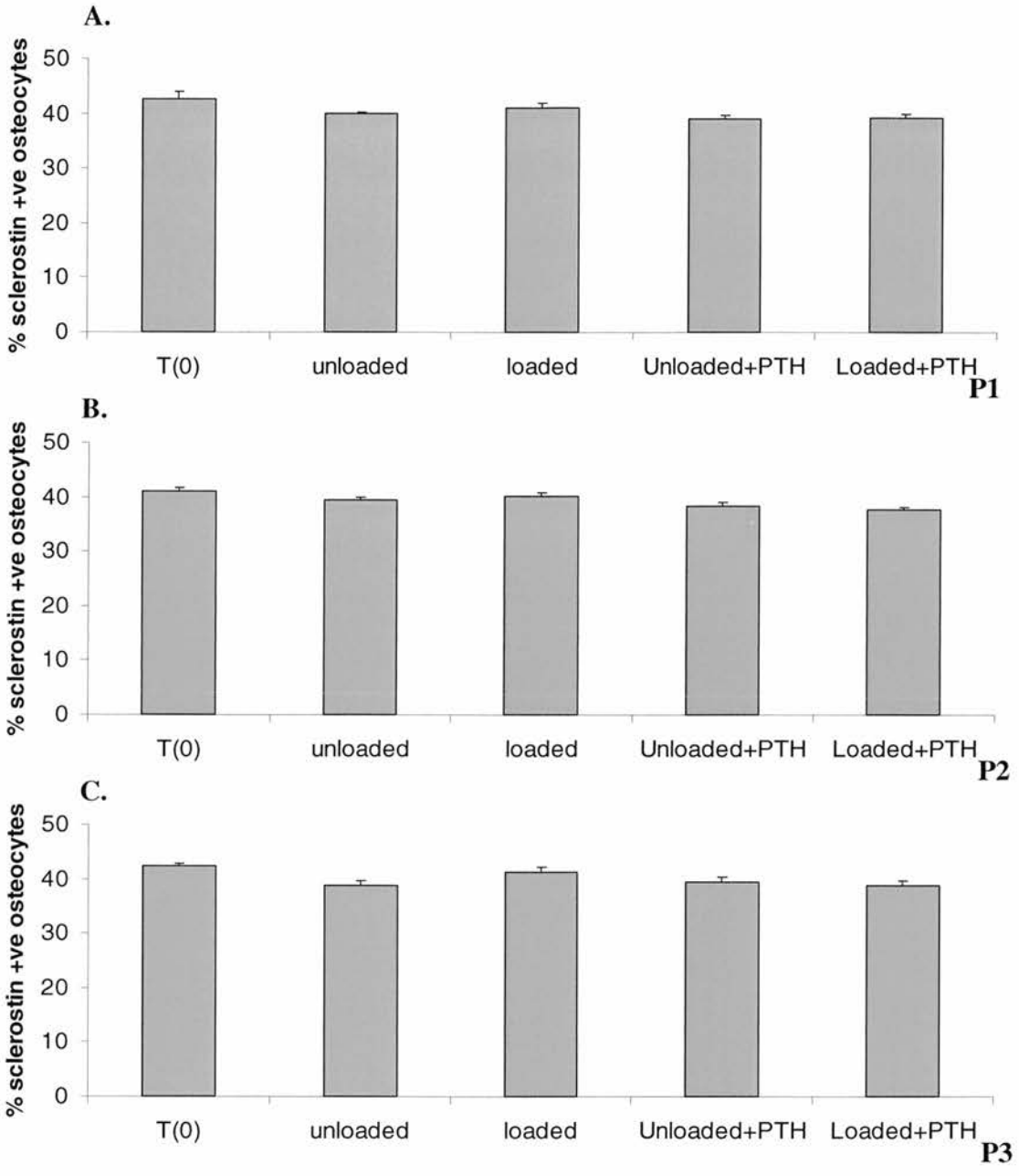

Figure 4.14 The percentage of sclerostin positive osteocytes in human trabecular explants in the presence or absence of mechanical stimulation and rhPTH. Sections obtained from the 2.5 mm distance for all three patients were analyzed for sclerostin expression on osteocytes (A-C). For P1 (A), P2 (B) and P3 (C) treatment of bone cores with rhPTH either in the presence or absence of mechanical stimulation had no effect on the percentages of osteocytes expressing sclerostin.. Results are expressed as the percentage of sclerostin positive osteocytes ± S.E.M

4.3.5 The effect of rhPTH on SOST gene expression in the presence or absence of mechanical stimulation.

Total RNA from bone cores from the three different patients was extracted and transcribed into cDNA which was then subjected to quantitative real-time PCR to measure the mRNA levels of SOST in samples subjected to mechanical stimulation in the presence or absence of rhPTH (Figure 4.15A-C). In all three patient samples SOST gene expression was significantly higher in the T (0) controls compared to both loaded and unloaded conditions in the presence or absence of rhPTH. In more detail in P1 mechanical stimulation in the presence or absence of rhPTH reduced SOST mRNA levels (A) compared to T (0) control (3 ± 5.4 vs. 33 ± 5.9, $p=0.03$, vs. 66 ± 5.4, $p<0.001$). Absence of mechanical stimulation in the presence or absence of rhPTH also reduced the mRNA levels of SOST (3 ± 1.63 vs. 29± 2.41, $p=0.12$). In P2 (B) similar observations to P1 were made with the presence of rhPTH in both loaded and unloaded conditions reducing the levels of SOST mRNA (1 ± 3.13 vs. 2 ± 0.81, $p>0.05$), however no statistically significant differences were noted. A reduction in SOST mRNA levels was observed in the presence or absence of mechanical stimulation compared to the T (0) control (3 ± 3.41 vs. 2± 2.41 vs. 30± 0.19, $p<0.001$). Similarly in P3 (C) the presence of rhPTH in loaded and unloaded conditions resulted in a reduction in SOST mRNA levels (2 ± 4.07 vs. 3 ± 0.63, $p>0.05$), with no statistically significant differences noted, as did the presence or absence of mechanical stimulation when compared to T (0) control (12 ± 0.81 vs 21 ± 0.10 vs. 96 ± 7.27, $p<0.001$).

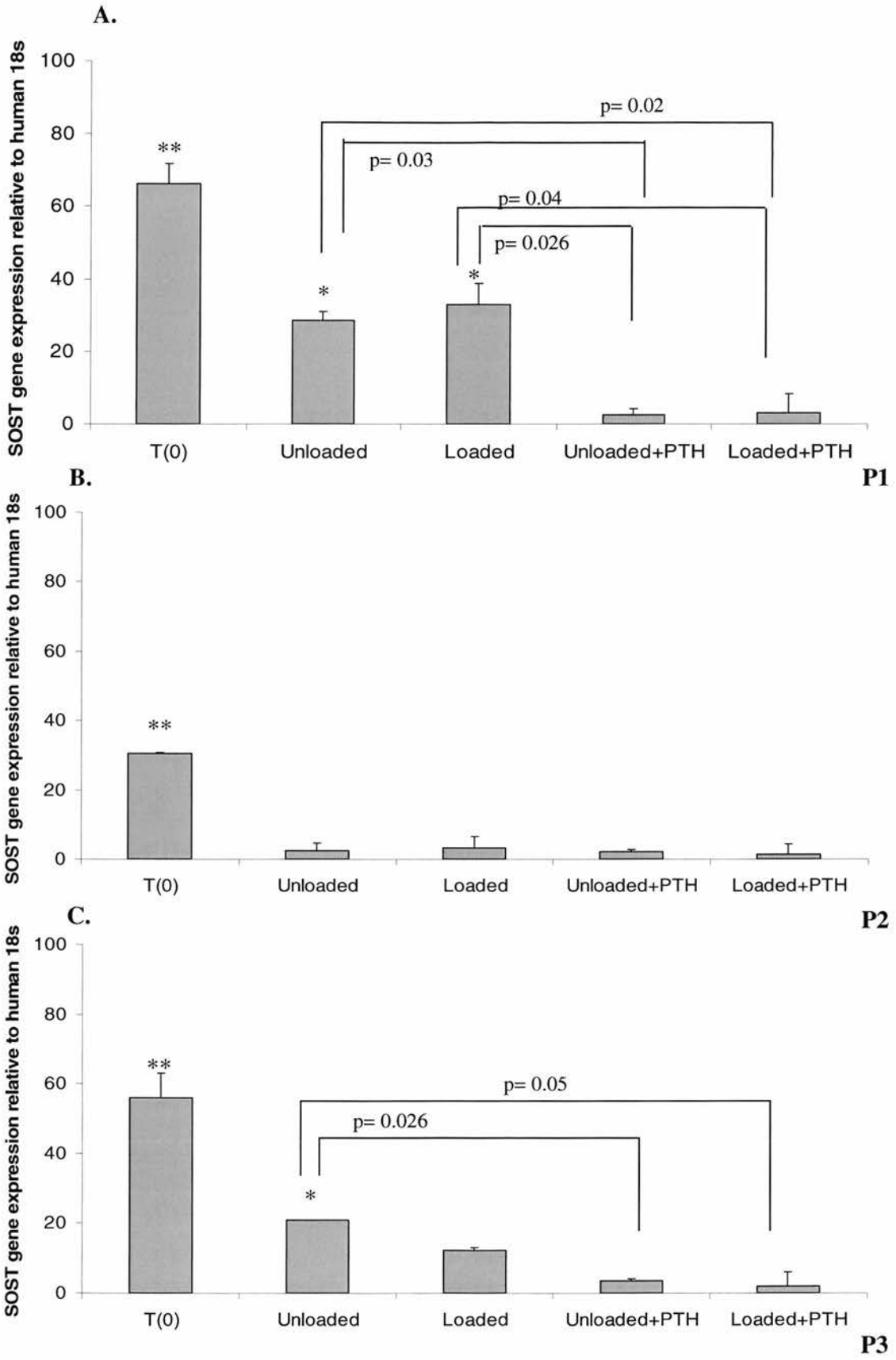
A.
SOST gene expression relative to human 18s
100
80
60
40
20
0
**
*
*
p= 0.02
p= 0.03
p= 0.04
p= 0.026
T(0)
Unloaded
Loaded
Unloaded+PTH
Loaded+PTH
P1
B.
SOST gene expression relative to human 18s
100
80
60
40
20
0
**
T(0)
Unloaded
Loaded
Unloaded+PTH
Loaded+PTH
P2
C.
SOST gene expression relative to human 18s
100
80
60
40
20
0
**
*
p= 0.05
p= 0.026
T(0)
Unloaded
Loaded
Unloaded+PTH
Loaded+PTH
P3

Figure 4.15 SOST gene expression in human trabecular explants subjected to mechanical stimulation in the presence or absence of rhPTH. RNA was extracted from whole bone cores using TRIZOL and subjected to cDNA synthesis used for quantitative real-time PCR for the SOST gene (A-C). For P1 (A) mechanical stimulation in the presence or absence of rhPTH reduced SOST mRNA levels as did the absence of mechanical stimulation in the presence or absence of rhPTH when compared to T(0) controls. Similarly in P2 (B) the presence of rhPTH in both loaded and unloaded conditions reduced the levels of SOST mRNA as did the presence or absence of mechanical stimulation compared to the T (0) control. Similar observations to P1 and P2 were made for P3 (C) in which the presence of rhPTH in loaded and unloaded conditions reduced SOST mRNA levels as did the presence or absence of mechanical stimulation when compared to T(0) control. Results are expressed as the SOST gene expression relative to human 18s ± S.E.M * = $p<0.05$ and ** = $p<0.001$ denote significant differences of T (0) to the other treatments.

4.4 Discussion

Data presented in previous chapters demonstrated a protective effect of rhPTH on the viability of rat osteocytes *in vivo* and murine osteocytes *in vitro*. The study presented in this chapter investigated the potential effects of rhPTH on the viability of human osteocytes *ex vivo* following 7 days in culture using the Zetos^{TM} bioreactor, in the presence or absence of physiological loading.

Over the years a line of evidence has accumulated to demonstrate the anabolic effects of mechanical loading within the physiological range of strains to bone (Mosley et al. 1997, Lanyon 1992) while unloading conditions induced bone resorption and bone loss. Organ and cell culture systems have provided important insights regarding the response of bone cells to mechanical stimulation or to growth factors and hormones (Rawlinson et al. 1995, Cheng et al. 1996, Zaman et al. 1997). However it has not been possible to maintain the tissue viable due to the inability of these systems to mimic the *in vivo* bone microenvironment (Jones et al. 2001) resulting in tissue necrosis mainly in the centre of the organ culture (Jones et al. 2001, Davies et al. 2004). Due to these difficulties, little is known regarding the viability of osteocytes, considered to be the mechanosensors (Lanyon 1993, Zhang et al. 1997, Noble et al. 2003) and transducers in bone (Lean et al. 1996, Aarden et al. 1996, Duncan and Turner 1995, Klein Nulend et al. 1995, Yellowley et al. 2000) based on the current ex vivo organ culture systems. In the study presented here the 3-D bioreactor system (Zetos^{TM}) was used to investigate the effects of rhPTH on human osteocytes from three patients over a seven day period in the presence or absence of mechanical stimulation.

For the determination of osteocyte viability following extraction from the patient, osteocytes were examined by means of their LDH activity in the T (0) controls. The distance analyzed was at 1 and 2.5 mm, in order to determine possible effects of the drilling process on osteocyte viability. It was observed that higher percentages of viable osteocytes were observed at 2.5 mm compared to 1mm in the T (0) cores possibly suggesting that the drilling process might have induced the loss of osteocytes observed in

the latter this finding is in line with previous work (Mann et al. 2006). Despite the loss of osteocytes at 1mm, the density of osteocytes per mm^2 (125-150 osteocytes per mm^2 at 1mm and 180-250 osteocytes per mm^2 at 2.5mm) was found to be within the range of viable osteocytes per mm^2 reported for human trabecular bone in the literature (Mullender et al. 1996, Tomkinson et al. 1998, Qiu et al. 2002, Mann et al. 2006). Because osteocyte viability at 2.5mm from the surface of the cores was higher than at the 1 mm distance all further analysis was carried out at this region of interest within each core.

Although the viability of osteocytes in the T (0) controls was found to be within the lowest range of viable osteocytes reported in human control samples (Mullender et al. 1996, Tomkinson et al. 1998, Qiu et al. 2002), maintenance of bone cores under unloading conditions in the bioreactor resulted in a decrease in the percentage of viable osteocytes, which was between 20-45% after 7 days in culture. However the viability of osteocytes was improved by almost 1.5 fold upon application of mechanical loading compared to the unloaded samples. Although in other *ex vivo* organ cultures such as the one in the study by Takai and colleagues (2004) it was shown that mechanical stimulation could not maintain osteocyte viability in bovine bone explants after 22 days in culture, possibly due to insufficient nutrient perfusion to osteocytes. In contrast to these findings in this system as it was shown by Mann and colleagues (2006) following 3, 7 and 27 days in culture, as well as by the experiments presented in this study there is sufficient and possibly homogeneous supply of feeding media throughout the thickness of the bone cores, as evidenced by the fact that osteocyte viability did not drop towards the centre of the bone cores.

The viability of osteocytes was examined by means of their metabolic activity. In more detail, the metabolic activity of the LDH enzyme was monitored following the addition of tetrazolium salts to cells as described in the methods section, which are reduced in viable cells to a coloured product by the action of dehydrogenases (Tisserat and Manthey 1996, Verleysen et al. 2004). On the basis of this assay only the living cells were coloured, since the colour observed is a product of metabolic activity in cells, whereas the non-

coloured cells were considered dead (Widholm 1972). In the current study this viability assay demonstrated that the non-viable cells were not detected due to the loss of enzyme activity, suggesting that only metabolically active cells were included in the measurement of viable cells. However, as described above necrotic cells would be excluded from the measurements, it may be possible that apoptotic cells would be included in the viable cell measurements, due to the fact that apoptosis is an active, ATP-dependent process (Kerr 1972) and therefore cells of the early apoptotic stages would still be metabolically active and would possibly show LDH activity. For these reasons the response of osteocytes to different treatments was further characterized by examining apoptotic indices using the in situ nick translation technique.

Apoptotic osteocytes were estimated based on DNA fragmentation, in the T (0) samples levels of apoptosis were similar to those reported in the literature for control human samples (Tomkinson et al. 1997, Mann et al. 2006). Culturing of bone explants in the absence of mechanical loading resulted in a 4 fold increase of osteocyte apoptosis compared to the T (0) samples. Similar findings has been previously reported by other studies showing that the absence of mechanical loading resulted in an increase in osteocyte apoptosis (Noble et al. 2003, Bakker et al. 2004, Basso et al. 2006, Mann et al. 2006). Moreover application of mechanical loading within the known osteogenic range (Mann et al. 2006) reduced osteocyte apoptosis compared to the unloaded samples. These findings are in accordance with previous studies that have demonstrated that application of mechanical stimulation within the physiological range is beneficial for osteocyte viability in rat bone either *in vivo* (Noble et al. 2003) or *ex vivo* (Lozupone et al. 1996) as well as for osteocyte viability and apoptosis in human bone.

Furthermore, following 7 days in culture and the application of loading in the presence or absence of rhPTH in the bioreactor there was an increase in alkaline phosphatase activity as indicated from the percentages of positively labeled bone surface compared to unloading conditions. These findings indicated that the mechanical strains or improved fluid flow produced by the bioreactor (Knothe et al., 2000) induced an osteogenic response in the bone cores. Although no fluorescent markers of bone formation had been administered due to the short duration of the experiments and no secure assessment of the

degree of bone formation could be formulated, the application of mechanical stimulus alone and in combination with rhPTH in patients 2 and 3 increased the percentage of ALP positive bone surfaces demonstrating a significant mechanoresponsiveness in the bioreactor system, these observations are in agreement with previous work done in our lab (Mann et al., 2006). On the other hand ALP positive bone surface was reduced in the unloaded samples.

It was shown previously that intermittent administration of PTH increases bone mass and improves bone structure *in vivo* (Li et al., 2003, Rosen et al., 2004). In light of these observations, rhPTH in the present study was administered intermittently as well. Both osteocytes and osteoblasts possess receptors for PTH (Dobnig and Turner, 1995), while osteoblasts are considered to be the primary target of PTH actions on bone (Jilka et al. 1999). The percentage of ALP positive labeled surfaces was increased in the presence of rhPTH in the presence or absence of mechanical stimulation suggestive of a synergistic effect of these two parameters on the osteoblast. Increased ALP activity has also been shown in other studies when osteoblasts were subjected to mechanical stimulation as well as in response to PTH treatment (Nasu et al. 200, Winter et al. 2003). Moreover SOST mRNA levels were decreased in patients 1 and 3 in response to rhPTH treatment as well as mechanical stimulation, which may further explain the enhanced osteoblast function as indicated by ALP staining.

Expression of sclerostin, the protein produced exclusively by osteocytes, was tested in this study via means of immunostaining and quantitative real-time PCR for SOST gene expression. Following rhPTH treatment in the presence or absence of mechanical stimulation sclerostin positive osteocyte numbers did not change when compared to T (0) and unloaded controls. However it should be noted that compared to rat bone as presented in chapter 3, the numbers of sclerostin positive osteocytes were higher in human bone. These findings may be due to the fact that sclerostin is a delayed secreted product of osteocytes, since newly embedded osteocytes will secrete sclerostin only after the local onset of mineralization, as such only matured osteocytes will secrete sclerostin (Poole et al. 2005). Another reason may be the fact that there was not a concentrated

region of cells that are affected enough to detect a change at the protein level using immunohostochemistry and possibly a more sensitive technique such as *in situ* hybridization would provide more information. On this basis it has been speculated that sclerostin functions as a final signal to osteoblasts (via osteocyte canaliculi) or to lining cells, when mineralization of the osteocyte surrounding matrix is completed, in order to limit osteoblast activity (Poole et al. 2005). Moreover only a subpopulation of osteocytes has PTH receptors in human bone, and newly embedded osteocytes do not express those, in order for them to be a PTH target (Langub et al. 2001).

On the other hand SOST mRNA levels were significantly reduced in response to rhPTH treatment in the presence or absence of mechanical stimulation, moreover loading and unloading conditions reduced the levels of SOST mRNA expression. Data presented here demonstrates that administration of intermittent rhPTH in the presence or absence of mechanical stimulation has downregulated SOST mRNA levels, demonstrating an rhPTH/loading-mediated effect on the regulation of SOST mRNA expression. However as mentioned SOST mRNA did not drop under unloading conditions as in murine models, possibly due to species-related differences, and it can be speculated that in human bone only PTH administration could prove effective in reducing sclerostin production. There is controversial data reported in the literature regarding the effects of intermittent PTH administration on SOST mRNA. Data presented in this study is in line with those of Keller and Kneissel (2005), Silvestrini et al (2007) who have reported a SOST mRNA reduction in mice and rat respectively, treated with PTH daily. Also Robling et al (2006) reported a decrease in SOST mRNA in response to mechanical loading in the rodent ulna loading model. On the other hand Bellido et al. (2005) have reported a fall in SOST mRNA in response to continuous infusion of PTH *in vivo* and *in vitro* while they failed to detect any changes in response to intermittent administration to PTH. In the presence of mechanical stimulation data presented here implicates SOST as a mechanically suppressed signal. With its known inhibitory effects of Lrp function and bone formation, it provides a possible regulatory mechanism that permits, enhanced Wnt signaling upon mechanical stimulation (Robling et al. 2006). Wnt signaling is important for the mechanotransduction cascade, as it was reported that Lrp5 deficient mouse

skeleton is unable to respond anabolically to mechanical stimulation (Sawakami et al. 2006). Intermittent PTH attenuates, while chronic administration does not affect osteoblast apoptosis (Bellido 2003) and reduces SOST mRNA (Bellido et al. 2005) in osteocytes; such that the precise role of SOST in intermittent PTH administration is not clear. SOST is clearly influenced by mechanical stimulation, as it is by PTH, and in the data presented here these two parameters in combination possibly exert a synergistic effect. PTH administration has also been shown to rapidly reduce sclerostin mRNA and protein production in osteocytes *in vitro* and in bone *in vivo* (Keller and Kneissel 2005, Silvestrini et al. 2007), raising the possibility that transient reduction of sclerostin output by osteocytes in response to intermittent PTH could mediate enhanced osteoblast differentiation and bone formation (Van Bezooijen et al. 2005), and reduced osteoblast apoptosis (Sutherland et al. 2004).

The beneficial bone responses to PTH therapy as well as mechanical stimulation are well known. *In vitro* studies using stretched osteocytes demonstrated that PTH and mechanical loading elevated IGF-I mRNA (Sekiva et al. 1999, Miyauchi et al. 2000). Such observations are suggestive of a potential mechanism between PTH signaling and mechanotransduction pathways. In the study by Chow et al. (1998) in normal and thyroparathyroidectomized rats, PTH (1-34) administration before or after mechanical stimulation restored the osteogenic response in the thyroparathyroidectomized rats suggesting that physiological levels of PTH are necessary for the mechanical responsiveness of bone. Similar findings were reported by Hagino et al. (2001) where a synergistic effect of mechanical loading and PTH administration was shown with bone formation increased by 4-point bending as well as by PTH administration with a significant interaction between loading and PTH.

In this study mechanical stimulation in the presence and more interestingly in the absence of rhPTH decreased the numbers of apoptotic osteocytes compared to unloading conditions in the absence of rhPTH. The anti-apoptotic effects of PTH have been demonstrated both *in vivo* and *in vitro* by Jilka and colleagues (1999) as well as in the previous chapter in this thesis were the anti-apoptotic effect of rhPTH on osteocytes *in*

vivo was highlighted. Frost (1988, 1992) proposed a strain threshold, called the 'set point' above which bone modeling and remodeling are activated. According to this theory hormones act to adjust the skeletal 'set point' that regulates bone mass relative to customarily encountered loading stimuli. The observations made in this study indicate that intermittent administration of rhPTH lowers this 'set point' such that identical loading stimuli are perceived as more intense in the rhPTH treated samples than in the controls. It has been shown in this study that rhPTH possibly acts synergistically with mechanical stimulation to decrease osteocyte apoptosis. Moreover rhPTH has been shown to exert its anti-apoptotic effects even in the absence of mechanical stimulation as demonstrated in the samples treated as such. In the study by Sakai et al (1999) it was reported that intermittent PTH (1-34) administration at 40μg/kg five times per week prevents immobilization related bone loss at the proximal tibia in the sciatic neurectomized mouse model (Sakai et al. 1999).

To my knowledge no other study exists in the literature to have reported the use of an *ex vivo* bioreactor to apply mechanical loads in the presence or absence of rhPTH. However in this study only a single dose of rhPTH was administered and the subsequent observations made should be interpreted with caution. Therefore it would be useful to conduct further studies to determine the dose-dependency of the effects of rhPTH on human osteocytes in response to mechanical stimulation. This study was based on samples obtained from three different patients and that can explain the variability observed in some of the treatment groups, however all three showed similar responses to loading and rhPTH in all parameters examined. This patient variability can be explained by the different genetic backgrounds, health problems and treatment received by each individual, alterations in the environment, age, nutrition, different trabeculae architecture and tha fact that males respond differently to load compared to females. Moreover findings of other studies examining indices tested here were reported in rat and mouse bone and there are potential species-related differences that should be acknowledged before comparing to human bone. Furthermore, it should be taken into account that the samples used were coming from patients undergoing elective hip arthoplasty and responses should be interpreted accordingly. The individuals were receiving various

prophylaxes for pain management but to my knowledge none was receiving any treatments in the form of HRT known to affect bone turnover. The degree of between-patient variability seen here is in agreement with previous work in our lab (Mann et al. 2006) and others (Tomkinson et al. 1997, Dunstan et al 1993) in which a range of variabilities in terms of apoptosis, viability as well as alkaline phosphatase positive surfaces are reported.

In summary this study has provided evidence that osteocytes undergo apoptosis in response to unloading which could be improved following application of mechanical stimulation within physiological levels in the Zetos^{TM} bioreactor in the presence or absence of rhPTH. Application of mechanical loading in the presence or absence of rhPTH induced an osteogenic response in terms of alkaline phosphatase positively labelled bone surfaces. Finally application of loading in the presence or absence of rhPTH decreased the mRNA levels of SOST gene expression, providing an indication of how loading and/ or rhPTH may be acting to enhance bone formation. However after PTH treatment in the presence or absence of mechanical stimulation, no differences were detected in sclerostin-positive osteocyte percentages in the different treatment groups; this data is in line with the data reported by Poole et al. (2005) who recorded no statistical differences between numbers of sclerostin-positive osteocytes in cortical and in cancellous normal human bone. Similar data was obtained for sclerostin positive rat osteocytes *in vivo* following rhPTH treatment as presented in chapter 3. An alternative explanation to this finding may provide future studies of protein expression using Western blots.

The use of the Zetos^{TM} system has enabled us to study the response of human osteocytes in response to mechanical stimulation in the presence or absence of rhPTH, since it would be difficult due to ethical issues to obtain human biopsies pre- and post-exercise in response to hormone treatment. The molecular mechanisms by which mechanical stimulation and rhPTH treatment increased osteocyte viability and decreased apoptosis in this system has not been the subject of investigation in this study. It is possible that the reduction in apoptosis is a product of increased nutrient supply and oxygen or due to an

CHAPTER 5

Differential Gene Expression Between Osteoblastic Populations at Different Anatomical Sites: Use of Laser Capture Microscopy and Microarray

Abstract

Anabolic treatments such as PTH and GH have been proposed to exert their effects selectively and specifically on the osteoblastic population at the periosteal and endosteal sites of bone. However, the cellular and molecular mechanisms by which these agents regulate osteoblastic cell behavior remain poorly understood. In the present study an attempt to unravel potential mechanisms of their actions on the osteoblast is presented. For the identification of genes of interest as potential drug targets for age related bone loss laser capture microdissection (LCM) technology, and gene microarray was used.

Thirty virgin female Sprague-Dawley rats at the age of 15 months were divided into five treatment groups. The control group received vehicle by gavage (n=6), treatment groups received rhPTH (1-34) once daily at a dose of 50 μg/kg (n=6), rhGH once daily at a dose of 2.5 mg/kg (n=6) by subcutaneous injection, Compound A twice daily by gavage at a dose of 100mg/kg (n=6), and Compound B once daily by gavage at a dose of 200mg/kg (n=6). Compounds A and B are of unknown nature (provided by NOVARTIS).The duration of the experiment was 14 days at the end of which tissue sections from the tibias of these animals where subjected to LCM to isolate pure osteoblastic cell populations. The tissue collected was then used for total RNA isolation.

In this study a technique for generating cryosections of native bone and the preparation of homogeneous osteoblast populations representing the state they adopt in their *in vivo* environment is presented. Gene expression analysis is presented for a limited number of samples and methodological pitfalls in the original study design as well as the methodology to solve these issues are discussed.

5.1 Introduction

In the previous chapters evidence has been presented regarding the protective effects of rhPTH and rhGH on murine osteocytes *in vitro*, rat osteocytes *in vivo* and human osteocytes *ex vivo* and their potential use as anabolic treatments to treat bone loss has been discussed. Osteocytes are derived from osteoblasts that become incorporated during bone remodelling. Recently anabolic agents have received lots of attention as they have been demonstrated to act by inducing bone formation by osteoblasts and/ or by inhibition of osteoblast apoptosis (Jilka et al., 1999). Both PTH and GH have the potential to be used as anabolic treatments (Allen et al, 2004). Thus exploring their bone forming activity may provide identification of novel molecules and mechanisms that may prove to be advantageous for osteoporosis treatment (Raouf and Seth, 2002, Onyia et al., 2005, Gonovi et al., 2006). In spite of the approval of rhPTH (1-34) produced by Lilly referred to as teriparatide as a therapeutic anabolic agent that increases bone mass, the discovery of other safe alternative therapies against osteoporosis continues to be a need. PTH results in increased osteoblast numbers and activity either via increased differentiation or survival or due to the ability to increase IGF-I and IGF-II in osteoblasts (Jilka et al. 1999, Robinson et al. 2006). GH on the other hand has been shown to up regulate bone formation markers as well as serum concentrations of IGF-I (Fernholm et al., 2000, Hedstorm et al. 2004) acting either directly on osteoblasts or indirectly via the stimulation and release of IGF-I (Govoni et al. 2006). Studies have shown differences in the osteogenic responses these agents elicit at different anatomical sites of bone (Andreassen and Oxlund, 2000) and it has been proposed, that each cell population responds differently both qualitatively and quantitatively to hormones and growth factors (Allen et al. 2004). Compared to endosteal, periosteal osteoblasts exhibit greater mechanosensitivity to strain, lower responsiveness to osteogenic compounds such as PTH and GH, more estrogen alpha receptors and higher levels of protein expression such as periostin, which is present in greater abundance in periosteum compared to other locations in bone (Allen et al. 2004). Such findings suggest that selective targeting of either periosteal or endosteal bone surfaces where osteoblasts reside could prove useful; however such an approach would require the identification of genes and proteins unique

to those sites or present in greater concentrations. However the interactions between periosteal and endosteal surfaces and the role that mechanical compensation plays in periosteal and/or endosteal expansion should not be undervalued, and necessitates more in-depth study. There is the possibility that specific drug targets are present within those sites that can possibly be activated independently. However the relatively small quantities of periosteum and endosteum at given sites as well as thinning of it with ageing, present hurdles that may be overcome by the use of laser capture microdissection (LCM) combined with molecular biology assays and tissue arrays. In the present chapter a pilot study looking into the gene expression of endosteal and periosteal osteoblastic populations in response to rhPTH and rhGH treatment using LCM is presented.

Bone is a compact, analytically difficult to handle mineralized tissue that undergoes continuous remodelling. Osteoblasts - the bone forming cells are synthesizing and secreting bone matrix proteins during remodelling, until about 10-20% of their population reaches the final differentiation stage that of osteocytes and eventually become embedded in bone matrix. It is clear that the osteoblast serves very important functions which are under the influence of a number of transcription factors (e.g., Cbfa-1/Runx-2), growth factors (e.g., TGF-β) and hormones (e.g., PTH, GH) (Mackie, 2003); and contributes to the interactions between bone cells under normal and pathological conditions; but the molecular physiology of the osteoblast is poorly understood. The maturation of the osteoblast is a complex process that involves a number of genotypic changes and although it is desirable to identify these changes for advancing diagnostic and therapeutic measures of diseased bone, there are very few reliable *in vivo* and *in vitro* studies in cell lines, particularly due to the difficulties in handling native bone tissue (Raouf and Seth, 2002, Onyia et al., 2005, Gonovi et al., 2006).

Transcript profiling appears to be a useful tool to study the global gene expression from tissues and cell lines (Shaffer et al., 2002, Nakazono et al. 2003) and could provide valuable information that would help towards the development of new drug targets for treating pathological bone conditions. However to apply this technology cells that exist in heterogeneous tissues, surrounded by other cell types, it is necessary to minimize

contamination of unwanted cells. LCM is a new tool that makes it possible, which allows the identification of cells, followed by their excision and subsequent RNA extraction. Successful microarray hybridization depends on the quality of the RNA samples subjected to analysis. The tissue preparations used in bone investigations are an unsatisfactory source of RNA; with the typical ones including formalin fixation, decalcification and paraffin embedding which generate chemically modified RNA molecules as well as affecting their integrity (Goldsworthy et al. 1999, Finkelstein et al. 1999, Srinivasan et al. 2002). Cryosections of bone are thought to provide the best source for obtaining intact RNA (Goldsworthy et al., 1999). However preparation of homogeneous populations of osteoblasts from frozen, undecalcified bone sections has proven to be difficult due to the low numbers of osteoblasts in the highly calcified tissue. Typically a minimum of 100ng of total RNA is required for indirect or direct labeling of cDNA to perform hybridization on one microarray chip to analyze gene expression (Xiang et al. 2002). Yields of this magnitude are usually not viable from typical LCM derived samples and as such amplification to make microarray analysis possible is required (Wang et al 2006). Collection of high quality RNA using LCM requires the application and optimization of various methodological steps including sectioning, staining, laser microdissection and successful RNA isolation; since it has not been determined to what extent each of the steps in LCM sample processing damages the RNA.

In the study presented here a short proof of concept study was undertaken to establish the feasibility of the Novartis study. For this study 2-3 months female virgin rats were used and ~ 10,000 periosteal and endosteal cells were collected using LCM and RNA extraction. These samples were evaluated and osteoblast lineage specific genes were identified. Following this study the Novartis study was initiated as discussed in this chapter.

In this chapter a pilot study is presented for the preparation of homogeneous osteoblast populations from cryosections of native rat bone, using laser microdissection

technology.Limited gene expression data is also presented and indicates methodological pitfalls in the original study design as well as the methodology to solve these issues.

5.2 Materials and Methods

All chemicals were purchased from Sigma, UK, unless otherwise stated. All LCM consumables were purchased from P.A.L.M. Microlaser Technologies.

5.2.1 Animals

The experimental design for the animals used in this study has been described 3.2.1; in the study described in chapter 3 only three groups where analyzed. In this study the second tibias of all five groups as outlined in diagram 5.1 where analyzed. More specifically the second tibias of all five animals from each of the five groups were sectioned and used for laser microdissection (LCM). Briefly animals were randomized into five treatment groups. The control group received vehicle by gavage using a stomach tube. The second group received synthetic recombinant human parathyroid hormone fragment 1-34 (rhPTH) (provided by NOVARTIS) once daily at a dose of 50 µg/kg body weight via subcutaneous injection, dissolved in 0.15M saline. The third group received recombinant human growth hormone (rhGH) (provided by NOVARTIS) once daily at a dose of 2.5 mg/kg body weight via subcutaneous injection, dissolved in distilled water. The fourth and fifth group received compounds A and B of unknown nature (provided by NOVARTIS),compound A was administered twice daily by gavage using a stomach tube at a dose of 100mg/kg body weight and compound B was administered once daily by gavage using a stomach tube at a dose of 200mg/kg body weight. The duration of the experiment was fourteen days, at the end of which all animals were killed by exsanguination, the tibias were harvested and dissected free of muscle, briefly immersed in 5% polyvinyl alcohol and chilled to –70°C in super cooled hexane (BDH, UK), prior to storage and analysis. Animal experimentation was conducted in compliance with national ethical guidelines.

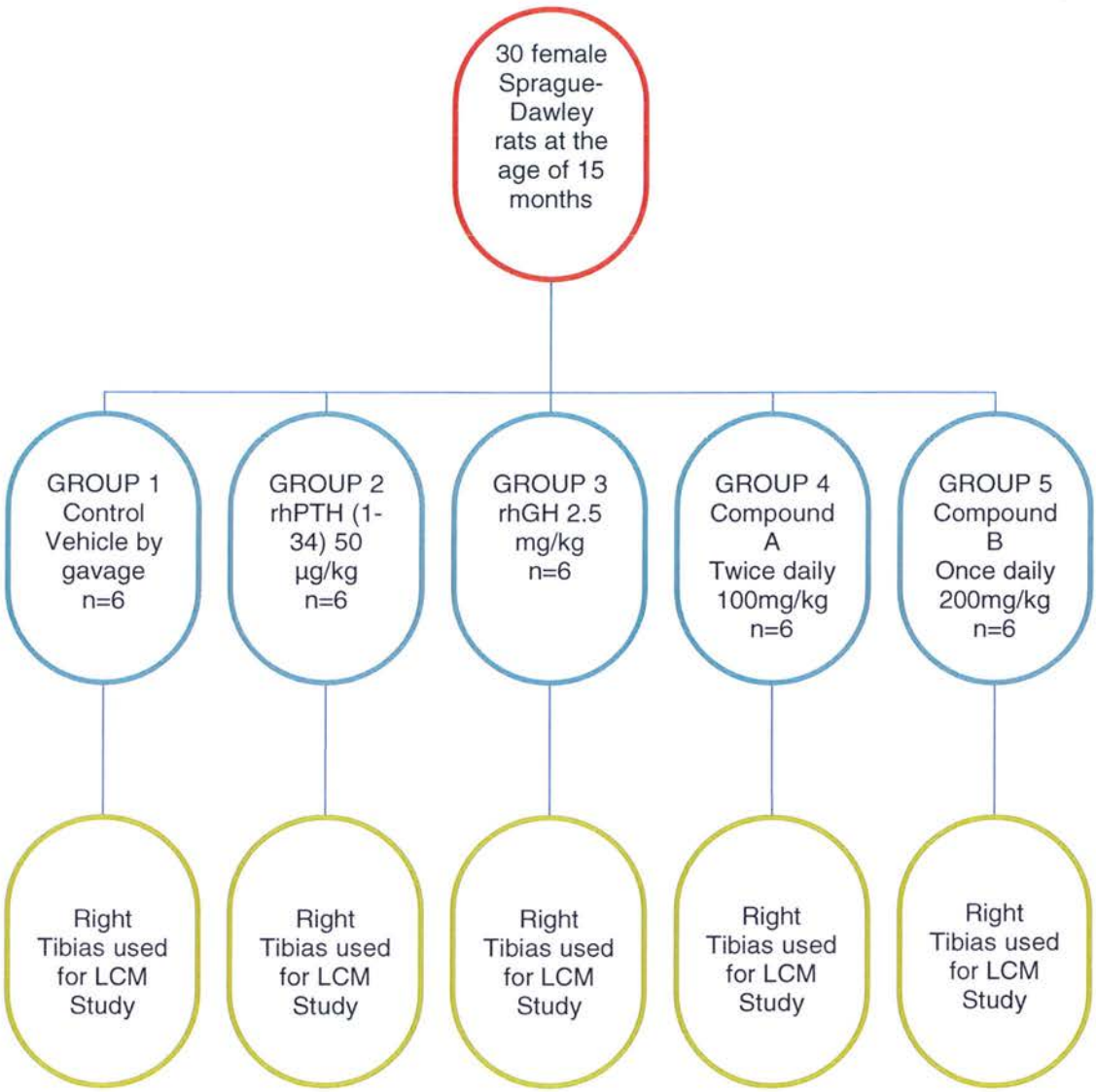

Diagram 5.1: Flow Diagram of *in vivo* experimental design. Thirty female animals were randomized in five treatment groups and tibias were subjected to cryosectioning and LCM.

5.2.3 Preparation of cryostat sections

Following their removal, bone specimens were immediately snap-frozen in hexane under RNase-free conditions. The sample was mounted on a chuck using polyvinyl alcohol in a freezing bath and was placed in the cryostat (Bright Instruments, Co. Ltd) to acclimatize at -26 to -28° C for 30 minutes prior to sectioning. Sectioning was performed using a tungsten carbide blade (Bright Instruments, Co. Ltd) at a thickness of 10 microns. For the identification of mid-diaphysis sections were examined every 20 sections following identification of the growth plate under the microscope. The absence of trabecular bone indicated the start of the diaphysis and sections were collected from that area of bone. Prior to LCM one slide (i.e. 4 sections) was stained with DAPI nuclear stain. Placed on the PALM microscope and number of cells per area (endosteum and periosteum) were counted per section and an average taken over the 4 sections in order to determine number of sections/area required to be LCM.

Subsequent sections were fixed by physical pressure on 1.35 μm thick PEN membrane slides (PALM). The slides were pre-treated to ensure RNAse free conditions, by dipping in RNase Away for 5 seconds and then washed twice in DEPC treated water; allowed to dry at room temperature prior to UV treatment for 30minutes at 254nm to polymerize the adhesive. Cryosections were stored at -80°C.

Prior to initiation of the Novartis study, preliminary studies as described in §5.3.2.1 were carried out to establish the techniques to be used. For these studies 2-3 month old female rat tibias were used for estimation of cell numbers using DAPI stain, to establish the best settings and conditions for laser microdissection and finally establish the most successful RNA extraction method, due to the difficulty to obtain animals of similar age as these of the *in vivo* study. The animals of the *in vivo* study were at the age of 18 months and the numbers of cells where found to be significantly lower compared to the younger animals of the preliminary studies (Figure 5.1).

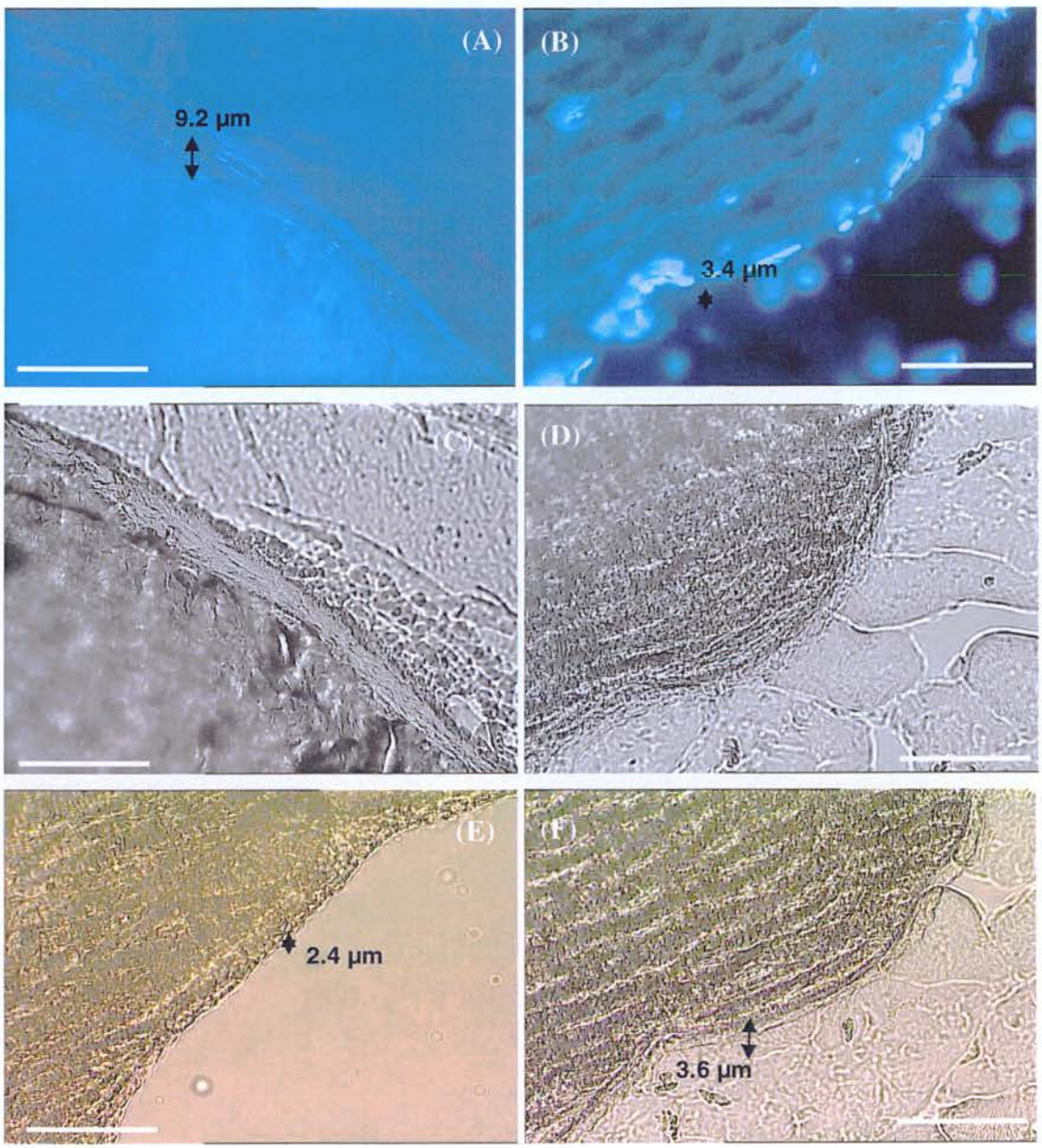

Figure 5.1. Representative images of periosteal and endosteal surfaces of young and old female rat tibias. DAPI stained and bright field periosteal surface of a 3 month old female rat tibia from the preliminary studies, with about 50 cells found on that surface (A, C), DAPI stained and bright field periosteal surface of an 18 month old female rat tibia from the *in vivo* study, with about 20 cells found on that surface (B, D). Bright field images of periosteal and endosteal surface from an 18 month old animal from the in vivo study (E, F).Bar represents 100µm.

5.2.4 Fixation and Staining of sections

Cryosections on slides were immediately fixed in pre-cooled 70% ethanol for 5 minutes followed by a 1 minute dip in eosin solution followed by washing in DEPC treated water. Cryosections were dehydrated by increasing grades of ethanol from 70% to 95% up to 100% for 15 seconds each. Cryosections were then allowed to dry at room temperature; when no leftover ethanol was obvious on the slides they were stored at -80°C until further use.

5.2.5 Micro Laser Dissection

LCM of the cryosections was performed using a 337-nm pulsed UVa-nitrogen laser (P.A.L.M Instruments, Germany) built in an inverse Zeis Axiovert 200/200m microscope (Figure 5.2). A pulsed ultra-violet (UV-A) laser of high beam quality is interfaced into the microscope and focused through an objective to a beam spot size of less than 1 micrometer in diameter for the cutting action. The principle of laser cutting is a locally restricted ablative process without heating of the adjacent material and results in a clear cut gap between the desired sample area and the surrounding tissue. After microdissection is complete, the isolated specimens are ejected out of the object plane and catapulted directly into a microfuge tube in a non-contact manner and such without the introduction of contamination (PALM MicroLaser Systems).

For collection of tissue 70µl of lysis buffer (10 ml's of RLT buffer (Qiagen) + 100 µl β-mercaptoethanol (Invitrogen)) were added into an eppendorf tube cap and the section was examined at x5 magnification to locate the area of interest. Upon identification of the area of interest laser dissection was performed using the PALM Robo software at 20 x magnifications with the laser energy and focus settings optimized according to the respective absorption behavior of the microdissected specimens (Figure 5.3, Figure 5.4). At the end of each collection the eppendorf cap was examined at x5 to ensure that laser dissection and catapulting were successful. The tube containing the laser dissected material was then centrifuged at 10, 000 rpm for 15 seconds to collect the sample at the bottom of the tube and stored at -80°C until further use.

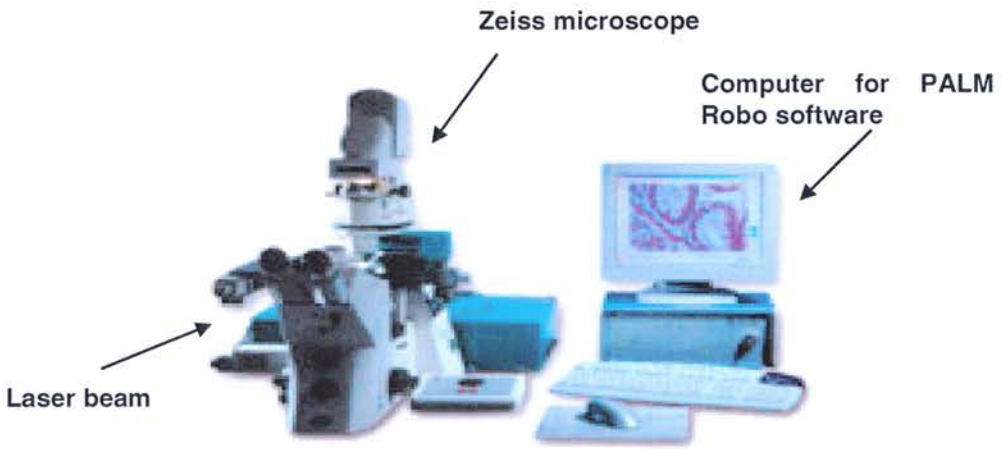

Figure 5.2. Zeiss/PALM system used for laser capture microdissection. Laser capture microdissection microscopy (LCMM) utilizes a UV laser pulsed micro beam for dissection. The isolated tissue is then catapulted into a microfuge tube cap for follow-up analysis.

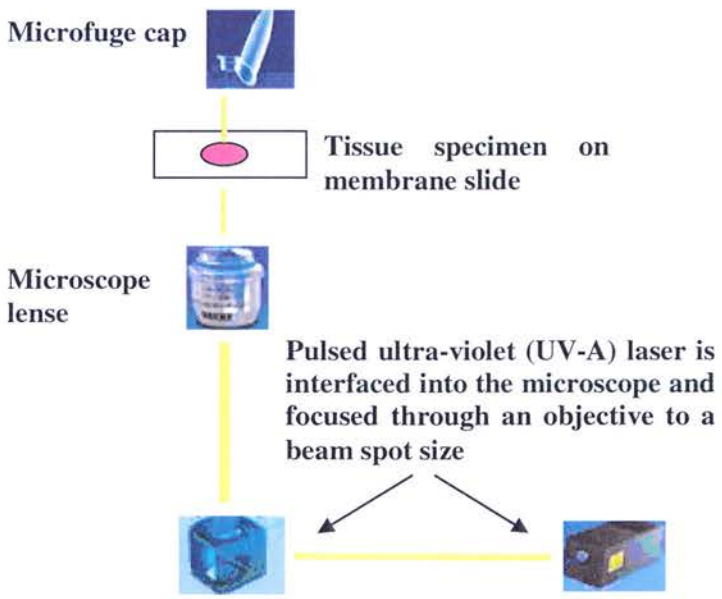

Figure 5.3. Principle of LCM. A pulsed ultra-violet (UV-A) laser is interfaced into the microscope and focused through an objective to a beam spot size for the cutting action. The principle of laser cutting is a locally restricted ablative process without heating of the adjacent material and results in a clear cut gap between the desired sample area and the surrounding tissue. After microdissection, the isolated specimens catapulted directly into the cap of a microfuge tube.

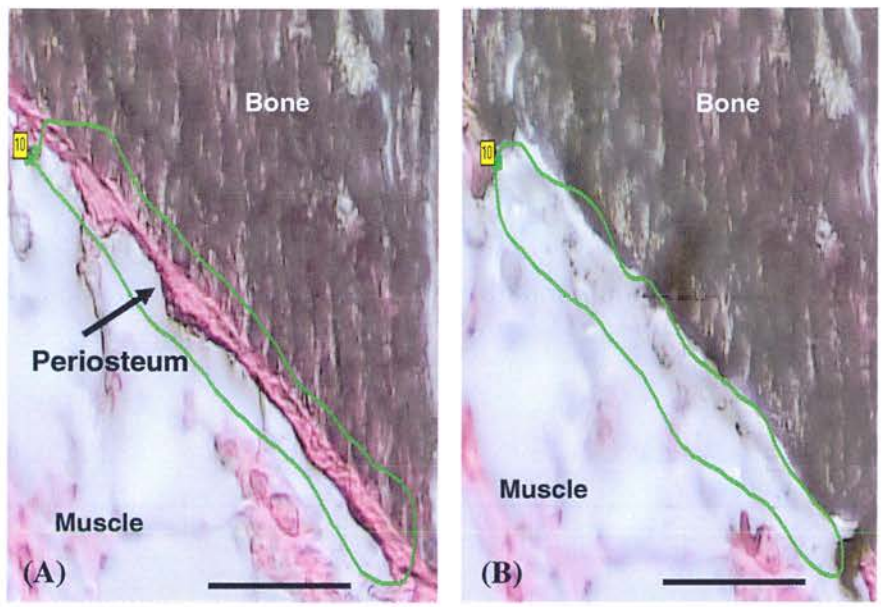

Periosteum prior LCM x20 Periosteum post LCM x20

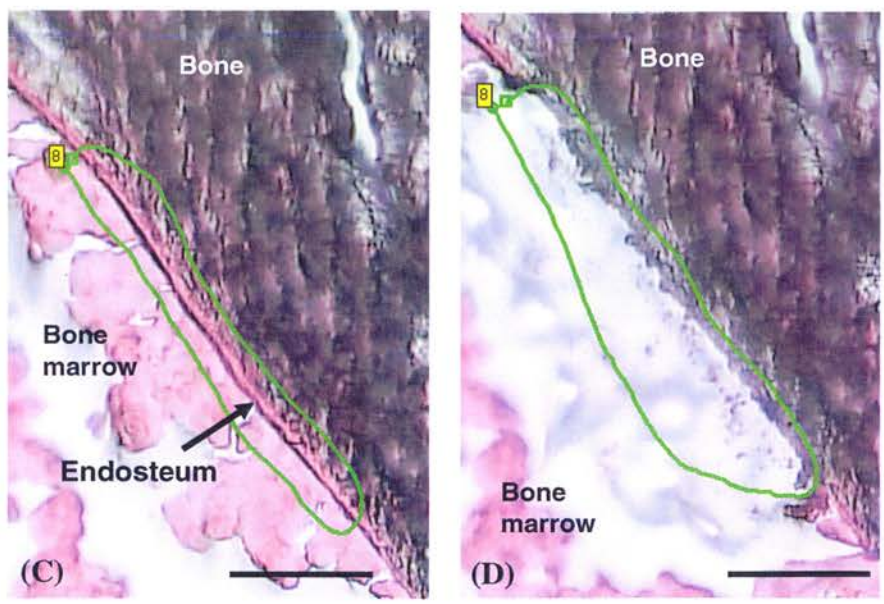

Endosteum prior LCM x20 Endosteum post LCM x20

Figure 5.4. Preparation of osteoblasts from bone cryosections using laser microdissection. Tibial mid-diaphysis specimens were dissected using a pulsed UVa-nitrogen laser. (A) Microdissection of periosteal osteoblasts prior LCM and (B) after LCM. (C) Microdissection of endosteal osteoblasts prior LCM and (D) after LCM. LCM was performed on fixed 10μm thick cryostat sections. Bar represents 100μm.

5.2.6 RNA Isolation

The RNA samples from which microarray data was obtained as described in §5.2.4 were extracted using the Qiagen Micro RNeasy Kit- for isolation of total RNA from microdissected tissue following manufacturer's protocol. In each case approximately 50,000 cells were LCM and RNA extracted. Limited microarray data was obtained from a small number of samples from the first set of RNA sent. No data was obtained from the second set of RNA samples as these were determined to be either sub-optimal or no RNA detectable. Therefore a number of RNA extraction methods and modifications trials were initiated using 50,000 LCM cells to try and improve the RNA quality. Four methods were used:

1) **Proteinase K** - Introduction of a Proteinase K digestion step to RNA extraction using Qiagen RNeasy Micro Kit.
2) **Trizol** (Invitrogen) following manufacturers protocol with two modifications (a) following homogenisation stage in Trizol solution samples were incubated for 10 minutes at room temperature with rotation prior to the addition of chloroform. (b) Glycogen carrier (20µg) was added to the aqueous phase prior to precipitation with isoprpanol.
3) **Decalcification** - Sections were de-calcified 10 minutes at room temperature in the decalcification mixture. Sections then underwent LCM and RNA extraction using either (a) Qiagen RNeasy Micro Kit or (b) Trizol followed by Qiagen Micro Kit Clean-up.
4) **Arcturus Pico Pure** - RNA was extracted from 50,000 LMD cells following Pico Pure RNA Isolation Kit Arcturus following manufacturer's protocol.

Total RNA was purified according to protocols provided by the suppliers as described below. Microdissected tissue was captured and lysed in buffers according to individual protocols.

5.2.6.1 Qiagen Micro RNeasy Kit - for isolation of total RNA from microdissected tissue

RNA was extracted from the micro dissected tissue using the RNeasy Micro Kit (Qiagen, UK). All the collections were pooled together into a single eppendorf tube at a 350 µl volume. The samples were then homogenized by passing through a 29 gauge (29G) needle. 350µl of 70% ethanol were added to the lysate and mixed by pipetting. The mixture was then applied onto an RNeasy MinElute Spin Column, and centrifuged (eppendorf Centrifuge 5415D) for 15secs at >8,000xg and another 350µl buffer RW1 were added to wash the column. To remove any genomic DNA contamination 10µl of DNaseI stock solution were added to 70µl buffer RDD and pipetted directly onto the membrane for 15 minutes at room temperature. To wash away the DNaseI mix, 350µl of buffer RW1 were pippeted onto the membrane.

The column was then transferred into a new collection tube and 500µl of buffer RPE was added onto the column to wash it further. Then 500µl of 80% ETOH was added to the column and centrifuged for 2 minutes at >8,000xg to dry the membrane. To elute the RNA the column was transferred into a 1.5 ml collection tube and 18µl of RNase free water was pippeted onto the membrane; the tube was then centrifuged for a minute at maximum speed. The RNA sample was then transferred on ice and stored immediately at -80°C.

5.2.6.2 Trizol

The tissue was collected in TRIZOL reagent (Invitrogen, UK) and stored at -80 °C until all collections were complete. The tissue was then pooled together into a single tube at a 500 µl volume and ground using a mortar and pestle for 1 minute. The homogenized sample was then incubated for 5 minutes at room temperature to allow the dissociation of nucleoproteins. The mix was then centrifuged (eppendorf centrifuge 5417R) to remove any debris and the supernatant was transferred to a new tube. 200 µl of chloroform was added and the samples vortexed for 15 seconds and incubated at room temperature for 2-3 minutes prior to centrifugation at 4°C for 15 minutes at 12,000 x g. The mixture then separates into a lower phenol-chloroform phase containing the DNA, an interphase that contains protein and a colorless upper aqueous phase containing the RNA. The upper aqueous phase was carefully aspirated into a new tube taking care to avoiding the interphase. An equal volume of room temperature isopropanol was added and the sample placed at -20 °C for a minimum of 20 minutes in order to precipitate the RNA. Following centrifugation at 12,000 x g for 10 minutes at 4°C the RNA was visible as a gel-like pellet at the bottom of the tube. The supernatant was then removed and the pellet washed three times with 1ml of 75% ethanol at 7,500 x g for 5 minutes at 4°C. All leftover ethanol was removed after the final wash and the pellet was allowed to air-dry for approximately 10 minutes. The RNA pellet was then dissolved in 15 µl of RNAse free water. The RNA sample was then transferred on ice and stored immediately at -80°C.

5.2.6.3 Qiagen Micro RNeasy Kit clean up

RNA samples extracted using the Trizol method were subjected to a clean up using the Qiagen Micro RNeasy kit, when there was an indication of co-contaminants in the samples. The sample was adjusted to 100µl with RNase-free water and 350µl of RLT buffer along with 250µl of 100% ethanol added and mixed thoroughly by pipetting. The sample was then loaded onto a column and centrifuged for 15 seconds at >8,000g. The flow through was then discarded and the column washed with 350µl of buffer RW1 centrifuged at >8,000g for 15 seconds. The flow through was then discarded and 500µl of buffer RPE was applied on to the column and centrifuged at >8,000g for 15 seconds. Another wash with 80% ethanol followed for 2 minutes at >8,000g. After the final wash the flow through was discarded and the column dried via centrifugation at full speed for 5 minutes. To elute the RNA 14µl of RNase free water were added to the column and centrifuged for 1 minute at maximum speed.

5.2.6.4 Arcturus Pico Pure RNA Isolation Kit

RNA was extracted from microdissected tissue using the Pico Pure RNA Isolation Kit by ARCTURUS (Arcturus, UK). The tissue was collected in 50 µl of extraction buffer provided with the kit into a microcentrifuge tube. At the end of each collection the tube was centrifuged and the collected cell extract was incubated at 42°C for 30 minutes and then stored at -80 ° C until all collections were completed and ready for the RNA extraction..

For the RNA isolation all collections were pooled together into one single eppendorf tube at a 250 µl volume. The column was pre-conditioned with 250µl of conditioning buffer for 5 minutes and then centrifuged at 16,000 g for 1 minute. The cell extract was then mixed with 70% ethanol and pippeted on the purification column, centrifuged at 100g for 2 minutes followed by an immediate centrifugation at 16,000g for 30 seconds. The column was then washed with 100 µl of wash buffer one and centrifuged at 8000g for 1 minute, followed by 100 µl wash with wash buffer two followed by centrifugation at 16000g for 2 minutes. After washing, the column was transferred into a new tube and 11

µl of the elution buffer was pippeted onto the column and incubated for 1 minute at room temperature prior to centrifuging at 1,000 g for 1 minute followed by an immediate centrifugation at 16,000g for 1 minute. The RNA sample was then transferred on ice and stored immediately at -80°C.

5.2.7 De-calcification of sections

Sections were de-calcified for the removal of hydroxyapatite. Following cryosectioning sections were incubated for 10 minutes at room temperature in the de-calcification mixture (50mM Tris/HCL containing 0.25mM EDTA at pH 7.4). Following de-calcification sections were gently washed with PBS followed by fixation and staining.

5.2.8 RNA quality and Quantity tests

In order to obtain successful microarray results both the quantity and quality of RNA are very important parameters. The RNA extracted in this study was tested both on the NanoDrop™ 1000 (Thermo Scientific) which is one of the most developed spectrophotometers, for quantity and the Agilent bioanalyser 2100 (Agilent, Palo Alto, CA, USA) for quality.

5.2.8.1 NanoDrop™ 1000

The NanoDrop™ 1000 Spectrophotometer (Thermo Scientific) enables highly accurate UV analyses of 1 µl samples. 2 µl of the RNA sample were loaded at the bottom pedestal of the instrument and then the other pedestal was lowered. Once a column was formed between the pedestals, using the NanoDrop™ software the quantity of RNA was measured and also the 260/280 and 260/230 ratios were given (Figure 5.6). At the end of the measurement the pedestals were washed with water. The 260/280 ratio is used to assess the purity of the nucleic acid. A ratio of ~2.0 is generally accepted as 'pure' for RNA preparations. If the ratio is lower that might indicate contamination of protein, phenol or salts. The 260/230 ratio was used as a secondary measure of purity and is usually higher than the 260/280 ratio. It is commonly in the range of 1.8-2.2. If this ratio is lower it is indicative of the presence of co-purified contaminants.

5.2.8.2 Agilent Bioanalyzer 2100

The Agilent 2100 bioanalyzer (Agilent Techonologies) is a microfluidics-based platform used for the analysis of DNA, RNA, proteins and cells. The data is generated within 30 minutes and indicates the quality and quantity of nucleic acids mainly by the RNA integrity number (RIN), scale from N/A to 10 which helps to estimate the integrity of the RNA not by the ratio of the ribosomal bands but by the entire electrophoretic trace of the RNA sample (Figure 5.7). RNA that was not degraded should have two clear bands representing the 28S and 18S rRNA, with ratios of 28S/ 18S absorbance exceeding 1.5. In addition, the RNA sample should be low in genomic DNA contamination, which would appear as bands larger than 28S rRNA. In the present study the pico chip was used, due to the low amounts of RNA obtained, the quantity of RNA detected with a pico chip is within 200-5000 pg/µl.

All the solutions were left at room temperature to equilibrate for half an hour. 1 µl of the dye concentrate was added in the filtered gel; vortexed and spun down to remove any residual dye. A pico chip was placed in the chip priming station and 9 µl of the gel-dye mix were pippeted in the designated well. The plunger was then held by the clip to evenly spread the gel throughout the chip and after 30 seconds it was released. Another 9µl of the gel-dye mix were added in the designated well. 9 µl of the conditioning buffer (providing the mixture with conditioning factors) were added in the appropriate well and 1 µl of the pico marker was added in the well marked as ladder. 1 µl of the samples to be tested were pippeted into each of the 10 wells. The chip was then vortexed in an adapter for 1 minute and placed into the Agilent Bioanalyzer within 5 minutes.

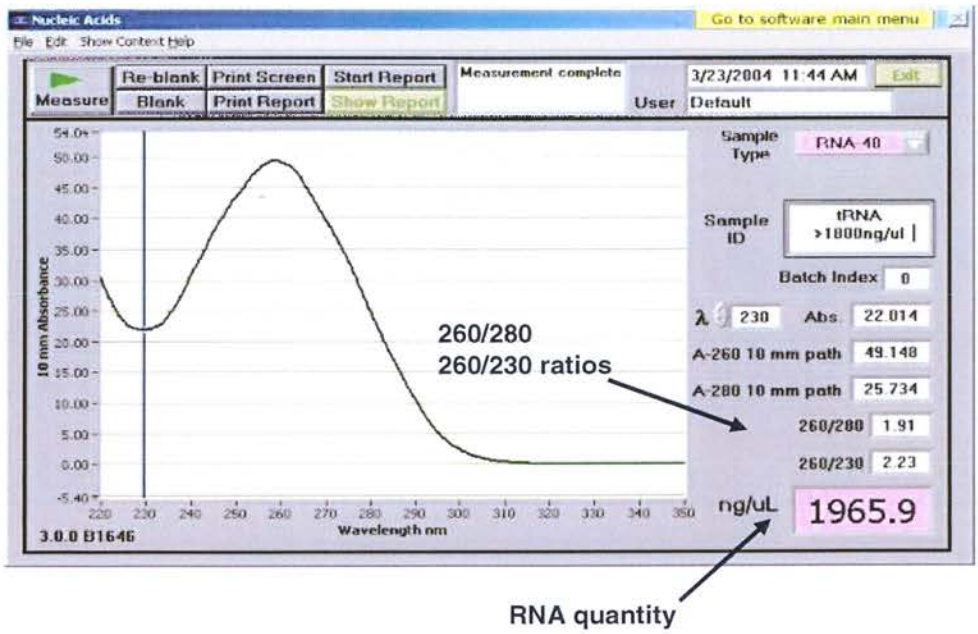

Figure 5.5 Typical analysis outcome of an RNA sample measurement with the NanoDrop™ 1000. A column with the RNA sample is formed between the pedestals and by using the NanoDrop™ software the quantity of RNA is measured and also the 260/280 and 260/230 ratios are given.

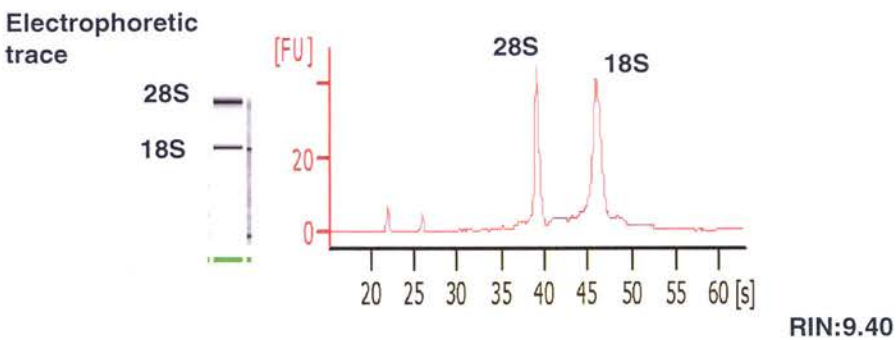

Figure 5.6 Typical analysis outcome of an RNA sample measurement with the Agilent 2100 bioanalyzer. The Agilent bioanalyzer is a microfluidics-based platform that provides information of the quality and quantity of nucleic acids, via an estimation of the RIN number which helps to estimate the integrity of the RNA not by the ratio of the ribosomal bands but by the entire electrophoretic trace of the RNA sample

5.2.9 Reverse Transcription Polymerase Chain Reaction (RT-PCR)

For RT-PCR successful reverse transcription depends on the integrity and purity of the RNA used as the template. Superscript™ III First Strand Synthesis System for RT-PCR (Invitrogen) was used to synthesize first strand cDNA. Superscript can copy DNA sequences from an oligo(dT) 16-18 primer which will anneal to mRNA poly-A tail. As per manufacturers instructions a 10 µl reaction was set up as follows:

1µl dNTP
1µl oligo (dT)
2µl RNA (20ng/µl)
6µl $_{DEPC}H_2O$

This mixture was heated at 65°C for 5 minutes before cooling on ice for >1 min, and addition of the following:

2µl 10xRT buffer
4µl $MgCl_2$
2µl 0.1 M DTT
1µl RNase OUT

This mixture was then heated to 42°C for 2 minutes and 1µl of Superscript mix was added directly into the mixture. It was then incubated at 42°C for 50 minutes and 70°C for 15 minutes on a thermocycler. The tube was then centrifuged and 1µl of RNase H was added directly into the mixture followed by incubation at 37 °C for 20 minutes. The resulting cDNA was then stored at -20°C until further use.

5.2.10 Polymerase Chain Reaction (PCR)

PCR is used to amplify specific regions of a DNA strand, which can be a single gene or part of a gene. The basic components of a PCR are a DNA template, one or more primers which are complementary to the DNA regions at the 5' and 3' ends of the DNA region, a DNA polymerase, deoxynucleoside triphosphates (dNTPs) which are the building blocks from which the DNA polymerases synthesizes the new DNA strand, a buffer solution that provides a suitable chemical environment for optimum activity and stability of the DNA polymerase, divalent cations, more commonly magnesium (Pavlov et al. 2004). Primers for use in PCR for the detection of actin were all designed in house. The sequences of the primers were:

β-actin: forward primers, 5'-ATCGTGGGGCGCCCCAGGCACC-3'

580 bp reverse primers, 5'-CTCCTTAATGTCACGCACGATTTC-3'

The PCR reaction was carried out in a 25µl volume by first preparing a master mix as follows using Taq DNA Polymerase (QIAGEN):

2µl	cDNA
2.5 µl	10xbuffer
0.5µl	dNTP's
0.5µl	Taq (5.5 units/25µl)
1.25µl	primer F
1.25µl	primer R
5µl	Q
12.1µl	H_2O

The reaction was performed by incubating the samples in an automatic DNA Thermal Cycler (Peltier Thermal Cycler, MJ Research PTC-200,) at appropriate temperatures corresponding to the three steps of the reaction of amplification-denaturation, annealing and extension. The thermal cycler program was as follows:

94°C 2 minutes
94°C 1 minute
60°C 1 minute
72°C 1 minute
Go to 2 x 25 times
72°C 7 minutes
4°C for ever

PCR products were visualized on agarose gels containing ethidium bromide and sized by running size markers.

5.2.11 Agarose Gel Electrophoresis

Agarose gels were made using SeaKem GTG Agarose (FMC Bioproducts). For the separation of products 1.2% agarose gels were cast. The required amount of agarose was dissolved in TBE buffer (89mM Tris Base, 89mM Boric Acid, 2mM EDTA sterilized with autoclaving), and the mixture was heated in a microwave oven for approximately 2 minutes until all agarose had dissolved. Agarose was cooled under running tap water for about 3 minutes. On cooling of the agarose 5 µl ethidium bromide (10mg/ml) was added and stirred, prior to gel being cast in the electrophoresis gel cast system. When the gel was set, the electrophoresis tank was filled with TBE buffer and samples were loaded using 3 µl of Orange G loading dye (1% w/v in dH_2O). 100 volts were applied across the gel until the dye front had migrated 2/3 from the end of the gel. Gels were visualized using a UV transilluminator (Uvidoc, UVItec, BTS-20-M). Ethidium bromide has the ability to bind to DNA/RNA and visibly fluoresces under UV light. The product size was measured relative to size markers (2 µl of Tracklt™ 100bp DNA ladder (Invitrogen)) which were run alongside samples.

5.2.12 Microarray and Bioinformatics

All microarray and bioinformatics analysis was carried out by the Novartis Genomics Unit (Basel, Switzerland). For cDNA synthesis since the starting total RNA was in the range of 10-100 ng per reaction, the 2-cycle cDNA amplification according to Affymetrix protocol was followed. For labeling and subsequent hybridizations to the arrays standard Affymetrix protocols were followed. The U34A oligonucleotide array (Affymetrix) was used for the microarray analysis. In figure 5.8, a summary of the steps involved in the two-cycle cDNA synthesis is presented.

DAY 1

Total RNA (100 ng)

↓

First Strand cDNA Synthesis using T7- oligo dT primer

↓

Second Strand cDNA Synthesis **(2)**

↓

In vitro Transcription using unlabelled ribonucleotides **(3)**

DAY 2

Clean-up of cRNA **(4)**

↓

First Strand cDNA Synthesis using random primers **(5)**

↓

Second Strand cDNA Synthesis using T7-oligo dT primer **(6)**

↓

Clean-up of Double Stranded cDNA **(7)**

↓

In vitro Transcription using biotinylated ribonucleotides **(8)**

DAY 3

Clean-up of cRNA **(9)**

Fragmentation and Hybridisation **(10)**
Carried out by MaC

Figure 5.7 Diagrammatic representation of the steps involved in the two-cycle cDNA synthesis for small samples. The process of the cDNA synthesis for small samples as per Affymetrix standard protocol.

5.2.12.1 Small Sample Protocol using the Affymetrix Two-Cycle Labelling Reagents First Cycle, First strand cDNA synthesis

Reagents were supplied by Affymetrix in the GeneChip Two-Cycle cDNA synthesis kit, the GeneChip IVT labelling kit, the GeneChip Sample Cleanup Module and Ambion in the MEGAscript High Yield Transcription Kit.

In more detail for **step 1**: (100ng) Total RNA - 2.5 µl
(5pmol/.l) diluted T7 Oligo d(T) primer 2µl
Diluted PolyA+ Cocktail 0.5 µl
Nuclease free dH2O. 0 µl

Made up to a total of 5 µl. Mixed by pipetting, spun briefly as necessary and then incubated at 70 °C for 6 minutes in a thermal cycler with a heated lid. The sample was cooled at 40 °C for 2 minutes; and spun briefly.

For the master mix: (5x) First Strand Buffer 2 µl
(0.1 M) DTT 1 µl
(10mM) dNTPs 0.5 µl
RNase Inhibitor 0.5 µl
Superscript II 1 µl

5µl of master mix were added to each reaction tube. Mixed by pipetting, spun briefly and incubated at 42 °C for 1 hour in a thermo-cycler with a heated lid. The reaction was incubated at 70 °C for 10 minutes in a thermo-cycler with a heated lid to inactivate the enzyme.The samples were cooled at 4 °C for 2 minutes and proceed immediately to "First Cycle, Second strand cDNA synthesis".

Step 2: Prepare a master mix: Nuclease free dH2O 4.8 µl
(17.5 mM) Freshly diluted MgCl2 4.0 µl
(10mM) dNTPs, 0.4 µl
E. coli DNA Pol I, 0.6 µl
RNase H, 0.2 µl

Mixed by pipetting and spun briefly.10 µl of the master mix were added to each of the first strand reaction tubes mixed by pipetting and incubated at 16 °C for 2 hours in a thermo-cycler without a heated lid, at 75 °C for 10 minutes and at 4 °C for 2 minutes. Following incubation tubes were placed on ice and proceed to "First Cycle, IVT Amplification of cRNA".

For step 3: Prepare a master mix:

10X Reaction buffer	5 µl
(75mM) ATP Solution	5 µl
(75mM) CTP Solution	5 µl
(75mM) GTP Solution	5 µl
(75mM) UTP Solution	5 µl
Enzyme Mix	5 µl

Mixed by pipetting and spun briefly. 30 µl of the master mix were added to the double-stranded cDNA from the previous reaction, and mixed thoroughly by pipetting. Tubes were then incubated at 37 °C for 16 hours in a thermo-cycler, spun briefly and proceed to "Clean-up of amplified cRNA".

For step 4: The samples were transferred to 1.5 ml microfuge tube and 50 µl of Nuclease free dH2O and 350 µl of IVT cRNA Binding Buffer were added and mixed thoroughly by pipetting. 250 µl of 100% ethanol were added and mixed by pipetting. The samples were then applied to an IVT cRNA Cleanup Spin Column and centrifuged at ≥8,000g for 15 seconds. The column was then transferred to a fresh 2ml collection tube and 500 µl of IVT cRNA Wash Buffer was added onto the spin column and spun at ≥8000g for 15 seconds. The collection tube was then emptied and 500 µl of 80% ethanol were added onto the spin column and spun at ≥8000g for 15 seconds. The collection tube was then emptied and the cap of the spin column opened and centrifuged at maximum speed for 5 minutes to completely dry the membrane. The spin column was transferred into a new 1.5ml collection tube and the sample was eluted by placing 13 µl of nuclease-free water directly onto the middle of the spin column membrane. The column was incubated at room temperature for 2 minutes and centrifuged at maximum speed for 1 minute. An aliquot of 2 µl was reserved for quality assessment and the remainder was used for the second cycle.

For step 5: A mix of the following was prepared:

600ng purified cRNA (from previous step) -	x µl
(0.2ug/ul) diluted Random Primers.	2 µl
Nuclease free dH2O -	x µl
Make up to a total of	11 µl

Mixed by pipetting and spun briefly. The mix was then incubated at 70 °C for 10 minutes, at 4 °C for 2 minutes and kept on ice.

For the master mix: (5x) First Strand Reaction Mix	4 µl
(0.1 M) DTT	2 µl
(10mM) dNTPs	1 µl
RNase Inhibitor	1 µl
Superscript II	1 µl

Mixed by pipetting and spun down briefly. 9 µl of the master-mix were added to the cRNA/random primer mix. Mixed by pipetting, and spun briefly. The mix was then

incubated at 42 °C for 1 hour in a thermo-cycler with a heated lid, cooled at 4 °C for 2 minutes, and spun briefly. 1 µl of RNase H was added to each sample mixed by pipetting and incubated at 37 °C for 20 minutes in a thermo-cycler with a heated lid, at 95 °C for 5 minutes cooled at 4 °C for 2 minutes, spun briefly and placed on ice.

Step 6: 4 µl of diluted T7 Oligo dT primer were added (5pmol/ µl) to each sample and mixed by pipetting. The samples were then incubated at 70 °C for 6 minutes in a thermal cycler with a heated lid and cooled at 4 °C for 2 minutes.

For the master mix:	RNase free dH2O	88 µl
	5x 2nd Strand Reaction Mix	30 µl
	(10mM) dNTPs	3 µl
	(10 U/ µl) E. coli DNA Pol I	4 µl

The master mix was then mixed by pipetting and 125 µl of the master mix were added to each sample for a final volume of 150ml.The mix was then incubated at 16 °C for 2 hours in a thermal cycler followed by addtitin of 2ml of T4 DNA polymerase. The mix was then incubated at 16 °C for 10 minutes and at 4 °C for 2 minutes. It was then placed on ice prior to the next step.

Step 7: The samples were transferred to a 1.5ml microfuge tube and 600 µl of cDNA Binding Buffer were added to the cDNA reaction. The samples were then applied to the cDNA Cleanup Spin Column and centrifuged at ≥8000g for 1 minute. The collection tube was then emptied and the column reloaded with the remaining cDNA mixture and centrifuged at ≥8000g for 1 minute. The column was then transferred into a new 2ml Collection tube and 750 µl of cDNA Wash Buffer were added onto the spin column and centrifuged at ≥8000g for 1 minute. The collection tube was emptied and the cap of the spin column was opened and centrifuge at maximum speed for 5 minutes, to completely dry the membrane. It was then transferred to a fresh 1.5ml collection tube. And the samples eluted by adding 14 µl of cDNA Elution Buffer directly onto the middle of the spin column membrane and incubated at room temperature for 1 minute followed by centrifugation at maximum speed for 1 minute.

Step 8: To prepare a master mix of the IVT reagents the following were mixed together:

Nuclease free dH20	8 µl
(10x) IVT labelling buffer	4 µl
Labelled NTP mix	12 µl
IVT labelling enzyme mix	4 µl

The mix was mixed by pippeting and 28 µl of master-mix were added to the double stranded cDNA for a final volume of and mixed by pipetting. The mix was the incubated at 37 °C for 16 hours and then at 4 °C for 2 minutes in a thermal cycler.

Step 9: The samples were transferred to a 1.5ml microfuge tube and 60 µl of nuclease free dH2O and 350 µl of IVT cRNA Binding Buffer were added into the sample and mixed thoroughly by pippetting. 250 µl of 100% ethanol were added and the sample was applied to an IVT cRNA Cleanup Spin Column and centrifuged at ≥8,000g for 15 seconds. The spin column was then transferred to a fresh 2ml collection tube and 500 µl of IVT cRNA Wash Buffer were added onto the spin column and spun at ≥8000g for 15 seconds. The collection tube was emptied and 500 µl of 80% ethanol were added onto the spin column and spun at ≥8,000g for 15 seconds. The collection tube was emptied and the cap opened and centrifuged at maximum speed for 5 minutes to completely dry the membrane. The spin column was then transferred into a new 1.5ml Collection tube and the sample eluted by placing 11 µl of nuclease-free water directly onto the middle of the spin column membrane. Incubated at room temperature for 2 minutes and centrifuged at maximum speed for 1 minute.

Step 10: For the fragmentation of cRNA in each tube x µl of cRNA (20µg), 4µl 5X fragmentation buffer and x µl RNase free dH_2O were added in the same tube to a final volume of 20µl. The mix was then incubated at 95 ^{o}C for 35 minutes. During incubation of cRNA, 20x eukaryotic hybridization controls and control oligonucleotide B2 were heated at 65 ^{o}C for 5 minutes and mixed gently by vortexing. After incubation, the microfuge tubes containing the cRNA were spun briefly to remove condensation from lid and 15µl of each replicate of the fragmentation reactions for each sample were transferred

into a clean tube. For the cocktail master mix, for each tube containing 15 µg fragmented 2X cRNA the following were added:

hybridization buffer	150µl
control oligonucleotide B2 (3nM)	5µl
20X eukaryotic hybridization controls	15µl
herring sperm DNA (10mg/ml)	3µl
acetylated BSA (50mg/ml)	3µl
DMSO (99.5% GC)	30µl
RNase free dH_2O	79µl

The master mix was pulsed-vortexed for 30 seconds and 285 µl of master mix were added to each 15 µl fragmented cRNA sample and mixed thoroughly.

For Hybridization:

1. Target Hybridization

The probe array was equilibrated to room temperature immediately before use and the array was wet by filling it through one of the septa with 200 µl of 1X MES hybridization buffer using a micropipetor. The probe was incubated at 45 ^{o}C for 10-15 minutes with rotation. The hybridization cocktail was heated to 99 ^{o}C for 5 minutes and then transferred to 45 ^{o}C for 5 minutes. The hybridization cocktails were spun at maximum speed in a microcentrifuge for 5 minutes to remove any insoluble material from the hybridization mixture. After 10-15 minutes of prehybridization, the buffer solution was removed from the probe array cartridge. The probe array was filled with 200 µl of the cocktail, avoiding any insoluble matter at the bottom of the tube and the probe array was placed in hybridization oven, loaded in balanced configuration around axis and rotated at 60rpm for 16 hours.

2. Post-hybridization wash and stain

The hybridization cocktail was removed from the probe array and set aside in a fresh eppendorf tube. The probe array was filled completely with non-stringent wash buffer.

The SAPE (Streptavidin-Phycoerythrin) stain solution was prepared (always fresh):

Final concentration	Volume (µl)
2XMES stain buffer	1X 600
DI H2O	540 µl
Acetylated BSA 50 mg/ml	2mg/ml 48 µl
SAPE 1mg/ml	10 µg/ml 12 µl

For the antibody solution:

Final concentration	Volume (µl)
2XMES stain buffer	1X 300
DI H2O	266.4 µl
Acetylated BSA 50 mg/ml	2mg/ml 24 µl
Normal goat IgG 10 mg/ml	0.1 mg/ml 6 µl
Biotinylated antibody 0.5 mg/ml	3µg/ml 3.6 µl

Target sequences for each chip were downloaded from the Affymetrix website and then compared to NCBI genome builds, to Uni-Gene and to RefSeq transcripts with BLAT.

5.3 Results

5.3.1 Proof of concept study

5.3.1.1 Optimization of staining and laser dissection

To improve laser dissection staining of tissues is helpful for the laser-excitation for cutting. Ethanol fixation and eosin staining were used in this study following reports by Schutze and Lahr (1998) and Goldsworthy and colleagues (1999) as it was found to be the stain with the least negative effect on RNA integrity along with ethanol fixation. To assess whether the use of staining with eosin affected the integrity of RNA, samples isloated from sections with or without eosin stain were analyzed. The quality of RNA as can be seen in figure 5.9 was similar in both cases indicating that staining had no negative effect in the quality of isolated RNA. RNA degradation as indicated by the degradation smears as well as by the RIN numbers (figure 5.9), appeared in both stained and unstained samples compared to RNA isolated from tissue culture cells, and therefore could not be attributed to the presence of eosin.

5.3.1.2 Isolation of RNA

For RNA isolation the Qiagen Micro RNeasy Kit for microdissected tissues was used as described in the §5.2.6.1. Both periosteal and endosteal osteoblasts were dissected using a 337-nm pulsed UVa-nitrogen microbeam laser built in an inverse microscope. Total RNA isolated was subjected to RT-PCR for cDNA synthesis followed by PCR. The PCR products were run on a 1.2% agarose gel. As can be seen in figure 5.10, in lanes 6 and 5 there is a visible product for actin in samples of laser micro-dissected (LMD) osteoblasts from periosteal and endosteal bone surfaces. Whole bone rat cryosections and 10,000 cultured osteoblasts and MLO-Y4 osteocyte-like cells were also subjected to RNA extraction and RT-PCR to provide the positive controls for the PCR. These results indicate the successful isolation of total RNA from 10,000 LMD periosteal and endosteal osteoblast samples and the expression of actin. The same samples were evaluated by the Novartis Genomics Unit and applied to microarray chips. Successful microarray data was obtained indicating the expression of genes of the osteoblast lineage (data not available).

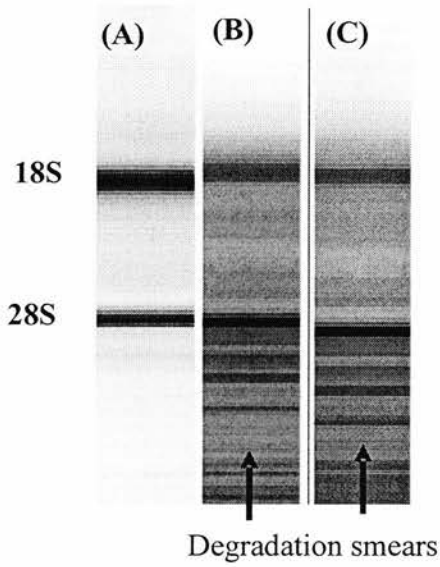

Figure 5.9 Effect of eosin staining and ethanol fixation on RNA integrity. Total RNA was prepared from mid-diaphysis tibial periosteal osteoblast microdissected material (10,000 cells) from a 3 month old animal. RNA was extracted using the RNeasy Micro kit (Qiagen) following manufacturers guidelines and analyzed by Agilent bioanalyzer, characterising RNA integrity on the basis of 18s and 28s rRNAs recovery by electrophoresis-gel-like images. (**A**) Control RNA, RIN: 9.3 from cultured osteoblasts (10,000 cells) (**B**) No staining, RIN: 5.8 (**C**) fixation and staining RIN: 5.3.

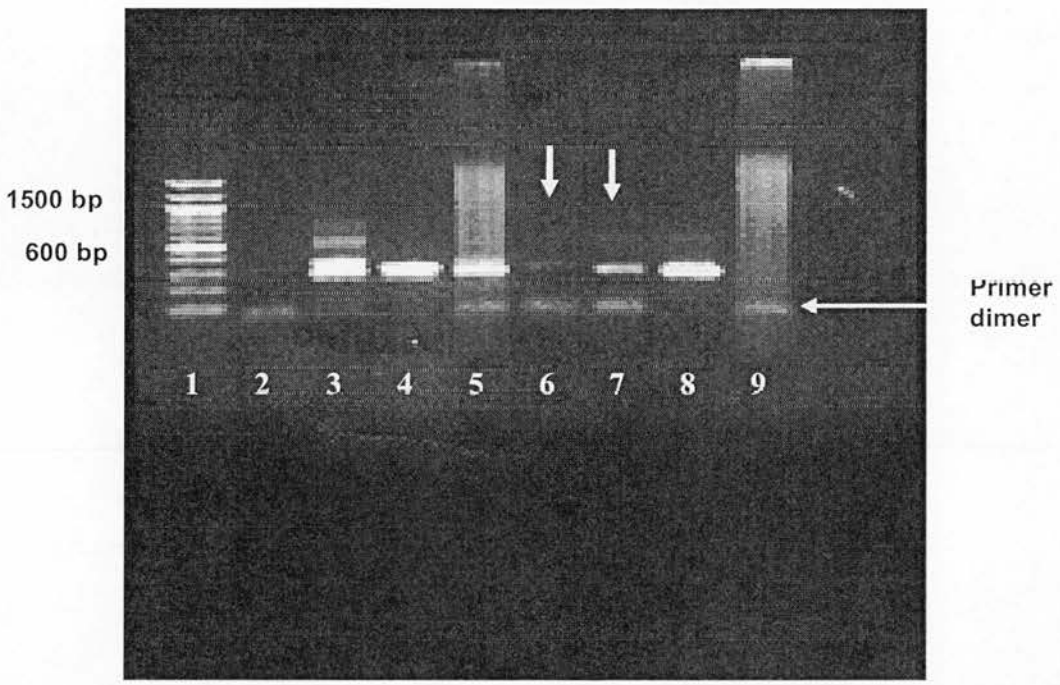

Lane 1: 100 bp DNA ladder

Lane 2: Actin with H_2O (cDNA negative control)

Lane 3: Actin with 1 rat section

Lane 4: Actin with cultured human osteobalsts (positive control)

Lane 5: Actin with 10 rat sections

Lane 6: Actin with 10,000 LMD endosteal osteoblasts

Lane 7: Actin with 10,000 LMD periosteal osteoblasts

Lane 8: Actin with MLO-Y4 (positive control)

Figure 5.10. Expression of actin in osteoblast preparations. The expression of actin was determined by RT-PCR in periosteal and endosteal osteoblast populations (lanes 6 and 7) as indicated by the arrows. RNA extracted from whole rat sections and 10,000 cultured osteoblasts and MLO-Y4 cells subjected to RT-PCR and actin expression served as controls.

5.3.2 Novartis study

5.3.2.1 RNA Isolation from the Control Group

Following the protocols developed for the proof of concept study, which indicate that the methods developed were successful for isolation of total RNA, the Novartis study samples from the *in vivo* experiment, were analyzed following the same protocols. Tibias were subjected to cryosectioning and LMD. For both periosteal and endosteal osteoblast samples ~50,000 cells were collected from either side and total RNA was isolated following the RNeasy Micro Kit extraction protocol. For the control group the NanoDrop profiles can be seen in Table 5.1 and the electropherogram in figure 5.11. Despite the fact that all samples extracted using the RNeasy Micro Kit provided a reading on the NanoDrop, we were unable to obtain an Agilent profile for some of the samples. As can been seen in table 5.1 260/230 ratios are low indicative of RNA degradation or co-contaminants, however the 260/280 ratios were close to 2 indicating that the RNA was clear of protein and DNA. Also as can be seen in figure 5.11, we were unable to obtain a profile on the Agilent bionalyzer on some samples indicative of no or very little RNA present; and for the samples that 18S and 28S peaks were detected degradation smears were observed as indicated by the intermediate bands in between the peaks and the low or non-applicable (N/A) numbers.

	ng/µl	260/280	260/230	Total RNA
ANIMAL 1				
PERIOSTEUM	1.4 ng/µl	1.72	0.35	16.8 ng
ENDOSTEUM	1.9 ng/µl	1.85	0.10	22.8ng
ANIMAL 2				
PERIOSTEUM	1 ng/µl	1.86	0.11	12 ng
ENDOSTEUM	1.2 ng/µl	1.78	0.37	16.8 ng
ANIMAL 3				
PERIOSTEUM	1.7 ng/µl	1.83	0.33	20.4 ng
ENDOSTEUM	1.9 ng/µl	1.87	0.37	22.8 ng
ANIMAL 4				
PERIOSTEUM	1.2 ng/µl	1.79	0.19	14.4 ng
ENDOSTEUM	2.2 ng/µl	1.84	0.13	26.4 ng
ANIMAL 5				
PERIOSTEUM	1.2 ng/µl	2.05	0.15	14.4 ng
ENDOSTEUM	1.9 ng/µl	1.77	0.33	22.8 ng

Table 5.1 NanoDrop readings for the control group RNA samples. 2 µl of the RNA samples were used for the NanoDrop. The 260/280 ratios were close to 2 indicative of RNA samples free of DNA and protein contamination but the 260/230 ratios were low indicative of the presence of co-contaminants.

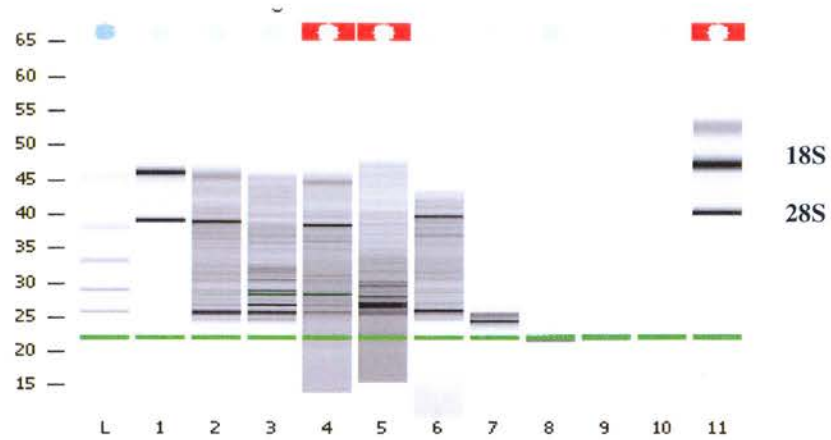
65
60
55
50
45
40
35
30
25
20
15
L 1 2 3 4 5 6 7 8 9 10 11
18S
28S

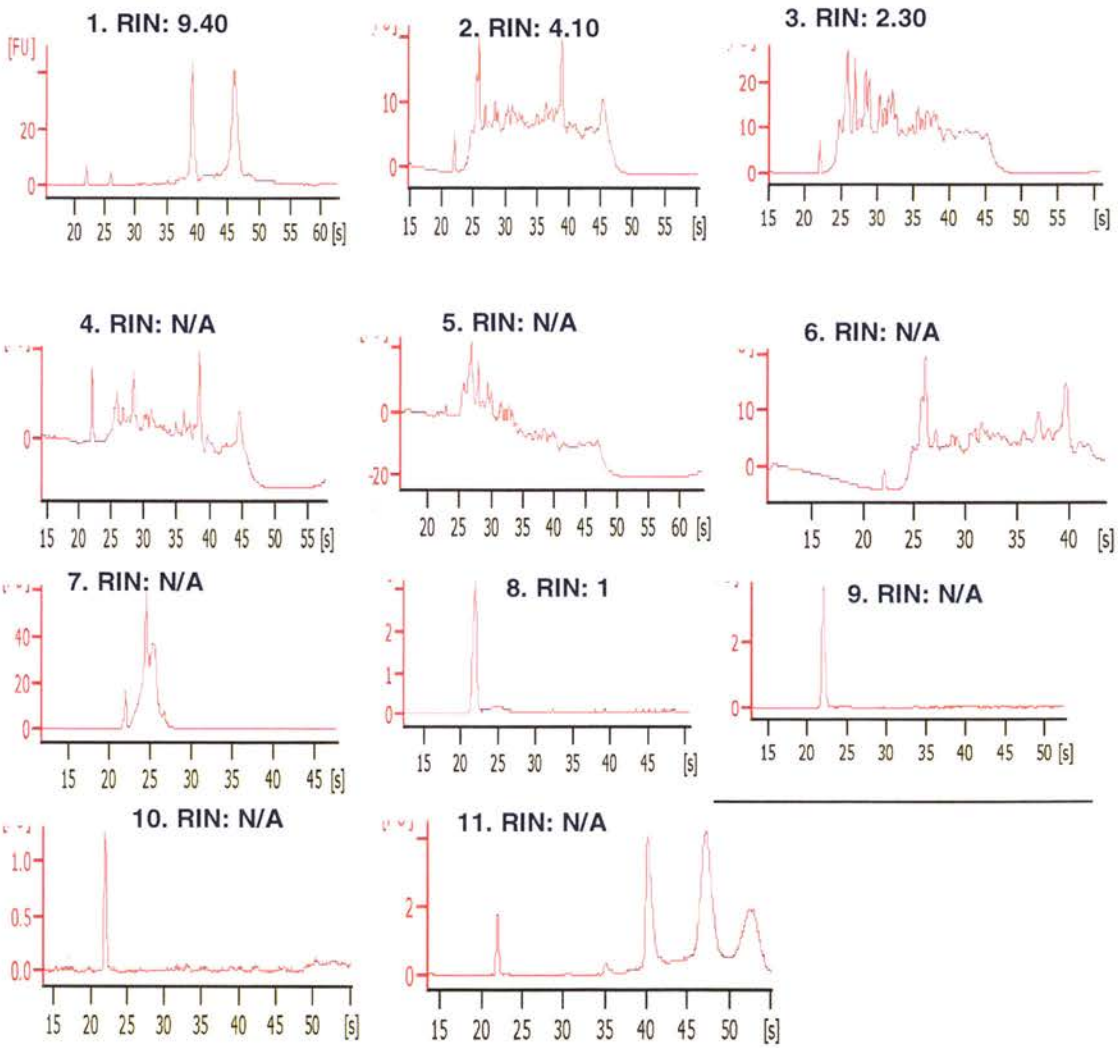
1. RIN: 9.40
[FU]
2. RIN: 4.10
3. RIN: 2.30
4. RIN: N/A
5. RIN: N/A
6. RIN: N/A
7. RIN: N/A
8. RIN: 1
9. RIN: N/A
10. RIN: N/A
11. RIN: N/A
[s]

L: Ladder

1. Control MLO-Y4 cells RNA

2. Periosteal sample Animal 1

3. Endosteal sample Animal 1

4. Periosteal sample Animal 2

5. Endosteal sample Animal 2

6. Periosteal sample Animal 3

7. Endosteal sample Animal 3

8. Periosteal sample Animal 4

9. Endosteal sample Animal 4

10. Periosteal sample Animal 5

11. Endosteal sample Animal 5

Figure 5.11 Agilent Bioanalyzer electropherogram and peaks of control total RNA isolation samples. Clear 18S and 28S peaks were observed for a few experimental samples, however degradation of these samples was observed as indicated by the low RIN numbers.

5.3.2.2 RNA Isolation from the Compound A

Tibias from the five animals that recived compound A twice daily at a dose of 100mg/kg were subjected to cryosectioning and LMD. Total RNA was isolated from these samples as described above for the control group. For compound A treatment group the NanoDrop profiles can be seen in Table 5.2 and the electropherogram in figure 5.12. Despite the fact that all samples extracted using the RNeasy Micro Kit gave a reading on the NanoDrop, we were unable to get an Agilent profile for all of the samples. Similarly to the control group RNA samples, the 260/280 ratios were close 2 but the 260/230 ratios were low, indicative of degradation or presence of co-contaminants. Moreover as can be seen in figure 5.12, we were unable to obtain a profile on the Agilent bionalyzer for most of the samples indicating that no or very little RNA, that is undetectable is present; for those samples in which 18S and 28S peaks were detected considerable degradation was observed as indicated by the contamination smears and the low RIN numbers.

ng/µl	260/280	260/230	Total

ANIMAL 1				
PERIOSTEUM	2.5 ng/µl	1.74	0.01	30 ng
ENDOSTEUM	3.0 ng/µl	1.72	0.24	36 ng
ANIMAL 2				
PERIOSTEUM	1.4 ng/µl	1.74	0.01	16.8 ng
ENDOSTEUM	2.3 ng/µl	1.67	0.25	27.6 ng
ANIMAL 3				
PERIOSTEUM	1.5 ng/µl	1.68	0.02	18 ng
ENDOSTEUM	3.1 ng/µl	1.75	0.18	37.2 ng
ANIMAL 4				
PERIOSTEUM	2.3 ng/µl	1.80	0.18	27.6 ng
ENDOSTEUM	4.8 ng/µl	2.1	0.01	57.6 ng
ANIMAL 5				
PERIOSTEUM	1.4 ng/µl	1.78	0.03	16.8 ng
ENDOSTEUM	1.2 ng/µl	1.65	0.01	14.4 ng

Table 5.2 NanoDrop readings for the Compound A group RNA samples. 2 µl of the RNA samples were used for the NanoDrop. For some of the samples the 260/280 ratios were close to 2 indicative of RNA samples free of DNA and protein contamination, however the 260/230 ratios were low indicative of the presence of co-contaminants

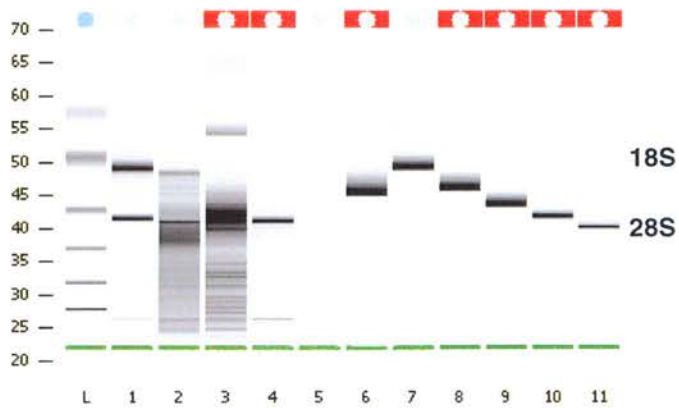
70
65
60
55
50
45
40
35
30
25
20
18S
28S
L 1 2 3 4 5 6 7 8 9 10 11

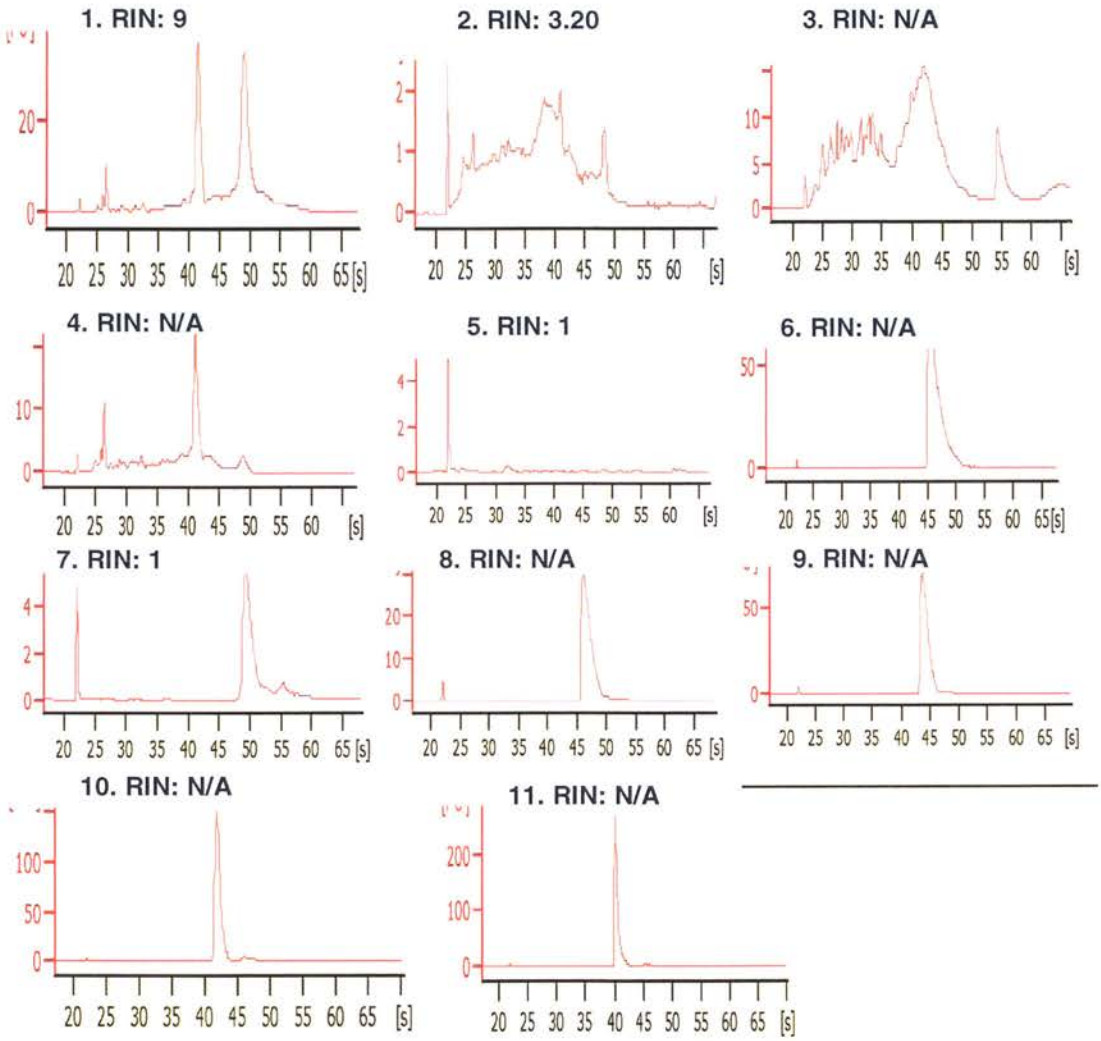
1. RIN: 9
2. RIN: 3.20
3. RIN: N/A
4. RIN: N/A
5. RIN: 1
6. RIN: N/A
7. RIN: 1
8. RIN: N/A
9. RIN: N/A
10. RIN: N/A
11. RIN: N/A
[s]

L: Ladder

1. Control MLO-Y4 cells RNA

2. Periosteal sample Animal 1

3. Endosteal sample Animal 1

4. Periosteal sample Animal 2

5. Endosteal sample Animal 2

6. Periosteal sample Animal 3

7. Endosteal sample Animal 3

8. Periosteal sample Animal 4

9. Endosteal sample Animal 4

10. Periosteal sample Animal 5

11. Endosteal sample Animal 5

Figure 5.12 Agilent Bioanalyzer electropherogram and peaks of Compound A total RNA extraction samples. Clear 18S and 28S peaks were observed for a few experimental samples, however degradation of these samples was observed as indicated by degradation smears and low or N/A RIN numbers.

5.2.3.3 RNA Isolation from the Compound B

Tibias from the five animals receiving compound B once daily at a dose of 200mg/kg were subjected to cryosectioning and LMD. Total RNA was extracted as described above for the other treatment groups. For compound B treatment group, the NanoDrop profiles can be seen in Table 5.3 and the electropherogram in figure 5.13. Despite the fact that all samples extracted using the RNeasy Micro Kit gave a reading on the NanoDrop, we were unable to get an Agilent profile for all of the samples. Similarly to the RNA samples discussed above the 260/280 ratios were close to 2 but the 260/230 ratios were low, indicative of degradation or presence of co-contaminants. Also as can be seen in figure 5.13, we were unable to obtain a profile on the Agilent bionalyzer for most of the samples indicating that no or very little RNA, that is undetectable is present; for the samples that 18S and 28S peaks were detected considerable degradation was observed.

	ng/µl	260/280	260/230	Total
ANIMAL 1				
PERIOSTEUM	2.2 ng/µl	1.80	0.22	22ng
ENDOSTEUM	1.3 ng/µl	1.90	0.44	15.6ng
ANIMAL 2				
PERIOSTEUM	1.0 ng/µl	1.68	0.03	12 ng
ENDOSTEUM	1.1 ng/µl	1.80	0.01	15.4 ng
ANIMAL 3				
PERIOSTEUM	1.0ng/µl	1.68	0.25	14 ng
ENDOSTEUM	1.8 ng/µl	1.85	0.01	25.2 ng
ANIMAL 4				
PERIOSTEUM	1.2 ng/µl	2.01	0.01	16.8 ng
ENDOSTEUM	1.2 ng/µl	2.1	0.02	16.8 ng
ANIMAL 5				
PERIOSTEUM	1.1 ng/µl	2.01	0.03	15.4 ng
ENDOSTEUM	1.8 ng/µl	1.81	0.06	25.2 ng

Table 5.3 NanoDrop readings for the Compound B group RNA samples. 2 µl of the RNA samples were used for the NanoDrop. Most of the experimental samples had high 260/280 ratios, however the 260/230 ratios similarly to other experimental samples from the other treatment groups were low indicative of the presence of co-contaminants

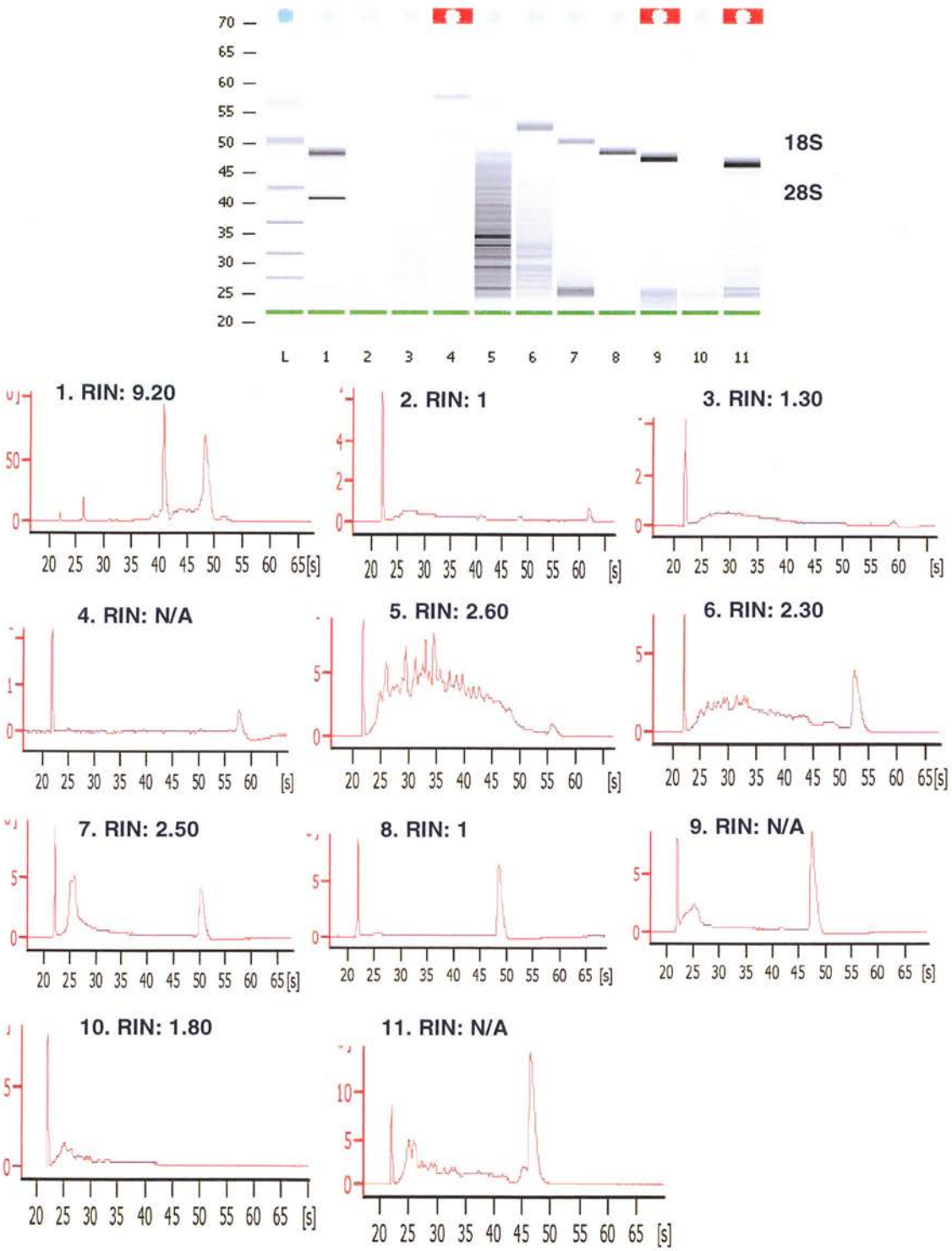
70
65
60
55
50
45
40
35
30
25
20
18S
28S
L 1 2 3 4 5 6 7 8 9 10 11
1. RIN: 9.20
2. RIN: 1
3. RIN: 1.30
4. RIN: N/A
5. RIN: 2.60
6. RIN: 2.30
7. RIN: 2.50
8. RIN: 1
9. RIN: N/A
10. RIN: 1.80
11. RIN: N/A
[s]

L: Ladder

1. Control MLO-Y4 cells RNA

2. Periosteal sample Animal 1

3. Endosteal sample Animal 1

4. Periosteal sample Animal 2

5. Endosteal sample Animal 2

6. Periosteal sample Animal 3

7. Endosteal sample Animal 3

8. Periosteal sample Animal 4

9. Endosteal sample Animal 4

10. Periosteal sample Animal 5

11. Endosteal sample Animal 5

Figure 5.13 Agilent Bioanalyzer electropherogram and peaks of Compound B total RNA extraction samples. Clear 18S and 28S peaks were observed for the control sample, but no RNA was detectable for all experimental samples of Compound B as no 18S or 28S peaks were detected.

5.2.3.4 RNA Isolation from the rhPTH Group

Tibias from the five animals receiving rhPTH once daily at a dose of 50μg/kg were subjected to cryosectioning and LMD. As for the treatment groups discussed above total RNA was isolated and tested on Agilent and NanoDrop. For the PTH treatment group the NanoDrop profiles can be seen in Table 5.4 and the electropherogram in figure 5.14. Despite the fact that all samples extracted using the RNeasy Micro Kit gave a reading on the NanoDrop, we were unable to obtain an Agilent profile for all of the samples. Similarly to RNA samples discussed above the 260/280 ratios were close to 2 but the 260/230 ratios were low, indicative of degradation or presence of co-contaminants. Also as can be seen in figure 5.14, we were unable to obtain a profile on the Agilent bionalyzer for most of the samples indicating that no or very little RNA, although 18S and 28S peaks are present degradation of the samples was observed as indicated by the degradation smears and the low or N/A RIN numbers.

	ng/µl	260/280	260/230	Total
ANIMAL 1				
PERIOSTEUM	2.0 ng/µl	1.90	0.05	28 ng
ENDOSTEUM	1.9 ng/µl	1.75	0.01	22.8ng
ANIMAL 2				
PERIOSTEUM	3.2 ng/µl	2.01	0.04	44.8 ng
ENDOSTEUM	3.4 ng/µl	1.68	0.15	47.6 ng
ANIMAL 3				
PERIOSTEUM	3.1 ng/µl	1.83	0.15	43.4 ng
ENDOSTEUM	2.9 ng/µl	1.87	0.08	40.6 ng
ANIMAL 4				
PERIOSTEUM	2.3 ng/µl	1.79	0.17	32.2 ng
ENDOSTEUM	2.1 ng/µl	1.84	0.22	29.4 ng
ANIMAL 5				
PERIOSTEUM	3.4ng/µl	1.82	0.13	47.6 ng
ENDOSTEUM	3.2 ng/µl	1.77	0.46	44.8 ng

Table 5.4 NanoDrop readings for the rhPTH group RNA samples. 2 µl of the RNA samples were used for the NanoDrop. Similarly to the RNA samples isolated from the other treatment groups in the rhPTH group samples had 260/280 ratios close to 2, however the 260/230 ratios similarly to the other experimental samples remain low indicative of the presence of co-contaminants.

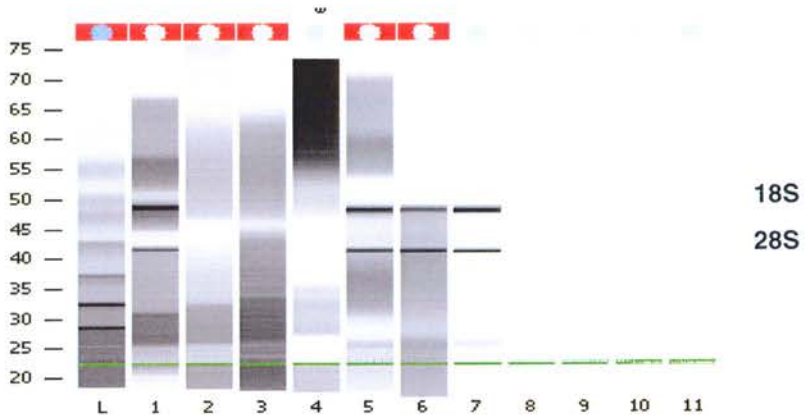
75
70
65
60
55
50
45
40
35
30
25
20
L 1 2 3 4 5 6 7 8 9 10 11
18S
28S

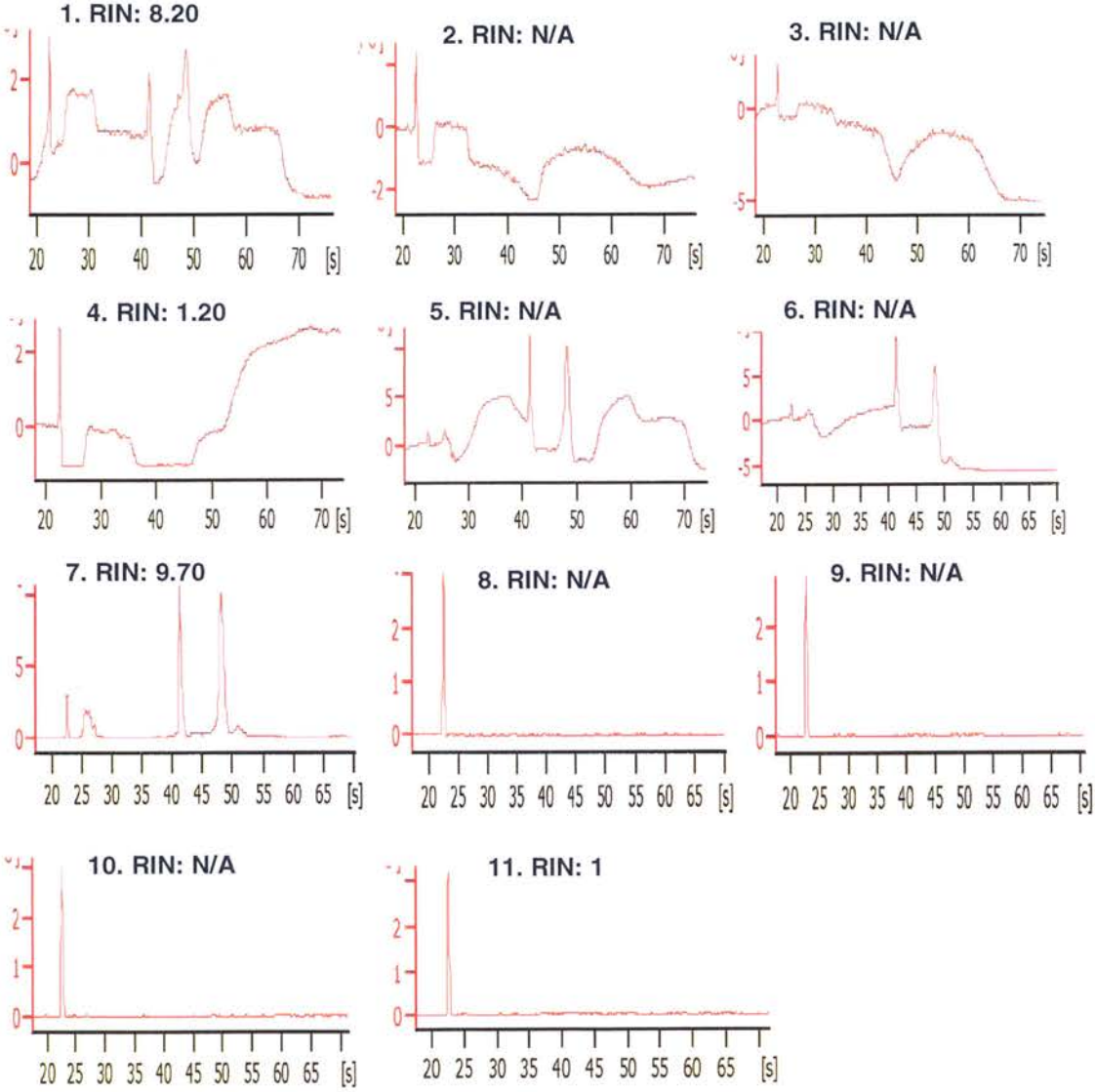
1. RIN: 8.20
2. RIN: N/A
3. RIN: N/A
4. RIN: 1.20
5. RIN: N/A
6. RIN: N/A
7. RIN: 9.70
8. RIN: N/A
9. RIN: N/A
10. RIN: N/A
11. RIN: 1
[s]

L: Ladder

1. Periosteal sample Animal 1

2. Endosteal sample Animal 1

3. Periosteal sample Animal 2

4. Endosteal sample Animal 2

5. Periosteal sample Animal 3

6. Endosteal sample Animal 3

7. Control MLO-Y4 cells RNA

8. Periosteal sample Animal 4

9. Endosteal sample Animal 4

10. Periosteal sample Animal 5

11. Endosteal sample Animal 5

Figure 5.14. Agilent Bioanalyzer electropherogram and peaks of rhPTH group total RNA extraction samples. Clear 18S and 28S peaks were observed for the control sample as well as 18S and 28S peaks for some of the experimental samples with degradation smears present and low RIN numbers.

5.2.3.4 RNA Isolation from the rhGH Group

Tibias from the five animals receiving rhGH once daily at a dose of 2.5mg/kg were subjected to cryosectioning and LMD. As for other treatment groups as described previously total RNA was extracted and subjected to Agilent and NanoDrop testing. For the rhGH treatment group the NanoDrop profiles can be seen in Table 5.5 and the electropherogram in figure 5.15. Despite the fact that all samples extracted using the RNeasy Micro Kit gave a reading on the NanoDrop, we were unable to get an Agilent profile for all of the samples. As for the RNA samples discussed previously the 260/280 ratios were close to 2 but the 260/230 ratios were low, indicative of degradation or presence of co-contaminants. Also as can be seen in figure 5.15, we were unable to obtain a profile on the Agilent bionalyzer for most of the samples. However samples that 18S and 28S peaks were detected considerable degradation was observed with obvious degradation smears in between peaks.

	ng/µl	260/280	260/230	Total
ANIMAL 1				
PERIOSTEUM	1.5 ng/µl	1.90	0.53	21 ng
ENDOSTEUM	1.9 ng/µl	1.75	0.04	22.8ng
ANIMAL 2				
PERIOSTEUM	2.2 ng/µl	1.77	0.32	30.8 ng
ENDOSTEUM	2.4 ng/µl	1.68	0.05	33.6 ng
ANIMAL 3				
PERIOSTEUM	3.6 ng/µl	1.93	0.10	50.4 ng
ENDOSTEUM	2.1 ng/µl	2.01	0.07	29.4 ng
ANIMAL 4				
PERIOSTEUM	3.4 ng/µl	1.79	0.07	47.6 ng
ENDOSTEUM	2.1 ng/µl	1.84	0.12	29.4 ng
ANIMAL 5				
PERIOSTEUM	1.5ng/µl	1.79	0.07	21 ng
ENDOSTEUM	2.1 ng/µl	1.79	0.12	29.4 ng

Table 5.5. NanoDrop readings for the rhGH group RNA samples. 2 µl of the RNA samples were used for the NanoDrop. Similarly to the RNA samples extracted from the other treatment groups, rhGH RNA samples had 260/280 ratios close to 2, however the 260/230 ratios similarly to the other experimental samples from other treatment groups were low.

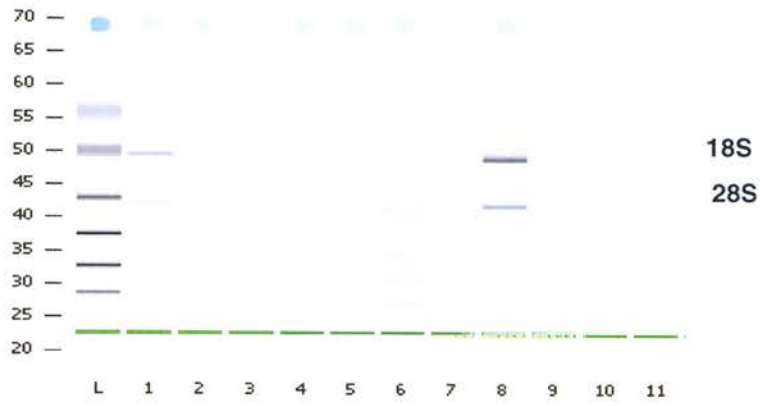
70
65
60
55
50
45
40
35
30
25
20
18S
28S
L 1 2 3 4 5 6 7 8 9 10 11

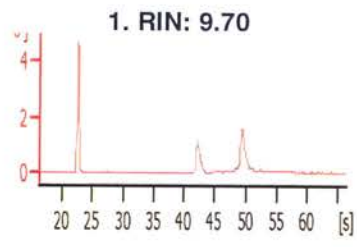
1. RIN: 9.70
20 25 30 35 40 45 50 55 60 [s]

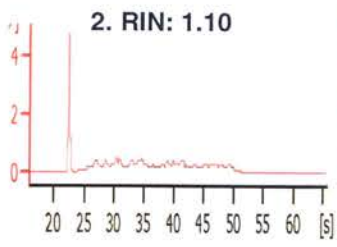
2. RIN: 1.10
20 25 30 35 40 45 50 55 60 [s]

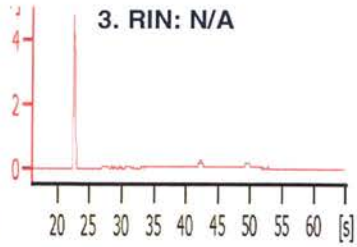
3. RIN: N/A
20 25 30 35 40 45 50 55 60 [s]

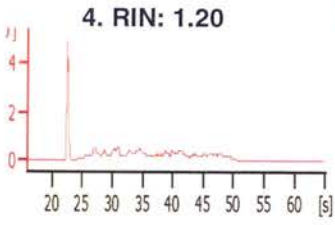
4. RIN: 1.20
20 25 30 35 40 45 50 55 60 [s]

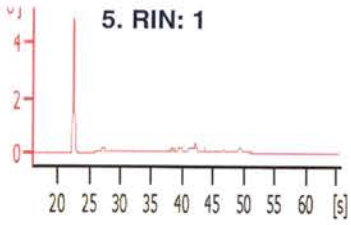
5. RIN: 1
20 25 30 35 40 45 50 55 60 [s]

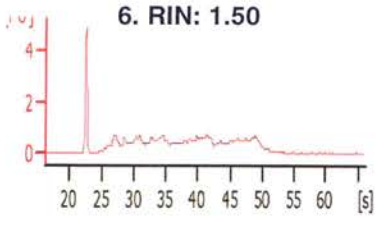
6. RIN: 1.50
20 25 30 35 40 45 50 55 60 [s]

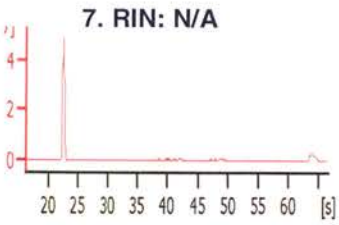
7. RIN: N/A
20 25 30 35 40 45 50 55 60 [s]

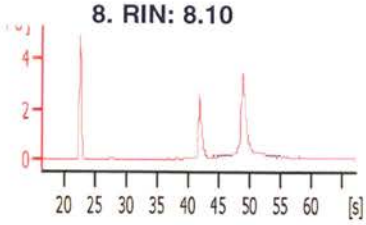
8. RIN: 8.10
20 25 30 35 40 45 50 55 60 [s]

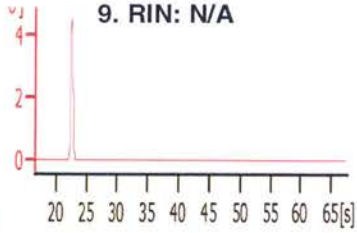
9. RIN: N/A
20 25 30 35 40 45 50 55 60 65[s]

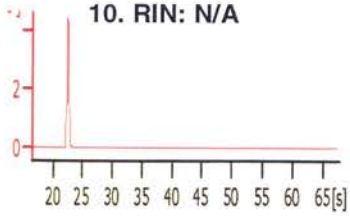
10. RIN: N/A
20 25 30 35 40 45 50 55 60 65[s]

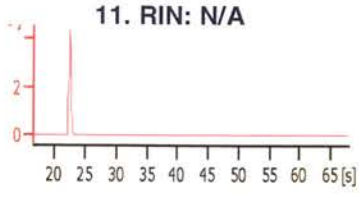
11. RIN: N/A
20 25 30 35 40 45 50 55 60 65[s]

L: Ladder

1. Periosteal sample Animal 1

2. Endosteal sample Animal 1

3. Periosteal sample Animal 2

4. Endosteal sample Animal 2

5. Periosteal sample Animal 3

6. Endosteal sample Animal 3

7. Periosteal sample Animal 4

8. Control MLO-Y4 cells RNA

9. Endosteal sample Animal 4

10. Periosteal sample Animal 5

11. Endosteal sample Animal 5

Figure 5.15. Agilent Bioanalyzer electropherogram and peaks of rhGH group total RNA extraction samples. Clear 18S and 28S peaks were observed for the control sample, and faint peaks for a few experimental samples with low RIN numbers and degradation smears present.

5.2.4 Preliminary Microarray data

All the RNA samples discussed above, extracted using the RNeasy Micro Kit (Qiagen) were evaluated by the Genomics Unit of Novartis (Basel, Switzerland). 5 animals from each group, 5 samples from each site (endosteal vs. periosteal) were arrayed. From the first set of samples which included the control and the rhPTH groups microarray data was obtained from a small number of samples, for the endosteal envelope (table 5.6) since most of them were found to be of sub-optimal quality to be further processed. No data was obtained from the second set of samples including the rhGH and Compounds A and B as these RNA samples were determined to be of either sub-optimal quality or no RNA detectable. No further RT-PCR was carried out to check for consistency to the data presented here, because of the small volume of the samples. Therefore a number of RNA extraction methods and modifications trials were initiated using ~50,000 LCM cells in an attempt to improve the RNA quality. These methods and the data obtained are discussed below. All trials discussed were performed at least three times each.

5.2.5 Gene expression in response to rhPTH treatment at the endosteal envelope

In order to identify genes regulated by rhPTH, rhGH and Compounds A and B at the endosteal and periosteal envelopes of old female rats the *in vivo* experiment as described in § 5.2.1 was set up. RNA samples from these treatment groups as well as the control group were tested by the Novartis Genomics Unit and only a few samples were found to be of optimal quality to be used for microarray analysis. Limited microarray data was obtained from the rhPTH and the control group for the endosteal envelope. Genes whose expression was changed by two-fold or more in response to rhPTH treatment compared to the control at the endosteal envelope of the rat tibia are listed in table 5.6. The genes showing most evident changes belong to mainly three categories: bone development, binding, catalysis and cell cycle.

Additional genes involved in signal transduction, apoptosis, cytokinesis and cell migration, cell proliferation as well as structural proteins and transcription factors were also upregulated in response to rhPTH treatment and are listed in Appendix 1.

Gene Symbol/Function	Gene Title	Fold Change (rhPTH/Control)
Development		
Irf6	interferon regulatory factor	45.97
Transcription		
Whsc1l1	Wolf-Hirschhorn syndrome candidate 1-like 1	11.89
Cell Cycle		
Pole2_predicted	Polymerase (DNA directed), epsilon 2 (p59 subunit)	33.7
Structural Protein		
Lamc2	lamimin, gamma 2	18.63
Binding		
Vps54	Vacuolar protein sorting 54	18.07
Sox6	SRY-box containing gene 6	8.292
Dtnbp1	distrobrevin binding protein 1	6.596
Lsm16_predicted	LSM16 homolog	13.45
Zfp91	zinc finger protein 91	4.744
Apoptosis		
Lrdd_predicted	leucine-rich and death domain containing	14.7
Birc3	baculoviral IAP repeat-containing 3	2.359
Cytokinesis/Motility		
Rcc2_predicted	regulator of chromosome condensation 2	12.23
Dock5_predicted	dedicator of cytokinesis 5	2.329
Proliferation		
Tff1	trefoil factor 1	6.73
Catalysis		

Fuca2	fucosidase, alpha-L- 2, plasma	6.761
Pde8b	Phosphodiesterase 8B	39.64
Signaling		
Rgs14	regulator of G-protein signaling 14	2.292
Tbc1d10a	TBC1 domain family, member 10a	2.235

Table 5.6 Gene expression changed two-fold or more in response to rhPTH treatment at the endosteal envelope of the rat tibia. The genes whose expression changed in response to rhPTH treatment mainly belong to three categories: bone development, binding, catalysis and cell cycle.

5.2.6 Improvement of RNA Quality

5.2.6.1. Qiagen RNeasy Micro RNA Isolation with addition of Proteinase K

~50,000 endosteal and periosteal osteoblast were LMD in lysis buffer (RLT + β-mercaptoethanol). For the control RNA 50,000 cultured osteoblasts were extracted using the RNeasy Micro kit method. For RNA isolation the manufacturer's protocol as described in the methods section was used with the introduction of a proteinase K step, known to inactivate the RNases and DNases in nucleic acid extractions. 5 µl (100µg) of proteinase K were added to the sample following homogenization in lysis buffer and then incubated at 55°C for 10 minutes prior to addition on an equal volume of 70% ethanol. The RNA samples were tested on the NanoDrop and the Agilent bionalyzer for quantity and quality (figure 5.16). As can be seen in figure 5.16 the 260/280 and 260/230 ratios were both low indicative of the presence of co-contaminants and on the Agilent profile no 18S and 28S peaks were detectable, indicative of no, or low amounts of RNA or highly degraded samples.

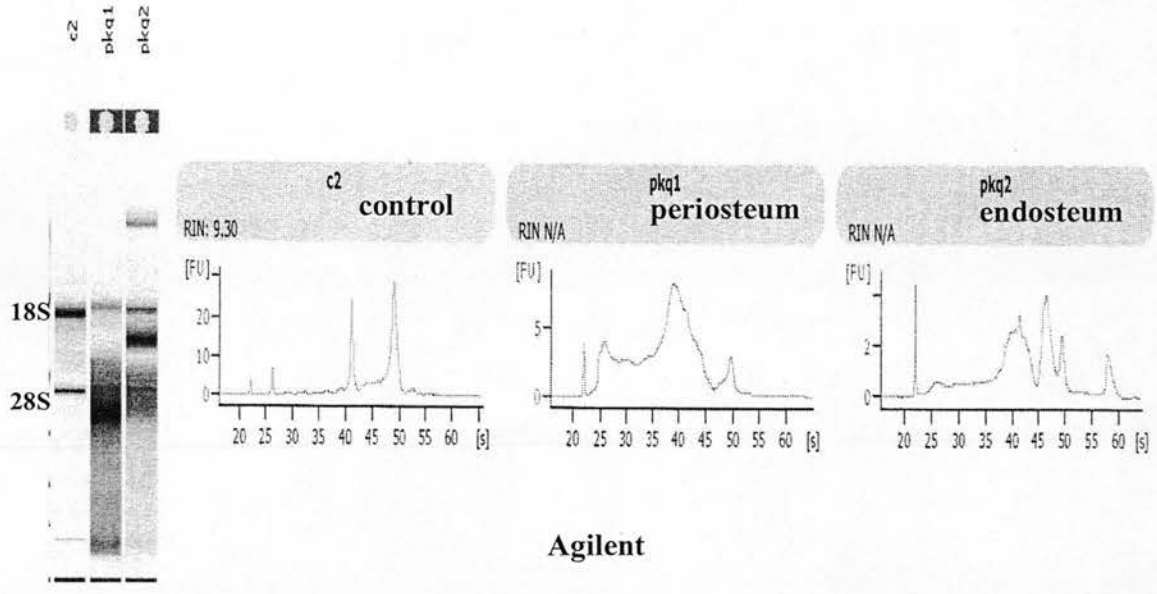

Agilent

Control	RNA Area	204.4			
	RNA Conc	6011pg/µl			
	RIN	9.3			
periosteum	RNA Area	254.5	**endosteum**	RNA Area	88.3
	RNA Conc	7484pg/µl		RNA Conc	2598pg/µl
	RIN	n/a		RIN	n/a

NanoDrop Readings	**260/280**	**260/230**	**ng/µl**
Periosteum	1.69	0.37	2.6
Endosteum	1.42	0.72	10.7
Control	2.0	2.06	1200

Figure 5.16. Agilent Bionalyzer profiles and NanoDrop data for total RNA samples of ~50,000 cells isolated using RNeasy Micro kit and addition of Proteinase K. 50,000 cells from periosteum and endosteum were LMD and RNA was isolated using the RNeasy Micro kit method with the addition of 100µg proteinase K. The 260/280 and 260/230 ratios were low for both samples indicative of co-contaminants. In the Agilent profiles no 18S and 28S peaks were detected for both samples while clear peaks were observed for the cultured osteoblast control sample indicative of degraded samples.

5.2.6.2. Trizol (Invitrogen) RNA isolation

~50,000 periosteal osteoblasts were LMD in trizol, which served as the lysis buffer. For the control RNA 50,000 cultured osteoblasts were lysed in trizol for RNA isolation, followed by the Qiagen clean-up. For RNA isolation the manufacturer's protocol as described in §5.2.6.2 was followed. The samples were then homogenized using a syringe and needle by passing 5-10 times through 29G needle attached to a sterile plastic syringe. The manufacturer's protocol was then followed for the extraction with two modifications:

a) On addition of Trizol reagent samples were left at room temp with rotation for 10 min's prior to addition of chloroform.
b) After aqueous layer was collected Glycogen carrier (20µg) was added prior to precipitation with isopropanol.

Following extraction 5µl of the sample were reserved for Nano-drop and Agilent analysis and the remaining sample was subjected to clean-up with Qiagen Micro Kit as described in §5.2.6.3. The RNA samples were tested on the NanoDrop and the Agilent bionalyzer for quantity and quality (figure 5.17). As can be seen in figure 5.17 the 260/280 and 260/230 ratios were both low indicative of the presence of co-contaminants while on the Agilent profile clear 18S and 28S peaks were detectable, indicative of RNA present, however low RIN numbers indicated RNA degradation. When the trizol extracted sample was subjected to clean-up considerable loss of RNA was observed with no significant improvements in either the 260/280, 260/230 ratios or RIN number.

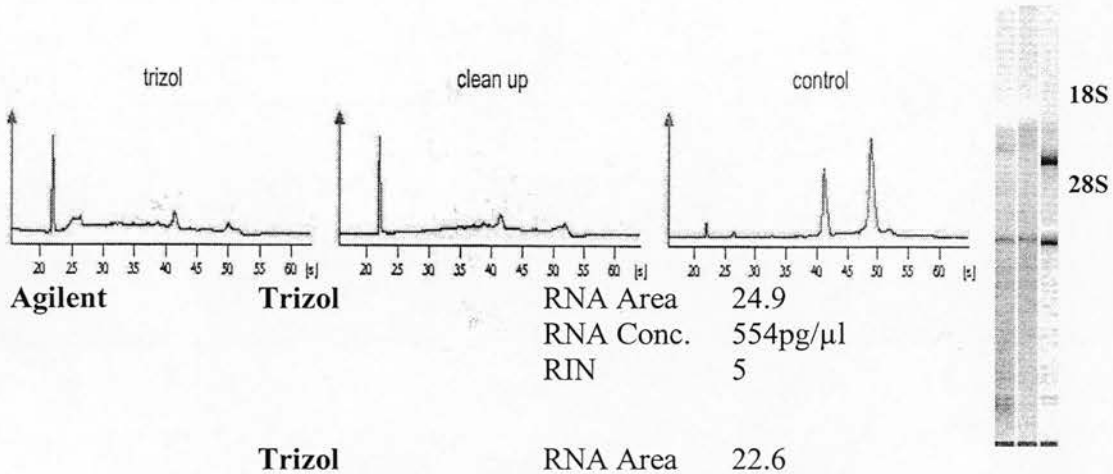

Agilent

Trizol	RNA Area	24.9
	RNA Conc.	554pg/µl
	RIN	5
Trizol + Clean up (Qiagen)	RNA Area	22.6
	RNA Conc.	502pg/µl
	RIN	4.1
Control (25,000 cultured Osteoblasts Diluted 1:10)	RNA Area	288.1
	RNA Conc.	2071pg/µl
	RIN	10

Nanodrop Readings

	260/280	260/230	ng/µl
Trizol	1.46	0.74	28.7
Trizol +clean up	1.44	0.31	15.1
Control	2.0	2.06	1200

Figure 5.17 Agilent Bionalyzer profiles and NanoDrop data for total RNA samples of ~50,000 cells isolated using Trizol and addition of glycogen carrier. ~50,000 cells from periosteum were LMD and RNA was isolated using Trizol with addition of 20µg of glycogen. The 260/280 and 260/230 ratios were low for both trizol and clean-up samples as can be seen from the NanoDrop reading indicative of co-contaminants. As can be seen in the Agilent profiles there are clear 18S and 28S peaks; however degradation was detected as the RIN number were low. Following clean-up of the sample there was no improvement in RNA quality with significant reduction in yield.

5.2.6.3 Section de-calcification followed by (a) Qiagen RNeasy Micro Kit and (b) Trizol followed by Qiagen Clean-up.

Although the trizol method improved the RNA quality significantly, further improvement was necessary for successful microarray analysis. In table 5.7 a summary of the RNA isolation methods discussed above is presented; with the modification of de-calcification of sections prior to LMD and RNA isolation using either a)the RNeasy Micro Kit or b)Trizol followed by the Qiagen clean-up. As can be seen from table 5.7 from the varying combinations tested there was no improvement in the 260/230 ratio. These samples were also tested using the Agilent and no profiles were obtained, demonstrating poor quality RNA unsuitable for further analysis. It can be concluded that the de-calcification step did not improve the RNA quality and resulted in significant reduction of RNA yield.

Extraction method	260/280	260/230	ng/µl
Qiagen+decalcification			
Periosteum	1.40	0.69	5.1
Endosteum	1.38	0.52	6.6
Qiagen No decalcification			
Periosteum	1.41	0.49	4.5
Endosteum	1.44	0.05	6.5
Trizol+decalcification			
Periosteum	1.39	0.33	12.5
Endosteum	1.45	0.42	22.5
Trizol No decalcification			
Periosteum	1.36	0.32	10.1
Endosteum	1.39	0.34	13.7
Clean up Trizol+decalc.			
Periosteum	1.54	0.45	6.9
Endosteum	1.49	0.13	8.3
Clean up Trizol No decalcification			
Periosteum	1.46	0.47	15.2
Endosteum	1.37	0.06	5.3

Table 5.7. Summary of RNeasy Micro Kit and Trizol total RNA isolation with or without de-calcification.

5.2.6.4. Arcturus Pico-Pure (Arcturus) RNA Isolation

The Arcturus Pico-Pure RNA isolation method was tested, since it has been postulated to be more sensitive with small LCM samples. ~50,000 periosteal osteoblasts were LMD in the lysis buffer provided by the supplier. Prior to extraction the sample was split in two samples each containing ~25,000 LMD osteoblasts. The extraction was carried out as described in §5.2.6.4. For the control RNA 1,000 cultured osteoblasts were used. The RNA samples were tested on the NanoDrop and the Agilent bionalyzer for quantity and quality. As can be seen in figure 5.18 the 260/280 and 260/230 ratios were low indicative of the presence of co-contaminants. The Agilent profiles showed clear 18S and 28S peaks for the control sample which was 25,000 cultured osteoblasts as well as for sample A1 but not for sample A2; with no real improvement in the RNA integrity as indicated by the RIN number for the for both A1 and A2 and poor reproducibility of the method.

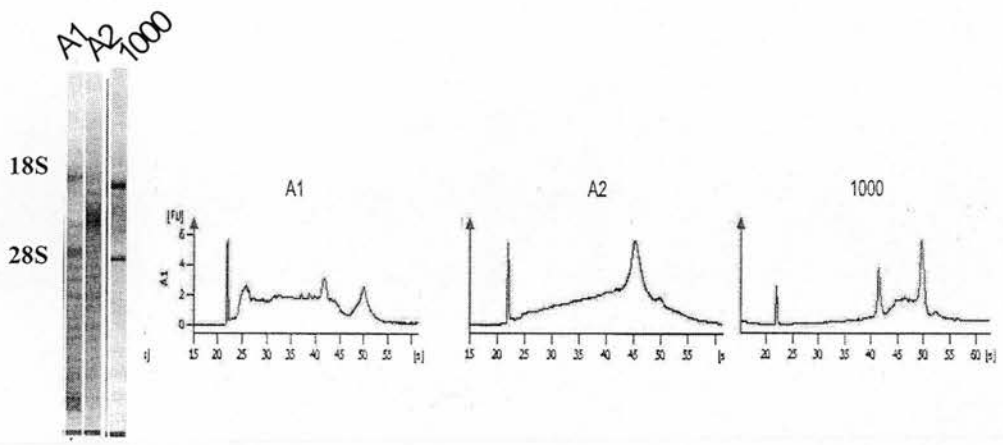

Agilent	A1	RNA Area	136.2	A2	RNA Area	204.4
		RNA Conc	979 pg/µl		RNA Conc	1469pg/µl
		RIN	3.1		RIN	N/A
	1000	RNA Area	149			
		RNA Conc	1071 pg/µl			
		RIN	8.1			

Nanodrop Readings

	260/280	**260/230**	**ng/µl**
A1	1.71	0.69	2.8
A2	1.55	0.75	9.4
Control (1000 cells)	1.6	1.15	26.8

Figure 5.18. Agilent Bionalyzer profiles and NanoDrop data for RNA samples of roughly 4,000 cells isolated using Arcturus Pico Pure RNA isolation kit. ~25,000 cells from periosteum of a 15 month old animal were LMD and RNA was isolated using the Arcturus Pico-Pure method. The 260/280 and 260/230 ratios were higher for the sample A1 compared to A2. As can be seen in the Agilent profiles there were clear 18S and 28S peaks for A1 but not for A2; however the samples were degraded as indicated by the low RIN numbers.

5.4 Discussion

Osteoblasts are the cells responsible for bone formation and have been proposed to respond differently to osteotropic agents at different anatomical sites, but the functional significance of such findings is not clear. One obstacle in understanding the response of osteoblasts to different anabolic treatments is that the cells are not accessible for study *in vivo*. Although it is possible to extract and culture osteoblasts from bones, the responses of such cells might be different from those *in vivo*. In the present study a technique to investigate osteoblast gene expression *in vivo*, in female rats previously treated with rhPTH, rhGH and Compounds A and B over an experimental period of 14 days using laser microdissection of bone tissue cryosections has been developed. The principle of this method is that only specific cell populations from heterogeneous tissues are isolated and RNA isolation can follow. Using this method, an attempt to investigate the gene expression in osteoblastic cells from the rat tibia at the endosteal and periosteal sites was made. Although limited gene expression was obtained, this technique forms the basis for future studies to investigate gene expression of specific cell populations.

In the present study female rats were subjected to rhPTH and rhGH treatment for 14 days. The animals used in this study were virgin 18 months of age females, which represents the female ageing skeleton; providing a good model for quiescent bone surfaces. During ageing, osteoblasts have a shorter life span and are more prone to apoptosis which may account for the deficit in bone formation observed in age-related osteopenia (Chan and Duque, 2002). The concept of apoptosis prevention in osteoblasts may explain the anabolic action of PTH and GH in ageing bone (Whitfield, 2006); however more research in terms of understanding the molecular profiles for such actions is necessary so that any differences in response to anabolic treatment could be documented and potentially be used for the design of drugs to prevent age-related bone loss.

Compact calcified bone, creates an analytically difficult to handle tissue. This is mainly the reason why the majority of the available data on osteoblasts stem from cell culture studies using cell lines, since obtaining pure populations of primary osteoblasts is

demanding. However such studies cannot provide much information regarding gene expression at the different anatomical sites of bone (periosteal vs. endosteal). To overcome these difficulties a powerful tool becoming more widely used is LCM, which allows the sampling of specific cell populations from heterogeneous tissues. In this study fixed cell samples were collected by LCM, however they differed in several aspects from fresh cells; as fixation introduced difficulty in the isolation of high quality RNA from these cells. It has been reported in other studies that RNA isolated from paraformaldehyde fixed, paraffin embedded cells was less reliable than RNA isolated from frozen ethanol fixed cells (Finke et al. 1993, Foss et al. 1994, Karlsen et al. 1994, Shibutani et al. 2000, Macabeo-Ong et al. 2002, Eisenberger et al. 2004). Ethanol fixation has been reported to introduce less chemical modifications, as it preserves nucleic acids through denaturation; in contrast to formalin which causes cross-linking of nucleotides and proteins, with subsequent poor RNA quality (Goldsworthy et al. 1999, Williams et al. 1999). In the present study the isolated RNA was to be used for microarray analysis, therefore it was necessary to minimize the potential modifications from fixation, as they would interfere with the amplification process. Furthermore, tissue was snap frozen in cold hexane, as it has been generally considered to be the best source of intact RNA, as well as maintaining better tissue morphology. To assess whether the stain of choice affected the integrity of RNA, sections fixed in 70% ethanol were subjected to staining or no staining, followed by LCM and RNA isolation. Following RNA examination it was found that staining and fixing generally affected the integrity of RNA to a certain extent when compared to RNA samples from fresh cells. Due to the study design it would not have been possible to perform the study without staining since it significantly improved the laser dissection process, as it helped laser-excitation for cutting. Although the morphology of sections was satisfactory and the regions of interest were well defined, it was troublesome to obtain such sections. For this reason it would be useful to consider using commercially available tape-transfer systems such as CryoJane for future studies, as it has been reported to produce frozen sections, fully intact and bonded to the microscope slide in less than 3 minutes that is ready for fixation and staining. The value of such systems is highlighted by the report of Eisenberger and colleagues (2004) of

successful isolation of intact osteocyte RNA using a tape-transfer system; however it may still need further testing and improvment.

Even when successfully isolated, RNA could have been subject to RNA degradation. RNases are present and active at fixation, however the tissues used in this study were immersion fixed in cold hexane and as such this possibility is remote. On the other hand the conditions pre and post fixation can introduce RNA degradation, these would include pre-fixation time, tissue processing; which would include cryosectioning, fixation and staining to LCM. To minimize the chances of RNA degradation, tissues, following surgical removal, were immediately fixed and all further processing from cryosectioning to LCM was performed under strict RNase free conditions with all solutions being RNase/DNase free as well as performing all steps in the minimum time necessary. During LCM, the room and microscope used were isolated and cleaned after each use to avoid introduction of RNases as well as minimizing the time of laser dissection to 30 minutes per slide, although it is possible to LCM tissues if completely dry for up to 2 hours.

Moreover the DNase treatment for removal of any residual genomic DNA present in the RNA sample as well as phenol/chloroform based extraction methods for example Trizol RNA isolation employed in this study may further reduce the final RNA yield considerably (Srinivasan et al. 2002). However in this study DNase treatment was a pre-requisite for subsequent microarray studies and thus could not be avoided. On the other hand RNA isolation using trizol did give some successful results; which unfortunately were not reproducible and the RNA yield was similar to the other RNA isolation methods employed in this study.

To determine whether LCM led to the expected collection of osteoblasts the presence of the actin gene was tested by PCR. Actin was found to be expressed in both the periosteal and endosteal preparations indicating successful isolation of osteoblastic populations with minimal contamination from the border regions when guiding the microdissection laser. Since the pilot study which was performed using young animals of about 3-5 months of age was successful, the same technique was applied in the animals of the study which

were 18 months of age. However the reproducibility was poor between different sets of samples, with RNA integrity being severely compromised in the tissues derived from the study samples. In an attempt to improve on the quality of the RNA various capturing media for microdissected material and RNA isolation methods were assessed. The RNeasy micro kit RNA isolation method which was the method of choice was proven successful as indicated by the limited microarray data obtained, however extensive degradation was detected. In an attempt to improve the method, a modification with the addition of proteinase K, which is known to inactivate RNases and DNases in nucleic acid extractions was introduced, with no improvement in the RNA quality as it was shown on the Agilent bionalyzer and poor 260/280, 260/230 ratios when quantified with the NanoDrop.

The next method that was tested was phenol based isolation of RNA using trizol with addition of glycogen carrier because of the low amounts of RNA present in these samples. For the removal of any carryover phenol a clean up step was performed, which did not improve the quality of the sample and resulted in significant yield reduction. Although the trizol method improved the quality of RNA extracted compared to the RNeasy method, the 260/280 and 260/230 ratios were low indicative of co-contaminants that were not removed following clean up of the samples as well as low RIN numbers indicative of RNA degradation.

Both RNeasy and trizol were viable methods for the purposes of this study, however there was clear evidence of co-contaminants and RNA degradation present. The 260/230 ratios were low, with absorption at 230 nm indicating salt contamination. As mineralized tissues are rich in hydroxyapatite and salts a de-calcification step with EDTA prior to fixation and staining was introduced. RNA was isolated using trizol and RNeasy micro kit, with no improvement in RNA quality as indicated by the 260/280 and 260/230 ratios as well as the inability to obtain Agilent profiles. These data may be explained by the fact that EDTA has been reported to compromise integrity and yield of nucleic acids (Williams et al. 1999), in future studies it would be useful to test other methods such as water or possibly shorter incubation times.

Finally RNA was extracted using the Arcturus pico pure RNA isolation method. This commercially available kit is hypothesized to successfully isolate RNA from as little as 100 cells. This RNA isolation method was found not to improve the integrity of RNA when compared to the other isolation methods. Although fewer cells were used for these extractions compared to the other methods it can be concluded that this method may be viable for studies of this nature, however it was found not to be reproducible.

Limited microarray data from the rhPTH treated group at the endosteal envelope was obtained. Genes whose expression was strongly elevated in response to rhPTH treatment were broadly grouped as being associated with development; binding, catalysis and cell cycle; other genes affected to a lesser extent by rhPTH treatment were categorized as being associated with signal transduction, apoptosis, cytokinesis and cell migration, cell proliferation as well as structural proteins and transcription factors. However no RT-PCR was performed to check for constistency due to time limitations, a major limitation which should be, addressed in future studies. PTH is known to regulate the expression of genes in these families (Qin et al. 2003), and similar findings have been reported *in vivo* and *in vitro* by other researchers (Onyia et al. 2005, Qin et al. 2003). However no other data is currently available in the literature regarding microarray data derived from different anatomical sites of bone and as such no direct comparisons to the data presented here can be made. These genes belong to different families based on their function, therefore further evaluation of the regulation and function of these genes is necessary to clarify their role in bone. It should be noted that this study is far from a complete representation of all PTH regulated genes and thus further investigations are necessary.

Osteoblasts pose receptors for both PTH (Fermor and Skerry, 1995) and GH (Lobie et al. 1992) and are thus directly stimulated by these hormones. It has been reported that the osteoblast and its progenitors are the primary *in vivo* targets for PTH action (Dempster et al., 1993), where stimulation of bone formation occurs primarily on endocortical surfaces (Oxlund et al., 1993). *In vitro* studies have shown that PTH promotes the commitment of osteoblast precursors (Ishizuya et al., 1997) and inhibits osteoblast apoptosis (Jilka et al., 1999). GH on the other hand has been shown to increase bone formation markers as well

as serum concentrations of IGF-I (Fernholm et al., 2000, Hedstorm et al. 2004). It is well known that GH either acts directly on specific tissues or by binding to its receptors and stimulating the release of IGF-I, however the interdependence of GH and IGF-I makes it difficult to independently assess the contribution of each compound to bone accretion (Govoni et al. 2006). The molecular events responsible for the different skeletal responses to PTH and GH are poorly understood. Therefore an attempt to ascertain the molecular networks responsible for the effects of these hormones, by identifying gene expression patterns and pathways associated with their processes in bone was undertaken.

In conclusion the data obtained and presented herein was not reproducible between different sets of samples. Although considerable effort over 36 months was put into this study, possibly due to the long term storage of the samples and the delays in analyzing data, might have affected the RNA integrity, since the first set of samples provided successful, though limited microarray data, compared to the second set of samples. While the older animals were the best model for a quiescent bone surface at the start of the experiment, obtaining high quality and quantity RNA from this age group was proving to be problematic and the quality and quantity of RNA obtained was inconsistent across the groups. This may have been due to the thinning of the periosteum and endosteum that occurs with ageing, which affects the number and activity of cells present at those sites, and therefore less RNA present and available to isolate. Finally during the laser dissection process in order to avoid contamination of the sample with extraneous tissue the muscle for the periosteal site and bone and bone marrow for the endosteal site were avoided, so it is a possibility that the area of interest undergoes damage as a result of the laser action when the width of periosteum to laser width ratio becomes to low which leads to increased tissue degradation. Although a challenging study with many difficulties, substantial work has been undertaken to provide the basis for future studies to assess how different hormonal and growth factors influence periosteal and endosteal cells. It's been long speculated that there are selective and specific drug targets within the periosteum and endosteum that can be independently activated, to improve bone strength and reduce fracture risk and studies like the one presented in this chapter highlight the importance of research that needs to be undertaken to identify these targets.

CONCLUSIONS AND FUTURE STUDIES

Conclusions and future work

The aim of this thesis was to provide support of the hypothesis, that rhPTH and rhGH can protect osteocytes from apoptosis and control differently osteoblastic cell populations at different anatomical sites. To examine this hypothesis a number of different experiments were carried out *in vitro* using the MLO-Y4 osteocyte-like cell line, *in vivo* using aged female rats and *ex vivo using* human bone cores in the presence or absence of mechanical stimulation. It has long been speculated that anabolic treatments can be used in the future to treat bone diseases. More specifically parathyroid and growth hormones have long been under investigation and associated with the prevention of osteocyte apoptosis and osteoblast actions to improve bone structure and integrity. However their effects and molecular mechanisms controlling these processes on osteocytes and osteoblasts have not been studied in response to injury, ageing or human *ex-vivo* explants.

In the second chapter of this thesis evidence has been presented of the protective effects rhPTH and rhGH exert on osteocytes in a cell wounding model *in vitro* using the osteocyte-like cell line MLO-Y4s, taken to represent microdamage *in vivo*. The data presented in chapter 2 may provide us with an insight of how osteocytes sense and respond to injury as well as the potential of therapeutical compounds to maintain osteocyte viability in disease and ageing. However studies in primary osteocytes rather than cell lines would be of more interest to explore their response to these hormones as well as injury. Further studies will be useful to establish the long-term fate of the wounded cells, since it is clear that is not necrosis of cells but we cannot rule out the possibility of apoptosis and the relation of such a response to rhPTH and rhGH. Finally the Zetos^{TM} bioreactor discussed in chapter 4 may be useful to induce microcracks in human bone and study the osteocyte response to cell wounding in its 3D dimensions in its native environment, since such a study would be difficult to design *in vivo*. The Zetos^{TM} bioreactor could be a useful system because it would allow the perfusion of growth factors as well as hormone treatments and perfusion of dyes to study histologically the fate and response of primary osteocytes to microdamage.

As MLO-Y4s are osteocyte-like cells they do not represent primary osteocytes and their responses during ageing. To study these parameters rhPTH and rhGH were administered in aged female rats as presented in chapter 3 to study their effects on the ageing osteocytic cell population. Evidence has been presented to show their protective effects on these cells as well as improving bone architecture as evidenced by micro-CT analysis. The effect of rhGH was not as pronounced as that of the rhPTH but these differences may be partially explained by the fact that osteocytes possess receptors for PTH but not for GH. Therefore GH treatment exerts indirect effects to the osteocytes possibly through the GH/IGF-I axis. Although the exact anti-apoptotic signaling pathways were not investigated in this thesis, sclerostin immunostaining may provide limited information as to the hormonal regulation of bone remodeling mediated by the osteocytes; further studies are however required to elucidate the possible involvement of sclerostin in other processes such as apoptosis or cell differentiation.

However studying the effects of anabolic compounds on osteocytes and osteoblasts in animal models is not representative of the *in vivo* situation in human bone. Therefore, to investigate the effects of rhPTH in the presence or absence of mechanical stimulation, following reports that they have synergistic effects on osteocyte viability and osteoblast indices in human trabecular bone explants, the Zetos^{TM} culture system was used. rhPTH in the presence or absence of mechanical stimulation decreased SOST gene expression, which supports the hypothesis of an anabolic effect of this hormone via the osteocyte. Possibly rhPTH prevented osteocyte SOST production and promoted osteogenesis by the rhPTH-stimulated apoptosis resisting osteoblasts in the BMUs of bones. However still more studies are required to elucidate the role of SOST and sclerostin in such systems and their biological significance in osteocyte-osteoblast communication. This system might prove to be valuable for the prolonged maintenance of bone samples in culture and questions regarding the time course of osteocyte or osteoblast apoptosis as well as the interactions of these cells might be answered by its use. Future work should explore whether rhPTH and rhGH, exert beneficial effects on osteocytes and osteoblasts and in combination with molecular biology techniques it might provide useful insights into the mechanisms and pathways employed by mechanical stimulation and/or rhPTH or rhGH

in the maintenance of osteocyte viability in human bone. Also the use of histomorphometric indices in longer duration experiments may provide useful information with regard to osteocytes and osteoblasts and their response to mechanical stimulation and growth factors. Due to time and compound availability limitations no experiments were carried out to study the effects of rhGH in this system. GH and exercise have been reported to increase osteogenesis at the periosteal envelope of bone (Kalu et al. 2000) and GH has been found to affect cortical and cancellous bone, however the complexity of the GH/IGF-I system as well as the effects of GH on muscle which may explain the enhanced mechanical properties of bone have made it hard to study these parameters together, the Zetos^{TM} may provide direct information as to the effects of these two parameters separately and in combination.

Finally both PTH and GH have been reported to exert anabolic actions by inducing bone formation by the osteoblasts and/or by inhibition of osteoblast apoptosis. The mechanisms by which they exert their anabolic effects remain unknown. However, the differences observed in the osteogenic responses these agents elicit at different anatomical sites of bone, suggest that selective targeting of either periosteal or endosteal bone surfaces would prove useful. This hypothesis served as the aim of the study in chapter 5 where an attempt to study the gene expression of osteoblasts using LCM has been presented. A number of pitfalls have been identified but this study could be the basis for the design of future studies to look into the molecular profiling of the osteoblast which is directly stimulated by rhPTH and rhGH and provide useful information that could serve towards the development of new drug targets for treating pathological bone conditions.

The data presented in this thesis highlights the protective effects of rhPTH and rhGH on osteocytes *in vitro, in vivo* and *ex vivo*. Also an attempt to study the osteoblast molecular profiling and its response to hormone treatment was made; unfortunately limited microarray data was obtained, in response to rhPTH treatment at the endosteal envelope that could form the basis for follow-up studies. Both rhPTH and rhGH exert complex actions on bone, and future studies are necessary to elucidate the mechanisms of these

actions. This could possibly lead to the design of compounds to treat age related bone loss.

REFERENCES

Aarden, E., Burger, E., Nijweide, P., 1994. Function of osteocytes in bone. *JCB:* 55:287-299.

Aarts M. M., Davidson D., Corluka A., Petroulakis E., Jun Guo, F., Bringhurst F. R., Galipeau J., Henderson J. E., 2001. Parathyroid Hormone-related Protein Promotes Quiescence and Survival of Serum-deprived Chondrocytes by Inhibiting rRNA Synthesis, The Journal of Biological Chemistry, 276 (41):37934–3794

Abizaid A, Schiavo L, Diano S., 2008. Hypothalamic and pituitary expression of ghrelin receptor message is increased during lactation. Neurosci Lett. 8;440(3):206-10

Abu EO, Bord S, Horner A, Chatterjee VK, Compston JE., 1997. The expression of thyroid hormone receptors in human bone. Bone. 21(2):137-42.

Actions of Anterior Pituitary Hormones: Growth Hormone (GH). Medical College of Georgia. 2007

Agarwala T., Gay CV., 1992. Specific binding of parathyroid hormone on living osteoclasts. JBMR 7:531-9

Aguirre JI, Plotkin LI, Gortazar AR, Millan MM, O'Brien CA, 2007.A Novel Ligand-independent Function of the Estrogen Receptor is Essential for Osteocyte and Osteoblast Mechanotransduction. *JBC.* 282(35):25501-25508

Aguirre, J.I., Plotkin, L.I., Stewart, S.A., Weinstein, R.S., Parfitt, A.M., Manolagas, S.C., Bellido, T., 2006. Osteocyte apoptosis is induced by weightlessness in mice and precedes osteoclast recruitment and bone loss. *JBMR* 21(4):605-15.

Ahmad AM, Hopkins MT, Fraser WD, Ooi CG, Durham BH, Vora JP, 2003. Parathyroid hormone secretory pattern, circulating activity, and effect on bone turnover in adult growth hormone deficiency. Bone 32:170-179

Ajubi, N., Klein-Nulend, J., Alblas, M., Burger, E., Nijweide, P., 1999. Signal transduction pathways involved in fluid flow-induced PGE_2 production by cultured osteocytes. *Am.J Physiol* 276:171-178.

Al-Badr W, Martin KJ.,2008. Vitamin D and Kidney Disease. Clin J Am Soc Nephrol.

Allen MR., Hock JM, Burr DB, 2004. Periosteum: biology, regulation, and response to osteoporosis therapies. Bone 35:1003– 1012

Amizuka N, Karaplis AC, Henderson JE, Warshawsky H, Lipman ML, Matsuki Y, Ejiri S, Tanaka M, Izumi N, Ozawa H, Goltzman D., 1996. Haploinsufficiency of parathyroid hormone-related peptide (PTHrP) results in abnormal postnatal bone development., Dev Biol., 175(1):166-76.

Andreassen TT, Melsen F, Oxlund H., 1996. The influence of growth hormone on cancellous and cortical bone of the vertebral body in aged rats. JBMR 11:1094-1102

Andreassen TT, Oxlund H., 2000. The influence of combined parathyroid hormone and growth hormone treatment on cortical bone in aged ovariectomized rats. JBMR 15:2266-2275

Aubin, J.E., Liu, F., Malaval, L., Gupta, A.K., 1995. Osteoblast and chondroblast differentiation. *Bone*. 17(2 Suppl):77S-83S.

Badi A., Samra A., Juppner H., Force T., Freeman MW., Kong X., Schipani E., Urena P., Richards J., Bonventre J., Potts J., Kronenberg H., Segre G. 1992, Expression cloning of a common receptor for parathyroid hormone and parathyroid hormone-related peptide from rat osteoblast-like cells: A single receptor stimulates intracellular accumulation of both cAMP and inositol trisphosphates and increases intracellular free calcium. Proc. Natl. Acad. Sci. USA 89: 2732-2736

Bagi CM, Brommage R, Deleon L, Adams S, Rosen D, Sommer A., 1994. Benefit of systemically administered rhIGF-I and rhIGF-I/ IGFBP-3 on cancellous bone in ovariectomized rats. JBMR 9:1301–1312

Bakker, A., Klein-Nulend, J., Burger, E., 2004. Shear stress inhibits while disuse promotes osteocyte apoptosis. *Biochem Biophys Res Commun* 320:1163-1168.

Barb CR, Hausman GJ, Lents CA., 2008. Energy metabolism and leptin: effects on neuroendocrine regulation of reproduction in the gilt and sow. Reprod Domest Anim. 43 Suppl 2:324-30

Barnard R, Ng KW, Martin TJ, Waters MJ, 1991. Growth hormone (GH) receptors in

Baron R, Tross R, Vugnery A., 1984. Evidence of sequential remodeling in rat trabecular bone: Morphology, dynamic histomorphometry, and changes during skeletal maturation. Anat Rec 208:137–145.

Baron, R., 1996. Anatomy and ultrastructure of bone. Primer on the metabolic bone diseases and disorders of mineral metabolism, Lippincott-Raven, New York, 3-10.

Baroncelli GI, Bertelloni S, Sodini F, Saggese G ,2003. Acquisition of bone mass in normal individuals and in patients with growth hormone deficiency. J Pediatr Endocrinol Metab 16 Suppl 2:327-335.

Basso, N., Heersche, J.N., 2006. Effects of hind limb unloading and reloading on nitric oxide synthase expression and apoptosis of osteocytes and chondrocytes. *Bone.* 39(4):807-14

Bellido T, Ali AA, Gubrij I, Plotkin LI, Fu Q, O'Brien CA, Manolagas SC, Jilka RL 2005. Chronic elevation of parathyroid hormone in mice reduces expression of sclerostin by osteocytes: a novel mechanism for hormonal control of osteoblastogenesis.

Bellido T., 2006, Downregulation of SOST/sclerostin by PTH: a novel mechanism of hormonal control of bone formation mediated by osteocytes.

Bentolila V, Boyce TM, Fyhrie DP, Drumb R, Skerry TM, 1998. Intracortical remodelling in adult rat long bones after fatigue loading. *Bone.* **23**, 275-281

Bilezikian JP., 2000. Combination anabolic and antiresorptive therapy for osteoporosis: opening the anabolic window.Curr Osteoporos Rep. 6(1):24-30.

Boissy P., Saltel F., Bouniol C., Jurdic P., Machuca-Gayet I., 2002. Transcriptional Activity of Nuclei in Multinucleated Osteoclasts and Its Modulation by Calcitonin. Endocrinology 143: 5 :1913-1921

Bonewald LF ,2004. Osteocyte biology: Its implications for osteoporosis. *J Musculoskel Neuron Interac.* 24, 101-104

Bonewald LF, Johnson ML, 2008. Osteocytes, mechanosensing and Wnt signalling. Bone. Apr;42(4):606-15

Bonewald LF., 2007. Osteocytes as dynamic multifunctional cells. Ann N Y Acad Sci. 1116:281-90

Bord S, Horner A, Beavan S, Compston J.2001. Estrogen receptors alpha and beta are differentially expressed in developing human bone. J Clin Endocrinol Metab 86:2309–14.

Bouillon R ,1991. Growth hormone and bone. Horm Res 36:49–55)

Boyde, A., 1980. Evidence against 'osteocyte osteolysis'. *Metab.Bone.Dis.Rel.Res* S239-255.

Boyden LM, Mao J, Belsky J, Mitzner L, Farhi A, Mitnick MA, Wu D, Insogna K, Lifton RP. 2002. High bone density due to a mutation in LDL-receptor-related protein 5. N Engl J Med. 346:1513-21.

Bringhurst FR, 2002. PTH receptors and apoptosis in osteocytes. JMNI 2(3):245-51

Bringhurst FR., 2002. PTH receptors and apoptosis in osteocytes. *JMNI* 2:245–251

Bronckers, A.L., Goei, W., van Heerde, W.L., Dumont, E.A., Reutlingsperger, C.P., van den Eijnde, S.M., 2000. Phagocytosis of dying chondrocytes by osteoclasts in the mouse growth plate as demonstrated by annexin-V labeling. *Cell Tissue Res.* 301(2):267-72

Brukner P, Bradshaw C, Khan KM, White S, Crossley K., 1966. Stress fractures: a review of 180 cases. *Clin J Sports Med.* 6, 85-89

Brunkow, M., Gardner, J., Van Ness, J., Paeper, B., Kovacevich, B., Proll, S., Skonier, J., Zhao, L., Sabo, P., Fu, Y., Alisch, R., Gillett, L., Colbert, T., Tacconi, P., Galas, D., Hamersma, H., Beighton, P., Mulligan, J., 2001. Bone dysplasia sclerosteosis results from loss of the SOST gene product, a novel cysteine knot-containing protein. *Am.J.Hum.Genet* 68:577–589

Burger, E.H., Klein-Nulend, J., van der Plas, A., Nijweide, P.J. , 1995. Function of osteocytes in bone--their role in mechanotransduction. *J Nutr.* 125(7 Suppl):2020S-2023S.

Burkhart JM, Jowsey J., 1997. Parathyroid and thyroid hormones in the development of immobilization osteoporosis. Endocrinology 81:1053-1062.

Burr D. 2005. Does early PTH treatment compromise bone strength? The balance between remodelling, porosity, bone mineral, and bone size. Curr. Osteoporos. Rep. 3:19-24.

Burr DB, Martin RB., 1993. Calculating the probability that microcracks initiate resorption spaces. J Biomech 26: 613-616.

Burr, D.B. ,Martin, R.B., Schaffler, M.B., Radin, E.L., 1985. Bone remodeling in response to in vivo fatigue microdamage. *J Biomech.* 18(3):189-200.

Cann CE, Arnaud CD, Roe S, Sanchez S. Localized bone response to drug modulated by local strains. Abstracts from Twenty-Seventh International Workshop on Hard Tissue Biology, Sun Valley, Idaho, August 1997

Carter, D., van der Meulen, M., Beaupre, G., 1996. Mechanical factors in bone growth and development. *Bone* 18(1), 5S-10S

Caverzasio J, Montessuit C, Bonjour JP., 1990. Stimulatory effect of insulin-like growth factor-1 on renal Pi transport and plasma 1,25-dihydroxyvitamin D3.Endocrinology. 127(1):453-9

Chan G, Duque G, 2002. Age-related bone loss: old bone, new facts. Gerontology 48: 62-71

Chavassieux, PM., Delmas, PD., 2006. Bone remodeling: biochemical markers or bone biopsy? *JBMR* 21(1):178-9.

Chen HT, Schuler LA, Schultz RD., 1998. Growth hormone receptor and regulation of gene expression in fetal lymphoid cells. *Mol Cell Endocrinol* 137:21–29

Chen X, Macica CM, Dreyer BE, Hammond VE, Hens JR, Philbrick WM, Broadus AE, 2006. Initial characterization of PTH-related protein gene-driven lacZ expression in the mouse., JBMR 21:113-23

Cheng, M.Z., Zaman, G., Rawlinson, S.C., Suswillo, R.F., Lanyon, L.E., 1996. Mechanical loading and sex hormone interactions in organ cultures of rat ulna. *JBMR* 11(4):502-11

Chenu C, Valentin-Opran A, Chavassieux P, Saez S, Meunier PJ, Delmas PD, 1990. Insulin like growth factor I hormonal regulation by growth hormone and by 1,25(OH)2D3 and activity on human osteoblast-like cells in short-term cultures. Bone 11:81–86.

Chow JW, Fox S., Jagger CJ, and Chambers TJ, 1998b. Role for parathyroid hormone in mechanical responsviness of rat bone, American Journal for Physiology, 274:E146-54

Claes Ohlsson, Bengt-Åke Bengtsson, Olle G. P. Isaksson, Troels E. Addreassen, Maria C. Slootweg , 1998, Growth Hormone and Bone Endocrine Reviews 19(1): 55–79

clonal osteoblast-like cells mediate a mitogenic response to GH. Endocrinology 128:1459–1464

Colopy SA, Benz-Dean J, Barrett JG, Sample SJ, Lu Y *et al.* ,2004. Response of the osteocyte syncytium adjacent to and distant from linear microcracks during adaptation to cyclical loading. Bone (4): 35:881-891

Compston JE., 2007, Skeletal actions of intermittent parathyroid hormone: Effects on bone remodelling and structure. Bone 40:1447–1452

Corpas E, Harman SM, Blackman MR., 1993. Human growth hormone and human aging. *Endocr Rev* 14:20–39

Cotman, C.W., Anderson, A.J., 1995. A potential role for apoptosis in neurodegeneration and Alzheimer's disease. *Mol Neurobiol.* 10(1):19-45.

Cowin S.C., 2002. Mechanosensation and fluid transport in living bone. JMNI 2(3):256-60

Danilovich N, Wernsing D, Coschigano KT, Kopchick JJ, Bartke A. 1999. Deficits in female reproductive function in GHR- KO mice: Role of IGF-1. *Endocrinology* 140:2637–2640.

David N. Herndon, M.D., Hal. K. Hawkins, Ph.D., M.D., Thuan T. Nguyen, M.D., Edgar Pierre, M.D., Robert Cox, M.S., and Robert E. Barrow, 1995. Characterization of Growth Hormone Enhanced Donor Site Healing in Patients with Large Cutaneous Burns. Annals of Surgery 221(6):649-659

Davidson MB., 1987. Effect of growth hormone on carbohydrate and lipid metabolism. *Endocr Rev* 8:115–131

Davies, C.M., Jones, D.B., Stoddart, M.J., Koller, K., Smith, E., Archer, C.W., Richards, R.G., 2006. Mechanically loaded ex vivo bone culture system 'Zetos': systems and culture preparation. *Eur Cell Mater.* 12 (11):57-75.

Dempster DW, Cosman F., Parisein M., Shen V. and Lindsay R., 1993. Anabolic actions of parathyroid hormone on bone. Endocrine Reviews, 14: 690- 709

DiGirolamo D., Mukherjee A., Fulzele K., Gan Y., Cao X., Frank S., Clemens T. ,2007. Mode of Growth Hormone Action in Osteoblasts. The Journal of Biological Chemistry 282(43):31666–31674

DiGirolamo JD., Mukherjee A., Fulzele K., Gan Y., Cao X., Frank SJ., Clemens TL., 2007. Mode of Growth Hormone Action in Osteoblasts. JBC, 282 (43): 31666-31674.

Divieti P, Inomata N, Chapin K., Singh R., Juppner H and Bringhurst FR, 2001. Receptros for the carboxyl-terminal region of pth (1-84) are highly expressed in osteocytic cells.Endocrinology, 142:916-25

Divietti P., 2005. PTH and osteocytes. JMNI 5(4):328-330

Dobnig H, Turner RT. 1995. Evidence that intermittent treatment with parathyroid hormone increases bone formation in adult rats by activation of bone lining cells. Endocrinology 136:3632–3638.

Dobnig H. and Turner RT., 1997. The effects of programmed administration of human parathyroid hormone fragment (1–34) on bone histomorphometry and serum chemistry in rats. Endocrinology 138: 4607–12.

Dodd JS, Raleigh JA, Gross TS, 1999. Osteocyte hypoxia: a novel mechanotransduction pathway. *Am J Cell Physiol.* 277(46), C598-C602

Dragovich, T., Rudin, C., Thompson, C., 1998. Signal transduction pathways that regulate cell survival and cell death. *Oncogene* 17:3207-3213.

Drüeke TB, Massy ZA, 2003. Advanced oxidation protein products, parathyroid hormone and vascular calcification in uremia.. *Blood Purif.* 20 (5): 494-7

Ducy, P., Schinke, T., Karsenty, G., 2000. The Osteoblast: A sophisticated fibroblast under central surveillance. *Science* 289:1501-1504

Dunstan CR, Lauren PD, Somers NM, Evans RA., 1993.Measurement of osteoclasts and bone resorption by automated image analysis. JBMR 8(2):139-45

Dunstan CR, Somers NM, Evans RA., 1993. Osteocyte death and hip fracture. *Calcif Tissue Int.* 53(Suppl1):S113–S116

Eichinger A, Fiaschi-Taesch N, Massfelder T, Fritsch S, Barthelmebs M, Helwig JJ.,2002. Transcript expression of the tuberoinfundibular peptide (TIP)39/PTH2 receptor system and non-PTH1 receptor-mediated tonic effects of TIP39 and other PTH2 receptor ligands in renal vessels. Endocrinology. 143(8):3036-43.

Einhorn, T. 1996.The bone organ system: Form and function. Osteoporosis, R. Marcus, D. Feldman and J. Kelsey, eds., Academic Press, California, 3-21.

Eisenberger S., Godehard H., Pyerin W., Ackermann K., 2004. High-quality RNA preparation for transcript profiling of osteocytes from native human bone microdissections , Analytical biochemistry, 335(2): 260-266

Ejersted C, Oxlund H, Eriksen EF, Andreassen TT., 1998. Withdrawal of parathyroid hormone treatment causes rapid resorption of newly formed vertebral cancellous and endocortical bone in old rats. Bone 23:43-52.

Eriksen EF, Eghbali-Fatourechi GZ, Khosla S, 2007. Remodeling and vascular spaces in bone. JBMR 22:1–6

Eriksen EF., Kasem M., Langdahl B., 1996. Growth hormone, insulin-like growth factors and bone remodeling.European Journal of Clinical Investigations 26, 525-534

Ernst M, Froesch ER, 1988. Growth hormone dependent stimulation of osteoblast-like cells in serum-free cultures via local synthesis of insulin-like growth factor I. Biochem Biophys Res Commun 151:142–147

Eschen C, Andreassen TT., 1995. Growth hormone normalizes vertebral strength in ovariectomized rats. Calcif Tissue Int. 57:392-396

Estepa JC, Aguilera Tejero E, Lopez I, Almaden Y, Rodriguez M, Felsenfeld AJ, 1999. Effect of phosphate on parathyroid hormone secretion in vivo. JBMR 14:1848–1854

Felsenfeld, A.J., Rodriguez, M., 1999. Phosphorus, regulation of plasma calcium, and secondary hyperparathyroidism: a hypothesis to integrate a historical and modern perspective. *J Am Soc Nephrol.* 10(4):878-90.

Fermor, B., Skerry, T.M., 1995. PTH/PTHrP receptor expression on osteoblasts and osteocytes but not resorbing bone surfaces in growing rats. *JBMR* 10(12):1935-43

Fernholm R, Bramnert M, Hagg E, Hilding A, Baylink DJ, Mohan S, and Thoren M, 2000. Growth hormone replacement therapy improves body composition and increases bone metabolism in elderly patients with pituitary disease. *J Clin Endocrinol Metab* 85: 4104–4112.

Fielding, J., Gilbert, N. Understanding social statistics. 2000. London. Sage

Finke J, Fritzen R, Ternes P, Lange W, Dolken G., 1993. An improved strategy and a useful housekeeping gene for RNA analysis from formalin-fixed, paraffin-embedded tissues by PCR. Biotechniques 14:448–53

Finkelstein S., Dhir R., Rabinovitz M., Bischeglia M., Swalsky P., DeFlavia P., Woods J., Bakker A., Becich M., 1997. Cold-temperature plastic resin embedding of liver for DNA- and RNA-based genotyping, *J. Mol. Diagn.* 1:17–22

Foss RD, Guha-Thakurta N, Conran RM, Gutman P., 1994. Effects of fixative and fixation time on the extraction and polymerase chain reaction amplification of RNA from paraffin-embedded tissue. Comparison of two housekeeping gene mRNA controls. Diagn Mol Pathol 3:148–55.

Franceschi RT and Xiao G, 2003. Regulation of the osteoblast-specific transcription factor, Runx2:responsiveness to multiple signal transduction pathways. JCB 88:446-54

Frank A. Gesek and Peter A. Friedman, 1992, On the Mechanism of Parathyroid Hormone Stimulation of Calcium Uptake by Mouse Distal Convoluted Tubule Cells. J. Clin. Invest. 1992. 749-758

Frost HM, 1988. Vital biomechanics: proposed general concepts for skeletal adaptations to mechanical usage. Calcif Tissue Int 42:145–156

Frost HM, 1992. The role of changes in mechanical usage set points in the pathogenesis of osteoporosis. JBMR 7:253–261

Frost, H. 1960. In vivo osteocytes death. J.Bone Joint Surg Am 42-A (1):138-143.

Frost, H., 1969. Tetracycline-based histological analysis of bone remodeling. *Calc.Tiss.Res* 3:211-237.

Frost, H.M., 1988. Vital biomechanics: proposed general concepts for skeletal adaptations to mechanical usage. *Calcif Tissue Int.* 42(3):145-56

Fuller, K., Chambers, T.J., 1995. Localisation of mRNA for collagenase in osteocytic, bone surface and chondrocytic cells but not osteoclasts. *J Cell Sci.* 108 (Pt 6):2221-30.

Gasser JA., 1998. Preclinical studies and clinical experiences with parathyroid hormone and its analogues. Curr Opin Orth 9:1-6

Gensure RC, Ponugoti B, Gunes Y, Papasani MR, Lanske B, Bastepe M, Rubin DA, Jüppner H. 2004. Identification and characterization of two parathyroid hormone-like molecules in zebrafish. Endocrinology. 145(4):1634-9

Giordano R, Bonelli L, Marinazzo E, Ghigo E, Arvat E., 2008. Growth hormone treatment in human ageing: benefits and risks. Hormones (Athens). 7(2):133-9.

Goldsworthy S., Stockton P., Trempus C., Foley J., Maronpot R., 1999. Effects of fixation on RNA extraction and amplification from laser capture microdissected tissue, *Mol. Carcinogen.* 25: 86–91

Govoni K.E., Keun Lee S., Chadwick R.B., Yu H., Kasukawa Y., Baylink D. J., Mohan S., 2006.Whole genome microarray analysis of growth hormone-induced gene expression in bone: T-box3, a novel transcription factor, regulates osteoblast proliferation. *Am J Physiol Endocrinol Metab* 291: E128–E136

Gowen, L.C., Petersen, D.N,. Mansolf, A.L., Qi, H., Stock, J.L., Tkalcevic, G.T., Simmons, H.A., Crawford, D.T., Chidsey-Frink, K.L., Ke, H.Z., McNeish, J.D., Brown, T.A., 2003. Targeted disruption of the osteoblast/osteocyte factor 45 gene (OF45) results in increased bone formation and bone mass. *JCB.* 278(3):1998-2007.

Goyeneche A., Harmon JM. , Telleria CM. 2006. Cell death induced by serum deprivation in luteal cells involves the intrinsic pathway of apoptosis. Reproduction 131: 103–111.

Green H, Morikawa M, Nixon T., 1985. A dual effector theory of growth-hormone action. *Differentiation* 29:195–198

Gu G, Hentunen TA, Nars M, Harkonen PL, Vaananen HK., 2005. Estrogen protects primary osteocytes against glucocorticoid-induced apoptosis. *Apoptosis.* 10:583–595

Gu Y., Preston M., Magnay J., El Haj A., Publicover S., 2001. Hormonally-Regulated Expression of Voltage-Operated Ca21 Channels in Osteocytic (MLO-Y4) Cells. Biochemical and Biophysical Research Communications 282, 536–542

Guchelaar, H., Vermes, A., Haanen, C., 1997. Apoptosis: molecular mechanisms and implications for cancer chemotherapy. *Pharm. World Sci.* 19:119-125

Hadjiargyrou, M., Rightmire, E., Ando, T., Lombardo, F., 2001. The E11 osteoblastic lineage marker is differentially expressed during fracture healing. *Bone.* 29(2):149-154

Hagino H., Okano T., Akhter M., Enokida M., Teshima R., 2001. Effect of parathyroid hormone on cortical bone response to in vivo external loading of the rat tibia. J Bone Miner Metab 19:244–250

Hall, PA., Coates, PJ. Ansari, B., Hopwood, D., 1994. Regulation of cell number in the mammalian gastrointestinal tract: the importance of apoptosis. *J Cell Sci.* 107 (Pt 12):3569-77

Ham, A.W. and Harris, W.R., 1956. Repair and transplantation of bone. Bourne, G.H. Editor, *The Biochemistry and Physiology of Bone* (First edn. ed.), Academic Press, New York, pp. 475–506

Hamaya, M., Mizogushi, I., Sakakura, Y., Yajima, T. Abiko, Y., 2002. Cell death of osteocytes occurs in rat alveolar bone during experimental tooth movement. *Calc.Tiss.Inter.* 70: 117-126.

Hamill OP, Martinac B, 2001. Molecular basis of mechanotransduction in living cells. *Physiol Rev* 81:685–740

Hanks J., 1976, Hanks' balanced salt solution and pH control. Tissue Culture Manual. 3

Harrington EK, Roddy GW, West R, Svoboda KK., 2007. Parathyroid hormone/parathyroid hormone-related peptide modulates growth of avian sternal cartilage via chondrocytic proliferation. Anat Rec (Hoboken). 290(2):155-67

Hazenberg JG, Taylor D, Lee C, 2007. The role of osteocytes and bone microstructure in preventing osteoporotic fractures. *Osteoporos Int.* 18, 1-8

Hedstrom M, Saaf M, Brosjo E, Hurtig C, Sjoberg K, Wesslau A, and Dalen N., 2004. Positive effects of short-term growth hormone treatment on lean body mass and BMC after a hip fracture: a double-blind placebo-controlled pilot study in 20 patients. *Acta Orthop Scand* 75: 394–401

Hildahl J., Power D.M., Björnsson B.D., Einarsdóttir I.E., 2008. Involvement of growth hormone-insulin-like growth factor I system in cranial remodeling during halibut metamorphosis as indicated by tissue- and stage-specific receptor gene expression and the presence of growth hormone receptor protein. Cell Tissue Res 332:211–225

Hill P. A., Bone remodeling, 1998, British Journal of Orthodontics, 25:101-107

Hill PA, Reynolds JJ, Meikle MC ,1995. Osteoblasts mediate insulin- like growth factor-I and -II stimulation of osteoclast formation and function. Endocrinology 136:124–131

Huber C, Collishaw S, Mosley JR, Reeve J, Noble BS., 2007. Selective estrogen receptor modulator inhibits osteocyte apoptosis during abrupt estrogen withdrawal: implications for bone quality maintenance. Calcif Tissue Int. 81(2):139-44

Hughes, D., Dai, A., Tiffee, J., Li H., Mundy, G., Boyce, B., 1996. Estrogen promotes apoptosis of murine osteoclasts mediated by TGF-beta. *Nat.Med.* 10:1132-6.

Hughes, DE., Boyce, BF., 1997. Apoptosis in bone physiology and disease. *Mol Pathol.* 50(3):132-7.

Hughes, DE., Dai, A., Tiffee, JC., Li, HH., Mundy, GR., Boyce, BF., 1996. Estrogen promotes apoptosis of murine osteoclasts mediated by TGF-beta. *Nat Med.* 2(10):1132-6.

Ibbotson KJ, Orcutt CM, D'Souza SM, Paddock CL, Arthur JA, Jankowsky ML, BoyceRW, 1992. Contrasting effects of parathyroid hormone and insulin-like growth factor I in an aged ovariectomized rat model of postmenopausal osteoporosis. JBMR 7:425–432

Ikeda, T., Yamagushi, A., Yokose, S., Nagai, Y., Yamato, H., Nakamura, T., Tsurukami, H., Tanizawa, T., Yoshiki, S., 1996. Changes in biological activity of bone cells in ovariectomised rats revealed by in situ hybridization. *JBMR* 11:780-788.

Ingber DE, 1997. Tensegrity: The architectural basis of cellular mechanotransduction. *Annu Rev Physiol* 59:575–599

Inman, CL., Warren, GL., Hogan, HA., Bloomfield, SA., 1999. Mechanical loading attenuates bone loss due to immobilization and calcium deficiency. *J Appl Physiol.* 87(1):189-195.

Isaksson, O. G. P., Jansson, J.-O., Gause, I. A. M. 1982. Growth hormone stimulates longitudinal bone growth directly. *Science* 216:1237-39

Ishizuya T., Yokose S., Hori M., Noda T., Suda T., Yoshiki S., Yamaguschi A.,1997. Parathyroid hormone exerts disparate effects on osteoblast differentiation depending on exposure time in rat osteoblastic cells., Journal Clinical Investigations, 99:2961-70

Janssens K., Dijke P., Janssens S., Van Hul W., 2005. Transforming Growth Factor-ß1 to the Bone. Endocrine Reviews 26 (6): 743-774

Jee WS, Tian XY., 2005. The benefit of combining non-mechanical agents with mechanical loading: a perspective based on the Utah Paradigm of Skeletal Physiology. JMNI 5(2):110-8

Jilka RL, 2007. Molecular and cellular mechanisms of the anabolic effect of intermittent PTH. Bone 40(6):1434-46

Jilka RL, Weinstein RS, Bellido T, Roberson P, Parfitt AM, Manolagas SC., 1999. Increased bone formation by prevention of osteoblast apoptosis with parathyroid hormone. J Clin Invest 104:439-446

Jilka, RL., Weinstein, R., Bellido, T., Parfitt, A., Manolagas, S., 1998. Osteoblast programmed cell death (apoptosis): modulation by growth factors and cytokines. *JBMR* 13:793-802.

Johansson AG, Lindh E, Blum WF, Kollerup G, Sorensen OH, Ljunghall S ,1996. Effects of growth hormone and insulin-like growth factor I in men with idiopathic osteoporosis. J Clin Endocrinol Metab 81:44–48

Johansson AG, Lindh E, Ljunghall S ,1992. Insulin-like growth factor I stimulates bone turnover in osteoporosis. Lancet 339:1619

John J. K., Andry J. M., 2000. Growth Hormone (GH), GH Receptor, and Signal Transduction Molecular Genetics and Metabolism 71, 293–314

Jones, DB., Boudriot, U., Kratz, M., Koller, K., Mertens, F., Smith, EL., 2001 A trabecular bone and marrow bioreactor. *Eur Cell Mater.* (1) S1:53.

Jones, DB., Broeckmann, E., Pohl, T., Smith, EL., 2003. Development of a mechanical testing and loading system for trabecular bone studies for long term culture. *Eur Cell Mater.* 5:48-59.

Jude E. Onyia , Leah M. Helvering , Lawrence Gelbert , Tao Wei , Shuguang Huang , Peining Chen , Ernst R. Dow , Avudaiappan Maran , Minzhi Zhang, Sutada Lotinun , Xi Lin , David L. Halladay , Rebecca R. Miles , Nalini H. Kulkarni , Emily M. Ambrose , Yanfei L. Ma , Charles A. Frolik , Masahiko Sato , Henry U. Bryant , Russell T. Turner, ,2005. Molecular profile of catabolic versus anabolic treatment regimens of parathyroid hormone (PTH) in rat bone: an analysis by DNA microarray., JCB. 95(2):403-18

Jüppner H 1994. "Molecular cloning and characterization of a parathyroid hormone/parathyroid hormone-related peptide receptor: a member of an ancient family of G protein-coupled receptors". *Curr. Opin. Nephrol. Hypertens.* 3 (4): 371–8

Juppner H., 1999. Receptors for parathyroid hormone and parathyroid hormone-related peptide: exploration of their biological importance. Bone, 25:87-90

Kakizaki, I., Zechner, G., Altmann, F., 1971. The osteocytes of the human labyrinthine capsule. *Arch Otolaryngol.* 94(2):139-50.

Kalu D. N., Banu J., Wang L., 2000. How cancellous and cortical bones adapt to loading and growth hormone. JMNI 1:19-23

Kameda, T., Mano, H., Yuasa, T., Mori, Y., Miyazawa, K., Shiokawa, M., Nakamaru, Y., Hiroi, E., Hiura, K., Kameda, A., Yang, NN., Hakeda, Y., Kumegawa ,M., 1997. Estrogen inhibits bone resorption by directly inducing apoptosis of the bone-resorbing osteoclasts. *J Exp Med.* 186(4):489-95.

Kaneko. H., Ogiuchi, H., Shimono, M., 1997. Cell death during tooth eruption in the rat: surrounding tissues of the crown. *Anat Embryol (Berl).* 195(5):427-34.

Kang S, Bennett CN, Gerin I, Rapp LA, Hankenson KD, Macdougald OA, 2007. Wnt signaling stimulates osteoblastogenesis of mesenchymal precursors by suppressing CCAAT/enhancerbinding protein alpha and peroxisome proliferator-activated receptor gamma. JBC 282:14515-14524.

Kanzaki S, Baxter RC, Knutsen R, Baylink DJ, Mohan S., 1995. Evidence that human bone cells in culture secrete insulin-like growth factor (IGF)-II and IGF binding protein-3 but not acid-labile subunit both under basal and regulated conditions. JBMR 10:854–858

Karaplis AC, Luz A, Glowacki J, Bronson RT, Tybulewicz VL, Kronenberg HM, Mulligan RC., 1994. Lethal skeletal dysplasia from targeted disruption of the parathyroid hormone-related peptide gene.,Genes Dev., 8(3):277-89.

Karlsen F, Kalantari M, Chitemerere M, Johansson B, Hagmar B., 1994. Modifications of human and viral deoxyribonucleic acid by formaldehyde fixation. Lab Invest 71:604–11.

Kassem M., Blum W., Ristelli J., Mosekilde L., Eriksen EF., 1993. Growth Hormone Stimulates Proliferation and Differentiation of Normal Human Osteoblast-Like Cells *In Vitro*. Calcif Tissue Int (1993) 52:222-226

Kato Y, Boskey A, Spevak L, Dallas M, Hori M, Bonewald LF, 2001. Establishment of an osteoid preosteocyte-like cell MLO-A5 that spontaneously minerilizes in culture. JBMR 16:1622-33

Kato Y, Windle JJ, Koop BA, Mundy GR, Bonewald LF, 1997. Establishment of an osteocyte-like cell line, MLO-Y4. JBMR 12:2014-23

Kawakami, A., Eguchi, K., Matsuoka, N., Tsuboi, M., Koji, T., Urayama, S., Fujiyama, K., Kiriyama, T., Nakashima, T., Nakane, PK., Nagataki, S., 1997. Fas and Fas ligand interaction is necessary for human osteoblast apoptosis. JBMR 12(10):1637-46.

Keaveny, TM., Yeh, OC., 2002. Architecture and trabecular bone - toward an improved understanding of the biomechanical effects of age, sex and osteoporosis. *JMNI* 2(3):205

Keller H, Kneissel M., 2005. SOST is a target gene for PTH in bone. Bone.,37(2):148-58.

Kelly PA, Ali S, Rozakis M, Goujon L, Nagano M, Pellegrini I, Gould D, Djiane J, Edery M, Finidori J, *et al.* ,1993. The growth hormone/prolactin receptor family. Recent Prog Horm Res 48:123–164

Kelly PA, Djiane J, Postel-Vinay MC, Edery M., 1991. The prolactin/ growth hormone receptor family. *Endocr Rev* 12:235–251

Kenzora, J., Steele, R, Yosipovitch, Z., Glimcher, M., 1978. Experimental osteonecrosis of the femoral head in adult rabbits. *Clin.Orthop.* (130):8-46.

Kerr, J., Wylie, A., Currie, A., 1972. Apoptosis: a basic biological phenomenon with wide-ranging implications in tissue kinetics. *Br.J.Cancer* 26:239-257.

Khosla S., Westendorf J.J, Oursler M.J. Building bone to reverse osteoporosis and repair fractures. *J. Clin. Invest.* 118:421–428

Klein-Nulend, J., Van der Plas, A, Semeins, C., Ajubi, N., Frangos, J., Nijweibe, P., Burger, E., 1995. Sensitivity of osteocytes to biomechanical stress in vitro. *FASEB* 9: 441-445.

Kneissel M, Boyde A, Gasser JA. 2001. Bone tissue and its mineralization in aged estrogen-depleted rats after longterm intermittent treatment with parathyroid hormone (PTH) analog SDZ PTS 893 or human PTH(1-34). Bone 28: 237–250.

Knothe Tate ML, Adamson JR, Tami AE, Bauer TW, 2004. The osteocyte. Int. J Biochem Cell Biol, 36:1-8.

Knothe Tate ML, Niederer P, Knothe U, 1998. In vivo tracer transport through the lacunocanalicular system of rat bone in an environment devoid of mechanical loading. *Bone,* 22, 107–117

Kobayashi H, Oikawa S, Umemura S, Hirosawa I, Kawanishi S., 2008. Mechanism of metal-mediated DNA damage and apoptosis induced by 6-hydroxydopamine in neuroblastoma SH-SY5Y cells. Free Radic Res. 42(7):651-60

Kogianni G, Mann V, Noble BS., 2008. Apoptotic Bodies Convey Activity Capable of Initiating Osteoclastogenesis and Localised Bone Destruction. JBMR

Kogianni, G., Mann, V., Ebetino, F., Nuttal, M., Nijweide, P., Simpson, H., Noble, B., 2004. Fas/CD95 is associated with glucocorticoid-induced osteocyte apoptosis. *Lif.Sci.* 75:2879-2895.

Kojima M, Hosoda H, Date Y, Nakazato M, Matsuo H, Kangawa K 1999 Ghrelin is a growthhormone-releasing acylated peptide from stomach. Nature 402:656-660

Komori T, Yagi H, Nomura S, Yamaguchi A, Sasaki K, Deguchi K, Shimizu Y, Bronson RT, Gao YH, Inada M, Sato M, Okamoto R, Kitamura Y, Yoshiki S, Kishimoto T. Targeted disruption of Cbfa 1 results in a complete lack of bone formation owing to maturational arrest of osteoblasts. Cell, 89:755-64

Kopchick ., Andry JM., 2000. Growth Hormone (GH), GH Receptor, and Signal Transduction. Molecular Genetics and Metabolism 71, 293–314

Kosaku Kurata, Terhi J Heino, Hidehiko Higaki, H Kalervo Väänänen, 2006. Bone Marrow Cell Differentiation Induced by Mechanically Damaged Osteocytes in 3D Gel-Embedded Culture. JBMR 21:616–625

Kostenuik PJ, Harris J, Halloran BP, Turner RT, Morey-Holton ER, Bikle DD., 1999. Skeletal unloading cause's resistance of osteoprogenitor cells to parathyroid hormone and to insulin-like growth factor-I., JBMR 1:21-31.

Krempien B, Manegold C, Ritz E, Bommer J., 1976. The influence of immobilization on osteocyte morphology: osteocyte differential count and electron microscopical studies. Virchows Archiv A:55-68

Kroneberg H., 2003. Developmental regulation of the growth plate:Nature, 417:332-335

Lancer SR, Bowser EN, Hargis GK, 1976. The effect of growth hormone on parathyroid function in rats. Endocrinology 98:1289–1293

Landry, P., Sadasivan, K., Marino, A., Albright, J., 1997. Apoptosis is coordinately regulated with osteoblast formation during bone healing. *Tissue Cell.* 29(4):413-9.

Lanfranco F, Gianotti L, Giordano R, Pellegrino M, Maccario M, Arvat E., 2003. Ageing, growth hormone and physical performance. J Endocrinol Invest. 26(9):861-72.

Langub C., Monier-Faugere C. , Quanle Qi, Z. Geng, Koszewski N. , Malluche H., 2001. Parathyroid Hormone/Parathyroid Hormone–Related Peptide Type 1 Receptor in Human Bone. JBMR 16:448–456

Lanske B, Karaplis AC, Lee K, Luz A, Vortkamp A, Pirro A, Karperien M, Defize LHK, Ho C, Mulligan RC, Abou-Samra AB, Juppner H, Segre GV, Kronenberg HM, 1996. PTH/PTHrP receptor in early development and Indian hedgehog-regulated bone growth. Science 273:663–666

Lanyon, L.E., 1993. Osteocytes, strain detection, bone modeling and remodeling. *Calcif Tissue Int* 53 Suppl 1:S102-6; S106-7.

Lanyon, L.E., 1996. Using functional loading to influence bone mass and architecture: objectives, mechanisms, and relationship with estrogen of the mechanically adaptive process in bone. Bone. 18(1 Suppl):37S-43S

Lean, J.M., Mackay, A.G., Chow, J.W., Chambers, T.J., 1996. Osteocytic expression of mRNA for c-fos and IGF-I: an immediate early gene response to an osteogenic stimulus. Am J *Physiol.* 270(6 Pt 1):E937-45.

Lecoeur H, 2002. "Nuclear apoptosis detection by flow cytometry: influence of endogenous endonucleases". *Exp. Cell Res.* 277 (1): 1–14

Leder B., Bringhurst FR, 2005, Regulation of calcium and phosphate homeostasis. In: DeGroot LJ, Jameson J (eds.) Endocrinology. Saunders, Philadelphia,PA,USA, pp. 1465-1498.

Lee, F.Y., Choi, Y.W., Behrens, F.F., DeFouw, D.O., Einhorn, T.A., 1998. Programmed removal of chondrocytes during endochondral fracture healing. *J Orthop Res.* 16(1):144-50.

Leupin O, Kramer I, Collette NM, Loots GG, Natt F, Kneissel M, Keller H., 2007. Control of the SOST bone enhancer by PTH using MEF2 transcription factors. JBMR 22(12):1957-67

Lewinson D, Shenzer P, Hochberg Z, 1993. Growth hormone involvement in the regulation of tartrate-resistant acid phosphatasepositivecells that are active in cartilage and bone resorption. Calcif Tissue Int 52:216–221

Li X, Qin L, Bergenstock M, Bevelock LM, Novack DV, Partridge NC., 2007. Parathyroid hormone stimulates osteoblastic expression of MCP-1 to recruit and increase the fusion of pre/osteoclasts. JBC. 282(45):33098-106

Liang JD, Hock JM, Sandusky JE, Santerre RF and Onyia JE, 1999. Immunohistochemical localization of selected early response genes expressed in trabecular bone of young rats given hPTH 1-34. Calcified Tissue International, 65:369-73

Ling Q., Ping Q., Luquan Wang, X. L., Swarthout J. T., Soteropoulos P., Tolias P., Partridge N. C., 2003. Gene Expression Profiles and Transcription Factors Involved in Parathyroid Hormone Signaling in Osteoblasts Revealed by Microarray and Bioinformatics. The Journal of Biological Chemistry 278 (22):19723–19731.

Ling Qin , Liza J. Raggatt and Nicola C. Partridge, 2004. Parathyroid hormone: a double-edged sword for bone metabolism. Trends in Endocrinology and Metabolism, 15(2):60-65

Lobie PE, Garcia-Aragon J, Wang BS, Baumbach WR, Waters MJ., 1992. Cellular localization of the growth hormone binding protein in the rat. Endocrinology 130:3057-3065

Locklin RM, Khosla S, Turner RT, Riggs BL, 2003. Mediators of the biphasic responses of bone to intermittent and continuously administered parathyroid hormone. JCB 89:180–190

Lozupone, E., Palumbo, C., Favia, A., Ferretti, M., Palazzini, S., Cantatore, FP., 1996. Intermittent compressive load stimulates osteogenesis and improves osteocyte viability in bones cultured "in vitro". *Clin Rheumatol.* 15(6):563-72.

Lupu F, Terwilliger JD, Lee K, Segre GV, Efstratiadis A., 2001. Roles of growth hormone and insulin-like growth factor 1 in mouse postnatal growth.Dev Biol. 229(1):141-62

Ma YL, Cain RL, Halladay DL, Yang X, Zeng Q, Miles RR, Chandrasekhar S, Martin TJ, Onyia JE, 2001. Catabolic effects of continuous human PTH (1–38) *in vivo* is

associated with sustained stimulation of RANKL and inhibition of osteoprotegerin and gene-associated bone formation.., Endocrinology, 142:4047–54.

Macabeo-Ong M, Ginzinger DG, Dekker N, McMillan A, Regezi JA, Wong DT, et al., 2002. Effect of duration of fixation on quantitative reverse transcription polymerase chain reaction analyses. Mod Pathol 15:979–87.

MacDougall, M., Simmons, D., Gu, T., Dong, J., 2002. MEPE/OF45, a new dentin/bone matrix protein and candidate gene for dentin diseases mapping to chromosome 4q21. Connet. Tissue. Res 43(2-3) : 320-330.

Mackie EJ., 2003. Osteoblasts: novel roles in orchestration of skeletal architecture., Int J Biochem Cell Biol. 35(9):1301-5.

Mann V, Huber C, Kogianni G, Jones D, Noble B. , 2006. The influence of mechanical stimulation on osteocyte apoptosis and bone viability in human trabecular bone.

Mann V, Jones DB, Noble BS., 2004. The effect of mechanical stimulation on osteocyte viability in bone. JMNI (OR-S2) 4(2):206-209.

Mann V., Huber C., Kogianni G., Collins F., Noble B., 2006. The antioxidant effect of estrogen and Selective Estrogen Receptor Modulators in the inhibition of osteocyte apoptosis *in vitro*. Bone. 40(3) :674-684

Mannstadt M, Jüppner H, Gardella TJ, 1999. "Receptors for PTH and PTHrP: their biological importance and functional properties". *Am. J. Physiol.* 277 (5 Pt 2): F665–75.

Maor G, Hochberg Z, Silbermann M, 1989. Growth hormone stimulates the growth of mouse neonatal condylar cartilage *in vitro*. Acta Endocrinol (Copenh) 120:526–532

Maor G, Hochberg Z, von der Mark K, Heinegard D, Silbermann M, 1989. Human growth hormone enhances chondrogenesis and osteogenesis in a tissue culture system of chondroprogenitor cells. Endocrinology 125:1239–1245

Marotti, G., 1996. The structure of bone tissues and the cellular control of their deposition. *Ital.J.Anat.Embryol.* 101(4):25-79.

Marotti, G., Cane, V., Palazzini, S., Palumbo, C., 1990. Structure-function relationships in the osteocytes. *Ital.J.Min.Electrolyte Metab.* 4:93-106.

Marotti, G., Farneti, D., Remaggi, F., Tartari, F., 1998. Morphometric investigation on osteocytes in human auditory ossicles. *Ann Anat.* 180(5):449-53.

Massas R. and Benayahu D. 1998. Parathyroid Hormone Effect on Cell-to-Cell Communication in Stromal and Osteoblastic Cells. JCB 69:81–86

Matthew R. A., Hock J. M., Burr D. B., 2004. Periosteum: biology, regulation, and response to osteoporosis therapies. Bone 35: 1003– 1012

Mazziotti G, Giustina A, Canalis E, Bilezikian JP. 2007. Glucocorticoid-induced osteoporosis: clinical and therapeutic aspects. Arq Bras Endocrinol Metabol. 51(8):1404-12

McClung MR, San Martin J, Miller PD, Civitelli R, Bandeira F, Omizo M, Donley DW, Dalsky GP, Eriksen EF., 2005. Opposite bone remodeling effects of teriparatide and alendronate in increasing bone mass. Arch Intern Med. 2005 165(15):1762-8.

McLung M., 2004. Parathyroid hormone for the treatment of osteoporosis. Obstet. Gynecol. Surv., 59:826-32

McNeil P.L., Miyake K., Vogel S. S, 2003. The endomembrane requirement for cell surface repair, PNAS , vol. 100 no. 8,4592–4597

McNeil P.L., Steinhardt R. A., 1997. Loss, Restoration, and Maintenance of Plasma Membrane Integrity. JCB 137: (1)1–4

McNeil PL, 2002. Repairing a torn cell surface: Make way, lysosomes to the rescue. *J Cell Sci* 115:873–879

McNeil PL, Kirchhausen T., 2005. An emergency response team for membrane repair. Nat Rev Mol Cell Biol. 6(6):499-505

McNeil PL, Steinhardt RL, 1997. Loss, Restoration, and Maintenance of Plasma Membrane Integrity. *JCB* 137, 1-4

McNeil PL, Terasaki M, 2001. Coping with the inevitable: How cells repair a torn surface membrane. *Nat Cell Biol* 3:E124–E129

McNeil, P.L., 1993. Cellular and molecular adaptations to injurious mechanical forces, Trends Cell. Biol. 3, 302-307

Meng XW, Liang XG, Birchman R, Wu DD, Dempster DW, Lindsay R, Shen V, 1996. Temporal expression of the anabolic action of PTH in cancellous bone of ovariectomized rats. JBMR 11(4):421-9

Merendino JJ., Insogna KL., Milstone LM., Broadus AE., Stewart AF., 1986. A parathyroid hormone-like protein from cultured human keratinocytes, Science, 231: 388-390

Miao D, He B, Karaplis AC, Goltzman D, 2002. Parathyroid hormone is essential for normal fetal bone formation. J Clin Invest 109:1173–1182

Miao D, He B, Lanske B, Goltzman D, Karaplis AC, 2001. Targeted disruption of the PTH gene leads to abnormalities in skeletal development and calcium homeostasis. JBMR 16:S161

Midura RJ, Su X, Morcuende JA, Tammi M, Tammi R. 2003. Parathyroid hormone rapidly stimulates hyaluronan synthesis by periosteal osteoblasts in the tibial diaphysis of the growing rat. JBC 278(51):51462– 8.

Miller SC, Bowman BM, Smith Jm, Jee WS, 1980. Characterization of endosteal bone-liing cells from fatty marrow bone sites in adult beagles. Anat. Rec., 198:163-73.

Misof BM, Roschger P, Cosman F, Kurland ES, Tesch W, Messmer P, Dempster DW, Nieves J, Shane E, Fratzl P, Klaushofer K, Bilezikian J, Lindsay R., 2003. Effects of intermittent parathyroid hormone administration on bone mineralization density in iliac crest biopsies from patients with osteoporosis: a paired study before and after treatment.J Clin Endocrinol Metab. 88(3):1150-6.

Miyake K., McNeil PL., 2003. Mechanical injury and repair of cells, Crit Care Med 31[Suppl.]:S496 –S501

Miyauchi A, Notoya K, Mikuni-Takagaki Y, Takagi Y, Goto M, Miki Y, Takano-Yamamoto T, Jinnai K, Takahashi K, Kumegawa M, Chihara K, Fujita T., 2000.

Parathyroid hormone-activated volume-sensitive calcium influx pathways in mechanically loaded osteocytes., JBC 275(5):3335-42

Miyauchi A, Notoya K, Takagaki YM, Takagi Y, Goto M, Miki Y, Yamamoto TT, Jinnai K, Takahashi K, Kumegawa M, Chihara K, Fujita T, 2000. Parathyroid hormone-activated volume-sensitive calcium influx pathways in mechanically loaded osteocytes. JBC 275:3335–3342

Miyauchi A., Notoya K., Mikuni-Takagaki Y.,Takagi Y., Goto M., Miki Y., Takano-Yamamoto T., Jinnai K., Takahashi K., Kumegawa M., Chihara K., Fujita T., 2000. Parathyroid Hormone-activated Volume-sensitive Calcium Influx Pathways in Mechanically Loaded Osteocytes. The Journal of Biological Chemistry 275 (5): 3335–3342

Mochizuki H, Hakeda Y, Wakatsuki N, Usui N, Akashi S, Sato T, Tanaka K, Kumegawa M, 1992. Insulin-like growth factor-I supports formation and activation of osteoclasts. Endocrinology 131: 1075–1080

Mohan S, Richman C, Guo R, Amaar Y, Donahue LR, Wergedal J, Baylink DJ., 2003. Insulin-like growth factor regulates peak bone mineral density in mice by both growth hormone dependent and -independent mechanisms. Endocrinology.144(3):929-36.

Moore A, Donahue CJ, Bauer KD, Mather JP ,1998. "Simultaneous measurement of cell cycle and apoptotic cell death". *Methods Cell Biol.* 57: 265–78

Morel G, Chavassieux P, Barenton B, Dubois PM, Meunier PJ, Boivin G ,1993. Evidence for a direct effect of growth hormone on osteoblasts. Cell Tissue Res 273:279–286

Mori, S., Burr, D.B., 1993. Increased intracortical remodeling following fatigue damage. *Bone.* 14(2):103-9.

Mori, S., Harruff, R., Ambrosius, W., Burr, D.B., 1997. Trabecular bone volume and microdamage accumulation in the femoral heads of women with and without femoral neck fractures. *Bone.* 21(6):521-6.

Mosley, J.R., March, B.M., Lynch, J., Lanyon, L.E., 1997. Strain magnitude related changes in whole bone architecture in growing rats. *Bone.* 20(3):191-8.

Mullender, M.G., Huiskes, R., 1997. Osteocytes and bone lining cells: which are the best candidates for mechano-sensors in cancellous bone? *Bone* 20(6):527-32.

Mundy, G. Factors regulating bone resorbing and bone forming cells. Bone remodeling and its disorders 1995, Martin Dunitz Publishers, 39-65.

Murray T.M., Rao L.G, Divieti P., Bringhurst F.R., 2005. Parathyroid Hormone Secretion and Action: Evidence for Discrete Receptors for the Carboxyl-Terminal Region and Related Biological Actions of Carboxyl-Terminal Ligands. Endocrine Reviews 26(1):78–113

Murray TM, Rao LG, Divieti P, Bringhurst FR. 2005. Parathyroid hormone secretion and action: evidence for discrete receptors for the carboxyl-terminal region and related biological actions of carboxyl- terminal ligands. Endocr Rev. 26(1):78-113.

Nagaraja S, Lin ASP, Guldberg RE, 2007. Age-related changes in trabecular bone microdamage initiation. *Bone,* 40, 973-980

Nakashima K, Zhou X, Kunkel G, Zhang Z, Deng JM, Behringer RR, de Crombrugghe B. 2002. The novel zinc finger-containing transcription factor osterix is required for osteoblast differentiation and bone formation.

Nasu M., Sugimoto T., Kaji H., Chihara K., 2000. Estrogen modulates osteoblast proliferation and function regulated by parathyroid hormone in osteoblastic SaOS-2 cells: role of insulin-like growth factor (IGF)-I and IGF-binding protein-5, *Journal of Endocrinology* 167:305–313

Nijweide, P. and Mulder, R., 1986. Identification of osteocytes in osteoblast-like cell cultures using a monoclonal antibody specifically directed against osteocytes. *Histochemistry* 84(4-6):342-7.

Nilsson A, Swolin D, Enerback S, Ohlsson C, 1995. Expression of functional growth hormone receptors in cultured human osteoblast- like cells. J Clin Endocrinol Metab 80:3483–3488

Nilsson O, Marino R, De Luca F, Phillip M, Baron J, 2005. Endocrine regulation of the growth plate. Horm Res 64:157-165.

Nishida S, Yamaguchi A, Tanizawa T, Endo N, Mashiba T, Uchiyama Y, Suda T, Yoshiki S, Takahashi HE, 1994. Increased bone formation by intermittent parathyroid hormone administration is due to the stimulation of proliferation and differentiation of osteoprogenitor cells in bone marrow. Bone. 6:717-23

Nishiyama K, Sugimoto T, Kaji H, Kanatani M, Kobayashi T, Chihara K, 1996. Stimulatory effect of growth hormone on bone resorption and osteoclast differentiation. Endocrinology 137:35–41

Niu T. and Rosen C.J., 2005. The insulin-like growth factor-I gene and osteoporosis: A critical appraisal. Gene 361: 38-56

Noble B., 2003. Bone microdmage and cell apoptosis. European Cells and Materials, 6 :45-6

Noble BS, 2008. The osteocyte lineage, Archives of Biochemistry and Biophysics 473: 106–111.

Noble BS, Peet N, Stevens HY, Brabbs A, Mosley JR, Reilly GC, Reeve J, Skerry TM, Lanyon LE, 2003. Mechanical loading: biphasic osteocyte survival and targeting of osteoclasts for bone destruction in rat cortical bone. Am J Physiol Cell Physiol 284: C934-C943

Noble BS, Reeve J, 2000. At the cutting edge: Osteocyte function, osteocyte death and bone fracture resistance. *Mol Cell Endocrinol.* 159¸7-13

Noble BS, Stevens H, Mosley JR, Pitsillides AA, Reeve J, Lanyon L (1997b) Osteocyte apoptosis and functional strain in bone. JBMR 12: 5

Noble, B., Peet, N., Stevens, H., Brabbs, A., Mosley, J., Reilly, G, Reeve, J., Skerry, T., Lanyon, L., 2003. Mechanical loading: biphasic osteocyte survival and targeting of osteoclasts for bone destruction in rat cortical bone. *Am.J.Physiol.Cell Physiol* 284(4):934-43.

Noble, B., Stevens, H., Reeve, J., Loveridge, N., 1997. Identification of apoptotic changes in osteocytes in normal and pathological human bone. *Bone* 20(3): 273-282.

O'Brien FJ, Hardimann DA, Hazenberg JG, Mercy MV, Mohsin S *et al.*, 2005. The behaviour of microcracks in compact bone. *Eur J Morphol.* 42, 71-79

Offermanns S, Iida-Klein A, Segre GV, Simon MI, 1996. "G alpha q family members couple parathyroid hormone (PTH)/PTH-related peptide and calcitonin receptors to phospholipase C in COS-7 cells". *Mol. Endocrinol.* 10 (5): 566–74.

Ogita M, Rached MT, Dworakowski E, Bilezikian JP, Kousteni S. 2008. Differentiation and Proliferation of Periosteal Osteoblast Progenitors are Differentially Regulated by Estrogens and Intermittent PTH Administration. Endocrinology.

Ohlsson C, Lovstedt K, Holmes PV, Nilsson A, Carlsson L, Tornell J., 1993. Embryonic stem cells express growth hormone receptors: Regulation by retinoic acid. *Endocrinology* 133: 2897–2903

Okazaki Ken, Jingushi Seiya, Ikenoue Takashi, Urabe Ken, Sakai Hiroaki, Iwamoto Yukihide, 2003. Expression of parathyroid hormone-related peptide and insulin-like growth factor I during rat fracture healing. Journal of Orthopaedic Research 21(3): 511-520

Olle G. P. Isaksson, Staffan Eddn, and John-Olov Jansson, 1985. Mode of action of pituitary growth hormone on target cells. Ann. Rev. Physiol. 47:483499

Ono N, Nakashima K, Schipani E, Hayata T, Ezura Y, Soma K, Kronenberg HM, Noda M, 2007. Constitutively active parathyroid hormone receptor signaling in cells in osteoblastic lineage suppresses mechanical unloading-induced bone resorption. JBC 282(35):25509-16

Otto F, Thornell Ap, Crompton T, Denzel A, Gilmour KC, Rosewell IR, Stamp GW, Beddington RS, Mundlos S, Olsen BR, Selby PB, Owen MJ, 1997. Cbfa 1, a candidate gene for cleidocranial dysplasia syndrome, is essential for osteoblast differentiation and bone development. Cell, 89:765-71

Oxlund H., Ejersted C., Andreassen TT., Torring O., Nilsson MH, 1993. Parathyroid hormone (1-34) and (1-84) stimulate cortical bone formation both from periosteum and endosteum.Calcified Tissue International, 53: 394-9

Ozeki, N., Mogi, M., Nakamura, H., Togari, A., 2002. Differential expression of the Fas-Fas ligand system on cytokine-induced apoptotic cell death in mouse osteoblastic cells. *Arch Oral Biol.* 47(7):511-7.

Palokangas H, Mulari M and Vaananen HK, 1997. Endocytic pathway from the basal plasma membrane to the ruffled border membrane in bone-resorbing osteoclasts. J. Cell Sci. 110 (Pt 15):1767-80

Palumbo C, Palazzini S, Marotti G, 1990b. Morphological study of intercellular junctions during osteocyte differentiation. Bone, 11:401-6

Papapoulos, S., 1997. Bisphosphonates: Pharmacology and rationale for their use in the prevention and treatment of glucocorticoid-induced osteoporosis. Glucocorticoids and Bone: the Clinical Problem, Boerhaave Committee for Postgraduate Education of medicine, Leiden University, The Netherlands, 83-92.

Parfitt AM, 1977. The cellular basis of bone turnover and bone loss:a rebuttal of the osteocytic resorption-bone flow theory. Clin. Orthop:236-47

Parfitt AM, Schipani E, Rao DS, Kupin W, Han ZH, Juppner H, 1996. Hypercalcemia due to constitutive activity of the parathyroid hormone (PTH)/PTH-related peptide receptor: comparison with primary hyperparathyroidism. J Clin Endocrinol Metab 81:3584–3588

Parfitt M. 2002. PTH and periosteal bone expansion. JBMR 17:1741-1743

Parfitt, A. M., Drezner, M. K., Glorieux, F. H., Kanis, J. A., Malluche, H., Meunier, P. J., Ott, S. M., and Recker, R. R. 1987. Bone histomorphometry: Standardization of nomenclature, symbols, and units. Report of the ASBMR histomorphometry nomenclature committee. JBMR 2:595– 610;

Parfitt, A., 1976. The actions of parathyroid hormone on bone: relation to bone remodeling and turnover, calcium homeostasis, and metabolic bone disease. Part III of IV parts; PTH and osteoblasts, the relationship between bone turnover and bone loss, and the state of the bones in primary hyperparathyroidism. *Metabolism*. 25(9):1033-69.

Parfitt, A., 1994. Osteonal and hemiosteonal remodelling: the spatial and temporal framework for signal traffic in adult human bone. *J.Cell.Biochem*. 55:273-286.

Parfitt, A., 2002. Targeted and non targeted bone remodeling: Relationship to basic multicellular unit origination and progression. *Bone* 30(1):5-7.

Parfitt, AM., 2001. The bone remodeling compartment: a circulatory function for bone lining cells. *JBMR* .16(9):1583-5.

Park SR, Oreffo RO and Triffitt JT, 1999. Interconversion potential of cloned human marrow adipocytes in vitro. Bone, 24:549-54

Petersen, DN., Tkalcevic, GT., Mansolf, AL., Rivera-Gonzalez, R., Brown, TA., 2000. Identification of osteoblast/osteocyte factor 45 (OF45), a bone-specific cDNA encoding an RGD-containing protein that is highly expressed in osteoblasts and osteocytes. *JBC* 275(46):36172-80.

Philbrick WM, Dreyer BE, Nakchbandi IA, Karaplis AC., 1998. Parathyroid hormone-related protein is required for tooth eruption., Proc Natl Acad Sci U S A., 95(20):11846-51.

Pioszak AA, Xu HE., 2008. Molecular recognition of parathyroid hormone by its G protein-coupled receptor., Proc Natl Acad Sci U S A.105(13):5034-9

Pitsillides, AA., Rawlinson, SC., Suswillo, RF., Bourrin, S., Zaman, G., Lanyon, LE., 1995. Mechanical strain-induced NO production by bone cells: a possible role in adaptive bone (re)modeling? *FASEB J.* 9(15):1614-22.

Plotkin L, Mathov I, Aguirre J, Parfitt A. *et al.*, 2005. Mechanical stimulation prevents osteocyte apoptosis: requirement of integrins, Src kinases, and ERKs. *Am J Physiol.* 289, C633-C643

Plotkin, L., Weintein, R., Parfitt, A., Roberson, P., Manolagas, S., Bellido, T., 1999. Prevention of osteocytes and osteoblast apoptosis by bisphosphonates and calcitonin. *J. Clin.Invest* 104:1363-1374

Poole K, Reeve J, 2005. "Parathyroid hormone - a bone anabolic and catabolic agent." Curr Opin Pharmacol 5 (6): 612-7).

Poole K. E., Reeve J., 2005. Parathyroid hormone- a bone anabolic and catabolic agent, Current opinion in Pharmacology, 5: 1-6

Poole, KE., van Bezooijen, RL., Loveridge, N., Hamersma, H., Papapoulos, SE., Lowik, CW., Reeve, J., 2005. Sclerostin is a delayed secreted product of osteocytes that inhibits bone formation. *FASEB J.* 19(13):1842-4.

Potts JT, Gardella TJ, 2007. Progress, paradox, and potential: parathyroid hormone research over five decades. Ann N Y Acad Sci.:1117:196-208

Power, J., Loveridge, N., Rushton, N., Parker, M. ,Reeve, J., 2002. Osteocyte density in aging subjects is enhanced in bone adjacent to remodeling harvesian systems. *Bone* 30:859-865.

Pradhan, D., Krahling, S., Williamson, P., Schlegel, RA., 1997. Multiple systems for recognition of apoptotic lymphocytes by macrophages. *Mol Biol Cell.* 8(5):767-78.

Prockop, D., 1997. Marrow stromal cells as stem cells for nonhematopoietic tissues. *Science* 276(4): 71-74.

Puzas, J., 1996. Osteoblast-cell biology-lineage and functions. Primer on the metabolic bone diseases and disorders of mineral metabolism, Lippincott-Raven, New York 11-16.

Qin L, Qiu P, Wang L, Li X, Swarthout JT, Soteropoulos P, Tolias P, Partridge NC., 2003. Gene expression profiles and transcription factors involved in parathyroid hormone signaling in osteoblasts revealed by microarray and bioinformatics. JBC 278(22):19723-31

Qiu S, Fyhrie DP, Palnitkar S *et al.* ,2005. The morphological association between microcracks and osteocyte lacunae in human cortical bone. *Bone,* 37, 10-15

Qiu S, Rao DS, Palnitkar S, Parfitt AM, 2002. Age and distance from the surface but not menopause reduce osteocyte density in human cancellous bone. Bone, 31:313-8

Qiu, S., Rao, DS., Fyhrie, DP., Palnitkar, S., Parfitt, AM., 2005. The morphological association between microcracks and osteocyte lacunae in human cortical bone. *Bone* 37:10-15

Ransjo¨ M, Lerner U, Ohlsson C ,1996. Growth hormone inhibits formation of osteoclast-like cells in mouse bone marrow cultures. JBMR 11 [Suppl]:T394

Rao, LG., Murray, TM., Heersche, JN., 1983. Immunohistochemical demonstration of parathyroid hormone binding to specific cell types in fixed rat bone tissue. *Endocrinology*. 113(2):805-10.

Raouf A, Seth A., 2002. Discovery of osteoblast-associated genes using cDNA microarrays. Bone. 30(3):463-71

Rawlinson, SC., Mosley, JR., Suswillo, RF., Pitsillides, AA., Lanyon, LE., 1995. Calvarial and limb bone cells in organ and monolayer culture do not show the same early responses to dynamic mechanical strain. JBMR 10(8):1225-32.

Recker RR, Kimmel DB, Parfitt AM, Davies KM, Keshawartz N and Hinders S, 1988. Static and tetracycline-based bone histomorphometric data from 34 postmenopausal females. JBMR 3:133-44

Reddi, A.H. 2001. Interplay between bone morphogenetic proteins and cognate binding proteins in bone and cartilage development: noggin, chordin and DAN. *Arthritis Res.* 3:1–5.

Reddien, PW., Cameron, S., Horvitz, HR.2001, Phagocytosis promotes programmed cell death in C. elegans. *Nature.* 412(6843):198-202.

Reijnders CM, Bravenboer N, Holzmann PJ, Bhoelan F, Blankenstein MA, Lips P, 2007. In vivo mechanical loading modulates insulin-like growth factor binding protein-2 gene expression in rat osteocytes. Calcif Tissue Int. 80(2):137-43

Reilly GC, Currey JD, 2000. The effects of damage and microcracking on the impact strength of bone. J Biomech 33: 337-43

Rittweger J., 2007. What is new in neuro-musculoskeletal interactions: mechanotransduction, microdamage and repair? JMNI 7(2):191-3).

Robling AG, Bellido T, Turner CH, 2006. Mechanical stimulation in vivo reduces osteocyte expression of sclerostin. JMNI 6:354

Robling AG., Niziolek PJ., Baldridge, LA. Condon KW., Allen MR., Alam I., Mantila SM., Gluhak-Heinrich J., Bellido TM., Harris SE.,. Turner CH. 2008. Mechanical Stimulation of Bone *in Vivo* Reduces Osteocyte Expression of Sost/Sclerostin. JBC 283 (9): 5866–5875

Robling, AG., Burr, DB., Turner, CH., 2000. Partitioning a daily mechanical stimulus into discrete loading bouts improves the osteogenic response to loading. *JBMR* 15(8):1596-602.

Rodan, G., 1992. Introduction to bone biology. *Bone*13 (Suppl 1):S3-6.

Rodan, G., Martin, J., 2000 Therapeutic approaches to bone diseases. *Science* 289:5484.

Rodan, GA., 1998. Control of bone formation and resorption: biological and clinical perspective. *JCB Suppl.*30-31:55-61.

Rogers, MJ., Frith, JC., Luckman, SP., Coxon, FP., Benford, HL., Monkkonen, J., Auriola, S., Chilton, KM., Russell, RG., 1999. Molecular mechanisms of action of bisphosphonates. *Bone.* 24(5 Suppl): 73S-79S.

Rosen C. J., 2004. What's new with PTH in osteoporosis: where are we and where are we headed? Trends in Endocrinology and Metabolism, 15:5

Rosingh, GE., James, J., 1968. Changes in cell nuclei of the ischaemic femoral head. *Calcif Tissue Res.* Suppl:38.

Roth BL., Poot M., Yue ST., Millard PJ., 1997. Bacterial viability and antibiotic susceptibility testing with SYTOX green nucleic acid stain. Appl Environ Microbiol. 63(6): 2421–2431

Rouleau MF., Mitchell J., Goltzman D., 1988. In vivo distribution of parathyroid hormone receptors in bone: evidence that a predominant osseous target cell is not the mature osteoblast, Endocrinology, 123:187-91

Rubin, CT., Lanyon, LE. Kappa Delta Award paper. 1987. Osteoregulatory nature of mechanical stimuli: function as a determinant for adaptive remodeling in bone. *J Orthop Res.* 5(2):300-10.

Rubin, CT., Lanyon, LE., 1984. Regulation of bone formation by applied dynamic loads. *J Bone Joint Surg Am.* 66(3):397-402.

Rubinacci A, Villa I, Dindi benelli F, Borgo E, Ferretti M, Palumbo C, Marotti G, 1998. Osteocyte-bone lining cell system at the origin of steady ionic current in damaged amphibian bone. Calcif. Tissue Int., 63:331-9

Russell RG, Espina B, Hulley P., 2006. Bone biology and the pathogenesis of osteoporosis. Curr Opin Rheumatol. Suppl 1:S3-10

Saggese G, Baroncelli GI, Federico G, Bertelloni S, 1995. Effects of growth hormone on phosphocalcium homeostasis and bone metabolism. Horm Res 44:55–63

Sakai A, Sakata T, Ikeda S, Uchida S, Okazaki R, Norimura T, Hori M, Nakamura T., 1999. Intermittent administration of human parathyroid hormone(1–34) prevents immobilization-related bone loss by regulating bone marrow capacity for bone cells in ddY mice. JBMR 14:1691–1699

Salmon W., Daughaday W. A hormonal controled serum factor which stimulates sulfate incorporation by cartilige in vitro. *J Lab Clin Med* 49:825, 1957

Sanders EJ, Harvey S., 2008. Peptide hormones as developmental growth and differentiation factors. Dev Dyn. 237(6):1537-52

Sass D., Jerome C., Bowman A., Bennett-Cain A, Ginn T., LeRoith D, Epstein S., 1997. Short-term effects of growth hormone and insulin-like growth factor I on cancellous bone formation in Rhesus Macaque monkeys. J Clin Endocrinol Metab 82:1202–1209

Savill J, Fadok V, 2000. Corpse clearance defines the meaning of cell death. *Nature.* 407, 784-788)

Savill, J., 1997. Recognition and phagocytosis of cells undergoing apoptosis. *Br Med Bull.* 53(3):491-508.

Sawakami, K., Robling, A. G., Ai, M., Pitner, N. D., Liu, D., Warden, S. J., Li, J., Maye, P., Rowe, D. W., Duncan, R. L., Warman, M. L., and Turner, C. H., 2006. The Wnt co-receptor LRP5 is essential for skeletal mechanotransduction but not for the anabolic bone response to parathyroid hormone treatment *JBC* 281, 23698–23711

Scheven B., Hamilton N., Fakkeldij T., Duursma S., 1991. Effects of recombinant human insulin-like growth factor I and II (IGF-I/-II) and growth hormone (GH) on the growth of normal adult human osteoblast-like cells and human osteogenic sarcoma cells. Growth Regul 1:160–167

Schiller P., D'Ippolito G., Brambilla R., Roos B., Howard G., 2001. Inhibition of gap-junctional communication induces the trans-differentiation of osteoblast to an adipocyte phenotype in vitro. JBC 276:14133-8

Schiller P., Mehta P., Roos B., Howard G., 1992. Hormonal regulation of intercellular communication:parathyroid hormone increase connexin 43 gene expression and gap-junctional communication in osteoblastic cells. Molecular Endrocrinology, 6: 1433-40.

Schipani E, Langman CB, Parfitt AM, Jensen GS, Kikuchi S, Kooh SW, Cole WG, Juppner H, 1996. Constitutively activated receptors for parathyroid hormone and parathyroid hormone-related peptide in Jansen's metaphyseal chondrodysplasia. N Engl J Med 335:708–714

Schulze, E., Witt, M., Kasper, M., Lowik, C.W., Funk, R.H., 1999. Immunohistochemical investigations on the differentiation marker protein E11 in rat calvaria, calvaria cell culture and the osteoblastic cell line ROS 17/2.8. *Histochem Cell Biol.* 111(1):61-9.

Sekiya H, Mikuni-Takagaki Y, Kondoh T, Seto K, 1999. Synergistic effect of PTH on the mechanical responses of human alveolar osteocytes. Biochem Biophys Res Commun 264:719–723

Selim AA., Mahon M., Juppner H., Bringhurst FR., Divieti P., 2006. Role of calcium channels in carboxyl-terminal parathyroid hormone receptor signaling. *Am J Physiol Cell Physiol* 291: C114–C121

Shibutani M, Uneyama C, Miyazaki K, Toyoda K, Hirose M., 2000. Methacarn fixation: a novel tool for analysis of gene expressions in paraffinembedded tissue specimens. Lab Invest 80:199–208.

Shikha Gaur, Mary E. Morton, G. Peter Frick, H. Maurice Goodman, 1998. Growth hormone regulates the distribution of L-type calcium channels in rat adipocyte membranes. *Am J Physiol Cell Physiol* 275:505-514

Shimizu, H., Sakamoto, M., Sakamoto, S., 1990. Bone resorption by isolated osteoclasts in living versus devitalized bone: differences in mode and extent and the effects of human recombinant tissue inhibitor of metalloproteinases. *JBMR* 5(4):411-8.

Sikavitsas, V., Temenoff, J., Mikos, A., 2001. Biomaterials and bone mechanotransduction. *Biomaterials* 22(19): 2581-2593.

Silvestrini G, Ballanti P, Leopizzi M, Sebastiani M, Berni S, Di Vito M, Bonucci E., 2007. Effects of intermittent parathyroid hormone (PTH) administration on SOST mRNA and protein in rat bone. J Mol Histol. 38(4):261-9

Silvestrini, G., Ballanti, P., Patacchioli, F.R., Mocetti, P., Di Grezia, R., Wedard, B.M., Angelucci, L., Bonucci, E., 2000. Evaluation of apoptosis and the glucocorticoid receptor

in the cartilage growth plate and metaphyseal bone cells of rats after high-dose treatment with corticosterone. *Bone* 26(1):33-42.

Skerry TM, Bitensky L, Chayen J, Lanyon LE. 1989. Early strain-related changes in enzyme activity in osteocytes following bone loading in vivo. JBMR 4(5):783-8.

Slootweg M., Most W., van Beek E., Schot L., Papapoulos S., Lowik C., 1992. Osteoclast formation together with interleukin-6 production in mouse long bones is increased by insulin-like growth factor-I. J Endocrinol 132:433–438

Slootweg M., van Buul-Offers S., Herrmann-Erlee M., van der Meer J., Duursma S., 1988. Growth hormone is mitogenic for fetalmouse osteoblasts but not for undifferentiated bone cells. J Endocrinol 116:R11–R13

Slootweg MC ,1993. Growth hormone and bone. Horm Metab Res 25:335–343

Slootweg MC, Salles JP, Ohlsson C, de Vries CP, Engelbregt MJ, Netelenbos JC., 1996. Growth hormone binds to a single high affinity receptor site on mouse osteoblasts: modulation by retinoic acid and cell differentiation. J Endocrinol 150:465–472

Slootweg MC, van Buul-Offers SC, Herrmann-Erlee MP, Duursma SA., 1988. Direct stimulatory effect of growth hormone onDNA synthesis of fetal chicken osteoblasts in culture. Acta Endocrinol (Copenh) 118:294–300

Sommerfeldt D. and Rubin C., 2001. Biology of bone and how it orchestrates the form and function of the skeleton. Eur Spine J 10:S86–S95

Srinivasan M., Sedmak D., Jewell S., 2002. Effect of fixatives and tissue processing on the content and integrity of nucleic acids. Am. J. Pathol. 161:1961-71

Srinivasan M., Sedmark D., Jewell S., 2002. Effect of fixatives and tissue processing on the content and integrity of nucleic acids, *Am. J. Pathol.* 161:1961–1971

Stanislaus D., Yang X., Liand JD., Wolfe J., Cain RL., Onyia JE., Falla N., Marder P., Bidwell JP., Queener SW., Hock JM., 2000. In vivo regulation of apoptosis in metaphyseal trabecular bone of young rats by synthetic human parathyroid hormone (1-34) fragment. Bone, 27:209-18

Stepan JJ, Alenfeld F, Boivin G, Feyen JH, Lakatos P, 2003. Mechanisms of action of antiresorptive therapies of postmenopausal osteoporosis. Endocrine Regulations 37(4):225-38.

Stracke H, Schulz A, Moeller D, Rossol S, Schatz H ,1984. Effect of growth hormone on osteoblasts and demonstration of somatomedin-C/IGF I in bone organ culture. Acta Endocrinol (Copenh) 107:16–24

Strewler GJ, 2000. The physiology of parathyroid hormone-related protein. New Eng J Med 342:177-185

Strewler, G.J., 2001. Local and systemic control of the osteoblast. *J Clin Invest.* 107(3):271-2.

Stryer, L. Biochemistry. W.H. Freeman and Company, New York, 1995, 497-498.

Suda T., Takahashi N., Udagawa N., Jimi E., Gillepsie MT., Martin TJ., 1999. Modulation of osteoclast differentiation and function by the new members of the tumor necrosi factor receptor and ligand families, Endocrinolgy Reviews, 20:345-57.

Sugimoto, M., Takahashi, S., Kotoura, Y., Shibamoto, Y., Takahashi, M., Abe, M., Ishizaki, K., Yamamuro, T., 1993. Osteocyte viability after high-dose irradiation in the rabbit. *Clin Orthop Relat Res.* 297:247-52.

Sutherland, M., Geoghegan, J., Yu C., Turcott E., Skonier J., Winkler D., Latham J.A., 2004. Sclerostin promotes the apoptosis of human osteoblastic cells: a novel regulation of bone formation.*Bone.* 35(4):828-35.

Suzuki A, Sekiguchi S, Asano S, Itoh M., 2008. Pharmacological topics of bone metabolism: recent advances in pharmacological management of osteoporosis. J Pharmacol Sci.106(4):530-5).

Swolin D, Ohlsson C, 1996. Growth hormone increases interleukin- 6 produced by human osteoblast-like cells. J Clin Endocrinol Metab 81:4329–4333

Takai E; Mauck RL., Hung CT., Guo XE , 2004. Osteocyte viability and regulation of osteoblast function in a 3D trabecular bone explant under dynamic hydrostatic pressure. *JBMR* 19:1403–1410.

Tam CS., Heersche JN., Murray TM., Parsons JA..,1982, Parathyroid hormone stimulates the bone apposition rate independently of its resorptive action: differential effects of intermittent and continuous administration. *Endocrinology* 110 :506–512.

Tan SD., Bakker AD., Semeins CM., Kuijpers-Jagtman AM., Klein-Nulend J., 2008. Inhibition of osteocyte apoptosis by fluid flow is mediated by nitric oxide. Biochem Biophys Res Commun. 369(4):1150-4.

Teitelbaum, S.L., 2000. Bone Resorption by Osteoclasts. *Science* 289: 1504-1508.

ten Dijke P, Krause C, de Gorter DJ, Löwik CW, van Bezooijen RL., 2008. Osteocyte-derived sclerostin inhibits bone formation: its role in bone morphogenetic protein and Wnt signaling. J Bone Joint Surg Am. 90 Suppl 1:31-5

Terasaki M, Miyake K, McNeil PL, 1997. Large plasma membrane disruptions are rapidly resealed by calcium dependent vesicle-vesicle fusion events. *JCB* 139, 63-74

Teti A., Rizzoli R., Zambonin-Zallone A., 1991. Parathyroid hormone binding to cultured avian osteoclasts, Biochem. Biophys. Commun. 174:1217-22

Thijssen J, 2001. Hormones and ageing. Maturitas, 38(1): 3-31

Tisserat, B. and Manthey, J.A., 1996. *In Vitro* sterile hydroponic culture to study iron chlorosis. *Journal of Plant Nutrition*. 19, (1): 129-143.

Tomkinson A, Reeve J, Shaw RW, Noble BS. 1997. The death of osteocytes via apoptosis accompanies estrogen withdrawal in human bone. *J Clin Endocrinol Metab.*82:3128–3135.,

Tomkinson, A., Gevers, E., Wit, J., Reeve, J., Noble, BS, 1998. The role of estrogen in the conrtol of rat osteocyte apoptosis. *JBMR* 13(8):1243-1250.

Turner RT, Evans GL, Cavolina JM, et al. 1998. Programmed administration of parathyroid hormone increases bone formation and reduces bone loss in hindlimb-unloaded ovariectomized rats. Endocrinology 139:4086–4091.

Turner, C. Editorial: Functional determinants of bone structure: Beyond Wolff's law of bone transformation. Bone 1992, 13: 403-409.

Ueland T. 2004. Bone metabolism in relation to alterations in systemic growth hormone. Growth Hormone & IGF Research 14: 404–417

Usdin TB, Bonner TI, Hoare SR, 2002. The parathyroid hormone 2 (PTH2) receptor. Recept. Channels 8 (3-4): 211–8.

Usdin TB, Gruber C, Bonner TI., 1995. Identification and functional expression of a receptor selectively recognizing parathyroid hormone, the PTH2 receptor.

Väänänen HK, Laitala-Leinonen T., 2008. Osteoclast lineage and function. Arch Biochem Biophys. 473(2):132-8

Väänänen HK., Zhao H., Mulari M., Halleen JM., 2000. The cell biology of osteoclast function. Journal of Cell Science 113, 377-381

van Bezooijen RL, Svensson JP, Eefting D, Visser A, van der Horst G, Karperien M, Quax PH, Vrieling H, Papapoulos SE, ten Dijke P, Löwik CW., 2007. Wnt but not BMP signaling is involved in the inhibitory action of sclerostin on BMP-stimulated bone formation. JBMR 22:19-28.

Van Bezooijen RL, ten Dijke P, Papapoulos SE, Lo¨wik CWGM , 2005. *SOST/* sclerostin, an osteocyte-derived negative regulator of bone formation. Cytokine Growth Factor Rev 16:319–327

Van Bezooijen RL, ten Dijke P, Papapoulos SE, Lowik CW, 2005. SOST/sclerostin, an osteocyte-derived negative regulator of bone formation. Cytokine Growth Factor Rev 16:319–327

van Bezooijen, RL., Papapoulos, SE., Lowik, CW., 2005. Bone morphogenetic proteins and their antagonists: the sclerostin paradigm. *J Endocrinol Invest.* 28(8 Suppl):15-7.

van Bezooijen, RL., Roelen, BA., Visser, A., van der Wee-Pals L., de Wilt, E., Karperien, M., Hamersma, H., Papapoulos, SE., ten Dijke, P., Lowik. CW., 2004. Sclerostin is an osteocyte-expressed negative regulator of bone formation, but not a classical BMP antagonist. *J Exp Med.* 6:805-14.

van der Plas A., Aarden EM, Feijen JH., de Boer AH., Wiltink A., Alblas MJ., de Leij L., Nijweide PJ., 1994. Characteristics and properties of osteocytes in culture, JBMR 9:1697-704

VanHouten J., Dann P., McGeoch G., Brown E., Krapcho K., Neville M., Wysolmerski J., 2004. The calcium-sensing receptor regulates mammary gland parathyroid hormone–related protein production and calcium transport. Clin Invest., 113(4): 598–608.

Veldhuis JD, Bowers CY, 2003. Human GH pulsatility: an ensemble property regulated by age and gender. J Endocrinol Invest 26:799-813

Verborgt O, Gibson GJ, Schaffler MB, 2000. Loss of osteocyte integrity in association with microdamage and bone remodeling after fatigue *in vivo*. JBMR 15: 60-67

Verleysen, H., Samyn, G., Van Bockstaele, E., Debergh, P., 2004. Evaluation of analytical techniques to predict viability after cryopreservation. *Plan Cell, Tissue and Organ Culture* 77 (1): 11-21

Waldorff EI, Goldstein SA, McCreadie BR., 2007. Age-dependent microdamage removal following mechanically induced microdamage in trabecular bone in vivo. Bone.40(2):425-32

Watanabe, Y., Kawai, K., Hirohata, K., 1989. Histopathology of femoral head osteonecrosis in rheumatoid arthritis: the relationship between steroid therapy and lipid degeneration in the osteocyte. *Rheumatol Int.* 9(1):25-31.

Wei S, Tanaka H, Kubo T, Ono T, Kanzaki S, Seino Y, 1997. Growth hormone increases serum 1,25-dihydroxyvitamin D levels and decreases 24,25-dihydroxyvitamin D levels in children with growth hormone deficiency. Eur J Endocrinol 136:45–51

Weiner, S. and Wagner, H., 1998. The material bone: Structure-mechanical function relations. Annu.Rev.Mater.Sci. 28: 271-298.

Weiner, S., Traub, W., Wagner, H.D. 1999. Lamellar bone: structure-function relations. *J Struct Biol.* 126(3):241-55.

Weinstein RS, Nicholas RW, Manolagas SC. 2005. Apoptosis of osteocytes in glucocorticoid-induced osteonecrosis of the hip. *J Clin Endocrinol Metab.* 85:2907–2912

Weinstein, R., Jilka, R., Parfitt, A., Manolagas, S. 1998. Inhibition of osteoblastogenesis and promotion of apoptosis of osteoblasts and osteocytes by glucocorticoids. *J.Clin.Invest* 102(2): 274-282.

Westbroek, I., de Rooij, K., Nijweibe, P. 2002. Osteocyte-specific monoclonal antibody mAb OB7.3 is directed against Phex protein. *JBMR* 17 (5): 845-853.

Wetterwald, A., Hoffstetter, W., Cecchini, M.G., Lanske, B., Wagner, C., Fleisch, H., Atkinson, M. 1996. Characterization and cloning of the E11 antigen, a marker expressed by rat osteoblasts and osteocytes. *Bone.* 18(2):

Whitfield JF, 2006. Osteoporosis-treating parathyroid hormone peptides: What are they? What do they do? How might they do it? Current Opinion in Investigational Drugs 7(4):349-359

Wilmiams C., Ponten F., Moberg C., Soderkvist P., Uhlen M., Ponten J.et al. 1999. A high frequency of sequence alterations is due to formalin fixation or archival specimens. Am. J. Pathol. 155: 1476-71.

Winter L., Walboomers X., Bumgardner J., Jansen J., 2003. Intermittent versus continuous stretching effects on osteoblast-like cells *in vitro,* J Biomed Mater Res 67A: 1269–1275

Wiren KM, Toombs AR, Semirale AA, Zhang X. 2006. Osteoblast and osteocyte apoptosis associated with androgen action in bone: requirement of increased Bax/Bcl-2 ratio. *Bone* 38:637–651

Wolff J. Das gasetz der transformation der knochen. Berlin, 1892, In: Hirchwald A, editor (An English translation of this monograph has been published by Springer-Verlag in 1986)

Wong MS, Tembe VA, Favus MJ., 2000. Insulin-like growth factor-I stimulates renal 1, 25-dihydroxycholecalciferol synthesis in old rats fed a low calcium diet. J Nutr 130:1147–52.

Wong SY, Evans RA, Needs C, Dunstan CR, Hills E, Garvan J, 1987. The pathogenesis of osteoarthritis of the hip. Evidence for primary osteocyte death. Clin Orthop Relat Res : 305-12.

Wronski TJ, Pun S, Liang H. 1999. Effects of age, estrogen depletion, and parathyroid hormone treatment on vertebral cancellous wall width in female rats. Bone 25:465– 468.

Wysolmerski JJ, Philbrick WM, Dunbar ME, Lanske B, Kronenberg H, Broadus AE.,1998. Rescue of the parathyroid hormone-related protein knockout mouse demonstrates that parathyroid hormone-related protein is essential for mammary gland development. Development.125(7):1285-94

Xiang CC, Kozhich OA, Chen M, Inman JM, Phan QN, Chen Y, Brownstein MJ. 2002. Amine-modified random primers to label probes for DNA microarrays. *Nat Biotechnol.* 20:738–742

Xing L and Boyce BF, 2005. Regulation of apoptosis in osteoclasts and osteoblastic cells. Biochem. Biophys. Res. Commun, 328:709-20

Yasuda H., Shima N., Nakagawa N., yamaguchi K., Kinosaki M., Mochizuki S., Tomoyasu A., Yano K., Goto M., Murakami A., Tsuda E., Morigana T., Higashio K., Udagawa n., Takahashi N., Suda T. 1998b. Osteoclast differentiation factor is a ligand for osteoprotegerin/osteoclastogenesis-inhibitory factor and is identical to TRANCE/RANKL., Pro. Natl., Acad. Sci. U S A, 95:3597-602

Yellowley, CE., Li, Z., Zhou, Z., Jacobs, CR., Donahue, HJ. 2000. Functional gap junctions between osteocytic and osteoblastic cells. *JBMR* 15(2):209-17.

Yoshizato H, Fujikawa T, Soya H, Tanaka M, Nakashima K. 1998. The growth hormone (GH) gene is expressed in the lateral hypothalamus: Enhancement by GH-releasing hormone and repression by restraint stress. *Endocrinology* 139:2545–2551

Zaman, G., Suswillo, RF., Cheng, MZ., Tavares, IA., Lanyon, LE. 1997. Early responses to dynamic strain change and prostaglandins in bone-derived cells in culture. *JBMR* 12:769-777

Zar, J. Biostatistical Analysis. Prentice-Hall Int. Editions, Second Edition, 1984

Zhao G, Monier-Faugere MC, Langub MC, Geng Z, Nakayama T, Pike JW, Chernausek SD, Rosen CJ, Donahue LR, Malluche HH, Fagin JA, Clemens TL. 2000. Targeted overexpression of insulin-like growth factor I to osteoblasts of transgenic mice: increased trabecular bone volume without increased osteoblast proliferation. Endocrinology 141(7):2674-82

Zhou Y, Xu BC, Maheshwari HG, He L, Reed M, Lozykowski M, Okada S, Cataldo L, Coschigamo K, Wagner TE, Baumann G, Kopchick JJ, 1997. A mammalian model for Laron syndrome produced by targeted disruption of the mouse growth hormone receptor/binding protein gene (theLaron mouse). *Proc Natl Acad Sci USA* 94:13215–13220

APPENDIX 1

APPENDIX 1

Gene Symbol	*Gene Title*
Irf6_predicted	interferon regulatory factor 6 (predicted)
Pde8b	Phosphodiesterase 8B
---	Transcribed locus
---	Transcribed locus
Pole2_predicted	Polymerase (DNA directed), epsilon 2 (p59 subunit) (predicted)
---	---
RGD1311934_predicted	similar to RIKEN cDNA 1810036H07 (predicted)
---	Transcribed locus
---	Transcribed locus
---	Transcribed locus
---	Transcribed locus
---	Transcribed locus
Atp6v0a2_predicted	ATPase, H+ transporting, lysosomal V0 subunit a isoform 2 (predicted)
Lamc2	lamimin, gamma 2
RGD1566014_predicted	Similar to Factor VIII associated protein (predicted)
Pex11a	peroxisomal biogenesis factor 11A /// peroxisomal biogenesis factor 11A
Vps54	Vacuolar protein sorting 54 (yeast)
MGC94464	similar to RIKEN cDNA 2500002L14; EST C77350
Lrdd_predicted	leucine-rich and death domain containing (predicted)
---	---
Lsm16_predicted	LSM16 homolog (EDC3, S. cerevisiae) (predicted)
Slc16a6	Solute carrier family 16 (monocarboxylic acid transporters), member 6
Rcc2_predicted	regulator of chromosome condensation 2 (predicted)
RGD1305441	similar to RIKEN cDNA 5730453I16
Whsc1l1_predicted	Wolf-Hirschhorn syndrome candidate 1-like 1 (predicted)
Slc22a5	solute carrier family 22 (organic cation transporter), member 5
---	---
---	---
Panx1	Pannexin 1
Sox6	SRY-box containing gene 6
Fuca2	fucosidase, alpha-L- 2, plasma
Tff1	trefoil factor 1
Dtnbp1	distrobrevin binding protein 1
---	CDNA clone IMAGE:7380769
Zfp91	zinc finger protein 91
RGD1561261_predicted	similar to Zinc finger protein ZIC 3 (Zinc finger protein of the cerebellum 3) (predicted)
RGD1309034	similar to Expressed sequence AW060207
LOC312777	Similar to TEL protein
---	Transcribed locus
---	Transcribed locus

Hgs	HGF-regulated tyrosine kinase substrate
Pgm3_predicted	phosphoglucomutase 3 (predicted)
Rhog	Ras homolog gene family, member G
Luc7l2_predicted	LUC7-like 2 (S. cerevisiae) (predicted)
RGD1306704_predicted /// RGD1561485_predicted	Hypothetical LOC295483 (predicted) /// Similar to Rho GTPase activating protein 20 (predicted)
---	Transcribed locus, strongly similar to NP_075738.1 yippee-like 1 [Mus musculus] /// Transcribed locus, strongly similar to NP_075738.1 yippee-like 1 [Mus musculus]
LOC498662	Similar to RIKEN cDNA 2610019F03
RGD1310433_predicted	similar to mKIAA1757 protein (predicted)
RGD1311595	similar to KIAA2026 protein
Birc3	baculoviral IAP repeat-containing 3 /// baculoviral IAP repeat-containing 3
Dock5_predicted	dedicator of cytokinesis 5 (predicted)
Rgs14	regulator of G-protein signaling 14
---	Transcribed locus, strongly similar to XP_574462.1 PREDICTED: similar to hypothetical protein C230069C04 [Rattus norvegicus]
Tbc1d10a	TBC1 domain family, member 10a
---	Transcribed locus
Srrm1_predicted	serine/arginine repetitive matrix 1 (predicted)
Chd2_predicted	chromodomain helicase DNA binding protein 2 (predicted)
---	Transcribed locus
---	Transcribed locus
---	Transcribed locus, strongly similar to NP_032322.1 heat shock factor 1 [Mus musculus]
RGD1563803_predicted	Similar to Lmnb2 protein (predicted)
RGD1308876_predicted	similar to 2610027C15Rik protein (predicted)
Pole4_predicted	polymerase (DNA-directed), epsilon 4 (p12 subunit) (predicted)
---	Transcribed locus
Akt1	Thymoma viral proto-oncogene 1
Aurkaip1	aurora kinase A interacting protein 1
Senp6_predicted	SUMO/sentrin specific peptidase 6 (predicted)
Steap3	STEAP family member 3 /// STEAP family member 3
Csnk1a1	Casein kinase 1, alpha 1
Ubc	ubiquitin C /// ubiquitin C
RGD1311678	Similar to 4921517L17Rik protein
Rhoa	ras homolog gene family, member A /// ras homolog gene family, member A
LOC678860 /// LOC690109	similar to 3-oxoacid CoA transferase 1 /// similar to 3-oxoacid CoA transferase 1
B2m	Beta-2 microglobulin
---	Transcribed locus
Gatad2a	GATA zinc finger domain containing 2A
LOC498022	similar to Cd300D antigen
---	Transcribed locus
LOC684800	similar to stromal membrane-associated protein 1
Pomgnt1	protein O-linked mannose beta1,2-N-

	acetylglucosaminyltransferase
Rps15	ribosomal protein S15
Rbm18_predicted	RNA binding motif protein 18 (predicted)
Impa1	Inositol (myo)-1(or 4)-monophosphatase 1
Glud1	glutamate dehydrogenase 1
Commd3	COMM domain containing 3
Rps2 /// RGD1559516_predicted /// LOC501171 /// LOC682718 /// LOC688473	ribosomal protein S2 /// similar to ribosomal protein S2 (predicted) /// similar to 40S ribosomal protein S2 /// similar to 40S ribosomal protein S2 /// similar to 40S ribosomal protein S2
Uqcrh	ubiquinol-cytochrome c reductase hinge protein /// ubiquinol-cytochrome c reductase hinge protein
Gabarap	gamma-aminobutyric acid receptor associated protein
---	Transcribed locus
Src	Rous sarcoma oncogene
---	Transcribed locus
RGD1563268_predicted	similar to Probable serine/threonine-protein kinase KIAA1811 (predicted)
---	Transcribed locus
Psenen	presenilin enhancer 2 homolog (C. elegans)
---	---
Alg3	Asparagine-linked glycosylation 3 homolog (yeast, alpha-1,3-mannosyltransferase)
---	Transcribed locus, strongly similar to XP_215477.3 PREDICTED: similar to RIKEN cDNA 1500031M22 [Rattus norvegicus]
RGD1561961_predicted	Similar to IQ motif and WD repeats 1 (predicted)
Ppfia1_predicted	protein tyrosine phosphatase, receptor type, f polypeptide (PTPRF), interacting protein, alpha 1 (predicted)
Lrp1	low density lipoprotein receptor-related protein 1 /// low density lipoprotein receptor-related protein 1
Pfn1	profilin 1
LOC361420	similar to TAFI95
Spg21	spastic paraplegia 21 homolog (human)
LOC317312 /// LOC686087	similar to RIKEN cDNA 1810018L05 /// similar to motile sperm domain containing 1
RGD1565966_predicted	Similar to male sterility domain containing 1 (predicted)
Ralb	v-ral simian leukemia viral oncogene homolog B
Cd59	CD59 antigen
Slc38a2	solute carrier family 38, member 2
---	---
Nfe2l2	nuclear factor, erythroid derived 2, like 2 /// nuclear factor, erythroid derived 2, like 2
---	---
Ei24	etoposide induced 2.4 mRNA
---	Transcribed locus
RGD1309450_predicted	similar to KIAA2010 protein (predicted)
Fcgr3	Fc receptor, IgG, low affinity III /// Transcribed locus, weakly similar to XP_421392.1 PREDICTED: similar to Protein phosphatase 1, regulatory (inhibitor) subunit 13B [Gallus gallus]
Eif3s6	eukaryotic translation initiation factor 3, subunit 6

Eef2	eukaryotic translation elongation factor 2 /// eukaryotic translation elongation factor 2
Sacm1l	SAC1 (suppressor of actin mutations 1, homolog)-like (S. cerevisiae)
---	Transcribed locus, moderately similar to XP_580018.1 PREDICTED: hypothetical protein XP_580018 [Rattus norvegicus]
RGD1305823	similar to RIKEN cDNA 0610037P05
Rpl23	ribosomal protein L23
LOC680227	LRRGT00193
---	Transcribed locus, strongly similar to NP_695208.1 serine/threonine protein kinase 6 [Rattus norvegicus]
LOC314964	similar to PHD finger protein 20-like 1 isoform 1
Smarca4	SWI/SNF related, matrix associated, actin dependent regulator of chromatin, subfamily a, member 4
Stxbp3	syntaxin binding protein 3
Rpl19	ribosomal protein L19
Bicd2	bicaudal D homolog 2 (Drosophila)
Hrmt1l3	heterogeneous nuclear ribonucleoprotein methyltransferase-like 3 (S. cerevisiae) /// heterogeneous nuclear ribonucleoprotein methyltransferase-like 3 (S. cerevisiae)
Cfl1	cofilin 1, non-muscle
Sod1	superoxide dismutase 1 /// superoxide dismutase 1
Ppp1r2	protein phosphatase 1, regulatory (inhibitor) subunit 2
RGD1562933_predicted /// LOC690789	similar to product is unknown~seizure-related gene (predicted) /// similar to Ornithine decarboxylase antizyme 2 (ODC-Az 2) (AZ2)
Coro1b	coronin, actin-binding protein, 1B
Pfdn1_predicted	prefoldin 1 (predicted)
Rpl28	ribosomal protein L28
Gng11	guanine nucleotide binding protein (G protein), gamma 11
RGD1309995_predicted	similar to CG13957-PA (predicted)
Arbp	acidic ribosomal phosphoprotein P0
Zfp592_predicted	zinc finger protein 592 (predicted)
---	Transcribed locus
Itgb3bp	integrin beta 3 binding protein (beta3-endonexin)
Pdlim1	PDZ and LIM domain 1 (elfin)
Rpl26	ribosomal protein L26
Sdhd	succinate dehydrogenase complex, subunit D, integral membrane protein /// succinate dehydrogenase complex, subunit D, integral membrane protein
Arhgef3_predicted	Rho guanine nucleotide exchange factor (GEF) 3 (predicted)
Rab28	RAB28, member RAS oncogene family
Rps13 /// LOC683961 /// LOC684988	ribosomal protein S13 /// similar to ribosomal protein S13 /// similar to ribosomal protein S13
Dnase1l1	deoxyribonuclease 1-like 1
RGD1565591_predicted	similar to Ski protein (predicted)
Uba52	ubiquitin A-52 residue ribosomal protein fusion product 1
Cdc23	CDC23 (cell division cycle 23, yeast, homolog)
Ptprf	protein tyrosine phosphatase, receptor type, F
Med31_predicted	mediator of RNA polymerase II transcription, subunit 31

	homolog (yeast) (predicted)
Adh4 /// Gtf2h4	Alcohol dehydrogenase 4 (class II), pi polypeptide /// General transcription factor II H, polypeptide 4
Pdha1 /// LOC685778 /// LOC686201	pyruvate dehydrogenase E1 alpha 1 /// similar to Pyruvate dehydrogenase E1 component alpha subunit, somatic form, mitochondrial precursor (PDHE1-A type I) /// similar to Pyruvate dehydrogenase E1 component alpha subunit, somatic form, mitochondrial precursor (PDHE1-A type I)
RGD1305453	similar to RIKEN cDNA 2410166I05
Rpl7a_predicted	ribosomal protein L7a (predicted)
RGD1307729_predicted	similar to KIAA0853 protein (predicted)
Ca3	carbonic anhydrase 3 /// carbonic anhydrase 3
---	Transcribed locus
Calm1	calmodulin 1 /// calmodulin 1
Sui1-rs1_predicted /// RGD1559924_predicted /// RGD1560994_predicted /// LOC678808 /// LOC686076 /// LOC691877	suppressor of initiator codon mutations, related sequence 1 (S. cerevisiae) (predicted) /// similar to Eukaryotic translation initiation factor 1 (eIF1) (predicted) /// similar to suppressor of initiator codon mutations, related sequence 1 (predicted) /// similar to suppressor of initiator codon mutations, related sequence 1 /// similar to suppressor of initiator codon mutations, related sequence 1 /// similar to suppressor of initiator codon mutations, related sequence 1
Irx3_predicted	Iroquois related homeobox 3 (Drosophila) (predicted)
RGD1304726	similar to RIKEN cDNA 6330509G02
---	---
Pole3	polymerase (DNA directed), epsilon 3 (p17 subunit)
---	Transcribed locus, strongly similar to XP_214253.3 PREDICTED: similar to muscleblind-like 2 isoform 1 [Rattus norvegicus]
---	Transcribed locus
Cpd	Carboxypeptidase D
MGC124824	similar to 2310002F18Rik protein
Grpel1	GrpE-like 1, mitochondrial
Arf3	ADP-ribosylation factor 3
P4hb	prolyl 4-hydroxylase, beta polypeptide
Rpl27a_predicted	ribosomal protein L27a (predicted)
RGD1564938_predicted	similar to MYLE protein (Dexamethasone-induced protein) (predicted)
Cse1l_predicted	chromosome segregation 1-like (S. cerevisiae) (predicted)
Ceacam3	Carcinoembryonic antigen-related cell adhesion molecule 3 /// Transcribed locus, strongly similar to XP_216910.3 PREDICTED: similar to Methionine-tRNA synthetase [Rattus norvegicus]
Ssu72	Ssu72 RNA polymerase II CTD phosphatase homolog (yeast)
Chd4	chromodomain helicase DNA binding protein 4
---	Transcribed locus
LOC685462	similar to EMI domain containing 1
---	Transcribed locus, strongly similar to XP_238334.3 PREDICTED: similar to putative homeodomain transcription factor 2 [Rattus norvegicus]
---	Transcribed locus

---	Transcribed locus
---	CDNA clone IMAGE:7317367
---	Transcribed locus
Hmgcs1	3-hydroxy-3-methylglutaryl-Coenzyme A synthase 1 /// 3-hydroxy-3-methylglutaryl-Coenzyme A synthase 1
Psma2	proteasome (prosome, macropain) subunit, alpha type 2 /// proteasome (prosome, macropain) subunit, alpha type 2
RGD1560155_predicted	Similar to mKIAA0934 protein (predicted)
Nfatc3_predicted	Nuclear factor of activated T-cells, cytoplasmic, calcineurin-dependent 3 (predicted)
Wdr41_predicted	WD repeat domain 41 (predicted)
Rpl14	ribosomal protein L14
LOC681415	Similar to Enhancer of rudimentary homolog
Rpl34_predicted /// LOC680170 /// LOC684829	ribosomal protein L34 (predicted) /// similar to ribosomal protein L34 /// similar to ribosomal protein L34
Cdc42	cell division cycle 42 homolog (S. cerevisiae)
Ndufb4	NADH dehydrogenase (ubiquinone) 1 beta subcomplex, 4, 15kDa
Dpm1_predicted	dolichol-phosphate (beta-D) mannosyltransferase 1 (predicted)
Bcl6_predicted	B-cell leukemia/lymphoma 6 (predicted)
Arl2bp	ADP-ribosylation factor-like 2 binding protein
RGD1309550	similar to hypothetical protein D12Ertd771e
Zfp212	Zinc finger protein 212
Camk2b	calcium/calmodulin-dependent protein kinase II, beta
Naca_predicted	nascent-polypeptide-associated complex alpha polypeptide (predicted)
Rps27a	ribosomal protein S27a
---	Transcribed locus, strongly similar to XP_340756.1 PREDICTED: similar to tumorous imaginal discs protein Tid56-like protein long form; TID1L; mTid-1L [Rattus norvegicus]
LOC499779	similar to RIKEN cDNA 2900010J23
Tagln2	transgelin 2
---	Transcribed locus
Thrap1_predicted	Thyroid hormone receptor associated protein 1 (predicted)
LOC368070	similar to Pinin
Tef	thyrotroph embryonic factor
Gnas /// Xlas	GNAS complex locus /// XLas protein
---	Transcribed locus
Actb	actin, beta
Pfn2	profilin 2 /// profilin 2
Rpl35	ribosomal protein L35
Cidea_predicted	Cell death-inducing DNA fragmentation factor, alpha subunit-like effector A (predicted)
LOC500715	similar to cyclin K
Ncl	nucleolin
Nfia	nuclear factor I/A
LOC619558	hypothetical protein LOC619558
Mtmr6_predicted	myotubularin related protein 6 (predicted)

Six5_predicted	sine oculis-related homeobox 5 homolog (Drosophila) (predicted)
---	Transcribed locus
Dlgh1	Discs, large homolog 1 (Drosophila)
LOC311352	similar to Adenosine deaminase CG11994-PA
MGC112883	LOC500651
---	Transcribed locus
Zfp281	Zinc finger protein 281
---	Transcribed locus
Edf1_predicted	endothelial differentiation-related factor 1 (predicted)
LOC361990	similar to DKFZP547E1010 protein
Eif3s9	eukaryotic translation initiation factor 3, subunit 9 (eta)
Pacsin2	protein kinase C and casein kinase substrate in neurons 2
Prss35	Protease, serine, 35 /// Protease, serine, 35
LOC683839 /// LOC688495	hypothetical protein LOC683839 /// hypothetical protein LOC688495
Ddx5	ddx5 gene
Psmb7	proteasome (prosome, macropain) subunit, beta type 7 /// proteasome (prosome, macropain) subunit, beta type 7
---	Transcribed locus
Prdx1	peroxiredoxin 1 /// peroxiredoxin 1
Rpl22l1_predicted	ribosomal protein L22 like 1 (predicted)
Ifitm2	interferon induced transmembrane protein 2 (1-8D)
Armc1_predicted	armadillo repeat containing 1 (predicted)
Fstl3	follistatin-like 3
MGC72957	similar to 60S ribosomal protein L18a
Sdpr	serum deprivation response protein
---	Transcribed locus
Rps14	ribosomal protein S14
---	Transcribed locus
Atp2a2	ATPase, Ca++ transporting, cardiac muscle, slow twitch 2
Tmem55a	transmembrane protein 55A
Numb	Numb gene homolog (Drosophila)
RGD1559716_predicted	similar to protein kinase/endoribonuclease(IRE1) alpha (predicted)
Prdm15_predicted	PR domain containing 15 (predicted)
RGD1562952_predicted	similar to Erbb2 interacting protein isoform 2 (predicted)
DERP6	dermal papilla derived protein 6
Isoc1	isochorismatase domain containing 1
Fkbp1a	FK506 binding protein 1a
LOC498453	similar to transcription elongation factor A 1 isoform 2
RGD1305466	similar to RIKEN cDNA 1300002A08
Itpr1	inositol 1,4,5-triphosphate receptor 1
Eif3s5_predicted	eukaryotic translation initiation factor 3, subunit 5 (epsilon) (predicted)
---	---
Cma1	chymase 1, mast cell
Stim1_predicted	stromal interaction molecule 1 (predicted)
LOC499745	Similar to Notch-regulated ankyrin repeat protein
Tgfbi	transforming growth factor, beta induced
---	Transcribed locus

RGD1560511_predicted	similar to Vps41 protein (predicted)
Osbpl5	oxysterol binding protein-like 5
Vmac	Vimentin-type intermediate filament associated coiled-coil protein
Dscr2_predicted	Down syndrome critical region homolog 2 (human) (predicted)
Mknk2	MAP kinase-interacting serine/threonine kinase 2
Rps15a	ribosomal protein S15a
Bsg	basigin
Cdc40_predicted	cell division cycle 40 homolog (yeast) (predicted)
---	Transcribed locus
---	Transcribed locus
Plg	plasminogen /// plasminogen
---	Transcribed locus
Cdc42ep4_predicted	CDC42 effector protein (Rho GTPase binding) 4 (predicted)
Pvrl3_predicted	poliovirus receptor-related 3 (predicted)
---	---
RGD1564876_predicted	similar to Solute carrier family 35, member E3 (predicted)
LOC687090	hypothetical protein LOC687090
LOC311078	similar to T-Brain-1 /// similar to T-Brain-1
Aqp1	aquaporin 1
---	Transcribed locus
Rnf25	ring finger protein 25
Dok4_predicted	docking protein 4 (predicted)
RGD1565591_predicted	similar to Ski protein (predicted)
Syncrip	synaptotagmin binding, cytoplasmic RNA interacting protein
---	Transcribed locus
Slc26a1	Solute carrier family 26 (sulfate transporter), member 1
Zfpn1a5_predicted	zinc finger protein, subfamily 1A, 5 (predicted)
Ap1s2_predicted	adaptor-related protein complex 1, sigma 2 subunit (predicted)
Csrp1	cysteine and glycine-rich protein 1
Serpinb6a	serine (or cysteine) peptidase inhibitor, clade B, member 6a
---	---
LOC502710 /// LOC679252	similar to Myeloid/lymphoid or mixed-lineage leukemia protein 3 homolog (Histone-lysine N-methyltransferase, H3 lysine-4 specific MLL3) /// similar to Myeloid/lymphoid or mixed-lineage leukemia protein 3 homolog (Histone-lysine N-methyltransferase, H3 lysine-4 specific MLL3)
Pebp1	phosphatidylethanolamine binding protein 1
LOC687899 /// LOC691534	similar to nucleolar protein family A, member 3 /// similar to nucleolar protein family A, member 3
Znf142_predicted	zinc finger protein 142 (clone pHZ-49) (predicted)
---	Transcribed locus, moderately similar to XP_529790.1 PREDICTED: hypothetical protein XP_529790 [Pan troglodytes]
RGD1304717_predicted	Similar to CDNA sequence BC024561 (predicted)
Hsf2	heat shock factor 2
Uqcrfs1	ubiquinol-cytochrome c reductase, Rieske iron-sulfur polypeptide 1

Anp32e	Acidic (leucine-rich) nuclear phosphoprotein 32 family, member E
RGD1307034_predicted	similar to hypothetical protein CG003 (predicted)
Rpsa	ribosomal protein SA
Psrc2	proline/serine-rich coiled-coil 2
Ttc3_predicted	tetratricopeptide repeat domain 3 (predicted)
Rab1	RAB1, member RAS oncogene family
---	Transcribed locus
Fkbp3_predicted	FK506 binding protein 3 (predicted)
---	Transcribed locus
Esam	endothelial cell adhesion molecule
RGD1310769_predicted	similar to HSPC288 (predicted)
Hig1	hypoxia induced gene 1
Tbc1d2b	TBC1 domain family, member 2B
Prpf4	PRP4 pre-mRNA processing factor 4 homolog (yeast)
Gpx4	glutathione peroxidase 4 /// glutathione peroxidase 4
Wbp5_predicted	WW domain binding protein 5 (predicted)
Eef1g	eukaryotic translation elongation factor 1 gamma
Dag1	dystroglycan 1
Faah	Fatty acid amide hydrolase
Gata4	GATA binding protein 4
---	Transcribed locus
Rela	v-rel reticuloendotheliosis viral oncogene homolog A (avian) /// v-rel reticuloendotheliosis viral oncogene homolog A (avian)
RGD1306495	similar to EST AA792894
---	Transcribed locus
---	Transcribed locus
Hspa14	heat shock 70kDa protein 14
---	Transcribed locus
Nme2	expressed in non-metastatic cells 2 /// expressed in non-metastatic cells 2
LOC680726	similar to RNA binding motif, single stranded interacting protein 3 isoform 1
---	Transcribed locus, weakly similar to XP_359938.1 hypothetical protein MG11009.4 [Magnaporthe grisea 70-15]
Rab12	RAB12, member RAS oncogene family
---	Transcribed locus
LOC687789	similar to ubiquitin-conjugating enzyme E2D 1, UBC4/5 homolog
LOC686809	similar to protein 7 transactivated by hepatitis B virus X antigen
Usp9x_predicted	ubiquitin specific peptidase 9, X chromosome (predicted)
Pdcd11_predicted	Programmed cell death protein 11 (predicted) /// CDNA clone IMAGE:7933354, with apparent retained intron
---	Transcribed locus
RGD1565641_predicted	RGD1565641 (predicted)
Abce1	ATP-binding cassette, sub-family E (OABP), member 1
Mtmr4_predicted	myotubularin related protein 4 (predicted)
RGD1309095_predicted	similar to hypothetical protein BC015148 (predicted)
Unc50	Unc-50 homolog (C. elegans)

---	Transcribed locus
RGD1563869_predicted	Sim ilar to glucocorticoid induced gene 1 (predicted)
---	Transcribed locus, strongly similar to XP_230983.3 PREDICTED: similar to MLTK-beta [Rattus norvegicus]
Pdcd5_predicted	programmed cell death 5 (predicted)
RGD1565253_predicted	similar to D-glucuronyl C5-epimerase (predicted)
---	Transcribed locus, strongly similar to NP_722482.1 BCL2-associated transcription factor 1 isoform 2 [Mus musculus]
---	---
Tm2d3_predicted	TM2 domain containing 3 (predicted)
---	Transcribed locus
Cmkor1	chemokine orphan receptor 1
---	Transcribed locus /// Transcribed locus
Rps2	ribosomal protein S2
Psmd11_predicted	proteasome (prosome, macropain) 26S subunit, non-ATPase, 11 (predicted)
Psme1	proteasome (prosome, macropain) 28 subunit, alpha
Ube2a	ubiquitin-conjugating enzyme E2A, RAD6 homolog (S. cerevisiae)
Lztr1_predicted	leucine-zipper-like transcriptional regulator, 1 (predicted)
Sec31l1	SEC31-like 1 (S. cerevisiae)
Fcgr3	Fc receptor, IgG, low affinity III
MGC72942	similar to CG6105-PA
---	Activity and neurotransmitter-induced early gene 11 (ania-11) mRNA, 3' UTR
---	Transcribed locus
Prdm15_predicted	PR domain containing 15 (predicted)
RGD1560248_predicted	similar to formin-like 2 isoform B (predicted)
---	Transcribed locus
Myct1_predicted	myc target 1 (predicted)
---	---
RGD1307982	similar to RIKEN cDNA 2810409H07
Nbr1	neighbor of Brca1 gene 1
---	---
LOC500954	Ubiquitin-Like 5 Protein
Usp12_predicted ///	ubiquitin specific protease 12 (predicted) /// similar to
RGD1561481_predicted /// LOC684318	ubiquitin specific protease 12 (predicted) /// similar to ubiquitin specific protease 12
Cryab	crystallin, alpha B /// crystallin, alpha B
Plec1	plectin 1
Ets2_mapped	v-ets erythroblastosis virus E26 oncogene homolog 2 (avian) (mapped)
---	Transcribed locus
Pxn	paxillin /// paxillin
RGD1560909_predicted	similar to DNA segment, Chr 1, Brigham & Womens Genetics 0212 expressed (predicted)
Sdc4	syndecan 4
Rbx1	ring-box 1 /// ring-box 1
Efnb3_predicted	ephrin B3 (predicted)
Wdr1	WD repeat protein 1
Dnase2	deoxyribonuclease II
Ccnc	Cyclin C /// Cyclin C

Mterfd2	MTERF domain containing 2
---	Transcribed locus
LOC686471 /// LOC690263	hypothetical protein LOC686471 /// hypothetical protein LOC690263
Noxo1_predicted	NADPH oxidase organizer 1 (predicted)
---	Transcribed locus, strongly similar to XP_578163.1 PREDICTED: similar to hypothetical protein, expressed [Rattus norvegicus] /// Transcribed locus, strongly similar to XP_578163.1 PREDICTED: similar to hypothetical protein, expressed [Rattus norvegicus]
Lrrc8	leucine-rich repeat-containing 8
LOC362855	P55
---	Transcribed locus
Arl1	ADP-ribosylation factor-like 1
Itgb4	Integrin beta 4
---	---
---	Transcribed locus
---	Transcribed locus
Vps28_predicted	vacuolar protein sorting 28 (yeast) (predicted)
---	Transcribed locus
Alg12_predicted	asparagine-linked glycosylation 12 homolog (yeast, alpha-1,6-mannosyltransferase) (predicted)
Rps6ka5_predicted	Ribosomal protein S6 kinase, polypeptide 5 (predicted)
Anxa2	annexin A2
---	Transcribed locus
---	Transcribed locus
Samd4b	sterile alpha motif domain containing 4B
Tpcn2_predicted	two pore segment channel 2 (predicted)
RGD1562438_predicted	similar to amyloid beta (A4) precursor protein-binding, family B, member 2 (predicted)
RGD1308139_predicted	similar to RIKEN cDNA 1200014J11 (predicted)
Pfn2	profilin 2
mrpl24	mitochondrial ribosomal protein L24
---	---
RGD1306142_predicted	similar to RIKEN cDNA B930096L08 (predicted)
RGD1311045_predicted	similar to RIKEN cDNA 4933428G09 (predicted)
Gls	glutaminase
LOC690599	Similar to Transmembrane anchor protein 1
RGD1560268_predicted	similar to AT motif-binding factor (predicted)
---	Transcribed locus
---	Transcribed locus, strongly similar to XP_343327.2 PREDICTED: similar to Myeloid/lymphoid or mixed-lineage leukemia protein 2 (ALL1-related protein) [Rattus norvegicus]
RGD1565969_predicted	similar to 5730405I09Rik protein (predicted)
RGD1308059	similar to DNA segment, Chr 4, Brigham & Womens Genetics 0951 expressed
---	Transcribed locus
Emp2	epithelial membrane protein 2
Gnaq	Guanine nucleotide binding protein, alpha q polypeptide
Trim2	tripartite motif protein 2
---	---

Gm963_predicted	Gene model 963, (NCBI) (predicted)
---	Transcribed locus
---	Transcribed locus
Wdr20	WD repeat domain 20
---	---
Jun	Jun oncogene
Rnd2	Rho family GTPase 2
RGD1305677	similar to RIKEN cDNA 1810020E01
Elavl1_predicted	ELAV (embryonic lethal, abnormal vision, Drosophila)-like 1 (Hu antigen R) (predicted)
---	Transcribed locus
---	Transcribed locus
MGC108896	similar to glutathione transferase GSTM7-7
Rab34	RAB34, member of RAS oncogene family
Centb2	Centaurin, beta 2
---	Transcribed locus
---	---
Mrpl49	mitochondrial ribosomal protein L49
Crygd	crystallin, gamma D
---	Transcribed locus
Kctd12_predicted	Potassium channel tetramerisation domain containing 12 (predicted)
Rbbp5_predicted	Retinoblastoma binding protein 5 (predicted)
---	Transcribed locus
RGD1310681_predicted	similar to RIKEN cDNA 6720467C03 (predicted)
RGD1563737_predicted	Similar to transmembrane protein 44 isoform a (predicted)
Cpd	carboxypeptidase D
Nedd4a	Neural precursor cell expressed, developmentally down-regulated gene 4A
Kif2	kinesin heavy chain family, member 2
Lrrc17	leucine rich repeat containing 17
LOC686179	hypothetical protein LOC686179
Cacnb4	calcium channel, voltage-dependent, beta 4 subunit
Camk2g	calcium/calmodulin-dependent protein kinase II gamma
Pofut2_predicted	protein O-fucosyltransferase 2 (predicted)
RGD1561852_predicted	similar to Protein C20orf29 (predicted)
Hnrpf	heterogeneous nuclear ribonucleoprotein F
RGD1305457	similar to RIKEN cDNA 1700023M03
---	Transcribed locus
Tax1bp3	Tax1 (human T-cell leukemia virus type I) binding protein 3
Mal	myelin and lymphocyte protein, T-cell differentiation protein
---	---
RGD1310357_predicted	similar to RIKEN cDNA 2810457I06 (predicted)
---	Transcribed locus
---	Transcribed locus
---	---
Art1_predicted	ADP-ribosyltransferase 1 (predicted)
Inpp4a	inositol polyphosphate-4-phosphatase, type 1
---	Transcribed locus

Hoxc6	homeo box C6 /// homeo box C6
RGD1562115_predicted	similar to TAFA5 (predicted)
LOC498353	similar to Sec1 family domain containing protein 2 (Syntaxin binding protein 1-like 1) (Neuronal Sec1)
RGD1563072_predicted	similar to hypothetical protein FLJ38984 (predicted)
Pik3r1	Phosphatidylinositol 3-kinase, regulatory subunit, polypeptide 1
Limd1_predicted	LIM domains containing 1 (predicted)
RGD1563990_predicted	similar to 8430411H09Rik protein (predicted)
---	Transcribed locus /// Transcribed locus
LOC679942 /// LOC684489	similar to angiopoietin-like 1 /// similar to angiopoietin-like 1
Zfp496_predicted	zinc finger protein 496 (predicted)
---	Transcribed locus
LOC684050	similar to procollagen C-endopeptidase enhancer 2 /// similar to procollagen C-endopeptidase enhancer 2
Selp	selectin, platelet
---	Transcribed locus
---	Transcribed locus
Ly6c /// RGD1565410_predicted	Ly6-C antigen /// similar to Ly6-C antigen gene (predicted)
Trim28	tripartite motif protein 28
Scarb1	scavenger receptor class B, member 1
LOC311134	hypothetical LOC311134
Ddx3x	DEAD/H (Asp-Glu-Ala-Asp/His) box polypeptide 3, X-linked
Wfdc1	WAP four-disulfide core domain 1
Synj2bp	synaptojanin 2 binding protein
---	Transcribed locus
Ftsj3	FtsJ homolog 3 (E. coli)
Slc12a7	Solute carrier family 12 (potassium/chloride transporters), member 7
Cldn1	claudin 1
Gpc3	glypican 3
LOC301124	hypothetical LOC301124
---	Transcribed locus
Kctd6_predicted	potassium channel tetramerisation domain containing 6 (predicted)
---	Transcribed locus
RGD1305166_predicted	similar to RIKEN cDNA 4930521E07 (predicted)
Mmp3	matrix metallopeptidase 3 /// matrix metallopeptidase 3
RGD1559610_predicted	similar to CGI-94 protein (predicted)
---	Transcribed locus
Siah2	seven in absentia 2
Ercc8_predicted	excision repair cross-complementing rodent repair deficiency, complementation group 8 (predicted)
Hps4_predicted	Hermansky-Pudlak syndrome 4 homolog (human) (predicted)
---	Transcribed locus
Mvp	Major vault protein
LOC300284	similar to RIKEN cDNA 4833435D08
Als2cr13_predicted	amyotrophic lateral sclerosis 2 (juvenile) chromosome

	region, candidate 13 (predicted) /// amyotrophic lateral sclerosis 2 (juvenile) chromosome region, candidate 13 (predicted)
Postn_predicted	periostin, osteoblast specific factor (predicted) /// periostin, osteoblast specific factor (predicted)
---	Transcribed locus
---	---
Snph_predicted	syntaphilin (predicted)
---	---
Trfp /// LOC501098	Trf (TATA binding protein-related factor)-proximal protein homolog (Drosophila) /// similar to ubiquitin specific protease 49 (predicted)
---	Transcribed locus
RGD1309105_predicted	Similar to RIKEN cDNA 2310005N03 gene
Ppp2r1a	protein phosphatase 2 (formerly 2A), regulatory subunit A (PR 65), alpha isoform
Gja7	gap junction membrane channel protein alpha 7
Nt5e	5' nucleotidase, ecto
RGD1307525_predicted	similar to intracellular protein transport like (XM453) (predicted)
LOC687381 /// LOC691853	similar to COX10 homolog, cytochrome c oxidase assembly protein, heme A: farnesyltransferase /// similar to COX10 homolog, cytochrome c oxidase assembly protein, heme A: farnesyltransferase
Sema5b_predicted	sema domain, seven thrombospondin repeats (type 1 and type 1-like), transmembrane domain (TM) and short cytoplasmic domain, (semaphorin) 5B (predicted)
Arhgef15_predicted	Rho guanine nucleotide exchange factor (GEF) 15 (predicted)
RGD1306762_predicted	similar to RIKEN cDNA 2510005D08 (predicted)
LOC682957	similar to Homeobox protein Hox-D9 (Hox-4.4) (Hox-5.2)
RGD1560745_predicted	similar to OTTHUMP00000018508 (predicted)
---	Transcribed locus
Mfap4	microfibrillar-associated protein 4 /// microfibrillar-associated protein 4
---	Transcribed locus, weakly similar to XP_580018.1 PREDICTED: hypothetical protein XP_580018 [Rattus norvegicus]
---	---
LOC499951	Similar to Transcription factor GATA-5 (GATA binding factor-5)
RGD1565095_predicted	similar to hypothetical protein MGC52110 (predicted)
---	Transcribed locus
---	Transcribed locus
RGD1562228_predicted	similar to E2-induced gene 2 protein (predicted)
Prg-2	plasticity-related protein PRG-2
---	Transcribed locus
RGD1305235	similar to RIKEN cDNA 1700052N19
LOC498331	similar to protein Tyr phosphatase /// similar to protein Tyr phosphatase
RGD1559727_predicted	similar to lipoma HMGIC fusion partner-like 3 (predicted)
Zfp537_predicted	zinc finger protein 537 (predicted)
Fbxo11	F-box only protein 11

Trdn	triadin
Klhl22_predicted	kelch-like 22 (Drosophila) (predicted)
Tpr	translocated promoter region
Fndc5	Fibronectin type III domain containing 5
RGD1563912_predicted	RGD1563912 (predicted)
Ptprk	Protein tyrosine phosphatase, receptor type, K, extracellular region
Pcdh3	protocadherin 3
Akr1b4	Aldo-keto reductase family 1, member B4 (aldose reductase)
---	Transcribed locus
Wdr50_predicted	WD repeat domain 50 (predicted)
Pros1	protein S (alpha) /// protein S (alpha)
MGC72614	Unknown (protein for MGC:72614)
Serpina3n	serine (or cysteine) peptidase inhibitor, clade A, member 3N /// serine (or cysteine) peptidase inhibitor, clade A, member 3N
Slc25a19	solute carrier family 25 (mitochondrial deoxynucleotide carrier), member 19
Tomm70a	translocase of outer mitochondrial membrane 70 homolog A (yeast)
---	Transcribed locus
---	Transcribed locus
RGD1305090_predicted	Similar to CD2-associated protein (predicted)
---	Transcribed locus
LOC306805	Similar to asporin precursor
Cdc42ep2	CDC42 effector protein (Rho GTPase binding) 2 /// CDC42 effector protein (Rho GTPase binding) 2
LOC688310	similar to CG5500-PA
LOC680687 ///	hypothetical protein LOC680687 /// hypothetical protein
LOC687274	LOC687274
Fmo5	flavin containing monooxygenase 5 /// flavin containing monooxygenase 5
---	Transcribed locus
Csrp2	cysteine and glycine-rich protein 2
Tex2	testis expressed gene 2
---	Transcribed locus
---	Transcribed locus
---	Transcribed locus
Akap5	A kinase (PRKA) anchor protein 5
---	---
---	Transcribed locus
---	Transcribed locus
---	Transcribed locus, strongly similar to XP_341639.2 PREDICTED: similar to Nedd4-binding brain specific protein BEAN [Rattus norvegicus]
Prkab2	Protein kinase, AMP-activated, beta 2 non-catalytic subunit
Stk16 /// RGD1560911_predicted /// RGD1306622_predicted	Serine/threonine kinase 16 /// Similar to BC026645 protein (predicted) /// Similar to KIAA0954 protein (predicted)
Col18a1	procollagen, type XVIII, alpha 1

Uxt	ubiquitously expressed transcript
LOC688999	Similar to Homeobox protein Hox-D8 (Hox-4.3) (Hox-5.4)
Polr2c	polymerase (RNA) II (DNA directed) polypeptide C
Stip1	stress-induced phosphoprotein 1
LOC362156	membrane-associated DHHC5 zinc finger protein
Crispld2	cysteine-rich secretory protein LCCL domain containing 2
Tnn_predicted	tenascin N (predicted)
---	Transcribed locus, moderately similar to NP_084125.1 hypothetical protein LOC77043 [Mus musculus]
---	Transcribed locus, weakly similar to XP_575132.1 PREDICTED: similar to LRRGT00012 [Rattus norvegicus]
Cdc26	cell division cycle 26
---	Transcribed locus
LOC678810 /// LOC685448	hypothetical protein LOC678810 /// hypothetical protein LOC685448
Coch_predicted	coagulation factor C homolog (Limulus polyphemus) (predicted) /// coagulation factor C homolog (Limulus polyphemus) (predicted)
RGD1359349	similar to hypothetical protein MGC34760
---	Transcribed locus
RGD1562438_predicted	similar to amyloid beta (A4) precursor protein-binding, family B, member 2 (predicted)